INVESTIGATIONS ON THE RADIATION CHARACTERISTICS OF BROADBAND STRIP LOADED SLOTTED MICROSTRIP ANTENNAS

A thesis submitted by

SARIN V.P

in partial fulfillment of the requirements for the degree of

DOCTOR OF PHILOSOPHY

Under the guidance of

PROF. K. VASUDEVAN

DEPARTMENT OF ELECTRONICS
FACULTY OF TECHNOLOGY
COCHIN UNIVERSITY OF SCIENCE AND TECHNOLOGY
KOCHI-22, INDIA

January **2012**

Investigations on the Radiation Characteristics of Broadband Strip Loaded Slotted Microstrip Antennas

Ph.D. Thesis under the Faculty of Technology

Author

Sarin V.P.
Research Scholar
Department of Electronics
Cochin University of Science and Technology
Kochi - 682022
Email: sarincrema@gmail.com

Supervising Guide

Dr. K. Vasudevan
Professor
Department of Electronics
Cochin University of Science and Technology
Kochi - 682022
Email: vasudevankdr@gmail.com

January 2012

I love him who lives for knowledge and who wants knowledge

Dedicated to my parents, teachers,

brother and to all my friends ....

DEPARTMENT OF ELECTRONICS
COCHIN UNIVERSITY OF SCIENCE AND TECHNOLOGY,
KOCHI – 682 022

Dr. K Vasudevan	Ph: 9447 357328
Professor	E-mail: vasudevankdr@gmail.com

Certificate

This is to certify that this thesis entitled "**Investigations on the Radiation Characteristics of Broadband Strip Loaded Slotted Microstrip Antennas**" is a bonafide record of the research work carried out by Mr. Sarin V.P under my supervision in the Department of Electronics, Cochin University of Science and Technology. The results embodied in this thesis or parts of it have not been presented for any other degree.

Cochin-22
30th January 2012

Dr. K. Vasudevan
(Supervising Teacher)

$\mathcal{D}$eclaration

I hereby declare that the work presented in this thesis entitled "**Investigations on the Radiation Characteristics of Broadband Strip Loaded Slotted Microstrip Antennas**" is a bonafide record of the research work done by me under the supervision of Dr. K. Vasudevan, Professor, Department of Electronics, Cochin University of Science and Technology, India and that no part thereof has been presented for the award of any other degree.

Cochin-22
30th January 2012

Sarin V.P.
Research Scholar
Department of Electronics
Cochin University of Science
and Technology

Words of Gratitude...

It is with a deep sense of gratitude that I wish to place on record my indebtedness to my supervising guide Dr. K. Vasudevan, Professor, Department of Electronics, Cochin University of Science and Technology, whose guidance and constant encouragement was indispensable for the progress and completion of this thesis. I remember the timely care he had given me throughout my research period.

I also thank Prof. P. Mohanan and Prof. C.K Aanandan, Department of Electronics, Cochin University of Science and Technology, for their whole hearted support, constant encouragement, and for extending the facilities of Department of Electronics for my research. I also wish to thank them for their valuable suggestion in my research.

Let me thank Prof. K. T Mathew and Prof. P.R.S Pillai, Head of the Department, Department of Electronics, for their whole hearted support, constant encouragement and valuable suggestions.

My sincere thanks to Dr. Tessamma Thomas, Dr. James Kurian, Dr. M.H. Supriya, all other faculty members and non teaching staffs of Department of Electronics for the help and cooperation extended to me.

I wish to express my sincere indebtedness to Dr. Thomaskutty Mathew, my teacher, School of Technology and Applied Sciences, Edappally for his timely care in my research, valuable suggestions and constant encouragement, which helped me very much to improve my research work.

I express my special thanks to Mrs. Nishamol M.S who had been with me throughout the research period as a motivation and the discussions with her really helped me to complete my research work successfully.

Dr. Rohith K. Raj, Dr. Manoj Joseph and Dr. Suma M.N had been with me throughout my research period. I take this opportunity to express my gratitude for their

valuable suggestions and encouragement which were of immense value to me. I really enjoyed very much my period of association with them.

I take this opportunity to express my sincere thanks to Dr. Gijo Augustine and Dr. Deepu V for extending me an unparalleled way of support, constant encouragement, and fruitful discussions on my research topic.

My sincere thanks to Mr. Sujith R, Mr. Tony D, Mrs. Laila D, Mrs. Shameena V.A and Mrs. Sarah Jacob for their whole hearted support, helps and above all, the association with me.

I express my sincere thanks to Mr. M. Gopikrishna and Mrs. Deepti Das Krishna for their valuable suggestions and help throughout my research period.

I am thankful to Mr. Dinesh R., Mr. Nijas, Mr. Deepak, Mr. Paulbert Thomas, Mr. Ullas G. Kalappura, Mr. Lindo A.O and Ms. Anju Mathews for their valuable help, fruitful discussions and constant encouragement.

My words are boundless to thank all my research colleagues in Centre for Research in Electromagnetics and Antennas, CUSAT centre for Ocean Electronics (CUCENTOL), Microwave Tomography and Material Research Laboratory (MTMR) and Audio and Image Research Lab (AIRL), Department of Electronics, Cochin University of Science and Technology.

In the course of my research work I received Junior and Senior Research fellow ships from University Grants Commission (UGC), Govt. of India. These financial supports are gratefully acknowledged.

My parents and my brother for their boundless love, care and their seamless effort, which gave me courage and stiffness to complete this work in this form.

Sarin V.P

Preface

With the recent progress and rapid increase in mobile terminals, the design of antennas for small mobile terminals is acquiring great importance. In view of this situation, several design concepts are already been addressed by the scientists and engineers. Compactness and efficiency are the major criteria for mobile terminal antennas. The challenging task of the microwave scientists and engineers is to device compact printed radiating systems having broadband behavior, together with good efficiency. Printed antenna technology has received popularity among antenna scientists after the introduction of microstrip antenna in 1970s. The successors in this kind such as printed monopoles and planar inverted F are also equally important. Scientists and Engineers are trying to explore this technology as a viable coast effective solution for forthcoming microwave revolution. The transmission line perspectives of antennas are very interesting. The concept behind any electromagnetic radiator is simple. Any electromagnetic system with a discontinuity is radiating electromagnetic energy. The size, shape and the orientation of the discontinuities controls the radiation characteristics of the system such as radiation pattern, gain, polarization etc. It can be either resonant or non resonant structure.

Microstrip antennas are suitable for wireless applications due to their low cost, high gain and ease of fabrication. But the major disadvantage of microstrip antennas is their inherent narrow bandwidth. A lot of techniques are introduced by the researchers all over the world to enhance the bandwidth of microstrip patch antennas. The thesis addresses an attempt to enhance the bandwidth of microstrip patch antennas by incorporating impedance matching strip as a part of the microstrip patch antenna. The first part of the thesis deals with the broadband operation of the tilted square slot and polygonal slot loaded square microstrip patch antennas. The resonant mechanisms are clearly mentioned using the simulation and experimental studies. The bandwidth of the polygonal slotted broadband patch antenna is again enhanced by implementing an L-strip feed mechanism. In the second major part of the thesis, a novel gain enhancement technique for single band and broadband square microstrip patch antennas is achieved by implementing offset stacked configurations.

.....ജ്ഞാ.....

CONTENTS

Chapter -4

INVESTIGATIONS ON A STRIP LOADED SLOTTED BROADBAND SQUARE MICROSTRIP ANTENNA FOR WIDEBAND APPLICATIONS

Chapter -5

INVESTIGATIONS ON STACKED OFFSET SINGLE BAND AND BROADBAND MICROSTRIP ANTENNAS FOR ENHANCED GAIN PERFORMANCE ....**159 - 198**

Chapter -6

CONCLUSION AND FUTURE PERSPECTIVE ....199 - 204

Appendix -A

A COMPACT PLANAR DUAL BAND ANTENNA FOR 2.4/5.2 GHZ
WIRELESS LAN APPLICATIONS...205 - 221

.....ೞഏ.....

Chapter **1**

INTRODUCTION

This chapter starts with a brief overview of the progress in antenna research. The invention of microstrip antennas is discussed in detail and the principle behind the radiation mechanism is explained using the fringing field model. The chapter also presents the feeding techniques used for microstrip antennas and the different models/techniques used for the analysis of different microstrip antenna configurations available. Finally, the motivation behind the development of broadband microstrip antennas and the thesis organization are described.

1.1 Introduction

The electromagnetic research industry got a punch in 1864, When James Clark Maxwell theoretically formulated the existence of electromagnetic waves [1]. The experimental validation of Maxwell's equations was done first by Heinrich Rudolf Hertz, known as the father of electromagnetics, 12 years later, in 1886. He generated, transmitted and received electromagnetic energy by means of an end loaded half wave dipole as the transmitter and a square loop antenna as the receiver [2]. This experiment leads to the birth of a new field called the antenna. "Antennas are like electronic eyes and ears" [3]. They act like an interface between free space and circuitry. In 1897, J.C Bose, the talented Indian Scientist gave his first public demonstration of electromagnetic waves. The wavelength he used ranges from 2.5mm to 5mm. The early history of electromagnetic waves before 1900 is well reviewed by Ramsay [4].

Guglielmo Marconi in 1897 combined the discoveries made by Maxwell and Hertz. He successfully demonstrated the practical application of wireless communication by implementing continuous radio contact between the shore and ships traveling in the English Channel [5]. In 1901 Marconi again took a much greater step by performing the first transcontinental wireless communication, between England and Canada. This achievement triggered the scientists and engineers all over the world towards the field of wireless communications.

1.2 An overview of antenna research

Before World war II, the common types of antennas used were majorly single element or array form wire type antennas, such as long wire antennas, wire dipoles, helices, rhombuses etc. In 1926, Yagi-Uda antenna was invented

[6] by Shintaro Uda and Hidetsugu Yagi from Tohoku Imperial University and it was received a wide popularity due to its simplicity and directionality.

World War II was the most flourishing period in antenna research. During and after World War II, many other radiators were introduced. These include aperture type antennas like open ended wave guides, slots, horns, reflectors and lenses [7]. In 1950s a breakthrough in antenna evolution was created by V.H Ramsey [8] which extended the maximum bandwidth as great as 40:1 or more. The structure is specified entirely by angles, instead of linear dimensions, they offered an infinite bandwidth and popularly referred to as frequency independent antennas. According to Prof. J.D Kraus [3, 9] antennas can be classified on the basis of the material from which it is made of as

a)   Antennas made of conductors of wire or tubing

b)   Antennas made of sheet conductors

c)   Antennas made of dielectrics

d)   Array antennas

Different types of helices, linear conductor antennas and loops are coming in category (a). Category (b) consists of reflectors, guiding, slotted and microstrip antennas. Group (c) is constituted by lenses, polyrods and slabs. The last group is divided into driven, parasitic, adaptive, interferometric and digital beam forming arrays.

The rapid developments in the present day communication systems (personal communication systems, mobile satellite communication systems etc) demand planar low profile and conformal antennas. Microstrip antennas are

satisfying all the above requirements and therefore they are fast replacing conventional antennas in the above areas.

1.3 Microstrip Antennas

The concept of microstrip antenna was proposed by Deschamps in 1953 [10]. Since then it took 20 years for the first practical microstrip antenna to come up. The first practical microstrip antennas were developed by Howell [11] and Munson [12] in the early of 1970's and this set the pace of research and development in the area of microstrip antennas all over the world.

The basic configuration of a microstrip antenna is shown in figure 1.1. It consists of a planar radiating structure of any geometrical shape over a ground plane separated by a thin dielectric substrate. Commonly used microstrip radiating geometries are rectangular and circular. However other shapes are used depending upon the application.
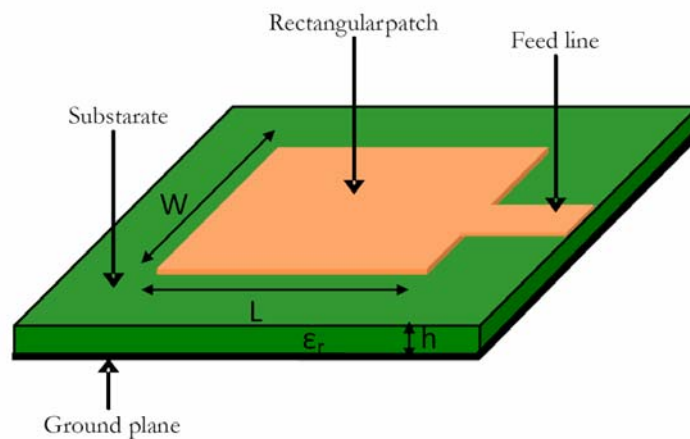
Fig. 1.1 Geometry of a conventional microstrip antenna excited using microstrip line

These antennas have got many important advantages like light weight, low volume, low profile planar configuration that can be made conformal , low

fabrication cost etc., compared to conventional microwave antennas. However they have some serious drawbacks like narrow bandwidth, low gain, radiation in one half plane, poor isolation between the feed and the radiating element etc.

1.4 Radiation from a microstrip antenna

The radiation from a microstrip antenna occurs from the fringing fields between the edges of the microstrip antenna conductor and the ground plane. For a rectangular microstrip antenna fabricated on a thin dielectric substrate and operating in the fundamental mode, there is no field variation along the width and thickness. The field varies along the length that is about a half wavelength long. The electric field configurations are shown in the figure 1.2
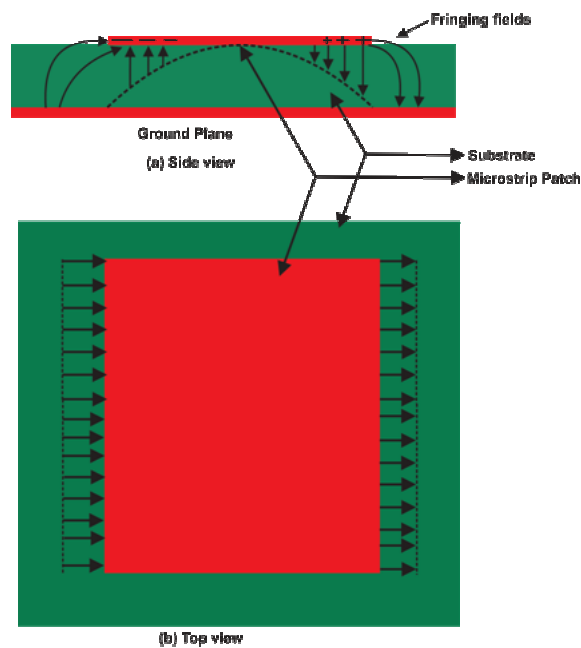
Fig. 1.2 Fringing field model for microstrip antenna

The radiation mechanism can be explained by resolving the fringing fields at the open circuited edges into normal and tangential components with

respect to the ground plane. The normal components are out of phase (as the patch is half wavelength long) and hence the far field produced by them cancels each other. Whereas the tangential components are in phase and the resulting fields are combined to give maximum radiation in the broadside direction.

1.5 Excitation Techniques

The selection of an appropriate feeding mechanism to couple power to a microstrip antenna is as important as the selection of the suitable geometry for a particular application. A variety of feeding mechanisms are available and some important techniques are discussed here.

1.5.1 Microstrip Feed

This is the simplest way to feed electromagnetic power to a microstrip antenna. Here, the antenna and the feed are fabricated simultaneously on the same side of the substrate as shown in figure 1.3. This type of feeding mechanism is very attractive in array environments.
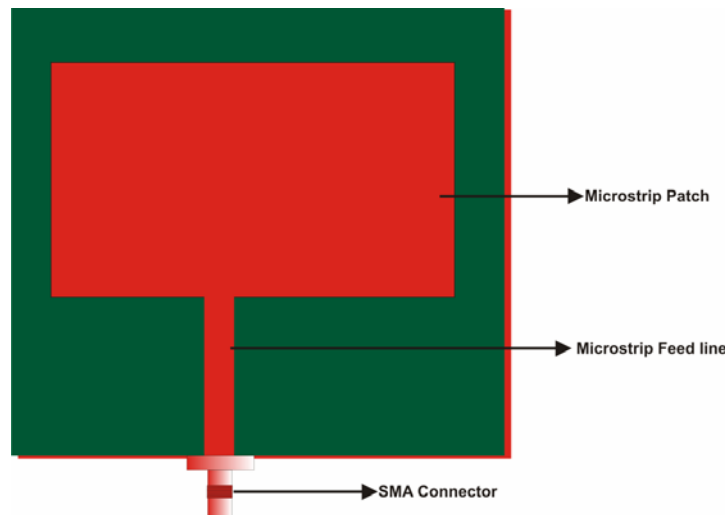
Fig. 1.3 Edge fed Microstrip Antenna

The most undesirable feature of this feeding mechanism is the spurious radiations from the bends, transitions, junctions, etc. These radiations adversely affect the side-lobe level and cross-polarization characteristics of the antenna. This drawback may be compensated by suitably selecting a high dielectric constant substrate. But it will reduce the radiation efficiency of the antenna. A compromise between the two is made depending upon the applications.

1.5.2 Coaxial feed

It is a conventional method for feeding a single patch antenna. Here, the coaxial connector is attached to the backside of the printed circuit board and the center conductor is attached to the antenna at the desired point. The coaxial feeding arrangement is shown in figure 1.4.
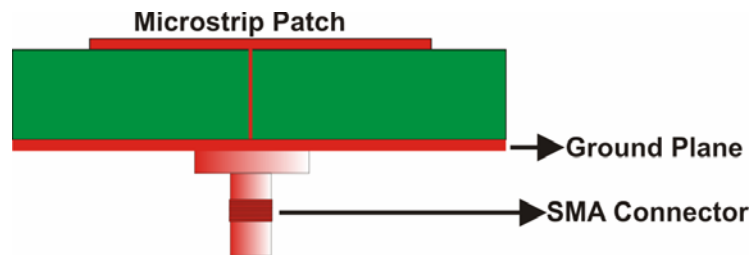
Fig. 1.4 Coaxial Feeding

Here, as the feed lies behind the radiating surface, there is no question of unwanted radiation from the feed for thin substrates. In fact, for thick substrates, the coupling between the adjacent feeds may deteriorate the performance. In array environment, the complete antenna and feeding arrangement cannot be etched simultaneously. This increases the feeding complexity, especially in large arrays. At high frequencies, it becomes very difficult to realize this type of feeding as it involves drilling holes through the substrate and proper soldering of the centre conductor to the patch.

1.5.3 Buried feed (Electromagnetic coupling)

In this type of feeding, the antenna and the feed are placed at different levels. i.e., the feed system is a covered microstrip line and the radiating element is etched on the covering substrate immediately above the open ended feed line. The radiating element is thus parasitically coupled to the feed line. The system can be considered as a microstrip patch on a double layer substrate sharing a common ground plane with the feed as shown in figure 1.5. Like the microstrip feed system, this arrangement also suffers from spurious radiation from the feed network. This may be minimized by using substrates of high dielectric constant for the feed line.

(a) Top view

(a) Side view
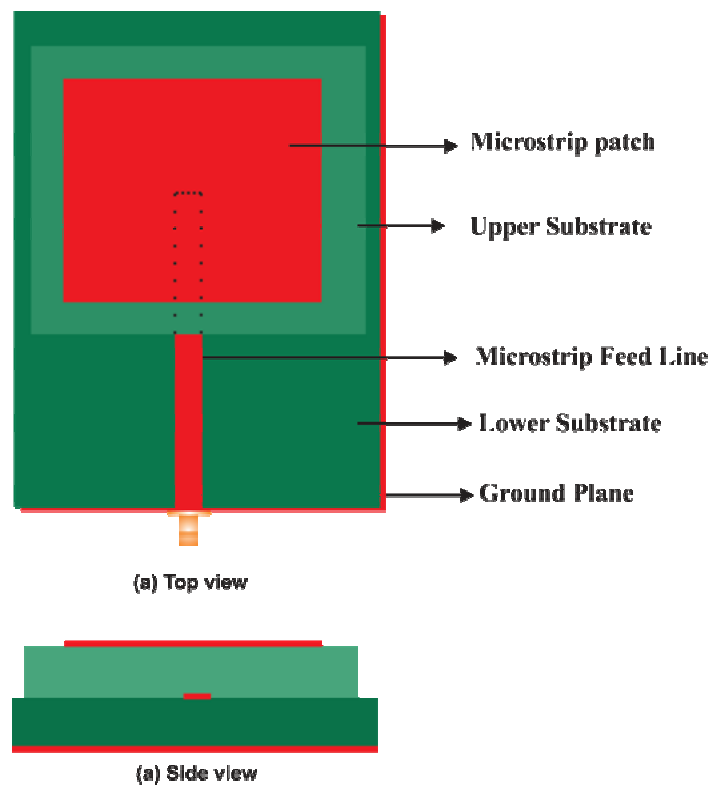
Fig. 1.5 Buried feed

1.5.4 Slot feed (Aperture coupling)

This feeding arrangement utilizes a common ground plane to separate the feed and the radiating geometry. The coupling between the two is provided by a slot etched on the ground plane. The aperture should be placed accurately below the patch and above the feed line as shown in figure 1.6. Here, spurious radiation from the feed is physically separated from that of the patch and can be completely avoided by enclosing the feed within the box. To avoid radiation towards the backside of the antenna, the slot must not resonate within the operating frequency band of the patch and should be placed far enough from the edge of the patch.
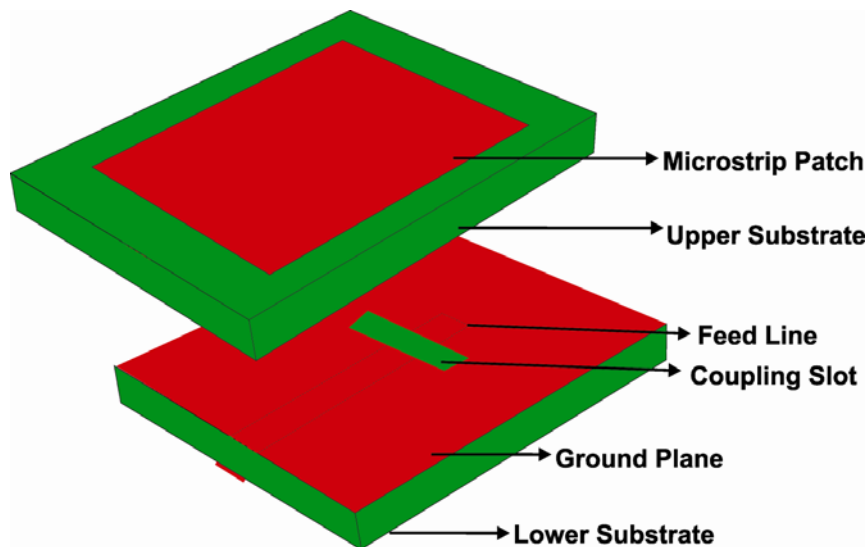
Fig. 1.6 Slot feed mechanism

1.6 Models/Techniques used in the analysis of microstrip antennas

Different methods are available in the literature for the analysis of microstrip antennas. For antennas having different geometrical shapes (rectangular), analytical techniques like cavity model and transmission line

model can be applied. For geometries which can be readily divided into few regular geometrical shapes, these analytical techniques could be applied along with segmentation technique. These techniques are suitable in the case of arbitrary shaped patches. Here numerical techniques like Finite Element Method (FEM), Finite Difference Time Domain method (FDTD), etc., could be used. Some important techniques used for the analysis of Microstrip antennas are described briefly in the following sections.

1.6.1 Transmission line model

This model was proposed by Munson [12] and Derneryd [13]. Here the microstrip resonator is represented by two radiating slots (corresponding to the two radiating edges) separated and connected by an approximately half wavelength ideal transmission line. The input impedance is determined as a function of the distance from the edge of the patch to the feed point. The different radiation characteristics are determined by assuming that the fields vary along the length of the patch and remain constant across the width. The main shortcoming of this model is that, it is applicable only to rectangular or square patch geometries.

1.6.2 Cavity model

Here, the microstrip geometry is considered as a cavity bounded at its top and bottom by electric walls and on its side by magnetic wall. The magnetic current flowing on the cavity side walls radiate at the resonant frequencies of the cavity, which is assumed to be surrounded by free space. This model is suitable for geometries in which the Helmholtz equation possesses an analytical solution such as disks, rectangles, triangles, ellipses etc.

1.6.3 Method of moments

In method of moments, the electric surface currents flowing over the patch metallization and the ground planes are evaluated by using the Richmond's reaction method [14]. The reaction integral equation is solved using the boundary conditions and method of moments. Now using suitable expansion functions for electric surface currents, the integral equations are reduced to algebraic equations. These equations are then solved for the unknown coefficients using any of the known numerical techniques. This technique is analytically simple and versatile, but it requires large amounts of computation. The limitation of this technique is usually the speed and storage capacity of the computer.

1.6.4 Finite element method (FEM)

The finite element method is a computer aided mathematical technique for obtaining approximate numerical solutions for the abstract equations of calculus that predicts the response of physical systems subjected to external influences. In the case of microstrip antennas, the fields interior to the antenna cavity can be determined by this method. Here the region of interest is subdivided into small areas or volumes depending upon the dimensions of the region. Usually these small regions are polygons such as triangles and rectangles for two dimensional problems and tetrahedral elements for three dimensional problems. The interior electric field, satisfying the inhomogeneous wave equation along with an impedance boundary condition on the perimeter walls, is solved for each of the elements subdividing the region of interest. This method is applicable to arbitrary shaped patches also.

1.6.5 Finite Difference Time Domain (FDTD) method

This is a method which can be applied to all kinds of antennas for all types of feeds [15-18]. This method consists of a discretisation and a solution of the

Maxwell's curl equations directly in the time domain. In FDTD, microstrip antennas are treated in the time domain for the analysis. The frequency dependence of the different parameters is determined from the Fourier transform of the transient current. However, this method becomes computationally costly and requires large amounts of memory when the structure becomes complex.

1.6.6 Green's function method

This method can be employed when the shape of the microstrip radiating structure is simple, such as rectangle, triangle or circle. The electric field inside the cavity is evaluated using Green's function and which in turn is used for the evaluation of the input impedance. This method is not suitable in the case of arbitrary geometrical shapes as the Green's functions are not available.

1.6.7 Segmentation Technique

When the geometrical shape of the microstrip antenna is neither simple nor completely arbitrary, but is a composite of simple geometrical shapes for which the Green's functions are available, the segmentation technique can be used. This method gives us the overall performance of the structure from knowledge of the contributions from the segments constituting it. Here the effect of radiation loss from the periphery is incorporated through impedance loading of the patch at the periphery. The main disadvantage of this method is that radiation losses should be known in advance. This is very difficult to estimate in the case of arbitrary shaped antennas. The suitability of different analytical techniques for antenna design is depended upon a variety of parameters and is well studied in [19]

1.7 Broadband microstrip antennas

One major drawback of microstrip antennas, which limits its widespread applications, is the narrow impedance bandwidth. There are   different

approaches for improving the impedance bandwidth of microstrip antennas. They include: using thicker substrates with low dielectric constant, addition of a parasitic patch on top of the original patch by using a separate dielectric substrate as support, using multiple patches in one plane and by means of proximity coupling of feed line to the patch antenna.

The use of thicker substrates for bandwidth enhancement is limited by the excitation of surface waves. In the case of using parasitic patches, each element resonates at adjacent frequencies and as a result the impedance bandwidth improves. The parasitic element will usually increase the overall surface area.

1.8   Outline of the present work

The fast development in the field of communication systems demands compact microstrip antennas suitable for use in MMIC's, satellite mobile communication systems, personal communication systems, etc. In this thesis, the experimental and simulated investigations towards the development of novel broadband and high gain microstrip antennas are presented. The experimental and simulation studies reveal that the proposed antennas exhibit simplicity in the structure yielding less fabrication complexities and broadband impedance matching and gain enhancement can be achieved using simple and novel techniques.

1.9   Chapter Organization

In chapter 2, a brief review of the important theoretical and experimental works done in the area of microstrip antennas is presented with an emphasis on broadband microstrip antennas.

In chapter 3, the methodology adopted for the investigations is presented. The details of the procedure used for the fabrication of microstrip antennas are presented. The techniques used for the measurement of different antenna characteristics like resonant frequency, reflection coefficient, radiation patterns etc. are described. Finally, the chapter highlights the numerical techniques used for the analysis of the antenna with due emphasis on Finite Difference Time Domain method. The fundamental and mathematical concept behind the FDTD method is elaborated.

The important observations and results of the experimental and simulation analysis carried out for enhancing the bandwidth of tilted square slotted and polygonal slotted microstrip antennas are presented in chapter 4. Feed modification of the polygonal slotted broadband microstrip antenna is done by incorporating a printed L-feed mechanism to enhance the impedance bandwidth further. Finally the time domain analysis of the structure is carried out to find out the pulse dispersion characteristics and is presented at the end of chapter 4.

Chapter 5 starts with a simple gain enhancement technique for single band microstrip antennas. Finally, the same technique is applied to the tilted square slot loaded and polygonal slot loaded broadband microstrip antennas to enhance the gain of the microstrip antenna over the entire frequency range.

The conclusions drawn from the experimental and simulation analysis are presented in chapter 6. Some possible applications of the newly developed antennas along with the scope for future work are also presented in this chapter.

The experimental woks done by the author in related fields are incorporated as appendix of this thesis.

1.10 References

[1]   K.Fujimoto and J.R.James, Mobile Antenna Systems Handbook, Artech House, 1994.

[2]   M.E Bialkowski, Wireless: From Marconi – The Way Ahead, IWTS 1997, Shah Alum, Malaysia 1997.

[3]   J.D Kraus, Antennas: Our Electronic Eyes & Ears, Microwave Journal, Jan. 1989, p.p 77-92.

[4]   Ramsay, Microwave Antennas and Waveguide Techniques before 1900, Proceedings of IRE vol. 42, issue 6, 1958, p.p 405-415.

[5]   T.S. Rappaport, Wireless Communications, Principles and Practice, Prentice Hall, 1996.

[6]   S. Uda, Wireless Beam of short electric waves, J. IEE (Japan), pp. 273-282, March 1926 and pp. 1209-1219, Nov. 1927.

[7]   W.V. T. Rusch, The current State of the Reflector Antenna Art-Entering the 1990's, Proc. IEEE, vol. 80, No.1, pp. 113-126, Jan. 1992.

[8]   V. H. Rumsey, Frequency Independent Antennas, 1957 IRE National Convention Record, Part 1, pp. 114-118.

[9]   J.D. Kraus, Ronald J. Marhefka, Antennas for all applications, TATA McGraw-Hill Edition, 3rd Edition, pp. 785-788

[10]   G.A. Deschamps, Microstrip Microwave Antennas, presented at the Third USAF symposium on Antennas, 1953

[11]   Howell, J.Q, Microstrip Antennas, presented in International symposium on Antennas and Propagation Soc. 1972,Williamburg

[12] R.E Munson, Conformal Microstrip Antennas and Phased Arrays, IEEE Trans. Antennas.& Propagation,Ap-22, pp. 74-77, 1974.

[13] A.G Derneryd, Linear Microstrip Antenna, Chalmer Univ. Technology, Report, Goteborge, Sweden, 1975.

[14] J.R Mosig and F.E Fred Gardiol, A Dynamic Radiation Model for Microstrip Structures, Advances in Electronics and Electron Physics, Vol. 59, 1982,pp. 139-234.

[15] K.S Yee, Numerical Solution of Initial Boundary Value Problems Involving Maxwell's Equations in Isotropic Media, IEEE Transactions on Antennas and Propagation, Vol-14, 1966, pp. 302-307.

[16] Titis Kokkinos, Costas D. Sarris, George Eleftheriades, Periodic FDTD Analysis of Leaky-Wave Structures and Applications to the Analysis of Negative-Refractive Index Leaky Wave Antennas, IEEE Transactions on Microwave Theory and Techniques, 2005, pp. 1-12.

[17] E. Nishiyama and M. Aikawa, FDTD Analysis of Stacked Microstrip Antenna with High Gain, Progress in Electromagnetics Research, Vol-33, 2001, pp. 29-43.

[18] S. Gao, FDTD Analysis of a Dual-Frequency Microstrip Patch Antenna, Progress in Electromagnetics Research, Vol-54, 2005, pp. 155-178.

[19] Demuynck. F, Petersen M, Choosing the Right EMSimulation Technology for Antenna Design and Analysis, European Conference on Antennas and Propagation, 26-30 March 2012, pp. 1296-1300.

.....౨౦౬.....

REVIEW OF LITERATURE

This chapter deals with the review of literature dealing with the development of broadband microstrip antennas. The chapter starts with the initial developments of microstrip antenna designs proposed by the research groups across the world. The different technologies so far proposed for the development of broadband microstrip antennas is discussed. The recent progress in the direction of broadband microstrip antenna research is then presented.

2.1 A Brief Review of Past Work

During the past few decades the researchers all over the world have studied the theoretical and experimental aspects of different types of microstrip antennas. Recently, development and analysis of broadband microstrip antennas have become an interesting area in personal communication systems due to the need of high speed data transmission. The relevant works in the field of microstrip antennas are reviewed with emphasis given to broadband microstrip antennas.

2.1.1 Microstrip Antennas – A Brief Review

Microstrip antenna was conceived by Deschamps [1] in 1953, in USA. In 1955, Gutton and Baissinot [2] in France patented a flat aerial that can be used in the UHF region. Lewin [3] studied the radiation from the discontinuities in striplines.

The first practical microstrip radiator was conceived by Byron [4] in the early 1970's. This antenna was a conducting strip, several wavelengths long and half wavelength wide separated from a ground plane by a dielectric strip. The strip was fed at regular intervals using coaxial connectors along the radiating edges and was used as an array. Munson [5] patented the microstrip element shortly thereafter.

The basic rectangular and circular patch antennas were designed by Howell [6]. His low profile antenna consisted of planar resonating element separated from the ground plane by a dielectric substrate whose thickness was very small compared to the wavelength. Feeding to the antenna was effected either by coaxial line from behind or by a microstrip line deposited on the same side. Design procedures were presented for linearly and circularly polarized

antenna and for dual frequency antennas from UHF through C band. The bandwidth obtained was very narrow and was found to be depending on the permittivity and thickness of the substrate.

During this time, different microstrip geometries were constructed for aircrafts and rockets. Of these, the cylindrical S band arrays constructed by Weinschel [7], the conformal array constructed by Sanford [8] for L band communication from KC-135 aircraft to ATS-6 satellite are of prime importance. Additional array designs were reported by James and Wilson [9] and Garvin *et al*. [10] when they constructed flush mounted low profile antennas for missiles.

Since the substrate properties are very important in microstrip antenna design, many workers were engaged in the investigation of substrate parameters. An elaborate study on different dielectric materials available in the market was done by Nowicki [11]. Polytetrafluroethylene substrates reinforced with glass random fiber or glass woven web were reported by Traut [12]. These filler materials take preferred orientations in the polymer matrix during the manufacturing process and give necessary mechanical and electrical properties desirable for antenna construction.

Substrates materials for specialized applications such as in aircraft where weight reduction is very important are reported by Murphy [13]. Two thin layers of PTFE bonded on both side s of a hex cell honeycomb structure have been discussed by Carver [14]. The dielectric constant ranges from 1.17 to 1.4 depending upon the thickness of the dielectric layers.

Microstrip antenna on Ferrite substrate is reported by Das and Choudhary [15]. The resonant frequency, bandwidth, efficiency and resonating length of a

rectangular microstrip patch on ferromagnetic substrates were derived. It was found that the size of the radiator can be reduced by constructing them on ferrite substrates since the ferrite has both dielectric and magnetic properties.

Theoretical analysis of microstrip radiator was first carried out by applying transmission line analogies. Derneryd [16, 17] utilized the transmission line theory to model the rectangular patch fed at the center of a radiating wall. The radiating edges were considered as narrow slots radiating into half space and separated by a half wavelength. This model gives the interpretation of the radiation mechanism and provides expressions for the radiated fields, radiation resistance, input impedance etc. This method is applicable only for patches of rectangular shape and was not adaptable for the inclusion of feed point and thus not adequate in many cases.

A more accurate method was developed by Lo et al. [18-20] in their cavity model. Here, the region between the ground plane and the microstrip patch is viewed as a thin TM cavity bounded by magnetic wall along the edge and electric walls from above and below. Thus the fields in the antenna may be assumed to be those of a cavity. The antenna parameters of different patch geometries with arbitrary feed points can be calculated using this approach. The different modes excited were also included in the calculation, by expanding the fields in modal functions, assuming that the perimeter of the microstrip antenna is enclosed in a perfect magnetic conductor without disturbing the fields. The radiation and other losses were represented in terms of substrate loss tangent.

Carver and Coffey [21-23] formulated the modal expansion model which is similar to cavity model. The fields between the patch and the ground plane are expanded in terms of a series of cavity resonant modes. Thus the patch is considered as a thin cavity with leaky magnetic walls. The impedance boundary

conditions are imposed on the four walls and the stored and radiated energy were investigated in terms of complex wall admittances. The calculations of wall admittance have been given by Hammerstad [24] and more accurately by Alexpoulos et al. [25].

James and Wilson [26] used the vector Kirchoff relationship for the known aperture fields to calculate the radiated fields of an open circuited microstrip line. Hammer et al. [27] extended the aperture concept to include the radiation from all sides of the patch, resonating in any mode. They have used the equivalence principle for evaluating the far fields. The excitation amplitude of individual modes for a particular feed point can be calculated using this method.

Agarwal and Bailey [28] suggested the wire grid model for evaluating the microstrip antenna characteristics. They modeled the radiating structure as a fine grid of wire segments and the currents on the current segments were calculated using Richmond's reaction theorem.

Alexopoulose [29] et al. discussed a dyadic Green's function technique for calculating the fields radiated by a Hertzian dipole printed on a ground substrate.

Mosig and Gardiol [30] developed a vector potential approach and applied the numerical techniques to evaluate the fields produced by microstrip antennas of any shape.

The modal expansion method is applicable to circular geometries also where the trigonometric expressions are replaced by Bessel functions. Mink [31] discussed the accuracy by which the wall admittance has to be known

especially in the case of a circular patch. He has shown that the wall admittance has to be evaluated to within 4% to predict the operating frequency to 0.5%.

The circular microstrip patch has been rigorously treated by Butler [32]. He solved the problem of centre fed circular microstrip antenna by considering the patch as a radiating annular slot, in which the radius of the outer ring is very large. Butler and Yung [33] analyzed the rectangular microstrip antenna using this technique.

For the microstrip antennas of arbitrary shapes the model expansion is much cumbersome and time consuming. Numerical methods have been developed for the analysis of these shapes.

For the numerical analysis of the patch antennas, Newman and Pozar [34, 35] developed the method of moments. They calculated the unknown surface currents flowing on the walls forming the microstrip patch, ground plane and magnetic walls using the Richmond's reaction method [36]. The reaction integral is solved using the method of moments.

Carver and Coffey [37] discussed a finite element approach for the numerical analysis of the fields interior to the microstrip antenna cavity. The analysis is done by a minimization process to seek the solution closest to the true solution. The equivalent aperture admittance is used as the boundary condition so as to mathematically decouple the interior and exterior regions.

Kerr [38] developed various configurations for dual frequency operation of the patch. One among them is the Shepherd crook feed for 1.22 m dish antenna. He mounted an L band patch antenna at the flange of an X-band wave guide which illuminates the dish antenna through a hole in the center of the L-band patch. The system worked at 1250 MHz and 9500 MHz. He also

employed a single rectangular patch with two feed points to obtain dual frequency operation. The impedance loading on one port is used to effect a measure of frequency control.

Schaubert and Farrar [39] discussed a piggyback antenna where one patch acts as the ground plane for the other. A quarter wave shorted parallel plate radiator resonant at 1140 MHz was mounted over a halfwave microstrip patch resonant at 990 MHz. Good isolation between the elements was achieved.

Carver [40] analyzed the circular microstrip patch and gave an accurate formula for the resonant frequency of the patch. He showed that for the radiating patch, the resonant frequency is complex since the wall admittance is complex. A thorough investigation on the dependence of resonant frequency on the various substrate parameters for the circular patch has been given by him.

Long and Walton [41] investigated the dual frequency behavior of stacked circular disc printed circuit antenna. Here, two discs of slightly different size are stacked together to obtain the dual frequency operation.

Long et al. [42, 43] measured the driving point impedance of a printed circuit antenna consisting of a circular disk separated by a dielectric from the ground. A theoretical RLC model is proposed for calculating the variation of input impedance with frequency and disc parameters. Resonant frequency of the circular disc antenna was also determined.

Shen [44] analyzed the elliptical patch microstrip patch and showed that the radiation from this antenna is circularly polarized in a narrow band when the eccentricity of the ellipse is small. Only a single feed is necessary to achieve circular polarization.

Microstrip disc antenna has been analyzed by Derneryd [45], by calculating the radiation conductance, antenna efficiency and quality factor associated with the circular disc antenna.

Kernweis [46] developed a dual frequency antenna by etching two 'ears' with a circular patch. With a 60^0 angular separation of the ears, good pattern and impedance characteristics were obtained at 1.99 GHZ and 3.04 GHz.

Mink [47] discussed a circular ring microstrip antenna which can give a substantially low resonant frequency than that of a circular patch antenna of the same size.

Newman and Tulyathan [48] analyzed the microstrip patch antennas of different shapes using moment method. The patch is modeled by surface currents and the dielectric by volume polarization current. The theory is capable of accurately predicting antenna parameters but requires precise computation.

Chang [49] proposed a graphical method for determining the size of a resonant patch for a specified frequency. It was found that by varying the aspect ratio it is possible to modify the Q factor of a resonant patch. Design curves were given in the form of Argand diagram for microstrip patches with fixed aspect ratios. Radiation was shown to be due to both the surface waves and space wave and for electrically thin substrates the surface wave radiation is not very significant.

Itoh and Menzel [50] suggested a method for analyzing the characteristics of open microstrip disk antenna. This method provided a number of unique and convenient features both in analytical and numerical phase. The theory was verified for experiments conducted on antenna constructed at 8.29 GHz.

2.1.2 Development of Wideband Microstrip Antennas

Schaubert and Farrar [51] reported that the use of parasitic elements can improve the bandwidth of microstrip antennas. Their antenna was a 12.7 cm x 12.7 cm rectangular patch on a 3.2mm Teflon fiber glass substrate. By placing two parasitic strips of 13 cm x 13.1 cm parallel to the non radiating edges they could match the antenna to 50 Ω feedline and achieve a 2:1 VSWR bandwidth of around 2.5 %.

Wood [52] suggested a method of doubling the bandwidth of rectangular microstrip antennas. He used two capacitively excited $\lambda/4$ short circuit parasitic elements placed parallel to the radiating edges. Here the driven patch and the parasitic patch together give two resonances. One of the resonances which has an antiphase voltage excitation has twice the bandwidth than that of the driven patch. The same technique has been used for bandwidth improvement of circularly polarized antennas also.

The use of an annual ring antenna instead of circular patch to achieve larger bandwidth was reported by Chew [53]. It was found that TM_{12} mode is suited for antenna performance where the stored energy is small yielding a small Q factor. For TM_{12} mode, the bandwidth increases with decrease in the outer to inner radius ratio of the annual ring.

Poddar et al. [54] obtained considerable improvement in bandwidth by constructing the patch antenna on stepped and wedge shaped dielectric substrates. They reported a 2:1 VSWR bandwidth of 28% on a wedge shaped substrate and 25% on a stepped substrate where the bandwidth of equivalent rectangular resonator is 13%.

It was Derneryd and Karlsson [55] who constructed a broadband microstrip antenna by using a thicker substrate of low dielectric constant. Here

the patch was fabricated on a thin glass fiber reinforced substrate and supported by low density foam above a ground plate. A bandwidth of 15% was obtained at 3 GHz with a 10mm spacing between the patch and the ground plane.

Log–periodic technique was employed by Hall [56- 58] to obtain broadband characteristics. With a series fed linear array of nine patch resonators in log-periodic arrangement, 30% bandwidth was obtained at X-band. The same arrangement fabricated on tapered substrate has still broader bandwidth. The radiation patterns show some frequency dependent characteristics.

Construction of conical microstrip antenna was reported by Das and Chatterjee [59]. Here, the conical patch antenna is modified by slightly depressing the patch configuration conically into the substrate. This conical antenna has a much larger bandwidth than that of an identical circular patch antenna. To maintain the substrate thickness small, the angle of depression of the cone was found to be greater than 80^0.

Jeddari et al. [60] computed the resonant frequency and bandwidth of conically depressed microstrip antennas. They have demonstrated impedance matching by feed probe position. The 2:1 VSWR bandwidth obtained was 12% at 3 GHz.

Pues et al. [61] also employed a log-periodic technique to achieve wide bandwidth. The various elements were fed by an open circuited feed line with branch lines. The input impedance and radiation patterns were theoretically predicted. A five element array yielded 2.2% bandwidth at S-band.

Lee [62] reported the design of a wide band quasi log-periodic microstrip antenna. The radiating elements which are circular patches are series-fed by

coplanar feeding network. A 2.3:1 bandwidth of 710 MHz was obtained at 3 GHz.

Pandharipande and Verma [63] presented a novel feeding scheme for the excitation of the patch array which gives broader bandwidth. The feed network consists of a stripline power divider using hybrid rings and the coupling from stripline to feed point is achieved by thin metal probe. A patch consisting of 8 elements gave 10%bandwidth at X-band.

Bhatnagar et al. [64] obtained larger bandwidth in triangular microstrip antennas using two parasitic resonators directly coupled to the non radiating edges and the third one gap coupled to the radiating edge. The system was called hybrid edge, gap and directly coupled triangular microstrip antenna (HEGDCOTMA). They obtained a bandwidth 11.28% at 3.19 GHz on 1.6mm substrate of relative permittivity 2.55, which is 5.4 times the bandwidth of a single triangular patch antenna. The half power beam width was also found to be reduced, but not remained constant over the entire band.

Bhatnagar et al. [65] proposed a stacked configuration of triangular microstrip antenna to obtain larger bandwidth. The parasitic patch was placed above the driven patch and the space between the two filled with foam. A bandwidth of 18% has been obtained at S-band.

Wood [66] suggested the use of circular and spiral microstrip lines as a compact and wideband circularly polarized microstrip antenna. The curved microstrip lines supporting travelling wave have a usable bandwidth of 40% at 10 GHz. He has also given an analysis technique for these types of antennas.

Hall et al. [67] reported the concept of multilayer substrate antennas to achieve broader bandwidth. These types of antennas constructed on Alumina

substrates give a bandwidth which is 16 times that of a standard patch antenna at the expense of increase in overall antenna height.

Sabban [68] constructed a stacked two layer microstrip antenna. It has a bandwidth of 15% for VSWR 2:1. The radiating element is excited via electromagnetic coupling by a feeding element located closer to the ground plane. This antenna has been used as an element for 64 element Ku band array.

Wolfon [69] improved the bandwidth of an electromagnetically coupled dipole by placing an additional resonant circuit between the feedline and the dipole. The additional resonator can increase the 1.5:1 VSWR bandwidth from 1.5%to 5.5%.

Dubost and Gueho [70] reported a wideband microstrip antenna with a deflected beam. Short circuited quarter wave dipoles are used as the radiators and are scattered along a transmission line fed at one end matched at the other end.

Fong et al. [71] described the construction of a wideband microstrip antenna on electrically thin multi layer substrates. A novel feeding technique suitable for thick substrate is also given.

Hori and Nakagima [72] designed a broadband circularly polarized microstrip antenna for public radio communication systems. By using a parasitic element the 1.5:1 VSWR bandwidth obtained is 13%. A 16 element array using coplanar feed network was constructed for demonstration.

Prior and Hall [73] showed that the addition of a short circuited ring to a microstrip disc antenna will double the bandwidth of the disc, with some reduction in the gain. This can be used as a compact antenna for reflector feed.

Dubost and Rabba [74] established that flat dipole printed on a substrate has its largest bandwidth when the dielectric constant is small and when it acts at both the third and fourth resonances.

Mosig and Gardiol [75] studied the effect of parasitic elements on microstrip antennas, using the integral equation techniques. The rectangular patch considered was 60 mm x 60 mm size on a 0.8mm substrate of dielectric constant 4.3. With a parasitic of dimension 62 mm x 8 mm kept parallel to the non radiating edge, the 2:1 VSWR bandwidth was found to be doubled.

Bandwidth improvement using parasitic elements has been extensively studied by Kumar and Gupta [76-78]. They showed that when the driven patch and the parasitic element are resonating at adjacent frequencies, a significant improvement in the bandwidth can be obtained. For this, they have proposed configurations like Radiating Edges Gap Coupled MIcrostrip Antennas (REGCOMA), Non-Radiating Edges Gap Coupled MIcrostrip Antennas (NEGCOMA), Four Edges Gap Coupled Microstrip Antennas(FEGCOMA) and Directly Coupled Multiple Resonator Microstrip Antennas(REDCOMA, NEDCOMA, FEDCOMA). Rigorous analysis method for these configurations has been proposed using segmentation and desegmentation techniques.

For the REGCOMA configuration, the bandwidth obtained was 6.9% at S band on a 3.18 mm PTFE substrate, which is 3.5 times than that of a rectangular patch antenna. Here the E-plane radiation pattern is found to be not uniform in the frequency band of interest. The direction of maximum radiation varies about 20^0 from the on axis with frequency change. The H-plane pattern however, was virtually unaffected.

For the NEGCOMA configuration, the measured bandwidth was 4 times the bandwidth of the corresponding rectangular patch. Here, the direction of H-Plane radiation varies with frequency and E-plane radiation remains unaltered.

For the FEGCOMA configuration, the bandwidth obtained was 6.7 times the bandwidth of rectangular patch antenna at S-band. Here both the E-plane and H-plane radiation patterns alter with frequency.

When the parasites are directly coupled to the radiating edges of the driven patch (REDCOMA), the bandwidth of the system is 5 times that of the isolated patch, for NEDCOMA it is 5.5 times and for FEDCOMA, it is 7.4 times. Here also, the radiation pattern varies with frequency.

Aanandan et al. [79, 80] has proposed a compact strip broadband microstrip antenna gap coupled with parasitic elements giving a bandwidth eight times higher than that of the standard single patch antenna of the same frequency. The proposed structure gives a less distorted radiation patterns with frequency. The even/odd mode analysis has been done and the theoretical results are compared with the experimental ones.

R. Garg and V.S Reddy [81] studied a coupled strip microstrip antenna exhibiting 23% bandwidth and an increased polarization purity. The even mode is responsible for the radiated power and the odd mode increases the bandwidth by shaping the impedance curve. It is concluded that increase in the number of strips increases the polarization purity.

Sang-Hyuk Wi et al. [82] developed a broadband microstrip antennas with U shaped parasitic elements incorporated along the radiating edges of the main patch. The prototype fabricated on FR4 substrate has a 2:1 VSWR

bandwidth of 27.3% and the radiation patterns are almost identical to a standard microstrip antenna.

The experimental study on a stacked two layer triangular patch antenna was proposed by P.S Bhatnagar et al. [83]. The antenna uses probe feeding and it achieves a bandwidth of 17.5% with good cross polarization characteristics.

Tsien Mink Au et al. [84] has conducted a theoretical analysis using the integral equations based Galerkin approach to study the effect of parasitic element on the characteristics of a microstrip antenna. Broadband nature of the antenna is analyzed using different parasitic patch sizes and its position and the optimum design yields 21.3% bandwidth.

H.R Hassani et al. [85] has analyzed a two layer stacked rectangular patch antenna using spectral domain techniques and the effect of variations in the alignment of patches and the sizes of the patches on the input impedance and radiation patterns were investigated. The displacement of the top patch in the direction of the resonance broadens the beam width in the E plane for the upper resonance at the expense of some distortions in the radiation patterns.

Frederic Croq and D.M Pozar [86] proposed an aperture stacked broadband microstrip antenna for millimeter wave applications having a bandwidth of the order of 20%. The antenna is analyzed using the integral equations solved using spectral domain by the method of moments.

Frederic Croq and Albert Papiernik [87] developed a slot coupled stacked broadband microstrip antenna with a dielectric protection cover on the top. The antenna exhibits a 1.6:1 VSWR bandwidth of 25% with good cross polar isolation in both the planes as compared to a standard rectangular microstrip

antenna. Parasitic radiation from the feeding aperture is minimal since the resonance of the slot aperture lies at a very far end from the patch resonances.

S.D Targonski and R.B Waterhouse et al. [88] has put forward a promising design of an aperture coupled stacked patch antenna fabricated on thick substrates. The antenna has a 2:1 VSWR bandwidth of 50% and the surface wave efficiency was found to be 80%.

U.K Revankar and A. Kumar [89] studied the mutual coupling between the stacked three layer circular microstrip antenna elements. The antenna achieves a bandwidth greater than 20% , relatively high gain and they concluded that for stacked antennas coupling via the radiating edge, there is a stronger coupling while coupling via the non radiating edge is weaker as compared to that of the single patch radiator.

R.B Waterhouse proposed a probe fed [90] and aperture fed stacked patch [91] arrays using a high dielectric constant substrate lower substrate (greater than 10) and a relative low dielectric laminate substrate as the top layer. It is observed that broad impedance bandwidth of the order of 25% over useful scanning ranges of $\pm 45^0$ in the principal planes can be attained.

Steven Mestdagh and vandenbosch et al. [92] designed an aperture coupled stacked patch antenna fed by coplanar wave guide without the use of separate feed substrate useful for millimeter wave applications. The antenna has a 2:1 VSWR bandwidth of 36.8% and a detailed systematic parametric analysis has been performed for the design guidelines.

Mohammod Ali et al. [93] designed a reconfigurable stacked microstrip patch antenna suitable for satellite and terrestrial links. Frequency reconfigurability is achieved by implementing p-i-n diodes.

Wayne S. Rowe and R.B waterhouse [94] proposed a microstrip line fed stacked two layer microstrip antenna with an upper dielectric cover. The relation between the dielectric layers, the sizes of the patches and the position of the feed line were studied in order to maintain broadband impedance matching behavior. The bandwidth of the antenna is found to be only 20%.

Shi-Chang Gao et al. [95] has developed a wideband two layer microstrip antenna coupled using an H-shaped aperture exhibiting a 2:1 VSWR bandwidth of 21.7%. The aperture feed is maintained to be non resonant and air spacers are used as the separation between the two patches so that the spacing parameter can be easily tuned for optimizing the antenna parameters.

K.M Luk and K.F Lee et al. [96] has designed a proximity coupled stacked circular microstrip antenna having two pairs of etched rectangular slots on the lower patch. The etched slots play a crucial role in obtaining a wide band behavior. The antenna exhibits a 2:1 VSWR bandwidth of 26% with good radiation performances having a cross polar isolation greater than -20 dB.

Ban-Leong Ooi et al. [97] proposed a novel design of a stacked patch antenna in which a square patch is loaded over the top of a probe fed E shaped patch. The antenna achieves a 2:1 VSWR bandwidth of 38.41%.

M.A Martin el al. [98] has stacked an E shaped patch antenna over a probe fed U slot microstrip antenna and the structure exhibits a relatively larger bandwidth as compared to the existing designs. The bandwidth of then antenna is found to be 59.7% and the radiation patterns are relatively stable over the entire bandwidth.

Rafi and Shafai [99] have extensively studied the effect of stacking over a V slotted patch antenna. It is concluded that the V slot patch stacked with a

rectangular patch can improve the bandwidth up to 47% and that stacked with another V slot patch can enhance the bandwidth up to 54%.

M.A Martin et al. [100] analyzed the behavior of a U slot patch antenna stacked with a rectangular patch. A simple circuit model is developed to study the reason for the resonances of the antenna. The antenna attains 56.8% impedance bandwidth with stable radiation patterns throughout the entire band of operation.

Nasimuddin and Z.N Chen [101] proposed a broadband microstrip antenna with low-high-low dielectric constant substrate combination using a microstrip line via feed to achieve a bandwidth of the order of 46.9%. The low dielectric constant substrates contain the feed line and the four parasitic patches while the high dielectric constant substrate contains the driven patch.

Volume reduction for the above structure is brought about by replacing the microstrip feed line with coplanar wave guide loop feed [102]. The antenna has 34% bandwidth with stable radiation patterns throughout the band of operation.

The promising design of an aperture stacked microstrip patch antenna was reported by S.D Targonski and Waterhouse et al. [103]. Here the resonant aperture along with the two stacked patches achieves a bandwidth of up to 70%. Impedance matching techniques like wide centered feed and dual offset feed lines are implemented to achieve broadband operation.

Broadband operation can be effectively achieved by properly inserting slots on the patch antenna geometry. Jui-Han Lu [104] proposed a single layer broadband circular microstrip antenna having a bandwidth 2.3 times higher than that of the standard antenna by properly inserting a pair of narrow arc shaped slots near the side edges of the patch.

Jui-Han Lu and Kin-Lu Wong et al. [105] has designed a dual frequency and broadband designs of an equilateral triangular microstrip patch antenna. Broadband operation is achieved by protruding a narrow slot close to the side edges of the triangular patch antenna. The antenna exhibits a bandwidth 2.6 times higher than that of a conventional triangular microstrip antenna.

Jui-Han Lu and Kin-Lu Wong et al. [106] achieved broadband circular operation on a triangular patch antenna by loading a narrow slot or a cross slot with unequal arm lengths.

Kin-Lu Wong et al. [107] proposed a slot loaded rectangular patch antenna with a bandwidth 2.4 times higher than that of the standard rectangular patch. Broadband operation is achieved by the combined effect of a pair of right angle slots and modified U slots on the rectangular microstrip antenna.

Amit A.Deshmukh and K.P Ray [108] developed a broadband microstrip antenna by integrating a half U slot and a rectangular slot inside a rectangular microstrip antenna giving twice the bandwidth as compared to that of the single half U-slot RMSA or RMSA with a rectangular slot.

T. Huynh and K.F Lee [109] proposed the first U-slot patch antenna for wide band operation. The antenna is coaxially fed and it can achieve a bandwidth up to 40% without using any parasitic elements.

M. Clenet and L. Shafai [110] discussed multiple resonances and the polarization characteristics of a U-slot patch antenna.

Steven Weigand and Greg H. Huff et al. [111] has proposed the analysis and design steps of the single layer U-slot loaded patch antenna. The design

rules are derived by the analysis of former experiments, method of moment simulations and experimental validations.

K.F lee and K.M Luk et al. [112] put forwarded the simulation and experimental studies of the U-slot patch antenna. They have concluded that for a foam substrate of thickness 0.08λ the antenna can offer 20-30% impedance bandwidth and the U-slot offers capacitive reactance which effectively suppresses the inductive reactance of the feeding probe. Modifications in the patch with and the patch width can excite dual frequency operation on the patch.

Ricky Chair and Ahmed A. Kishk et al. [113] reduced the size of the U-slot patch antenna by halving the patch along the line of symmetry without affecting the cross polarization characteristics. An area reduction of almost 50% with a bandwidth of 28.6% is achieved without affecting the radiation efficiency.

Fan Yang and Rahmat-Samii et al. [114] explored the wideband mechanism taking place inside an E-shaped patch antenna in which broad bandwidth of 30.3% is obtained by merging two resonances. The analysis of the antenna is done using Method of Moments with the vector triangular basis functions. The equivalent circuit modeling is done in order to explore the principle behind broadband operation.

Yuehe Ge and Karu P. Esselle et al. [115] proposed a size reduction technique by incorporating corrugations on the wings of the E shaped patch antenna. The antenna has 25% size reduction as compared to the E shaped patch antenna and has similar bandwidth and radiation characteristics as that of the E shaped patch antenna.

Yuehe Ge and Karu P. Esselle et al. [116] has studied the E shaped patches with probe feed and microstrip feed and designed prototypes of arrays for attaining polarization and space diversity inorder to implement it with PCMCIA cards.

Lin Peng and Yun Zhang et al. [117] developed a compact E shaped patch antenna for broadband operation. Reduction in the size is obtained by introducing a shorting wall and inserting slot at the radiating edge of the patch.

A.K Shackelford and K.M Luk et al. [118] has proposed a method to reduce the size of the probe fed U-slot rectangular patch antenna by incorporating shorting posts within the structure.

C.L Mak and K.F Lee et al. [119] put forward the implementation of shorted walls on one side of a halved U-slot patch antenna to achieve compactness without affecting the bandwidth and radiation characteristics of antenna as compared to that of the full structure.

K.F Lee and K.M Luk et al. [120] developed the theoretical and experimental analysis on broadband microstrip patch antennas with shorting walls. The analysis has been done on both fully shorted patch and partially shorted patch. They concluded that the use of partially shorting wall had the effect of reducing the resonant frequency of the antenna while the bandwidth of the antenna remains same as that of the fully shorted patch antenna.

Jeen-Sheen Row and Yen-Yu Liou [121] successfully implemented the usage of short circuiting walls on a slotted triangular microstrip patch antenna. The antenna exhibits a bandwidth greater than 25% with conical radiation patterns.

Debatosh Guha and Y.M.M Antar [122] developed a circular microstrip pach antenna loaded with balanced shorting pins. The bandwidth of the antenna is found to be doubled without sacrificing the radiation characteristics.

I-Fong Chen and Chia-Mei Peng [123] presented an edge shorted patch antenna for UHF band applications. The antenna comprises of an edge shorted patch, a director element and a metal reflector to achieve directional, high gain and broadband operation. The antenna offers almost 64% area reduction as compared to a standard microstrip patch working on the same frequency.

A simple technique to increase the bandwidth of microstrip antenna is to use thick substrates or increasing the height of the antenna. But when the substrate height is of the order of $0.05\lambda_0$, the increased inductive reactance of the probe deteriorates 50Ω impedance matching. This increased inductive reactance can be overcome by making modifications in the feed probe. C.L Mak and K.F lee et al. [124] proposed a proximity coupled U-slot patch antenna having a bandwidth of 20%. The microstrip feed line is made in the form of π shape in order to obtain broadband impedance matching characteristics.

K.M Luk [125] implemented the L-probe feed mechanism to a square patch antenna and the resulting structure has a 2:1 VSWR bandwidth of 35% without compromising the radiation characteristics.

C.L Mak and K.F Lee el al. [126] has modified the L-probe with a T shaped probe termination to a rectangular microstrip patch antenna. The antenna exhibits a bandwidth of 40% and it is concluded that the usage of two symmetrical T-probes substantially reduce the H-plane cross polarization power.

Ban-Leong Ooi [127] proposed a double π shaped microstrip line fed U-slot patch antenna having an impedance bandwidth of 26%. The design

attains better impedance matching characteristics than the single π stub antenna with stable radiation characteristics throughout the band of operation.

Yong-Xin Guo and K.F Lee et al. [128] has analyzed the L-probe proximity fed rectangular patch using the Finite difference Time Domain Method. They have conducted a detailed parametric analysis of all the parameters affecting broadband impedance matching performance.

C.L Mak and Y.L Chow et al. [129] performed experimental studies on the rectangular micostrip patch antenna with L-shaped probe. The antenna is having a 2:1 VSWR bandwidth of 36% and they have concluded that the L-probe does not have much effect on the resonant frequency. A two element array was designed and found that it can suppress the cross polarized radiation of the antenna.

Y.X Guo [130] implemented the L feed mechanism on a microstrip line fed U-slot patch antenna. The antenna exhibits 42.7% impedance bandwidth which is very much higher as compared to the normal U-slot patch antenna.

Yong-Xin Guo and K.F Lee et al. [131] extensively studied the radiation characteristics of the L-probe fed rectangular patch antenna using the Finite Difference Time Domain Analysis. They found that the input impedance almost remains constant for different ground plane dimensions for form substrates and the dependence of gain on ground plane size is found to be periodic as the radiation patterns strongly depend on the ground plane size.

Yong-Xin Guo and K.M Luk [132] experimentally studied the effect of L-feed on the performance of a probe fed circular patch antenna. The antenna can achieve 30% impedance bandwidth and can produce monopole like conical radiation patterns.

Sean M. Duffy [133] proposed the utilization of single and dual tuning stubs as the part of the microstrip line feed to increase the bandwidth of microstrip antennas. The bandwidth of conventional proximity coupled patch antenna is increased up to 8.4% and that of a stacked aperture coupled patch antenna up to 34.5%.

Y.W Jang [134] developed T shaped microstrip line fed U-slot coupled rectangular patch antenna having a bandwidth of 76.8%. The special feeding structure results in an increased coupling to the patch antenna giving three merged resonances offering broadband operation.

S. Mridula and P. Mohanan et al. [135] implemented a printed L-strip feeding mechanism to a standard microstrip line fed rectangular microstrip patch antenna having a bandwidth of 10%.

Chi Yuk Chiu and K.M Luk et al. [136] has proposed impedance matching technique for quarter wave short circuit wall embedded patch antennas. They have included a folded inner small patch as an extension of the probe feed in a U-slot and L-slit patch antenna. The maximum achieved bandwidth for the U-slot patch antenna is found to be 53% which is very much higher than that of the original U slot patch (28%).

Zhi Ning Chen [137] developed a novel feeding technique for enhancing the radiation performance of a suspended plate antenna by incorporating a probe fed half wave length strip. The proposed antenna effectively suppress the cross polar radiation and a cross polar isolation greater than 20 dB is observed throughout the entire operating bandwidth with stable radiation patterns.

P. Li and K.M Luk [138] has proposed a novel feeding technique by incorporating meandering feeding strip for a standard rectangular patch

antenna. Bandwidths up to 32% and a cross polar isolation greater than 20 dB in the entire bandwidth with high gain are achieved.

Ahmed A. Kishk and K.F Lee et al. [139] implemented the use of hook shaped feed as an alternative to the L feed to a shorted wall rectangular patch antenna. An area reduction of 25% was achieved with a bandwidth of 20% which is comparable as compared to the L fed shorted patch. The hook feed find applications where the size of the L strip is comparable as that of the patch dimensions.

Jongkuk Park [140] put forward a modified L-probe feeding mechanism by replacing the bent part of the L-probe with a printed strip on a suspended substrate and by placing the radiating patch underneath the substrate. It can achieve higher bandwidths as compared to the L-feed patch antenna by increasing the substrate thickness.

K.L Lau and K.M Luk [141] studied the combined effect of L-probe feeding and aperture coupling technique to attain wideband circularly polarized operation. The antenna utilizes Wilkinson power divider along with the dual feeding system to achieve wideband CP operation.

P. Li and K.L Lay et al. [142] studied the performance of the simple probe fed patch and the L-probe fed patch antennas on curved ground planes. It was observed that the usage of carved ground plane increases both the input impedance and the beam width of the patch antenna. An impedance bandwidth of 45.2% and a beam width of 89^0 are achieved for a simple probe fed patch.

K.L Lau and K.M Luk [143] proposed a compact wideband circular patch antenna by utilizing two pairs of symmetrical shorting walls combined with the

L-probe feeding mechanism. The antenna exhibits 27.1% bandwidth with monopole like radiation patterns throughout the band.

Xiu-Yin Zhang and Sheng-Li Xie et al. [144] implemented the principle of dual printed L-probes for achieving wideband low cross polarized patch antenna. The antenna attains a bandwidth of 45.25% with stable and symmetrical radiation patterns throughout the entire operating bandwidth.

Shing-Lung Steven and K.M Luk [145] designed a wideband L-probe patch antenna for pattern reconfiguration applications. Four shorting posts are implemented within the structure which can excite the conical mode and the broadside mode at overlapped frequencies.

Karlo Queiroz da Costa and Victor Dmitriev et al. [146] embedded passive loops with an L-fed rectangular patch antenna. The rectangular loops act as the magnetic dipoles and the rectangular patch as the electric dipole and the resonance caused by them merge together to achieve broadband impedance matching having a bandwidth of 15%.

I.Ang and B.L Ooi [147] demonstrated a semi-circle fed cross shaped microstrip patch antenna exhibiting a bandwidth of 63.7% which is very much higher as compared to a conventional L-probe fed patch antenna.

C.Y Chiu and C.H Chan et al. [148] achieved bandwidth broadening by using an E-shaped patch fed with a folded patch feed and size reduction is attained by implementing shorting walls. The antenna has a bandwidth more than 70% and the cause of resonance along with design guidelines are given for validation.

M.Naser and B.S Virdee et al. [149] developed a promising design which can achieve a bandwidth of 125%. The antenna utilizes a rectangular slot loaded

polygonal shaped patch and shorting pins to achieve compact broadband operation.

S.H Sun and T.P Wong [150] achieved broadband impedance matching over a U-slot loaded shorting planes trapezoidal patch antenna by implementing a modified T-shaped feeding mechanism.

Yong-Xin Guo and K.F Lee et al. [151] implemented L-probe feeding to a microstrip slot antenna. For TM_{11} mode, an impedance bandwidth of about 24% is achieved while for the TM_{12} mode, an impedance bandwidth of 27% is obtained.

K.L Lau and K.M Luk et al. [152] investigated the effect of folding the patch surface along with L-feed mechanism to achieve a wideband antenna exhibiting a very large bandwidth of 133.3%. But the cross polarization characteristic of the antenna is very poor.

In addition to the above techniques broadband impedance matching networks can be incorporated with the microstrip antenna element to broaden the bandwidth. H.W Pues and Van de Capelle [153] experimentally studied the effect of a shielded microstrip matching network consisting of two resonator elements etched on the same substrate as the patch. The bandwidth is improved by a factor of 3.9%.

F.S Fong and H.F Pues [154] reported a wideband multi layer patch antenna which makes use of feed probe inductance as a part of impedance matching network. A series capacitance located at the top end of the probe forms a series resonant circuit which is used for broadband matching of the parallel resonant circuit constituted by the resonant patch antenna. The bandwidth improvement data is not reported in this paper.

J.M Griffin and J.R Forest [155] achieved broadband impedance matching for a circular microstrip patch antenna in which the series resonance of the feed probe inductance is taken into account for broadband impedance matching. For a 6mm radius patch. A 1.5:1 VSWR bandwidth of the antenna is found to be 35%, but the radiation patterns shows frequency dependency over the entire operating bandwidth.

D.M Pozar and B. Kaufman [156] used a single stub impedance matching technique for increasing the bandwidth of an electromagnetically coupled microstrip patch antenna. In this model the input impedance of the microstrip patch antenna was measured by a network analyzer and the component values for the network model (a capacitance in series with the a parallel RLC) were obtained by computer aided model fitting procedure. A stub circuit was then designed to match the load.

Hongming and Van de Capelle et al. [157] proposed a simplified real frequency technique for increasing the bandwidth of microstrip patch antenna. Here the impedance matching network is built as a part of the microstrip line feed as band pass impedance steps and transitions. It was shown that band pass matching networks exhibits better performance than the low pass and high pass prototypes.

C.L Mak, K.M Luk et al. [158] proposed a microstripline fed L-strip patch antenna which achieves an impedance bandwidth of 49% with a foam substrate of total thickness $0.13\lambda_0$. The L-strip at the end of the microstrip feed line, like a step along the Z-axis, reduces the spacing between the patch and the feedline, which couples more electromagnetic energy into the patch thereby enhancing the bandwidth.

2.2 **Present Work**

As already mentioned, the bandwidth of microstrip antennas can be increased by increasing the substrate thickness, decreasing the dielectric constant, by the use of additional resonators gap coupled to the driven patch or by implementing broadband impedance matching networks as a part of the patch antenna. There are limitations in increasing the substrate thickness due to the excitation of surface waves. Also the dielectric constant cannot be decreased much due to practical difficulties. The usage of parasitic resonators increases the overall surface area. In some cases, the size is thrice as that of the isolated patch antenna and in some other cases even five times. Implementation of broadband matching networks as a part of the printed microstrip transmission line increases the complexities of fabrication.

In the present work, an attempt is made to remedy these drawbacks. Efforts are successfully implemented to bring the broadband impedance matching strip to the same plane of the patch antenna by loading a slot on the patch. Wide bandwidth is obtained by properly matching the resonances of the slot loaded patch antenna and the resonance caused by the metal strip. Since the strip is incorporated within the patch structure, additional external matching elements are not required which greatly reduces the antenna size. The design greatly reduces the fabrication complexities associated with the manufacturing process and it eliminates the need of additional spacers required for antenna mounting. Using this technique, the tilted square slot patch can achieve a bandwidth of 38%. Finally, the tilted square slot of the patch antenna is replaced with a polygonal slot and the validity of strip matching is confirmed through simulation and experimental studies. It is observed that the resonance mechanism of the polygonal slot patch antenna is same as that of the tilted square slot antenna, but it can give a higher bandwidth of the order of 45%. The

polygonal slotted patch antenna can be reconfigured to attain an even higher bandwidth by implementing L-strip feeding mechanism. The L-strip feed mechanism will excite higher order modes of the patch antenna and suitable strip dimension is selected to merge the newly generated resonances to the already existing resonances. The antenna can offer a bandwidth of 74% and it is an attractive choice for breast cancer imaging applications.

The second part of the thesis deals with the gain enhancement techniques for microstrip antennas. Here, principle of stacking is successfully implemented and the position of the parasitic patch is offsetted to enhance the gain of the antenna. The offsetting technique is successfully implemented on single band square microstrip patch antennas and on the tilted square slot loaded and the polygonal slot loaded microstrip patch antennas without deteriorating the matching performance of the antenna.

2.3 References

[1]   G.A Deschamps, "Microstrip Microwave Antennas", 3rd USAF Symposium on Antennas, 1953.

[2]   H. Gutton and G. Baissinot, "Flat Aerial for Ultra High Frequencies", French Patent No. 703113, 1955.

[3]   L. Levin, "Radiation from Discontinuities in Strip Lines", Proc. IEE, vil.107, Pt.c, pp 163-170, 1960.

[4]   E.V Byron, "A new Flush Mounted Antenna Element for Phased Array Applications", Proc. Phased Array Antenna Symp., pp.187-192, 1970.

[5]   R.E Munson, "Conformal MIcrostrip Antennas and Microstrip Phased Arrays", IEEE Trans. Antennas Propagat., vol.AP-22, pp.74-77, 1974.

[6]   J.Q Howell, "MIcrostrip Antennas", IEEE Trans. Antennas Propagat., vol.AP-23, pp.90-93, 1975.

[7]   H.D Weinschel, "Progress report on Development of Microstrip Cylindrical Arrays for Sounding Rockets", Phys. & Sci. Lab., New Mexico State Univ., Las Cruces, 1973.

[8]   G.G Sanford, "Conformal MIcrostrip Phased Array for Aircraft Tests with ATS-6", Proc.Nat.Electronic Conf., vol.29, pp. 252-257, 1974.

[9]   J.R James and G.J Wilson, "New Design Technique for Microstrip Antenna Arrays", Proc. 5th European Microwave Conf., Hamburg, pp-102-106, 1975.

[10]   G.W Garvin, R.E Munson, L.T Ostwald and K.G Schroeder, "Low Profile Electrically Small Missile Base Mounted MIcrostrip Antennas", Dig.Int.Symp.Antennas Propagat.Soc., Urbana, IL, pp-244-247, 1975.

[11]   T.E Nowicki, "Microwave Substrates, Present and Future", Proc. Workshop Printed Circuit Ant.Tech., New. M.S Univ. Las Cruces, pp.26/1-22. 1979.

[12]   G.R Traut, "Clad Laminates of PTFE Composites for Microwave Antennas", ibid., pp.27/1-17, 1979.

[13]   L.R Murphy, "SEASAT and SIR-A Microstrip Antennas", ibid., pp. 18/1-20, 1979.

[14]   K.R Carver, "Description of a Composite Hex cell Microstrip Antenna", Private Communication to J.W.Mink, 1979.

[15]   S.N Das and S.K Choudhary, "Rectangular Microstrip Antenna on a Ferrite Substrate", IEEE Trans. Antennas Propagat., vol.AP-30, pp.499-502, 1982.

[16]   A.G Derneryd, " Linear MIcrostrip Array Antenna", Chalmer Univ. Technol., Goteborge, Sweden, Tech. Report, T.R 7505, 1975.

[17]   A.G Derneryd, " Linear MIcrostrip Array Antenna", IEEE Trans. Antennas Propagat., vol.AP-24, pp.846-851, 1976.

[18]   Y.T Lo, D. Solomon and W.F Richards, "Theory and Experiment on Microstrip Antennas", IEEE AP-S Symposium (Japan), pp.53-55, 1978.

[19]   W.F Richards, Y.T Lo and D.D Harrison, "Improved Theory for MIcrostrip Antennas", Electron. Lett., Vol.15, pp.42-44, 1979.

[20]   Y.T Lo, D. Solomon and W.F Richards, "Theory and Experiment on Microstrip Antennas", IEEE Trans. Antennas Propagat., vol. AP-27, pp.137-145, 1979.

[21]   K.R Carver, " A Modal Expansion Theory for the Microstrip Antenna", Dig.Int.Symp.Antennas Propagat.Soc., Seattle, WA, pp.101-104, 1979.

[22]   K.R Carver and E.L Coffey, "Theoretical Investigations of the Microstrip Antenna", Tech.Rept. PT 00929, Physical Science Lab., New Mexico Science Univ., Las Cruces, 1979.

[23]   E.L Coffey and T.H Lehman, "A New Analysis Technique for Calculating the Self and Mutual Impedance of Microstrip Antennas", Proc. Workshop on Printed Circuit Antennas, New Mexico State Univ., pp.31/1-21, 1979.

[24]   E.O Hammerstad, "Equations for Microstrip Circuit Design", Proc. 5th European Microwave Conf. , Hamburg, pp.268-272, 1975.

[25]   N.G Alexopoulose and I.E Rana, " Mutual Impedance Computation Between Printed Dipoles", IEEE Trans. Antennas Propagat., vol. AP-27, pp.137-145, 1979.

[26] J.R James and C.J Wilson, "Microstrip Antennas and Arrays Part I Fundamental Action and Limitations", IEE Proc. Microwaves, opt. & Antennas, Vol.1, pp. 165-174, 1977.

[27] P. Hammer, D. Van Bouchante, D. Verschraevan and A. Van de Capelle, "A Model for Calculating the radiation Fields of Microstrip Antennas", IEEE Trans. Antennas Propagat., vol. AP-27, pp.267-270, 1979.

[28] P.K Agarwal and M.C Bailey, "An Analysis Technique for Microstrip Antennas", IEEE Trans. Antennas Propagat., vol. AP-25, pp.756-759, 1977.

[29] N.G Alexopoulose, N.K Uzunoglu and I.E Rana, "Radiation by Microstrip Patches", Dig.Int.Symp.Antennas Propagat., pp.722-727, 1979.

[30] J.R Mosig and F.E Gardiol, "The near Field of an Open Microstrip Structure", IEEE AP-S, Int.Synp. Digest, pp.379-381, 1979.

[31] J.W Mink, "Sensitivity of Microstrip Antennas to Admittance Boundary Variations", IEEE Trans. Antennas Propagat., vol. AP-29, pp.143-145, 1981.

[32] C.M Butler, "Analysis of a Coax-Fed Circular MIcrostrip Antenna", Proc.Workshop printed Circuit Antenna Tech., New Mexico State Univ., Las Cruces, pp.13/1-17.1979.

[33] C.M Butler and E.K Yung, "Analysis of a Terminated Parallel Plate Waveguide with a Slot on its Upper Plate", Ann. Telecommun., vol.34, No.9, 1979.

[34] E.L Newman, "Strip Antennas in a Dielectric Slab", IEEE Trans. Antennas Propagat., vol. AP-26, pp.647-653, 1978.

[35]   E.L Newman and D.M Pozar, "Electromagnetic Modeling of Composite Wire and Surface geometries", IEEE Trans. Antennas Propagat., vol. AP-26, pp.784-787, 1978.

[36]   J.H Richmond, "A Wire Grid Model for Scattering by Conductive Bodies", IEEE Trans. Antennas Propagat., vol. AP-14, pp.782-786, 1966.

[37]   K.R Carver and E.L Coffey, "Theoretical Investigations of the Microstrip Antenna", Physical and Science Lab., New Mexico State Univ., Las Cruces, pp.3/1-20, 1979.

[38]   J.L Kerr, "Microstrip Antenna Developments ", Proc.Workshop printed Circuit Antenna Tech., New Mexico State Univ., Las Cruces, pp.3/1-20, 1979.

[39]   D.H Schaubert and F.G Farrar, "Some Conformal Printed Circuit Antenna Design", Proc.Workshop printed Circuit Antenna Tech., New Mexico State Univ., Las Cruces, pp.5/1-21, 1979.

[40]   K.R Carver, "Practical Analytical Techniques for the Microstrip Antenna", Proc.Workshop printed Circuit Antenna Tech., New Mexico State Univ., Las Cruces, pp.7/1-20, 1979.

[41]   S.A Song and M.D Walton, "A Dual Frequency Stacked Circular Disc Antenna", IEEE Trans. Antennas Propagat., vol. AP-27, pp.270-273, 1979.

[42]   S.A Long, L.C Chen, M.D Walton and M.R Allerding, "Impedance of a circular Disk Printed Circuit Antenna", Electron Lett., vol.14, pp.684-686,1978.

[43]   L.C Chen, S.A Song, M.R Allerding and M.D Walton, "Resonant Frequency of a Circular Disc Printed Circuit Antenna", IEEE Trans. Antennas Propagat., vol. AP-25, pp.595-596, 1977.

[44]   L.C Chen, "The Elliptical Microstrip Antenna with Circular Polarization", IEEE Trans. Antennas Propagat., vol. AP-29, pp.95-99, 1981.

[45]   A.G Derneryd, "Analysis of Microstrip Disc Antenna Element", IEEE Trans. Antennas Propagat., vol. AP-27, pp.660-664, 1979.

[46]   J. McLLvenna and N. Kernweis, "Variations on the Circular MIcrostrip Antenna Element", Proc.Workshop printed Circuit Antenna Tech., New Mexico State Univ., Las Cruces, pp.25/1-15, 1979.

[47]   J.W Mink, "Circular Ring MIcrostrip antenna Elements", Dig.Int.Symp. Antennas Propagat.Soc., Quebec City, Canada, June 1980.

[48]   E.H Newman and P. Tulyathan, "Analysis of Microstrip Antennas using Moment Methods", ibib., pp.47-53, 1981.

[49]   D.C Chang, "Analytical Theory of an Unloaded Rectangular Patch", ibid., pp.54-62, 1981.

[50]   T. Itoh and W. Mentzel, "A Full Wave Analysis Method for open MIcrostrip Structures", ibid., pp.63-67, 1981.

[51]   D.H Schaubert an F.G Farrar, "Some Conformal Printed Circuit Antenna Designs", Proc.Workshop Printed Circuit Antenna Tech., New Mexico State Univ., Las Cruces, pp.5/1-21, Oct.1979.

[52]   C. Wood, "improved bandwidth of Microstrip Antenna Using Parasitic Elements", IEE Proc. Pt.H, vol.127, pp.231-234, 1980.

[53]   W.C Chew, "A Broadband Annual Ring MIcrostrip Antenna", IEEE Trans. Antennas Propagat., vol. AP-30, pp.918-922, 1982.

[54] D.R Poddar, J.S Chatterjee and S.K Choudhary, "On Some Broadband MIcrostrip Resonators", IEEE Trans. Antennas Propagat., vol. AP-31, pp.193-194, 1983.

[55] A.G Derneryd and I. Karlson, "Broadband Microstrip Antenna Element and Array", IEEE Trans. Antennas Propagat., vol. AP-24, pp.140- 1141, 1981.

[56] P.S Hall, "New Wide Band MIcrostrip Antenna Using Log Periodic Techniques", Electron Lett., vol.16, pp.127-128, 1980.

[57] P.S Hall, "Multi Octave Bandwidth Log-Periodic MIcrostrip Antenna Array", IEE Proc.. pt.H, vol.133, pp.127-136, 1986.

[58] P.S Hall, "Microstrip Antenna Array with Multioctave Bandwidth", Microwave J., vol.29, pp.123-130, 1986.

[59] N. Das and J.S Chatterjee, "Conically Depressed Microstrip Patch Antenna", IEE Proc.. pt.H, vol.130, pp.193-196, 1983.

[60] L. Jeddari, K. Mahdjoubi, C. Terret and J.P Daniel , "Broadband Conical MIcrostrip Antenna", Electron Lett., vol.21, pp.896-898, 1985.

[61] H. Pues, J. Bogaers, R. Peik and A. Van De Capelle, "Wideband Quasi Log Periodic MIcrostrip Antenna", IEE Proc., pt.H, vol.28, 1983.

[62] M.S Lee and S.S Lee, "Design of Wideband Quasi Log Periodic Microstrip Antenna", J.Korean Inst.Electron.Eng., vol.20, pp.40-44, 1983.

[63] V.N Pandharipande and K.G Verma , "Wideband Microstrip Patch Array at X-Band", J.Inst.Elec.Telecom.Eng, vol.29, pp.497-500, 1983.

[64] P.S Bhatnagar, J.P Daniel, K. Mehdjoubi and C. Terret , "Hybrid Edge, Gap and Directly coupled Triangular Microstrip Antenna", Electron Lett., vol.22, pp.853-855, 1986.

[65] P.S Bhatnagar, J.P Daniel, K. Mehdjoubi and C. Terret , "Experimental Study on Stacked Triangular MIcrostrip Antennas", Electron Lett., vol.22, pp.864-865, 1985.

[66] C. Wood , "Curved Microstrip Lines as Compact Wideband Circularly Polarized Antennas", IEE J.MOA, vol.126, pp.5-13, 1979.

[67] P.S Hall, C. Wood and C. Garrek, "Wideband MIcrostrip Antennas for Circuit Integration", Electron Lett., vol.15, pp.458-460, 1970.

[68] A. Sabban, "A New Broadband Stacked Two Layer Antenna", Dig., Int.Sump.Antennas and Propag. vol.1, pp.63-66, May 1983.

[69] R.I Wolfson and W.G Sterns, "A High Performance MIcrostrip, Dual Polarized Radiating Element", Dig., Int.Sump.Antennas and Propag.,Boston MA, USA, vol.2, pp.555-558, June 1984.

[70] G. Dobust and S. Gueho, "Theory of Large Bandwidth Microstrip Plane Array with A Deflected Beam", ibid., vol.2, pp.807-810,1984.

[71] K.S Fong, H.F Pues and M.J Withers, "Wideband Multilayer Coaxial Fed Microstrip Antenna Element", Electron Lett., vol.21, pp.497-499, 1985.

[72] T. Hori and N. Nakagima , "Broadband Circularly Polarized Array Antenna with Coplanar Feed", Trans. Inst.Electron. and Commun. Eng., Jpn, Part B, vol.J 68B, pp.515-522, 1985.

[73] C.J Prior and P.S Hall, "Microstrip Disc Antenna with a Short Circuited Annular Ring", Electron Lett., vol.21, pp.719-721, 1985.

[74] G. Dubost and A. Rabba, "Substrate Influence on Flat Folded Dipole Bandwidth", Electron Lett., vol.21, pp.426-427, 1985.

[75] J.R Mosig and F.E Gardiol, "The Effect of Parasitic Elements on Microstrip Antennas", IEEE AP-S Symposium, Vancouver, pp.397-400, 1985.

[76] G. Kumar and K.C Gupta, "Broadband MIcrostrip Antennas Using Additional r=Resonators Gap Coupled to the Radiating Edge", IEEE Trans. Antennas Propagat., vol. AP-32, pp.1375-1379, 1985.

[77] G. Kumar and K.C Gupta, "Non Radiating Edges and Four Edges Gap Coupled Multiple Resonator Broadband Microstrip Antennas", IEEE Trans. Antennas Propagat., vol. AP-33, pp.173-178, 1985.

[78] G. Kumar and K.C Gupta, "Directly Coupled Multiple Resonator Wideband MIcrostrip Antennas", ibid., vol. AP-33, pp.588-593, 1985.

[79] C.K Aanandan and K.G Nair, "Compact Broadband Microstrip Antenna", Electron Lett., vol.22, pp.1064-1065, 1986.

[80] C.K Aanandan, P. Mohanan and K.G Nair, "Broadband Gap Coupled Microstrip Antenna", IEEE Trans. Antennas Propagat., vol. AP-38, pp.1581-1586, 1991.

[81] Ramesh Garg and V.S Reddy, "A Broadband coupled Strips Microstrip Antenna", IEEE Trans. Antennas Propagat., vol. AP-39, pp.1344-1345, 2001.

[82] Sang-Hyuk Wi, Yong-Shik Lee and Jong-Gwan Yook, "Wideband Microstrip Patch Antenna with U Shaped Parasitic Elements", IEEE Trans. Antennas Propagat., vol. AP-55, pp.1196-1199, 2007.

[83] P.S Bhatnagar, J.P Daniel, K. Mahdjoubi and C. Terret, "Experimental Study on Stacked Triangular MIcrostrip Antennas", Electron Lett., vol.22, pp.864-865, 1986.

[84] Tsein Ming and Kwai Man Luk, "Effect of Parasitic Element on the Characteristics of Microstrip Antenna", IEEE Trans. Antennas Propagat., vol. 39, pp.1247-1251, 1991.

[85] H.R Hassani and D. Mirshekhar-Syahkal, "Analysis of Stacked Rectangular Patch Antennas with Non Aligned Patches or Unequal Patch Sizes", IEEE Trans. Antennas Propagat., vol. 42, pp.1333-1336, 1994.

[86] Frederic Croq and David M. Pozar, "Millimeterwave Design of Wideband Aperture Coupled Stacked Microstrip Antennas", IEEE Trans. Antennas Propagat., vol. 39, pp.1770-1776, 1991.

[87] Frederic Croq and Albert Papiernik, "Stacked Slot Coupled Printed Antenna", IEEE Microw. Guided Wave Lett., vol. 1, pp.288-290, 1991.

[88] S.D Targonski, R.B Waterhouse and D.M Pozar, "Wideband Aperture Coupled Stacked Patch Antenna Using Thick Substrates", Electron Lett., vol.32, pp.1941-1942, 1996.

[89] U.K Revankar and A. Kumar, "Mutual Coupling Between Stacked Three Layer Circular MIcrostrip Antenna Elements", Electron Lett., vol.30, pp.1997-1998, 1994.

[90] R.B Waterhouse, "Design and Scan Performance of Large, Probe fed Stacked MIcrostrip Patch Arrays", IEEE Trans. Antennas Propagat., vol. 50, pp.893-895, 2002.

[91] R.B Waterhouse, "Design and Performance of Large Phased Arrays of Aperture Stacked PAtches", IEEE Trans. Antennas Propagat., vol. 49, pp.292-297, 2001.

[92] Steven Mestdagh, Walter De Raedt and Guy A.E Vandenbosch, "CPW-Fed Stacked Microstrip Antennas", IEEE Trans. Antennas Propagat., vol. 52, pp.74-83, 2004.

[93] Mohammod Ali, Abu T.M. Sayem and Vijay K. Kunda, "A Reconfigurable Stacked MIcrostrip Patch Antenna for Satellite and Terrestrial Link", IEEE Trans. Vehicular Tech., vol. 56, pp.426-435, 2007.

[94] Wayne S.T Rowe and R.B Waterhouse, "Investigation into the Performance of Proximity Coupled Stacked Patches", IEEE Trans. Antennas Propagat., vol. 54, pp.1693-1698, 2006.

[95] Shi-Chang Gao, Le-Wei Li, Mook Seng Leong and Tat-Soon Yeo, "Wideband Microstrip Antenna With H-Shaped Coupling Aperture", IEEE Trans. Vehicular Tech., vol. 51, pp.17-27, 2002.

[96] K.M Luk, K.F Lee and Y.L Chow, "Proximity Coupled Stacked Circular Disc Microstrip Antenna with Slots", Electron Lett., vol.34, pp.419-420, 1998.

[97] Ban-Leong Ooi, Shen Qin and Mook-Seng Leong, "Novel Design of Broadband Stacked Patch Antenna", IEEE Trans. Antennas Propagat., vol. 50, pp.1391-1395, 2002.

[98] M.A Martin, B.S Sharif and C.C Tsimenidis, "Probe Fed Stacked Patch Antenna for Wideband Applications", IEEE Trans. Antennas Propagat., vol. 55, pp.2385-2388, 2007.

[99]   Gh. Rafi and L. Shafai, "Broadband MIcrostrip Patch Antenna with V-Slot", IET Proc. MIcrow. Antennas Propagat., vol. 151, pp.435-440, 2004.

[100] M.A Martin, B.S Sharif and C.C Tsimenidis, "Dual Layer Stacked Rectangular Microstrip Patch Antenna for Ultra Wideband Applications", IET Proc. MIcrow. Antennas Propagat., vol. 1, pp.1192-1196, 2007.

[101] Nasimuddin and Z.N Chen, "Wideband Microstrip Antenna with Sandwich Substrate", IET Proc. Microw. Antennas Propagat., vol. 2, pp.538-546, 2008.

[102] Nasimuddin and Z.N Chen, "Wideband Multi Layered Microstrip Antennas Fed By Coplannar Waveguide-Loop With and Without Via Combinations", IET Proc. Microw. Antennas Propagat., vol. 3, pp.85-91, 2009.

[103] S.D Targonski, R.B Waterhouse and D.M Pozar, "Design of Wideband Aperture Stacked Patch Microstrip Antennas", IEEE Trans. Antennas Propagat., vol. 46, pp.1245-1251, 1998.

[104] Jui-Han Lu, "Bandwidth Enhancement Design of Single Layer Slotted Circular MIcrostrip Antennas", IEEE Trans. Antennas Propagat., vol. 51, pp.1126-1129, 2003.

[105] Jui-Han Lu, Chia-Laun Tang and Kin Lu Wong, "Novel Dual Frequency and Broadband Designs of Slot Loaded Equilateral Triangular Microstrip Antennas", IEEE Trans. Antennas Propagat., vol. 48, pp.1048-1055, 2000.

[106] Jui-Han Lu, Chia-Laun Tang and Kin Lu Wong, "Single Feed Slotted Equilateral Triangular MIcrostrip Antenna for Circular Polarization", IEEE Trans. Antennas Propagat., vol. 47, pp.1174-1178, 1999.

[107] Jia-Yi Sze and Kin Lu Wong, "Slotted Rectangular Microstrip Antenna for Bandwidth Enhancement", IEEE Trans. Antennas Propagat., vol. 48, pp.1149-1152, 2000.

[108] Amit A. Deshmukh and K.P Ray, "Compact Broadband Slotted Rectangular Microstrip Antenna", IEEE Antennas Wireless Propag. Lett., vol. 8, pp.1410-1413, 2009.

[109] T. Huynh and K.F Lee, "Single-Layer Single-Patch Wideband MIcrostrip Antenna", Electron Lett., vol.31, pp.1310-1312, 1995.

[110] M.Clenet and L. Shafai, "Multiple Resonances and Polarization of U-Slot Patch Antenna", Electron Lett., vol.35, pp.101-103, 1999.

[111] Steven Weigand, Greg H. Huff, Kankan H. Pan and Jennifer T. Bernhard, "Analysis and Design of Broadband Single Layer Rectangular U-Slot Microstrip Patch Antennas", IEEE Trans. Antennas Propagat., vol. 51, pp.457-468, 2003.

[112] K.F Lee, K.M Luk, K.F Tong, S.M Shum, T. Huynh and R.O Lee, "Experimental and Simulation Studies of the Coaxially Fed U-Slot Rectangular Patch Antenna", IET Proc. Microw. Antennas Propagat., vol. 144, pp.354-358, 1997.

[113] Ricky Chair, Chi-Lun Mak, K.F Lee, K.M Luk and Ahmed A. Kishk, "Miniature Wideband Half U-Slot and Half E-Shaped Patch Antennas", IEEE Trans. Antennas Propagat., vol. 53, pp.2645-2652, 2005.

[114] Fang Yang, Xue-Xia Zhang, Xiaoning Ye and Yahya Rahmat Samii, "Wideband E-Shaped Patch Antennas for Wireless Communications", IEEE Trans. Antennas Propagat., vol. 49, pp.1094-1100, 2001.

[115] Yuehe Ge, Karu P. Esselle and Trevor S. Bird, "A Compact E-Shaped Patch Antenna", IEEE Trans. Antennas Propagat., vol. 54, pp.2411-2413, 2006.

[116] Yuehe Ge, Karu P. Esselle and Trevor S. Bird, "E-Shaped Patch Antennas for High Speed Wireless Networks", IEEE Trans. Antennas Propagat., vol. 52, pp.3213-3219, 2004.

[117] Lin Peng, Cheng-Li Ruan and Yun Zhang, "A Novel Compact Broadband Microstrip Antenna", Proc. Asia Pacific Microwave Conference. 2004.

[118] A.K Shackelford, K.F Lee, K.M Luk and R.C Chair, "U-Slot Patch Antenna With Shorting Pin", Electron Lett., vol.37, pp.729-730, 2001.

[119] C.L Mak, R. Chair, K.F Lee, K.M Luk and A.A Kishk, "Half U-Slot Patch Antenna With Shorting Wall", Electron Lett., vol.39, 2003.

[120] K.F Lee, Y.X Guo, J.A Hawkins, R. Chair and K.M Luk, "Theory and Experiment on Microstrip Patch Antennas With Shorting Walls", IET Proc. Microw. Antennas Propagat., vol. 147, pp.521-525, 2000.

[121] Jeen-Sheen Row and Yen-Yu Liou, "Broadband Short-Circuited Triangular Patch Antenna", IEEE Trans. Antennas Propagat., vol. 54, pp.2137-2141, 2006.

[122] Debatosh Guha and Yahia M. M Antar, "Circular MIcrostrip Patch Loaded With Balanced Shorting Pins for Improved Bandwidth", IEEE Trans. Antennas Wireless Propagat. Lett., vol. 5, pp.217-219, 2006.

[123] I-Fong Chen and Chia-Mei Peng, "A Novel Reduced Size Edge Shorted Patch Antenna for UHF Band Applications", IEEE Trans. Antennas Wireless Propagat. Lett., vol. 8, pp.475-477, 2009.

[124] C.L Mak, K.M Luk and K.F Lee, "Proximity Coupled U-Slot Patch Antenna", Electron Lett., vol.34, 1998.

[125] K.M Luk, C.L Mak, Y.L Chow and K.F Lee, "Broadband MIcrostrip Patch Antenna", Electron Lett., vol.34, 1998.

[126] C.L Mak, K.F Lee and K.M Luk , "Broadband Patch Antenna with a T-Shaped Probe ", IET Proc. Microw. Antennas Propagat., vol. 147, pp.73-76, 2000.

[127] Ban-Leong Ooi, "A Double π Stub Proximity Feed U-Slot Patch Antenna", IEEE Trans. Antennas Propagat., vol. 52, pp.2491-2496, 2004.

[128] Yong-Xin Guo, Chi-Lun Mak, K.M Luk and K.F Lee, "Analysis and Design of L-Probe Proximity Fed Patch Antennas", IEEE Trans. Antennas Propagat., vol. 49, pp.145-149, 2001.

[129] Chi-Lun Mak, K.M Luk and K.F Lee and Y.L Chow, "Experimental Study of a Microstrip Patch Antenna with an L-Shaped Probe", IEEE Trans. Antennas Propagat., vol. 48, pp.777-783, 2000.

[130] K.M Luk, Y.X Guo, K.F Lee and Y.L Chow, "L-Probe Proximity Fed U-Slot Patch Antenna", Electron Lett., vol.34, 1998.

[131] Yong-Xin Guo, K.M Luk and K.F Lee, "L-Probe Fed Thich-Substrate Patch Antenna Mounted on a Finite Ground Plane", IEEE Trans. Antennas Propagat., vol. 51, pp.1955-1963, 2003.

[132] Yong-Xin Guo, Michael Yan Wah Chia, Zhi Ning Chen and K.M Luk, "Wide-Band L-Probe Fed Circular Patch Antenna For Conical Pattern Radiation", IEEE Trans. Antennas Propagat., vol. 52, pp.1115-1116, 2004.

[133] Sean M. Duffy, "An Enhanced Bandwidth Design Technique for Electromagnetically Coupled Microstrip Antennas", IEEE Trans. Antennas Propagat., vol. 48, pp.161-164, 2000.

[134] Y.W Jang, "Broadband T-Shaped Microstrip Fed U-Slot Coupled Patch Antenna", Electron Lett., vol.38, 2002.

[135] S. Mridula, Sreedevi K. Menon, Lethakumary, Binu Paul,C.K Aanandan and P. Mohanan, "Plannar L-Strip Fed Broadband Microstrip Antenna", Microw. and Opt. Tech. Lett., vol.34, 2002.

[136] Chi Yuk Chiu, Kam Man Shum, Chi Hou Chan and K.F Lee, "Bandwidth Enhancement Technique For Quarter Wave Patch Antennas", IEEE Antennas Wireless Propag. Lett., vol. 2, pp.130-132, 2003.

[137] Zhi Ning and Michael Y.W Chia, "Broadband Suspended Probe-Fed Plate Antenna With Low Cross Polarization Levels", IEEE Trans. Antennas Propagat., vol. 51, pp.345-346, 2003.

[138] P.Li, H.W Lai, K.M Luk and K.L Lau, "A Wideband Patch Antenna With Cross Polarization Suppression", IEEE Antennas Wireless Propag. Lett., vol. 3, pp.211-214, 2004.

[139] Ahmed A. Kishk, K.F Lee, W.C Mok and K.M Luk, "A Wideband Small Size Microstrip Antenna Proximately Coupled to a Hook Shape Probe", IEEE Trans. Antennas Propagat., vol. 52, pp.59-65, 2004.

[140] Jongkuk Park, Hyung-gi Na and Seung-hun Baik, "Design of a Modified L-Probe Fed Microstrip Patch Antenna", IEEE Antennas Wireless Propag. Lett., vol. 3, pp.117-119, 2004.

[141] K.L Lau and K.M Luk, "A Novel Wideband Circularly Polarized Patch Antenna Based on L-Probe and Aperture Coupling Techniques", IEEE Trans. Antennas Propagat., vol. 53, pp.577-580, 2005.

[142] P.Li, K.L Lau and K.M Luk, "A Study of the Wideband L-Probe Fed Plannar Patch Antenna Mounted on a Cylindricalor Conical Surface", IEEE Trans. Antennas Propagat., vol. 53, pp.3385-3389, 2005.

[143] K.L Lau and K.M Luk, "A Wideband Planar Monopole Wire Patch Antenna for Indoor Base Station Applications", IEEE Antennas Wireless Propag. Lett., vol. 4, pp.155-157, 2005.

[144] Xiu-Yin Zhang, Quan Xue, Bin-Jie Hu and Sheng Li Xie, "A Wideband Antenna With Dual Printed L-Probes For Cross-Polarization Suppression", IEEE Antennas Wireless Propag. Lett., vol. 5, pp.388-340, 2006.

[145] Shing-Lung Steven Yang and K.M Luk, "Design of a Wide-Band L-Probe Patch Antenna for pattern Reconfiguration or Diversity Applications", IEEE Trans. Antennas Propagat., vol. 54, pp.433-438, 2006.

[146] Karlo Queiroz da Costa, Victor Dmitriev, D.C Nascimento and J.C da S. Lacava, "Broadband L-Probe Fed Patch Antenna Combined With Passive Loop Elements", IEEE Antennas Wireless Propag. Lett., vol. 6, pp.100-102, 2007.

[147] I. Ang and B.L Ooi, "Broadband Semi-Circle Fed Microstrip Patch Antennas", IET Microw. Antennas Propag., vol. 1, pp.770-775, 2007.

[148] C.Y Chiu, H. Wong and C.H Chan, "Study of Small Wideband Folded Patch Feed Antennas", IET Microw. Antennas Propag., vol. 1, pp.501-505, 2007.

[149] M. Naser-Moghadasi, A. Dadgarpour, F. Jolani and B.S Virdee, "Ultra Wideband Patch antenna With a Novel Folded patch Technique", IET Microw. Antennas Propag., vol. 3, pp.164-170, 2009.

[150] S.H Sun, K.F man, B.Z Wang and T.P Wong, "An optimized Wideband Quarter Wave Patch Antenna Design", IEEE Antennas Wireless Propag. Lett., vol. 4, pp.486-488, 2005.

[151] Yong-Xin Guo, K.M Luk and K.F Lee, "L-Probe Proximity Fed Annular Ring Microstrip Antennas", IEEE Trans. Antennas Propagat., vol. 49, pp.19-21, 2001.

[152] K.L Lau, Sai-Hong Wong and K.M Luk, "Wideband Folded Feed L-Slot Folded Patch Antenna", IEEE Antennas Wireless Propag. Lett., vol. 8, pp.340-343, 2009.

[153] H.W Pues and A.R Van de Capelle, "Wideband Impedance Matched Microstrip Resonator Antennas", IEE Second Inter. Conf. on Antennas and Propagat., pt.1, pp.402-405, 1981.

[154] F.S Fong, H.F Pues and M.J Withars, "Wideband Multi Layer Coaxial-Fed Microstrip Antenna Element", Electron. Lett., vol. 21, pp.497-498, 1985.

[155] J.M Griffin and J.R Forest, "Widebanding Circular Disc Microstrip Antenna", Electron. Lett., vol. 18, pp.266-269, 1982.

[156] D.M Pozar and B. Kaufman, "Increasing the Bandwidth of Microstrip Antenna by Proximity Coupling", Electron. Lett., vol. 23, pp.368-369, 1987.

[157] Homgminh An, Bart K.J.C Nauwelaers and Antonie R. Van de Capelle, "L-Probe Proximity Fed Annular Ring Microstrip Antennas", IEEE Trans. Antennas Propagat., vol. 42, pp.129-136, 1994.

[158] C.L Mak, K.M Luk and K.F Lee, "Me Fed L-Strip Patch Antenna", IET Microw. Antennas Propag., vol. 146, pp.282-284, 1999.

.....ℰℛ.....

METHODOLOGY

This chapter describes the experimental and simulation facilities utilized to characterize the behavior of the broadband microstrip antenna configurations. The microstrip feed line and the proposed antennas are fabricated using the in-house photolithography facility. The antenna characteristics such as return loss, radiation pattern and gain are measured using vector network analyzer and associated instrumentation. The Finite Element Method (FEM) based HFSS is employed for simulation studies of the antenna. Theoretical analysis of the antennas are done using in-house developed MATLAB based FDTD codes.

3.1   Fabrication of the microstrip antenna

The various steps involved in the fabrication of the broadband microstrip antenna are listed below.

3.1.1 Selection of substrate material

The first procedure in the microstrip antenna fabrication is the selection of suitable substrate with electrical and material properties matching the required application. The dielectric constant and loss tangent and their variation with temperature and frequency are important in fabrication. A large range of Polytetrafluroethylene (PTFE), polystyrene, polyolefin, polyphenylene, alumina, sapphire, quartz, ferromagnetic, rutile and semiconductor substrates permit considerable flexibility in the choice of substrates for a particular application. Traditional microstrip antennas at the microwave frequencies use substrates such as PTFE and quartz for good radiation efficiency. These offer excellent electrical performance, but the resulting substrate costs are often too high. So we selected FR4, a widely used substrate material for microwave applications. It is low cost, easily available and most suitable for effortless fabrication.

3.1.2 Photolithography

Since the dimensions of microstrip antennas are critical in microwave frequencies, photolithographic techniques were used to fabricate the desired antenna configurations in the selected substrate. Photolithography or Optical Lithography is the process of transferring geometric shapes from a photo-mask to the surface of a substrate. The major procedures involved in this technique are explained below.

In the first step, the double side copper coated FR4 substrates are chemically cleaned with acetone or Chloroform to remove particulate matter on the surface as well as any trace of organic, ionic and metallic impurities. A very thin film of photoresist is applied with the help of a spinner. There are two types of photoresists; positive and negative. For positive resists, the resist is exposed with UV light wherever the under lying material is to be removed. In these resists, exposure to the UV light changes the chemical structure of the resist so that it becomes more soluble in the developer solution. The exposed resist is then washed away by the developer solution, leaving windows of the bare underlying metallic region. The photomask, therefore, contains an exact copy of the pattern which is to remain on the substrate. The negative resist on the other hand, remains on the surface wherever it is exposed and the developer solution removes only the unexposed portions. Masks used for negative photo resist, therefore, contain the inverse of the pattern to be transferred. After developing, the unwanted metallic portions are cleared using Ferric Chloride solution. Fig 3.1 shows the different steps involved in the procedure.
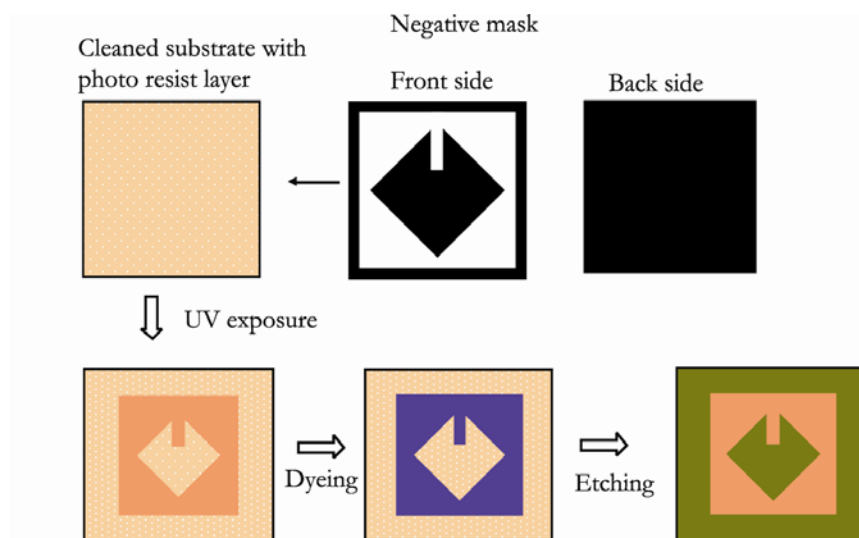
Fig. 3.1 Step by step process involved in Photo lithographic process

3.2 Excitation technique

In the present work, proximity coupling (Electromagnetic coupling) with a 50 Ω microstrip line is used to excite the patch antenna as described in section 1.5.3. The width of the microstrip line is designed for 50 Ω characteristic impedance using standard design equations. The impedance matching can be easily achieved by moving the patch along the surface of the microstrip feed line.

3.3 Facilities used for antenna measurements

A concise description of the basic facilities used for the antenna measurements is presented below.

3.3.1 HP 8510C vector network analyzer

It is the main equipment used for taking fast and accurate microwave measurements in both frequency and time domain. It can synthesis frequencies from 45 MHz to 50 GHz. The time domain response is displayed by taking the Inverse Fourier Transform of the measured frequency data. The time domain characteristics require both magnitude and phase data to perform the Inverse Fourier Transform. Moreover, phase data is required to perform the vector error correction for measurement accuracy [1].

The HP 8510C network analyzer comprises of a microwave generator, s-parameter test set, signal processor and the display unit as depicted in fig. 3.2. The synthesized sweeper generator, HP 83651B, uses an open loop YIG tuned element to generate the RF stimulus. The frequencies can be synthesized in step mode or ramp mode, depending upon the desired measurement accuracy. The antenna under test is connected to the two-port s-parameter Test unit, HP8514B. This module isolates the incident, reflected and transmitted signals at the two ports. The signals are then down converted to an intermediate

frequency and fed to the IF detector. These signals are suitably processed to display the magnitude and phase information of S-parameters in log-magnitude, linear-magnitude, or Smith chart formats. All these constituent modules of the network analyzer are connected using the HP1B system bus. A completely automated data acquisition is made possible using the HP-BASIC based MERLSOFT, developed indigenously at the Center for Research in Electromagnetics and Antennas (CREMA), Department of Electronics, Cochin University of Science and Technology.
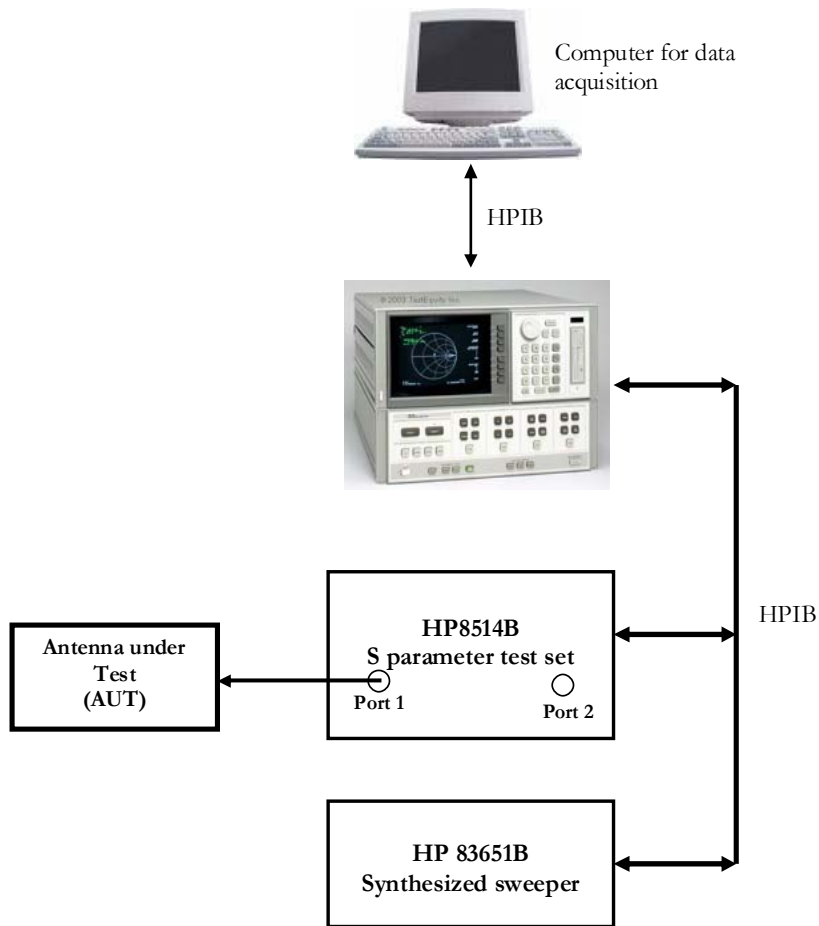
Fig. 3.2 Block diagram of HP 8510c network analyzer assembly

3.3.2 Anechoic chamber

The free space environment required in antenna pattern measurements is realized by making use of the anechoic chamber. It is a very big room compared to the wave length of operation, consists of microwave absorbers [2] fixed on the walls, roof and the floor to avoid the EM reflections. The tapered chamber with an average chamber reflectivity of -35 dB is used for making antenna measurements. The absorbers used in building the chamber are made from high quality, low density foam, infused with dielectrically and magnetically lossy medium. The wall of the chamber is covered with Carbon black impregnated polyurethane foam based pyramidal and flat absorbers of appropriate sizes. Aluminum sheets are used to shield the chamber from electromagnetic interferences from other equipments. The polyurethane foam structure gives the geometrical impedance matching, while the dispersed Carbon provides the required attenuation, for a wide frequency range of 500 MHz to 18 GHz. The photograph of the anechoic chamber used for the measurement is shown in fig. 3.3.

Fig. 3.3 Photograph of the anechoic chamber used for the antenna measurements

3.4 Antenna Measurements

Various antenna parameters like resonant frequency, S-parameters, bandwidth, gain, polarization, radiation pattern etc. are measured using different experimental setups as described below.

3.4.1 Measurement of Resonant Frequency, S-parameters and Bandwidth

The port-1 of the vector network analyzer is calibrated by using the suitable standard short, open and thru loads. Proper phase delay is introduced while calibrating, to ensure that the reference plane for all measurements in the desired frequency range is actually at 0^0, thus taking care of probable cable length variations. The broadband microstrip antenna is then connected to the first port of the network analyzer S-parameter test set as shown in fig. 3.2. The magnitude and phase of the measured S_{11} log map data is stored in ASCII format in the computer using the MERLSOFT. The resonant frequencies are determined from the return loss curves in the log map form, by identifying those frequencies for which the curve shows maximum dip. The experimental setup for these measurements is shown in figure 3.4.

The return loss is the number in dB that the reflected signal is below the incident signal. As the VSWR=2 corresponds to the reflection coefficient, ρ $= \dfrac{VSWR+1}{VSWR-1} = 1/3$, then 20 log(1/3)=-10 dB. Thus 2:1 VSWR bandwidths are determined by observing the range of frequencies (Δfr) about the resonant frequency, f_r for which the return loss curves show a -10 dB value. The bandwidth is then calculated as $\dfrac{\Delta fr}{fr}$. The input impedance of the microstrip antenna at the resonant frequencies are determined directly from the Smith Chart display in the network analyzer, where after calibration the centre corresponds to 50 Ω.

3.4.2 Measurement of Radiation Pattern

Radiation pattern measurement is carried out using the setup consisting of both the network analyzer and anechoic chamber as depicted in fig.3.3. An

automatic turn table assembly kept in the quiet zone is used to mount the test antenna inside the anechoic chamber. The principal E and H-plane radiation patterns (with both co and cross polar pattern) of the test antenna are measured by keeping the test antenna inside the chamber in the receiving mode. The block diagram of the experimental setup used for this measurement is shown in fig.3.4. A standard wide band ridge horn antenna is used as the transmitter. The horn is then connected to port-1 and the test antenna in port-2 of the S-parameter test set. The analyzer is configured to make the S_{21} measurements in the step mode with proper averaging. The radiation patterns of the antenna under test at multiple frequencies can be measured in a single rotation of the positioner using MERLSOFT.

With the test horn antenna aligned in bore sight for maximum reception and polarization matched, the thru response calibration is performed for the frequency of interest and saved in the calibration set. To eliminate spurious reflections from the neighborhood that are likely to interfere with the measured signal, a gate is turned on in the analyzer. This is done by switching it into the time domain and providing a gate span depending on the largest dimension of the test antenna. The turn table is then set to rotate the desired angle using the positioner. The positioner will stop at each step angle and take the S_{21} measurements till it reaches the stop angle. Measurements are repeated in the principal planes for both the co and cross-polar orientations of the test antenna and horn. From the stored data, different radiation characteristics like half power beam width, cross-polar level etc. in the respective planes are estimated.
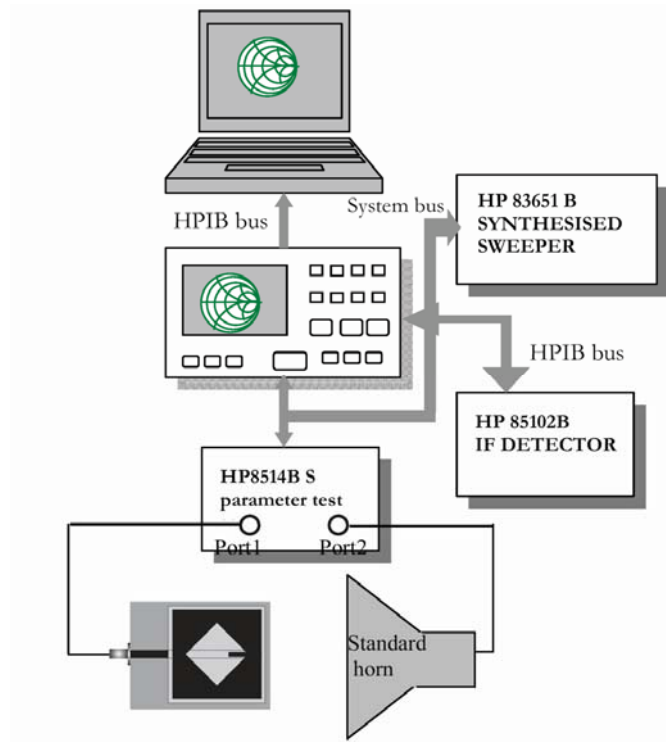
Fig. 3.4 Experimental setup for antenna characterization

3.4.3 Gain

The gain of the antenna under test is measured using the gain transfer method [3-4], utilizing a reference antenna of known gain. The experimental setup for the measurement of gain is same as that used for radiation pattern measurement. A standard antenna with known gain G_s operating in the same frequency band as the test antenna is used as the reference antenna. S_{21} measurements are then carried out to determine the reference power with the wide band horn as transmitter and the reference antenna as receiver. A Thru response calibration is performed for the frequency band of interest and saved in a new cal set. This is taken as the reference gain response (0 dB). The reference antenna is then replaced with the test antenna, retaining the earlier bore sight alignment. S_{21} is then measured with the new calibration on and

power received in dB, P_r is recorded. The gain G_t of the test antenna is calculated from the stored data based on Friis transmission formula as G_t (dB)= G_s (dB)+P_r (dB).

3.4.4 Polarization

Polarization of an antenna in a given direction is the polarization of the wave radiated or transmitted by the antenna, which is that property of the electromagnetic wave describing the time varying direction and relative magnitude of the electric field vector at a fixed location in space and the sense in which it is traced as observed along the direction of propagation. The experimental setup for polarization measurement is similar to that of the radiation pattern. The designed broadband microstrip antenna is kept in the transmitting mode and the wide band horn is used as receiver. RF signal and the DC voltage source are applied to the test antenna in the transmitting mode and the power received by the wide band horn in the vertical plane is stored as a function of frequency. The transmitting antenna is then rotated 90^0 to record the received power as a function of frequency in the horizontal plane. The analysis of the recorded data in both the planes gives the polarization of the test antenna throughout the entire band of operation.

3.4.5 Time domain analysis

Antennas intended for Ultra Wide Band (UWB) imaging applications need to possess superior pulse handling capabilities. Most of the UWB antennas have been characterized by frequency domain characteristics such as gain and reflection coefficient. Gain is a scalar quantity and does not reveal the phase variation of the far field, which may have serious impact on UWB antenna performance. For instance, even though an antenna's gain may appear well behaved, if the phase center of the antenna moves as a function of frequency, or

as a function of look angle θ and φ, then the antenna will radiate a dispersed wave form.

Analysis of the transient response of the antenna is performed by direct time domain measurements or by a frequency domain measurement followed by Fourier transformation. Measurement in the time domain is presented in [5]. Frequency domain measurements take advantage of the high dynamic range and the standardized calibration of the vector network analyzer and are equally accurate to the time domain measurements [6].

The source pulse used is the fourth order Rayleigh pulse with pulse given by,

$$V_{in}(t) = A\left[3 - 6\left(\frac{4\pi}{T^2}\right)t^2 + \left(\frac{4\pi}{T^2}\right)^2 t^4\right] e^{-2\pi(\frac{t}{T})^2} t^2 \frac{V}{m} \quad \text{-------------------- (3.1)}$$

The typical wave form is represented in fig. 3.5 with the amplitude constant A= 1.6 and the pulse duration parameter T= 67 pS to cover the operating bandwidth of the antenna.
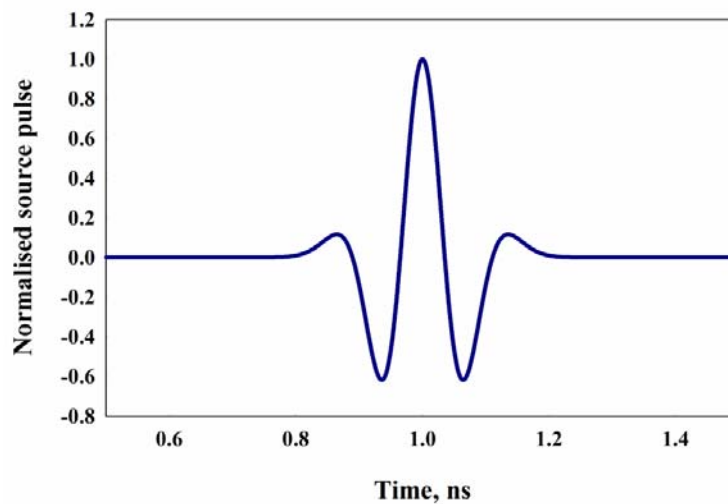
Fig. 3.5 Typical Fourth order Gaussian Pulse

The received wave form is determined by both the source pulse and the system transfer function. The transfer function measured by vector network analyzer is the frequency response of the system. However, the frequency domain raw data can be transformed to the time domain. Here, Hermitian processing is used for the data conversion. At first, the pass-band signal is obtained with zero padding from the lowest frequency down to DC; secondly, the conjugate of the signal is taken and reflected to the negative frequencies. The resultant double sided spectrum corresponds to a real signal, i.e. the system impulse response. It is then transformed to the time domain using Inverse Fast Fourier Transform (IFFT). Finally the system impulse response is convolved with the input pulse to achieve the received signal for both the scenarios, i.e. face to face and side by side orientations.

3.5 HFSS: 3D Electromagnetic simulator

HFSS utilizes a 3D full-wave Finite Element Method (FEM) to compute the electrical behavior of high-frequency and high-speed components [7]. With HFSS, one can extract the parameters such as S, Y, and Z, visualize 3D electromagnetic fields (near- and far-field), and optimize design performance. An important and useful feature of this simulation engine is the availability of different kinds of port schemes. It provides lumped port, wave port, incident wave scheme etc. The accurate simulation of coplanar waveguides and microstrip lines can be done using wave port.

In this thesis some parts of the investigations are done using HFSS. The optimization algorithm available with HFSS is very useful for antenna engineers to optimize the dimensions very accurately. There are many kinds of boundary schemes available in HFSS. Radiation boundary and PML boundary are widely used in this work. The vector as well as scalar representation of E, H, J values of

the device under simulation gives a good insight in to the problem under simulation.

The first step in simulating a system in HFSS is to define the geometry of the system by giving the material properties and boundaries for 3D or 2D elements available in HFSS window. The suitable port excitation scheme is then given. A radiation boundary filled with air is then defined surrounding the structure to be simulated. Now, the simulation engine can be invoked by giving the proper frequency of operations and the number of frequency points. Finally the simulation results such as scattering parameters, current distributions and far field radiation pattern can be displayed.

3.6 Finite Difference Time Domain method (FDTD)

The Finite Difference Time Domain (FDTD) method was first introduced by K.S.Yee in 1966 [8] and refined and reinvented by Taflove [9] in the 1970's. This method permits the modelling of electromagnetic wave interactions with a level of detail as high as that of the Method of Moments. Unlike MoM, however, the FDTD does not lead to a system of linear equations defined over the entire problem space. Updating each field component requires knowledge of only the immediately adjacent field components calculated one-half time step earlier. Therefore, overall computer storage and running time requirements for FDTD are linearly proportional to N, the number of field unknowns in the finite volume of space being modelled. The FDTD method has thus emerged as a viable alternative to the conventional Frequency Domain methods because of its dimensionally reduced computational burdens and ability to directly simulate the dynamics of wave propagation [10]. The rapid growth of FDTD in Computational Electromagnetics is presented in the survey paper by Shlager and Schneider [11]. Although FDTD and TLM are time domain methods there

are some fundamental differences that make them complement each other than compete each other. TLM is a physical model based on Huygens' principle using interconnected transmission lines, but the FDTD is an approximate mathematical model directly based on Maxwell's equations. In the two-dimensional TLM, the magnetic and electric field components are located at the same position with respect to space and time, whereas in the corresponding two-dimensional FDTD cell, the magnetic field components are shifted by half an interval in space and time with respect to the electric field components. Due to this displacement between electric and magnetic field components in Yee's FDTD, Chen et al. [12] modified the FDTD and the new formulation is exactly equivalent to the symmetric condensed node model used in the TLM method. This implies that the TLM algorithm can be formulated in FDTD form and vice versa. However, both algorithms retain their unique advantages. FDTD has a simpler algorithm where constitutive parameters are directly introduced, while the TLM has certain advantages in the modeling of boundaries and the partitioning of the solution region. Furthermore, the FDTD requires less than one-half of the CPU time spent by the equivalent TLM program under identical conditions. A detailed description of FDTD, the method used for the numerical analysis in the present investigation is presented in the following sections.

3.6.1 Numerical investigations: Finite Difference Time Domain

Finite difference Time Domain method proposed by Yee in 1966 is extensively used in many areas of science and technology. FDTD, a technique that discretizes the problem domain in both time and space gives time and frequency domain information of the electromagnetic problem of interest. FDTD provides a direct solution of time dependant Maxwell's equation for electric and magnetic field intensities in a finite, piecewise homogenous media. Due to the lack of analytical preprocessing and modeling, FDTD is a potential tool for planar antenna

problems. Specifically, certain characteristic strengths of FDTD attract the investigators to apply this algorithm in the antenna design and analysis. Following are the striking features of this powerful modelling, simulation and analysis tool.

- From the mathematical point of view, it is a direct implementation of Maxwell's curl equations. Therefore, analytical processing of Maxwell's equations is almost negligible.

- It can model complex antenna geometries and feed and other structures in the model.

- It can model any type of materials of importance to electromagnetic technology, including conductors, dielectrics, dispersive and non linear medium.

- Impulsive excitations in Time Domain gives a broadband response in frequency domain in a single FDTD run through concurrently run Fourier transform.

- The complex near field information is an intrinsic part of FDTD model and the near to far field transformation offers the calculation of far field radiation pattern in single FDTD run.

- FDTD is accurate: It is good model of the physical world. The ready availability of time domain and frequency domain data provides a deep physical insight to the problem in different perspectives. Visualization of fields in time provides a clear insight to the actual physics behind the antenna radiation.

3.6.2 Fundamental concepts of FDTD

Analysis of antenna problem using FDTD starts with dividing the structure into various regions based on the material properties. The unbounded

region, if any, is then bounded by terminating it with absorbing medium or a termination free from reflections. The entire structure is discretised in the form of number of cuboids of volume $\Delta x\Delta y\Delta z$ called Yee cells, whereΔx, Δy, Δz are the dimensions of cuboid in X, Y and Z directions. The Yee cell is the basic building block of the entire structure in which the Electric fields and Magnetic field are interleaved as shown in fig.3.6. The time domain is also discretised with interval Δt. The structure is then excited by an electromagnetic pulse. The wave thus launched by the pulse in the structure is then studied for its propagation behavior. The stabilized time-domain waveform is numerically processed to determine the time-domain and frequency domain characteristics of the structures. Convergence, stability, accuracy and consistency are some of the issues to be addressed while implementing FDTD method.
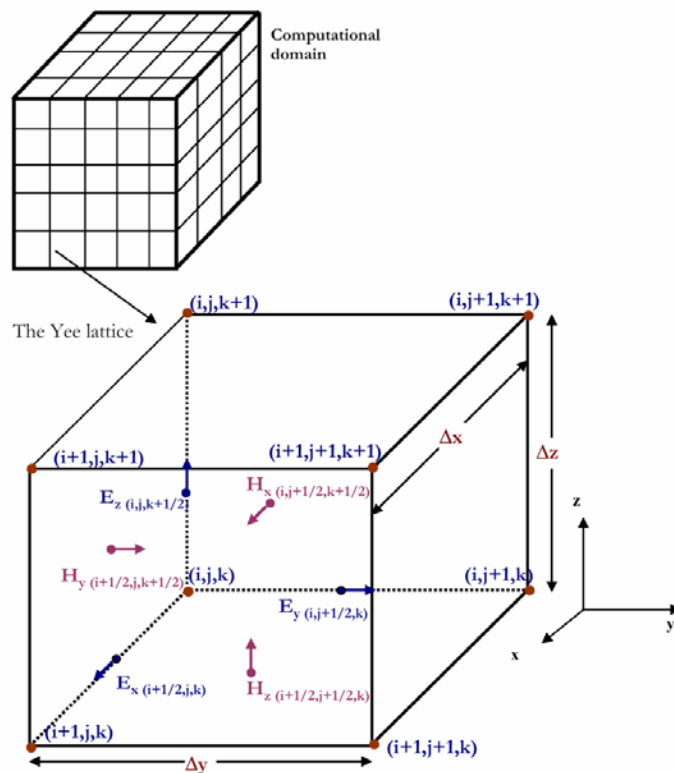
Fig 3.6 Yee cells illustrating E and H field vector placements

3.6.3 Implementation

FDTD method is a direct solution of Maxwell's time-dependent curl equations. The curl operators in the Maxwell's set of equation are discretized using central difference approximations of spatial and time derivatives. The orthogonal E field components (E_x, E_y, E_z) are staggered onto the edges of the Yee cell, where as H field components(H_x, H_y, H_z) are distributed at the face centers. Maxwell's Divergent equations are inherent in FDTD scheme if initial and boundary values are properly applied [13]. Yee defines the grid coordinates (i,j,k) as

$$(i, j, k) = (i\Delta x, j\Delta y, k\Delta z) \text{---} (3.2)$$

where Δx, Δy and Δz are the actual grid separations and i, j and k are the space indices in x, y and z directions. Following Yee's notation the grid points in the solution region are defined as

$$(i, j, k) = (i\Delta x, j\Delta y, k\Delta z) \text{ ---} (3.3)$$

and any function of space and time can be defined as

$$F^n(i, j, k) = F(i\Delta x, j\Delta y, k\Delta z, n\Delta t) \text{ ------------------------------------} (3.4)$$

where Δt is the time increment, n is the time index and Δx, Δy, Δz is the space increment along the three coordinate axes.

The spatial and temporal derivatives of F are written using central finite difference approximations as follows

$$\frac{\partial F^n(i, j, k)}{\partial x} = \frac{F^n(i+1/2, j, k) - F^n(i-1/2, j, k)}{\Delta x} \text{ ----------------------} (3.5a)$$

$$\frac{\partial F^n(i,j,k)}{\partial t} = \frac{F^{n+1/2}(i,j,k) - F^{n-1/2}(i,j,k)}{\Delta t} \quad \text{------------------------------} \quad 3.5b)$$

The starting point of the FDTD algorithm is the differential form of Maxwell's curl equations for an isotropic medium [Eqn 3.6 (a-b)].

$$\nabla \times \vec{E} = -\mu \frac{\partial \vec{H}}{\partial t} \quad \text{---} \quad (3.6a)$$

$$\nabla \times \vec{H} = \sigma E + \varepsilon \frac{\partial \vec{E}}{\partial t} \quad \text{--} \quad (3.6b)$$

These curl equations can be expended in Cartesian coordinates [Eqn. 3.7 (a-f)].

$$\frac{\partial Hx}{\partial t} = \frac{1}{\mu}\left(\frac{\partial Ey}{\partial z} - \frac{\partial Ez}{\partial y} \right) \quad \text{------------------------------------} \quad (3.7a)$$

$$\frac{\partial Hy}{\partial t} = \frac{1}{\mu}\left(\frac{\partial Ez}{\partial x} - \frac{\partial Ex}{\partial z} \right) \quad \text{------------------------------------} \quad (3.7b)$$

$$\frac{\partial Hz}{\partial t} = \frac{1}{\mu}\left(\frac{\partial Ex}{\partial y} - \frac{\partial Ey}{\partial x} \right) \quad \text{------------------------------------} \quad (3.7c)$$

$$\frac{\partial Ex}{\partial t} = \frac{1}{\varepsilon}\left(\frac{\partial Hz}{\partial y} - \frac{\partial Hy}{\partial z} - \sigma Ex \right) \quad \text{-------------------------------} \quad (3.7d)$$

$$\frac{\partial Ey}{\partial t} = \frac{1}{\varepsilon}\left(\frac{\partial Hx}{\partial z} - \frac{\partial Hz}{\partial x} - \sigma Ey \right) \quad \text{-------------------------------} \quad (3.7d)$$

$$\frac{\partial Ez}{\partial t} = \frac{1}{\varepsilon}\left(\frac{\partial Hy}{\partial x} - \frac{\partial Hx}{\partial y} - \sigma Ez \right) \quad \text{-------------------------------} \quad (3.7e)$$

By applying central difference approximations (Equn.3.7.a-3.7.b) to the above scalar equations, six coupled central difference equations (Equn.3.8.a-3.8.f) are obtained as

$$H_x^{n+1/2}(i, j+1/2, k+1/2) = H_x^{n-1/2}(i, j+1/2, k+1/2)$$

$$+ \left[\frac{\Delta t}{\mu.\Delta z} \right] \left(E_y^n(i, j+1/2, k+1) - E_y^n(i, j+1/2, k) \right)$$

$$- \left[\frac{\Delta t}{\mu.\Delta y} \right] \left(E_z^n(i, j+1, k+1/2) - E_z^n(i, j, k+1/2) \right) \text{....... (3.8a)}$$

$$H_y^{n+1/2}(i+1/2, j, k+1/2) = H_y^{n-1/2}(i+1/2, j, k+1/2)$$

$$+ \left[\frac{\Delta t}{\mu.\Delta x} \right] \left(E_z^n(i+1, j, k+1/2) - E_z^n(i, j, k+1/2) \right)$$

$$- \left[\frac{\Delta t}{\mu.\Delta z} \right] \left(E_x^n(i+1/2, j, k+1) - E_x^n(i+1/2, j, k) \right) \text{........ (3.8b)}$$

$$H_z^{n+1/2}(i+1/2, j+1/2, k) = H_z^{n-1/2}(i+1/2, j+1/2, k)$$

$$+ \left[\frac{\Delta t}{\mu.\Delta y} \right] \left(E_x^n(i+1/2, j+1, k) - E_x^n(i+1/2, j, k) \right)$$

$$- \left[\frac{\Delta t}{\mu.\Delta x} \right] \left(E_y^n(i+1, j+1/2, k) - E_y^n(i, j+1/2, k) \right) \text{........(3.8c)}$$

$$E_x^{n+1}(i+1/2, j,k) = E_x^n(i+1/2 j,k)$$

$$+\left[\frac{\Delta t}{\varepsilon.\Delta y}\right]\left(H_z^{n+1/2}(i+1/2, j+1/2,k)-H_z^{n+1/2}(i+1/2, j-1/2,k)\right)$$

$$-\left[\frac{\Delta t}{\varepsilon.\Delta z}\right]\left(H_y^{n+1/2}(i+1/2, j,k+1/2)-H_y^{n+1/2}(i+1/2, j,k-1/2)\right)......(3.8d)$$

$$E_y^{n+1}(i, j+1/2,k) = E_y^n(i, j+1/2,k)$$

$$+\left[\frac{\Delta t}{\varepsilon.\Delta z}\right]\left(H_x^{n+1/2}(i, j+1/2,k+1/2)-H_x^{n+1/2}(i, j+1/2,k-1/2)\right)$$

$$-\left[\frac{\Delta t}{\varepsilon.\Delta x}\right]\left(H_z^{n+1/2}(i+1/2, j+1/2,k)-H_z^{n+1/2}(i-1/2, j+1/2,k)\right)......(3.8e)$$

$$E_z^{n+1}(i, j,k+1/2) = E_z^n(i, j,k+1/2)$$

$$+\left[\frac{\Delta t}{\varepsilon.\Delta x}\right]\left(H_y^{n+1/2}(i+1/2, j,k+1/2)-H_y^{n+1/2}(i-1/2, j,k+1/2)\right)$$

$$-\left[\frac{\Delta t}{\varepsilon.\Delta y}\right]\left(H_x^{n+1/2}(i, j+1/2,k+1/2)-H_x^{n+1/2}(i, j-1/2,k+1/2)\right).......(3.8f)$$

To implement these equations, in Yee cell of dimension $\Delta x \Delta y \Delta z$, the there Electric field components and corresponding magnetic field components are interleaved at half discretization length and half time steps. Central difference approximation for time derivative is obtained by alternatively calculating the E and H fields at every half time step (Δt).The discretization in space and time which granted the name leap frog algorithm to this method is shown in Fig 3.7
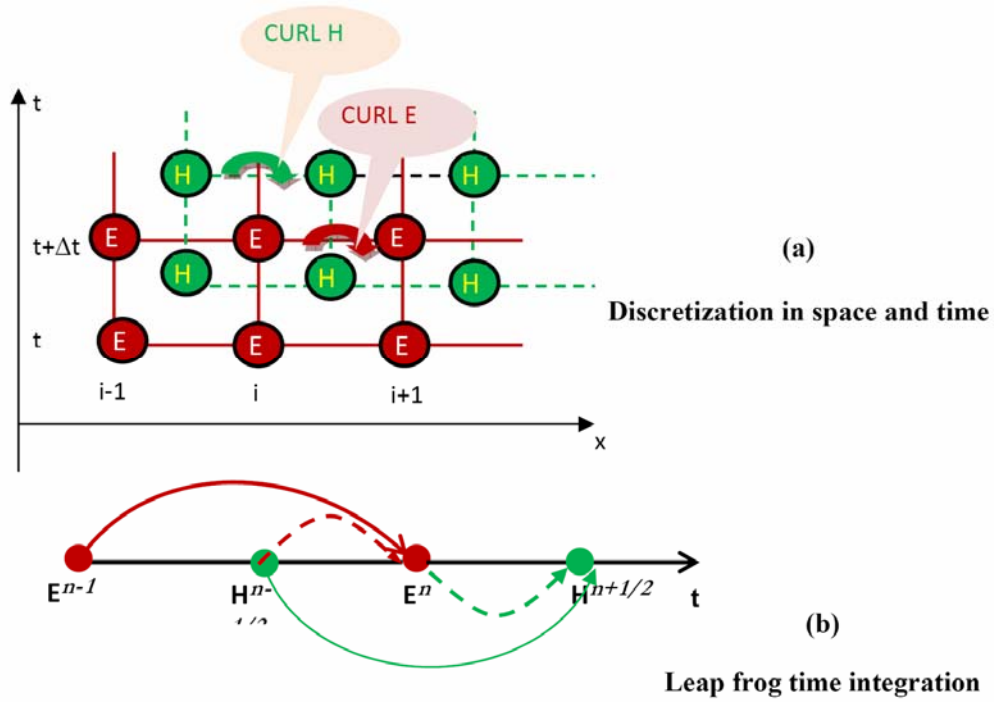
Fig 3.7 FDTD method proposed by Yee

Yee's algorithm is modified and simplified for easy programming by Sheen et al [14]. Hence for the computer implementation the explicit equations (Equn. 3.8.a-3.8.f)are modified as

$$H_{x,i,j,k}^{n+1/2} = H_{x,i,j,k}^{n-1/2} + \frac{\Delta t}{\mu \Delta z}\left(E_{y,i,j,k}^{n} - E_{y,i,j,k-1}^{n}\right) - \frac{\Delta t}{\mu \Delta y}\left(E_{z,i,j,k}^{n} - E_{z,i,j-1,k}^{n}\right) \quad ...(3.9a)$$

$$H_{y,i,j,k}^{n+1/2} = H_{y,i,j,k}^{n-1/2} + \frac{\Delta t}{\mu \Delta x}\left(E_{z,i,j,k}^{n} - E_{z,i-1,j,k}^{n}\right) - \frac{\Delta t}{\mu \Delta z}\left(E_{x,i,j,k}^{n} - E_{x,i,j,k-1}^{n}\right) \quad ...(3.9b)$$

$$H_{z,i,j,k}^{n+1/2} = H_{z,i,j,k}^{n-1/2} + \frac{\Delta t}{\mu \Delta y}\left(E_{x,i,j,k}^{n} - E_{x,i,j-1,k}^{n}\right) - \frac{\Delta t}{\mu \Delta x}\left(E_{y,i,j,k}^{n} - E_{y,i-1,j,k}^{n}\right) \quad ...(3.9c)$$

$$E_{x,i,j,k}^{n+1} = E_{x,i,j,k}^{n} + \frac{\Delta t}{\varepsilon \Delta y}\left(H_{z,i,j+1,k}^{n+1/2} - H_{z,i,j,k}^{n+1/2}\right) - \frac{\Delta t}{\varepsilon \Delta z}\left(H_{y,i,j,k+1}^{n+1/2} - H_{y,i,j,k}^{n+1/2}\right) \quad ...(3.9d)$$

$$E_{y,i,j,k}^{n+1} = E_{y,i,j,k}^{n} + \frac{\Delta t}{\varepsilon \Delta z}\left(H_{x,i,j,k+1}^{n+1/2} - H_{x,i,j,k}^{n+1/2}\right) - \frac{\Delta t}{\varepsilon \Delta x}\left(H_{z,i+1,j,k}^{n+1/2} - H_{z,i,j,k}^{n+1/2}\right) \quad ...(3.9e)$$

$$E_{z,i,j,k}^{n+1} = E_{z,i,j,k}^{n} + \frac{\Delta t}{\varepsilon \Delta x}\left(H_{y,i,j,k}^{n+1/2} - H_{y,i,j,k}^{n+1/2}\right) - \frac{\Delta t}{\varepsilon \Delta y}\left(H_{x,i,j+1,k}^{n+1/2} - H_{x,i,j,k}^{n+1/2}\right) \quad ...(3.9f)$$

using the above update equations present magnetic and electric fields are calculated from the immediate past corresponding fields and neighboring other fields. In each time step a set of electric and magnetic fields are used to generate a set of electric and magnetic field components at the next time step as shown in Fig.3.7(b).

3.6.4 Boundary conditions

Most of the Electromagnetic problems are unbounded or associated with open space regions. In the FDTD implementation of such problems requires exhaustive computational efforts and unlimited computational resources. Due to limited computational resources, the simulation domain requires truncation, which may introduce spurious fields from the boundaries unless appropriate measures are taken. Size of the computational domain is selected based on the problem under analysis. The Boundary condition should ensure that the outgoing wave is completely absorbed at the boundary, making domain appear infinite in extend with minimum numerical back reflection. The first most widely used ABC was devised by Mur in 1981 [15]. This boundary condition is derived from a one-way wave equation. However, the attenuation of waves incident on the Mur ABC degrades as the incident angle (away from the normal) increases until at the grazing angle, the boundary becomes perfectly reflecting. Hence for most of the

simulations using Mur's first order ABC at least 20cells are required between the boundary and the radiating structure. As the number of cells between the radiator and boundary is increased the outward propagating wave from the radiator approaches to the normal incidence at the truncated boundary and are subsequently absorbed better than the waves at the near grazing angle.

3.6.5 Perfect Electric Conductor (PEC) boundary

The PEC boundary is used to represent ideal conductors. This type of boundary condition deliberately reflects all incident wave energy back into the computational domain, thus limiting its size. The boundary conditions at a perfect electric conductor are such that the electric field components tangential to the surface must be zero, stated mathematically where $\vec{n}$ is a surface normal vector,

$$\vec{n} \times \vec{E} = 0 \quad \text{--} \quad (3.10)$$

in the Yee cell formulation the electric fields calculated at points on the surface of a PEC are always tangential to the surface. Thus by using the Yee cell in the FDTD scheme, the boundary condition at the surface of a PEC can be satisfied by simply setting $E_{tan} = 0$, they will remain *nearly* zero throughout the iterations. In materials finite conductivity, the update equation for the electric field component is

$$E^n = E^{n-1} \left[\frac{1 - \frac{\sigma \Delta t}{2\varepsilon}}{1 + \frac{\sigma \Delta t}{2\varepsilon}} \right] + \left[\frac{1}{1 + \frac{\sigma \Delta t}{2\varepsilon}} \right] \left[\frac{\Delta t}{\varepsilon} \right] \left(\nabla \times H^{n-\frac{1}{2}} \right) \quad \text{..............} \quad (3.11)$$

when $\sigma \gg 1$ in the above equation, $E^n \cong E^{n-1}$. In the FDTD iteration procedure, once the boundary conditions on the tangential fields are satisfied, the boundary conditions on the normal fields will be automatically valid. PEC

boundaries are used in the present investigation to model the finite ground plane and metallic strip of the printed strip monopole antenna.

3.6.6 Dielectric interface boundary

While modelling the microstrip antenna on a dielectric substrate at the interface between two media (Air and Dielectric) the discretization of Maxwell's equation become invalid. This is because in the difference equation only single value for material constants (ε and μ) are used, but in actual case there are two separate values on either side of the interface (ε_1 , $\mu._1$of air and ε_2 μ_2 of the dielectric). By applying the equivalent parameter approach introduced by Zhang and Mei [16] the condition at the interface is approximated as

$$\varepsilon_{eff} = \frac{\varepsilon_1 + \varepsilon_2}{2}$$ -- (3.12)

a detailed description of the Boundary condition applied for the truncation of the computational domain is presented in the following section.

3.6.7 First order Mur's ABC

Mur's first order ABC is derived from differential equations. Differential based ABC's are generally obtained by factoring the wave equation and by allowing a solution that permits only outgoing waves. Mur's ABC was proposed after the theoretical work by Enquist and Majda [17]. It provides satisfactory absorption for a great variety of problems and is extremely simple to implement. Mur's first order ABC looks back one step in time and one cell into the space location. For the structure considered in the thesis, the pulses on the radiating microstrip antenna will be normally incident to the outer boundary mesh walls and this leads to simple approximate boundary condition that the

tangential electric field at the outer boundary obeys one dimensional wave equation in the direction normal to the mesh wall. For the x normal wall the one dimensional wave equation can be written as

$$\left(\frac{\partial}{\partial x} - \frac{1}{c}\frac{\partial}{\partial t}\right)E_{\text{tan}} = 0 \text{ --- (3.13)}$$

by imposing above equation on a wave normally incident on planar surface, absorbing condition for a normal incident wave with out reflection can be obtained as

$$\frac{\partial E(x,t)}{\partial x} = \frac{1}{c}\frac{\partial E(x,t)}{\partial t} \text{ Where x=}\Delta x/2, \text{ t= (n+1/2) }\Delta t \text{------------------- (3.14)}$$

for updating of the electric field at

$$x = \Delta x / 2, t = (n+1)\Delta t$$.

in finite-difference form it can be written as follows:

$$\frac{E_1^{n+1/2} - E_0^{n+1/2}}{\Delta x} = \frac{1}{c}\frac{E_{1/2}^{n+1} - E_{1/2}^{n}}{\Delta t} \text{ --------------------------------------- (3.15)}$$

In this form, the finite-difference approximation is accurate to the second order in Δx and Δt. But the values at the half grid points and half time steps are not available, and can be averaged as

$$E_m^{n+1/2} = \frac{E_m^{n+1} + E_m^{n}}{2} \text{ --- (3.16)}$$

$$E_{m+1/2}^{n} = \frac{E_{m+1}^{n} + E_m^{n}}{2} \text{ --- (3.17)}$$

The equations 3.15, 3.16 and 3.17 yields a explicit finite difference equation

$$E_0{}^{n+1} = E_1{}^n + \left(\frac{c\Delta t - \Delta x}{c\Delta t + \Delta x}\right)(E_1{}^{n+1} - E_0{}^n) \quad \text{---------------------------------- (3.18)}$$

Where E_0 represents the tangential electric field component on the mesh wall and E_1 represents the tangential electric field component on node inside of the mesh wall. Similar expressions are obtained for the other absorbing boundaries by using the corresponding normal directions for each wall. But while implementing the Mur's first order boundary conditions for microstrip antenna, it should be noted that boundary walls are far enough from the radiating patch to ensure the normal incidence at the boundary walls. For the oblique incidence case the wave will reflected from the boundary walls.

For the analysis of broadband microstrip antennas presented in the thesis the above mentioned first order Mur's ABC based FDTD technique is implemented using MATLAB^{TM} . This MATLAB based code can be used for extracting antenna characteristics such as return loss, radiation pattern, gain and efficiency.

3.6.8 Numerical dispersion and stability criteria

The numerical algorithm for Maxwell's curl equation defined by finite difference equation requires that time increment Δt have a specific bound relative to the lattice dimensions Δx Δy and Δz. This bound is necessary to avoid numerical instability, an undesirable possibility of computed results to spuriously increase without the limit as time marching progresses. To ensure the computational stability it is necessary to satisfy a relation between the space increment and time increment. To ensure the stability of the time-stepping

algorithm, Δt is chosen to satisfy the Courant-Friedrichs-Lewy (CFL) Stability criterion:

$$\Delta t \leq \frac{1}{V_{max}} \frac{1}{\sqrt{1/\Delta x^2 + 1/\Delta y^2 + 1/\Delta z^2}} \qquad \text{..(3.19)}$$

V_{max} is the maximum velocity of light in the computational volume. Typically V_{max} will be the velocity of light in free space unless the entire volume is filled with dielectric. These equations will allow the approximate solution of E and H in the volume of the computational domain or mesh. In the present investigation the maximum time step is limited as 99.5% of the value given by the above equation.

The discretization of Maxwell's equations in space and time causes the variation of the phase constant of the propagating wave with frequency. For a fixed cell size different frequency components of a wave propagate at slightly different velocities. This phenomenon is referred to as numerical dispersion and is inherently present in the FDTD algorithm. Furthermore, velocity depends also on the angle of propagation with respect to the coordinate axis. This is called numerical anisotropy. For accurate and stable results, the grid dispersion error must be reduced to an acceptable level, which can be readily accomplished by reducing the cell size. Accuracy of computation can be ensured by selecting the grid size as 10 cells per wavelength (λ/10) or less at the highest frequency. In the analysis presented in the thesis the accuracy and stability are ensured by selecting Δx, Δy, Δz ≤ $\lambda_{min}/20$.

3.6.9 Luebbers feed model for fast FDTD convergence

With the transient excitation in FDTD, impedance and scattering parameters over a wide frequency band can be calculated. One difficulty with

FDTD is that for some applications, few thousands of time steps may be required for the transient fields to decay. This difficulty is common in the case of circuits having very high quality factor. One method to reduce the time steps required is to apply signal processing methods to predict the voltages and currents at later times from the results computed for early times. Instead of making FDTD calculations for the full number of time steps required for transients to dissipate, one might make actual FDTD calculations for some fraction of this total number of time steps, and use these results to predict those for the later times [18].

Applying the various prediction methods adds additional complexity to the FDTD calculation process. The prediction methods are complicated, and may require care and skill by the use to obtain accurate results. Most of the methods described require the use to determine the order of the prediction process, related to the number of terms of whatever expansion function is used to approximate the FDTD time signal. A poor choice for the order of the prediction model can result in larger precision errors.

Another simple approach is to include a source with internal resistance to excite the problem. By employing source with internal resistance which matches with the characteristic impedance of the transmission line provided accurate results while greatly reduces the number of time steps required for convergence.

3.6.10 Resistive source model

FDTD transient calculations are often excited by a hard voltage source, whose internal source resistance is zero ohms. These sources are very easy to implement in an FDTD code. The electric field at the mesh edge where the source is located is determined by some function of time rather than by the

FDTD update equations. A common choice is a Gaussian pulse, but other functions may also be used. The Gaussian pulse is significantly greater than zero amplitude for only a very short fraction of the total computation time, especially for resonant geometries such as many antennas and micro strip circuits.

Once the pulse amplitude drops the source voltage becomes essentially zero, the source effectively becoming a short circuit. Thus, any reflections from the antenna or circuit which return to the source are totally reflected. The only way the energy introduced into the calculation space can be dissipated is though radiation or by absorption by lossy media or lumped loads. For resonant structures, there are frequencies for which this radiation or absorption process requires a relatively long time to dissipate the excitation energy. Using a source with an internal resistance to excite the FDTD calculation provides an additional loss mechanism for the calculations.
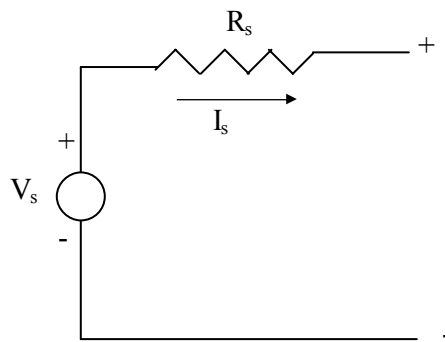
Fig 3.8 FDTD source with source resistance

Consider that it is desired to excite an FDTD calculation with a voltage source that corresponds to an electric field E in the z direction at a certain mesh location $i_s \Delta x, j_s \Delta y, k_s \Delta z$, described using the usual Yee notation. The

corresponding equivalent circuit for a voltage source which includes an internal source resistance Rs is illustrated in Fig. 3.8 If the source resistance Rs is set to zero then the usual FDTD electric field at the source location is simply given by

$$E_s^n (i_s, j_s, k_s) = \frac{V_s (n\Delta t)}{\Delta z}$$ --- (3.69)

Vs is any function of time, often a Gaussian pulse.

However, with the source resistance included, the calculation of the source field $E_s^{\ n}(i_s, j_s, k_s)$ at each time step is complicated slightly. To determine the terminal voltage V of Fig. 3.8 and, thus, the FDTD electric source field $E_s^{\ n}(i_s, j_s, k_s)$, the current through the source must be determined. This can be done by Ampere's circuital law, taking the line integral of the magnetic field around the electric field source location. The current through the source is then given by

$$I_s^{\ n-1/2} = \left(H_x^{\ n-1/2}(i_s, j_{s-1}, k_s) - H_x^{\ n-1/2}(i_s, j_s, k_s)\right)\Delta x +$$
$$(H_y^{\ n-1/2}(i_s, j_s, k_s) - H_y^{\ n-1/2}(i_{s-1}, j_s, k_s))\Delta y$$ ....(3.70)

so that by applying Ohm's law to the circuit of Fig. 3.8 the electric source field is given by

$$E_s^{\ n}(i_s, j_s, k_s) = \frac{V_s(n\Delta t)}{\Delta z} + \frac{I_s^{\ n-1/2} R_s}{\Delta z}$$ ....(3.71)

if Rs=0, in this equation, then the usual hard-voltage source results. The value of the internal resistance does not appear to be critical. A reasonable choice for Rs is to use the value of the characteristic impedance of the transmission line. In the thesis Rs is selected as 50Ω.

3.6.11 Staircase transition for microstrip line feed

The microstrip excitation presented in the thesis is implemented by using Luebber's [19] approach of stair cased FDTD mesh transition from electric field sources location to the full width of the microstrip transmission line. Compared to the "hard" voltage source excitation this approach provides accurate results with reduced computational time. For implementing the stair cased transition in microstrip line the substrate is discretized in order to incorporate more than one Yee cell. A gap feed model can be obtained by applying the excitation field between the microstrip line and the ground plane using a stair cased mesh transition as shown in Fig.3.9.
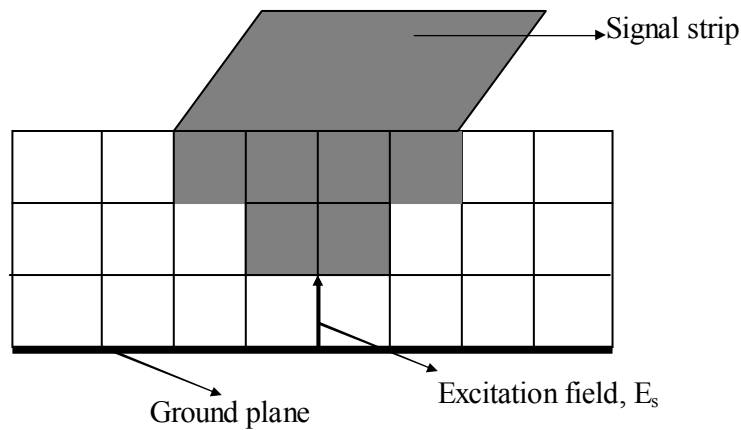
Fig 3.9 Stair cased feed model for microstrip line in FDTD

3.6.12 Excitation source modeling.

Proper excitation of the computational domain excites a field distribution closely resembling that of the physical structure. On the other hand, improper excitation leads to spurious solutions. For the antenna analysis in time-domain a narrow pulse is usually used as the excitation pulse to extract the frequency-domain parameters in the entire frequency range of interest by Fourier

transform of the transient results. The frequency band of interest decides the width of the pulse. A narrow pulse ensures wide band performance. To avoid the unnecessary noise appearing in the FDTD generated response, the excitation pulse and its spectrum must have a smooth roll off and low side lobes.

A sine wave or a Gaussian pulse can be used as the input signal for the 3D FDTD method. However, a Gaussian pulse plane wave is the most widely specified incident field as it provides a smooth roll off in frequency content and is simple to implement. In addition, the frequency spectrum of a Gaussian pulse is also Gaussian and will therefore provide frequency domain information from dc to the desired cut off frequency by adjusting the pulse width. The Gaussian input is of the form

$$g(t) = e^{-\left(\frac{(t-t_0)^2}{T^2}\right)}$$ --- (3.72)

where t_o is the pulse delay and T relates to the Gaussian half width, which sets the required cut off frequency. Writing in the discrete form,

$$g(n\Delta t) = e^{-\left(\frac{(n\Delta t - t_0)}{T}\right)^2}$$ --- (3.73)

where T = N Δt and t_o = 3T. Thus the pulse is sampled N times in a pulse half widthT. The Gaussian pulse and its spectrum are shown in Figure 3.10. It is evident from the figure that the pulse provides relatively high signal levels up to the desired frequency. The parameter N can be changed to achieve sharper frequency roll off. In the FDTD method, all functions are assumed to be causal. Therefore, to satisfy the initial condition of zero excitation at the zeroth time step, the time of origin of the Gaussian pulse must be shifted by t_o ($t_o \gg 1$). To ensure proper initial value conditions a time delayed Gaussian pulse $t_0 = 3*T$ is employed in the thesis.

In order to simulate a voltage source excitation in a Microstrip fed structure, a vertical electric field E_s can be imposed in between the ground plane and the microstrip line as shown in Fig 3.10. This electric field is defined using the Equn.3.74 with the voltage source as Gaussian pulse.

$$V_s = e^{-\left(\frac{(t-t_0)^2}{T^2}\right)} \text{--- (3.74)}$$
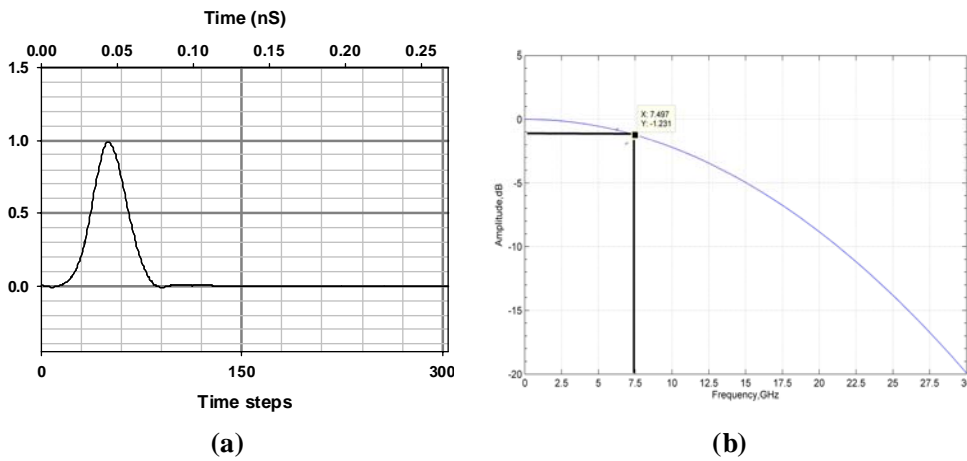
Fig. 3.10 (a) Gaussian pulse   (b) Gaussian spectrum

Gaussian pulse is usually used for the extracting the antenna characteristics such as return loss, impedance bandwidth, input impedance etc. Sinusoidal excitation is usually used to extract the radiation characteristics at a particular frequency of interest. A sinusoidal function of the following form is usually used for extracting the near field data at a particular frequency.

$$E(t) = E_0 Sin(2\Pi ft)$$

Where E_0 determines the peak amplitude and 't=n*Δt' is the current instant of time.

3.6.13 Flowchart of Yee algorithm

MATLAB based numerical code is developed for the parametric analysis of the antenna. The Flow chart used for extracting the antenna reflection characteristics are depicted in Fig.3.11
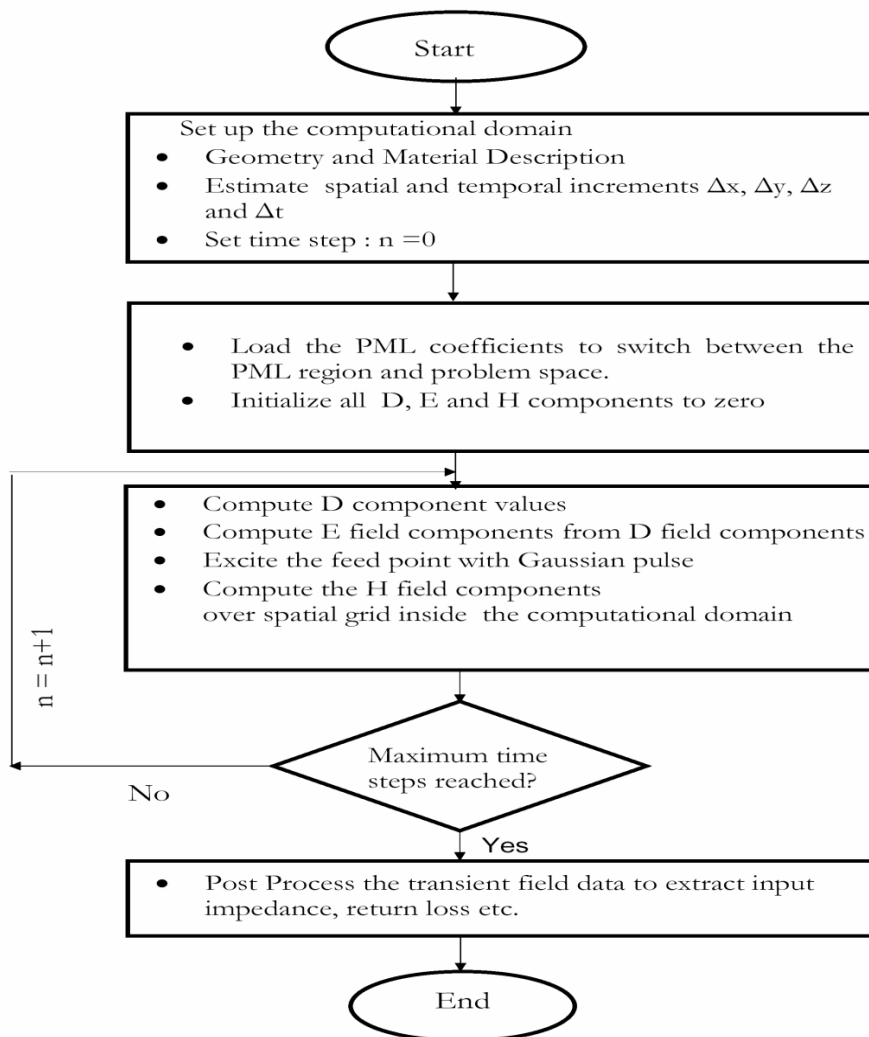
Fig.3.11 The FDTD flow chart

3.7 Antenna characteristics using FDTD

FDTD algorithm performs the transient analysis of the antenna under investigation .Fourier transform of the transient data gives the frequency domain information over the frequency range of interest. Current and voltage samples are taken from the fixed points in the FDTD grid and Fast Fourier Transform (FFT) is used to compute the frequency domain information. Since for our analysis FFT can provide results with god accuracy FFT is used instead of DFT. By suitably post processing this information the reflection characteristics can be extracted as outlined in the section below.

The voltage at the input port location is computed from the E_z field components at the feed point over the entire simulation time interval. The current at the feed point is calculated from the H field values around the feed point using Ampere's circuital law. The input impedance of the antenna is computed from the Eqn 3.75

$$Z_{in}(\omega) = \frac{FFT(V^n, P)}{FFT(I^{n-1}, P)}$$ -- (3.75)

Where P is the suitable Zero padding used for taking FFT, $V^n = E_z^n * \Delta z$

Since microstrip line is modeled using Leubber's staircase approach as explained in section 3.6.9, the internal impedance of source resistance Rs is taken as the characteristic impedance (Z_0) of microstrip line.

Reflection coefficient is given as $\Gamma(\omega) = \dfrac{Z_{in} - Z_0}{Z_{in} + Z_0}$ ....(3.76)

Return loss in dB, $S_{11} = 20\log_{10}\Gamma(\omega)$ ....(3.77)

The return loss computed in the above process is processed for extracting the fundamental resonant frequency and 2:1 VSWR bandwidth corresponding to the -10dB return loss.

3.8 References

[1]   HP8510C Network Analyzer operating and programming manual, Hewlett Packard, 1988.

[2]   Design, Development and Performance Evaluation of an Anechoic Chamber for Microwave Antennas Studies, E. J. Zachariah, K. Vasudevan, P. A. Praveen Kumar, P. Mohanan and K. G. Nair, Indian Journal of Radio and Space Physics, Vo. 13, February 1984, pp. 29-31.

[3]   C. A. Balanis, "Antenna Theory: Analysis and Design", Second Edition, John Wiley & Sons Inc. 1982.

[4]   John D. Kraus, "Antennas", Mc. Graw Hill International, second edition, 1988.

[5]   Jongh R.K, M. Hajian, L.P Lighthart, "Antenna time-domain measurement techniques", IEEE Antennas and Propagation Magazine, No. 39, Vol. 5, page No. 7-12.

[6]   Sorgel W, S. Knorzer, W. Wiesbeck, "Measurement and evaluation of ultra wide band antennas for communications", International ITG Conference on Antennas-INICA2003, Page No. 377-380.

[7]   HFSS User's manual, version 10, Ansoft Corporation, July 2005.

[8]   K.S.Yee, "Numerical solution of initial boundary value problems involving Maxwell's equations in isotropic media," *IEEE Trans. Antennas Propagat.,* vol.14, no.4, pp.302-307, May 1966.

[9]   Allen.Taflove, "Numerical issues regarding finite-difference time-domain modelling of Microwave structures," *Time-Domain Methods for Microwave structures – Analysis and Design,* Ed.Tatsuo Itoh and Bijan Houshmand, *IEEE Press..*

[10]   Allen Taflove and Morris E. Brodwin, "Numerical solution of steady – state electromagnetic scattering problems using the time-dependent Maxwell's equations," *IEEE Trans. Microwave Theory Tech.*, vol.23, pp.623-630, August 1975.

[11]   Kurt L.Shlager and John B.Schneider, "A selective survey of the Finite-Difference Time-Domain literature," *IEEE Antennas Propagat. Mag.*, vol.37, no.4, pp.39-57, August 1995.

[12]   Z. Chen, M. Ney, and W.J.R. Hoefer, "A new finite-difference time-domain formulation and its equivalence with the TLM symmetrical condensed node," *IEEE Trans. Micro. Theo. Tech.*, vol. 39, no. 12, Dec. 1992, pp. 2160–2169.

[13]   Andrew F. Peterson,Scott L Ray and Raj Mittra," Computational methods for Electromagnetics", University Press, India,2001,Ch.12.

[14]   David.M.Sheen, Sami.M.Ali, Mohamed D.Abouzahra and Jin Au Kong, "Application of the Three-Dimensional Finite- Difference Time-Domain method to the analysis of planar Microstrip circuits, "*IEEE Trans. Microwave Theory Tech.*, vol.38, no.7, pp.849-857, July 1990.

[15]   G. Mur, "Absorbing Boundary Conditions for the Finite Difference Approximation of the Time-Domain Electromagnetic Field Equations," *IEEE Trans. Electromagn. Compat.*, Vol .EMC-23, Nov. 1981, pp. 377-382.

[16] X.Zhang,J.Fang,y.Liu and K.K Mei, "Calculation of dispersive characteristics of Microstripes by time domain finite difference method", IEEE Trans.Mirowave theory and tech. vol 36,pp.263-267,1988.

[17] Enquist and Majada, "Absorbing Boundary Conditions for the Numerical simulation of waves", Mathematics of computation, Vol. 31, 1977, pp. 629-651.

[18] Sullivan Dennis M, "Electromagnetic simulation using the FDTD method", IEEE press series on RF and Microwave Technology, USA.

[19] R.J Leubbers and H.S Langdon., "A simple feed Model that reduces Time steps Needed for FDTD Antenna and Microstrip Calculations" IEEE Trans. Antennas and Propogat.Vol.44,No.7,July 1996, pp.1000-1005.

.....౹౦�খ.....

INVESTIGATIONS ON A STRIP LOADED SLOTTED BROADBAND SQUARE MICROSTRIP ANTENNA FOR WIDEBAND APPLICATIONS

The fundamental investigations towards the development of impedance matching strip loaded slotted square patch antennas are described in this chapter. A rectangular metal strip is incorporated on the top corner of the slot of a square patch antenna to achieve wideband impedance matching characteristics. The added metal strip achieves impedance matching for the resonant modes of the slotted patch with an additional third resonance which merges together with the matched resonances of the patch to broaden antenna bandwidth. Exhaustive parametric analysis has been carried out to find out the effect of the slot and strip dimensions on antenna reflection characteristics. The design equations of the antennas are formulated and are validated on different substrates. Experimental and simulation studies are conducted for both the tilted square slot loaded and polygonal slot loaded microstrip antennas. Finally, L-strip feeding mechanism is successfully implemented on the polygonal slotted strip loaded square patch antenna to enhance the bandwidth of the antenna further.

4.1   Metal strip for impedance matching: an overview

The latest trend in antenna design is to reduce the size and weight. The reduction in size of the antenna imposes fundamental limitations on the antenna performance. Along with reduction in size, the antenna should cater the requirements of high gain and wide bandwidth. In conventional wire monopole antennas, one simple way to reduce the size of a monopole antenna is to load a positive reactive component, such as a coil, at the feed point or a short circuited transmission line with a length less than a quarter wavelength etc. The resistance of short antennas becomes very low at the resonant frequency when the size of the antenna is reduced.

In the case of microstrip antennas, reduction in size is achieved by implementing slot or ring antennas. The resonant wavelength for the dominant mode of operation of a microstrip ring antenna is nearly equal to the average circumference of the ring. This mode achieves compact operation. But, the input impedance is large at the edge of the strip and only a slight variation is noted along the sides of the patch antenna. For a square ring microstrip antenna, the width of the slot (W_1) to that of the patch (W_2) plays a crucial role in impedance matching. It must be less than 0.4 to achieve 50 Ω impedance matching for probe feeding. A larger value of W_2/W_1 increases compactness, but the impedance matching performance deteriorates. This can be effectively overcome by loading the ring antenna. The field at the load will fix the field distribution on the rest of the ring. For a short circuit load the electric field will be zero at the load and the input impedance vary accordingly along the periphery of the ring. By properly selecting the feed position with respect to the load, 50 Ω impedance matching can be easily achieved. But, for a short circuited post, we cannot control the radiation characteristics of the antenna. Ramesh Garg [1] proposed a remedy to this problem by loading a rectangular

open circuited stub on the same plane of the edge fed microstrip ring antenna. It is found that two modes are existing in the loaded ring, one remains constant with the load and the other is the mode offered by the unloaded square ring antenna. The feed location can be optimized to excite any of the two modes depending upon its distance from the load.

The loaded metal strip can also be utilized to achieve broadband impedance matching for microstrip antenna. Lee et. al [2] utilized an L-shaped metal strip at the end of the microstrip transmission line, like a step along the Z-axis, to achieve broadband impedance matching characteristics for a rectangular microstrip antenna operating in the TM_{01} mode. The antenna is loaded at a height of $0.1245\lambda_0$ from the microstrip feed line, so that, without the L-strip, there exists only a weak electromagnetic coupling between the patch and the feed line and hence the antenna offers poor impedance matching characteristics. The L-strip introduced at the end of the feed line reduces the spacing between the feed line and the patch and it couples more electromagnetic energy into the patch and hence matching performance is improved. The horizontal part of the L-strip having a dimension less than $\lambda_0/4$ provides a capacitance to suppress the inductance introduced by the vertical part of the L-strip. The L-strip, in effect, acts like a series L-C resonant element connected in series with the parallel RLC resonant element of the patch, thereby enhancing the bandwidth.

In the present design, efforts have been attempted in order to bring the impedance matching strip on the same plane of the patch antenna. The design eliminates the need of additional spacers required for supporting the patch, thereby reducing the fabrication complexities. The strip incorporated on the top portion of the tilted square slotted and polygonal slotted square microstrip patch

antenna attains impedance matching for the resonant modes of the slot loaded square patch antenna and in addition, it contributes another resonance with the patch. This chapter is divided into three sections. The first section deals with the experimental and simulation studies towards the development of a tilted square slot loaded broadband microstrip patch antenna. Detailed parametric analysis are performed to find out the effect of antenna parameters on reflection characteristics and finally the current pattern of the antenna are analysed to find out the resonant mechanism behind broadband operation of the antenna. In the second section, a polygonal slot is taken into consideration. Similar analysis done in the first section is performed to find out the resonant mechanism of the antenna. In the final section, the L-strip feeding mechanism is implemented on the strip loaded polygonal slotted broadband patch antenna to achieve impedance matching for the higher order modes of the patch thereby enhancing the bandwidth of the antenna further.

4.2 Evolution of the antenna

In this section, the steps followed for attaining broadband operation of a square microstrip antenna are discussed. The evolution of the antenna is shown in fig 4.1. The initial design is an electromagnetically coupled Square Microstrip Patch Antenna (MPA) designated as Antenna I. Antenna I is the reference antenna since other structures are derived from this structure. A 45^0 tilted square slot is introduced at the centre of the square patch to yield Antenna II. The final antenna is obtained by incorporating a rectangular metal strip on the top portion of the slot of Antenna II and it is named as Antenna III. The experimental and simulation studies of the three antennas are discussed in the following sections.

セ
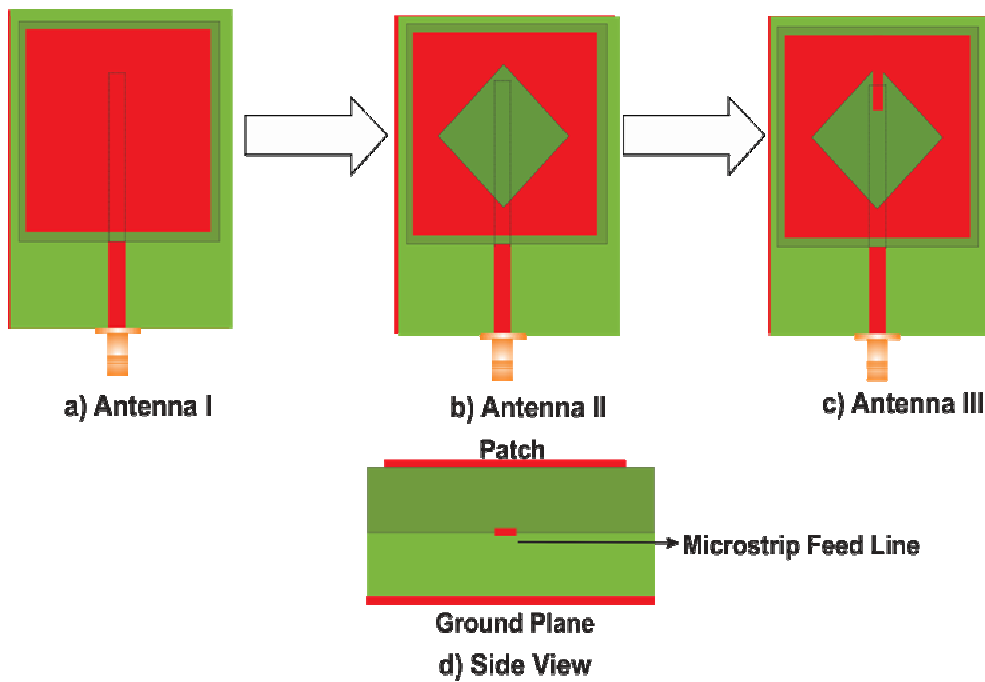
Fig. 4.1 Evolution of the antenna

4.2.1 Electromagnetically coupled square patch antenna

In this section, the simulation studies of a simple electromagnetically coupled patch antenna (antenna I) are taken into consideration. Initially a square patch of dimension $L_1 X \ L_1$ mm^2 is fabricated on a substrate of dielectric constant 4.2 and height h=1.6mm. The antenna is electromagnetically coupled using a 50 ohm microstrip transmission line fabricated using the same substrate. The width of the transmission line, W_f is calculated using the standard design equation of the microstrip transmission line [3]. The antenna fabrication is done by adopting standard photolithographic procedures. The geometry of the antenna is shown in fig. 4.2.
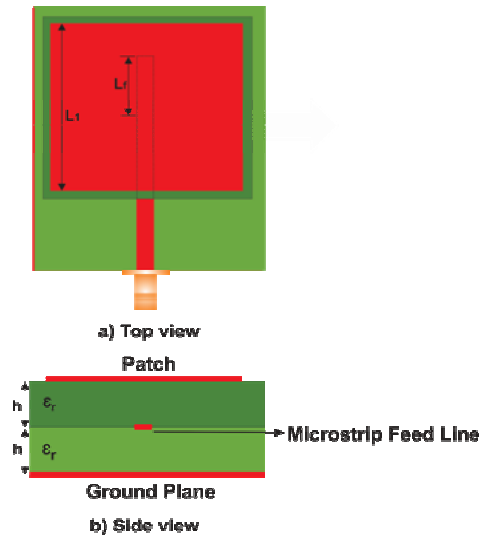
Fig. 4.2 Electromagnetically coupled square patch antenna (Antenna I)

The feed line lies along the line of symmetry of the patch along the X-axis. The feed offset parameter from the centre of the patch to the top end of the mirostrip transmission line is denoted by L_f and is maintained at 10.55mm. The total height of the antenna is 3.2mm. The Ground plane dimension is selected to be 44X55 mm^2 (W_gXL_g).

4.2.1.1 Reflection characteristics

The simulated reflection characteristics of the electromagnetically coupled square microstrip patch antenna at the selected feed point is taken with geometrical parameters held at L_1=35mm, L_f=10.55mm, W_f=3mm, L_g=55mm, W_g=44mm and h=1.6mm and is shown in fig 4.3(a). It can be seen that there is a poorly matched first resonance around 4.69 GHz and a well matched second resonance centered around 5.97 GHz. The reflection coefficient values at the resonances are found to be -7.38 dB and -24.27 dB respectively. The input impedance of the antenna is a good tool for finding the reason for the impedance mismatch. The input impedance variations of the proposed antenna are also

shown in fig 4.3(b). The input impedance at the resonances is found to be 28.8-j28.8 ohms and 47.7-j3.8 ohms respectively.
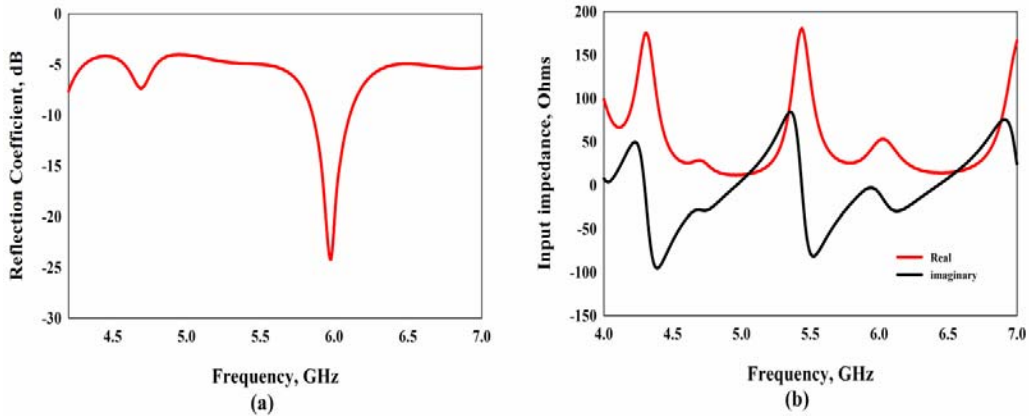
Fig. 4.3 a) Reflection characteristics and b) Input Impedance of antenna I

4.2.2 Electromagnetically coupled slot loaded square patch antenna

In order to incorporate the impedance matching strip on the same plane of the patch antenna, a 45^0 tilted slot of dimension L_2XL_2 mm^2 is etched on the centre of antenna I.
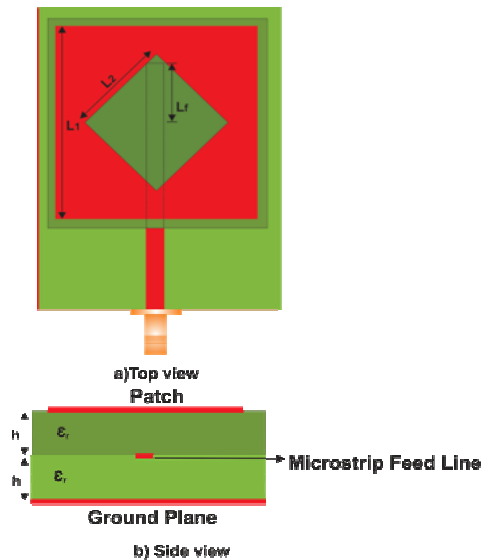
Fig. 4.4 Slot loaded square patch antenna (Antenna II)

The geometry of the proposed design (antenna II) is shown in fig 4.4. The antenna parameters are L_1=35mm, L_2=17.5mm, L_f=10.55mm, W_f=3mm, L_g=55mm, W_g=44mm and h=1.6mm.
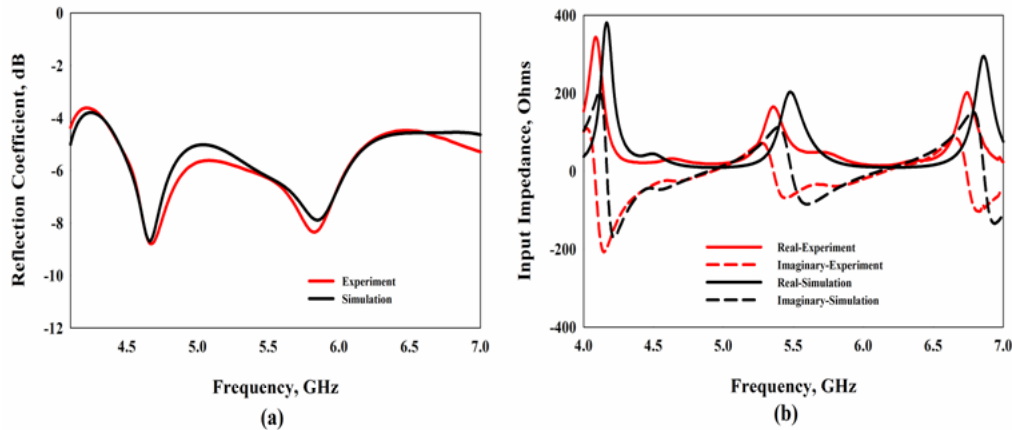
Fig. 4.5 a) Reflection characteristics and   b) Input Impedance of antenna II

The reflection characteristics of this slot loaded square microstrip antenna are shown in fig 4.5(a). The experimental and simulation results show good agreement. It is observed that the two resonant frequencies are found to be lowered as compared to the resonances of the antenna without the slot (Antenna I). The new lowered resonant frequencies are found to be at 4.67 GHz and 5.82 GHz. It is also seen that the impedance matching at both the resonant frequencies are found to be deteriorated. The reflection coefficient values at the resonances are found to be 8.8dB and 8.4dB respectively. The reason for poor impedance matching can be explained with the help of the input impedance plot of the antenna. Fig 4.5(b) shows the input impedance plot of the antenna. The input impedances are found to be 30-j26 ohms and 36-j36 ohms at the resonances. It can be concluded that the slot adds capacitive reactance for the second resonance which deteriorates the impedance matching performance at the resonances.

4.2.3 Electromagnetically coupled strip loaded square patch antenna

Broadband impedance matching for the slot loaded microstrip patch antenna (Antenna II) can be brought about by properly inserting a rectangular metal strip on the top portion of the slot. This will make the impedance matching strip on the same plane of the antenna, thereby reducing the complex fabrication of the impedance matching circuitry as an extension of the microstrip transmission line as in the case of [2]. The dimension of the strip is denoted by L_3XW mm^2. The geometry of the proposed design is shown in fig 4.6. The patch antenna layout used for the FDTD computational domain is also shown in the same figure.

a) Top view

c) Detailed view

b) Side view

c) Layout of the computational domain
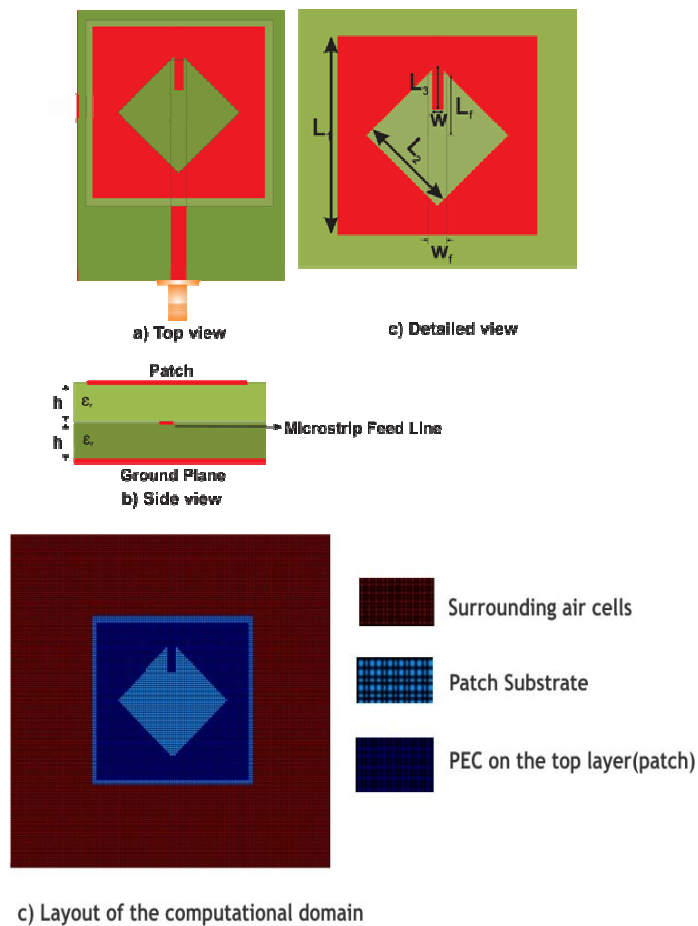
Fig. 4.6 Strip loaded antenna (Antenna III)

4.2.3.1 Reflection characteristics

The antenna is simulated using FDTD code implemented in MATLAB$^{TM.}$ The built in FFT function of the MATLAB is used to extract the frequency domain characteristics. The entire computational domain is divided into Yee cells of dimensions $\Delta x=\Delta y=0.5$mm and $\Delta z=0.4$mm which ensures the minimum discretization error. Maximum frequency of operation is selected as 7GHz so that spatial discretization is less than $\lambda/20$ of the maximum frequency of operation. The substrate is discretized as 4 cells in the Z direction and 10 air cells were assigned on each side of the substrate periphery to ensure the practical condition of surrounding air. The dielectric cells in contact with the air boundary are assigned the effective dielectric constant value to ensure the air dielectric interface. Microstrip feed is modeled using Leubber's technique as outlined in chapter 3. The input Gaussian pulse facilitates to extract the wideband characteristics of the printed microstrip antenna. The reflection characteristics of the antenna at the optimum design are shown in fig 4.7. The antenna parameters are $L_1=35$mm, $L_2=17.5$mm, $L_3=7.8$mm, $L_f=10.55$mm, $W_f=3$mm, $L_g=55$mm, $W_g=44$mm and $h=1.6$mm at the optimum design. The experimental, simulated and the computed results are in good agreement. It is observed that broadband impedance matching is obtained by merging three resonances centered around 4.5 GHz, 5.6 GHz and 6.14 GHz. The antenna has a 2:1 VSWR bandwidth of 38% from 4.3 GHz to 6.33 GHz. This frequency range is wide enough to cover IEEE 802.11a (5.15-5.35 GHz, 5.725-5.825 GHz), HIPERLAN2 (5.45-5.725 GHz) and HiSWANa (5.15-5.25 GHz) communication bands.
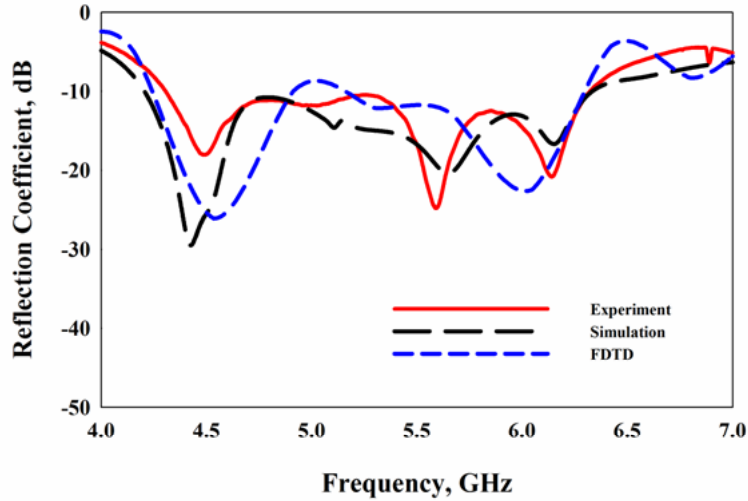
Fig. 4.7 Reflection characteristics of antenna III

4.2.3.2 Strip Length variation

The dimension of the added metal strip plays a crucial role in achieving broadband impedance matching performance of the antenna. It provides impedance matching for the two modes of the tilted square slotted patch antenna and the introduction of the strip provides another third resonance. These three resonances merge together to provide a wide bandwidth for the antenna. Therefore the selection of the strip length (L_3) and width (W) is the major step in the optimization process. A thorough parametric analysis has been performed to find out the effect of the strip length L_3 on reflection characteristics of the antenna. Fig 4.8.a shows the effect of strip length on reflection characteristics of the antenna with strip width (W) maintained at 2mm. Here, the strip length L_3 is varied from 1.8mm to 9.8mm in steps of 1mm.

It can be seen that without the strip there exists only two poorly matched resonances, one at 4.67 GHz and the other at 5.82 GHz which is same as the reflection characteristics of antenna II. As the strip length increases impedance matching corresponding to the two resonances

increases and an optimum length of L$_3$=7.8mm is selected to obtain the maximum achievable bandwidth. Also, the two resonances are shifted towards the lower side with increase in L$_3$. The strip also produces an additional third resonance which merges together with the initial two resonances to give broadband operation.
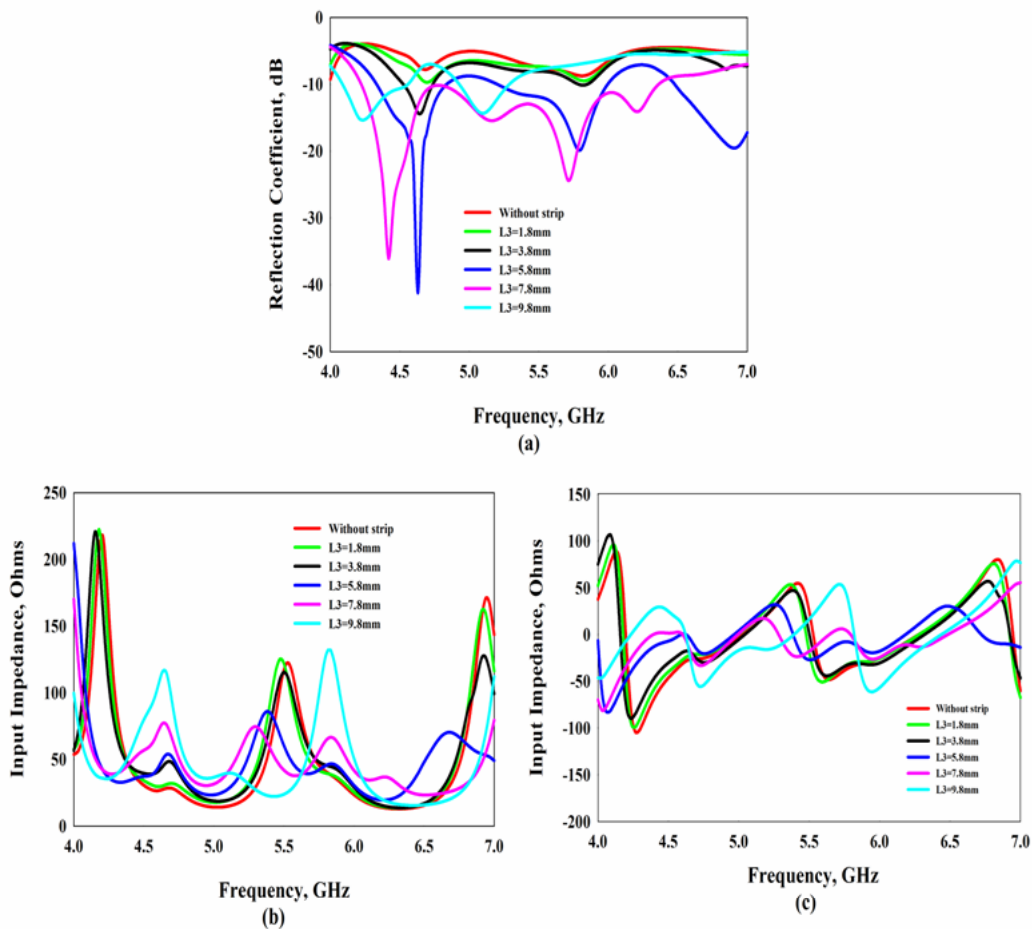
Fig. 4.8 Effect of strip length variation on a) Reflection characteristics, b) Real impedance and c) Imaginary impedance

The strip has a crucial role on the impedance matching performance of the antenna. The input impedance variation of the antenna with strip length

is also shown in fig 4.8. It can be seen that without the strip the input impedances are found to be 27.5-j27.6 ohms and 38.7-j33.8 ohms respectively for the first two resonances. The impedance mismatch can be accounted due to the presence of the high capacitive reactance. Increasing the strip length increases the real part of the impedance for both the resonances and the imaginary part shifts towards the inductive side. Thus, the strip effectively suppresses the high capacitive reactance offered by the slot and we can conclude that the strip acts as a series LC circuit connected in series with the slot antenna to improve the impedance matching performance of the slot loaded antenna.

4.2.3.3 Effect of slot and strip dimensions

The previous section deals with the strip length variation when the slot dimension (L_3) held at 17.5mm and the strip width (W) at 2mm. Here, the parameters under consideration are the slot and strip dimensions. For each slot dimension the strip length is varied for different strip widths. The results are illustrated from fig. 4.9 to fig. 4.28. From this parametric analysis, the broadband design which yields a lower initial resonant frequency having maximum bandwidth is selected as the optimum design. The optimum dimensions of the slot and strip are found to be L_2=17.5mm, L_3=7.8mm and W=2mm.

$L_2=15.5mm$
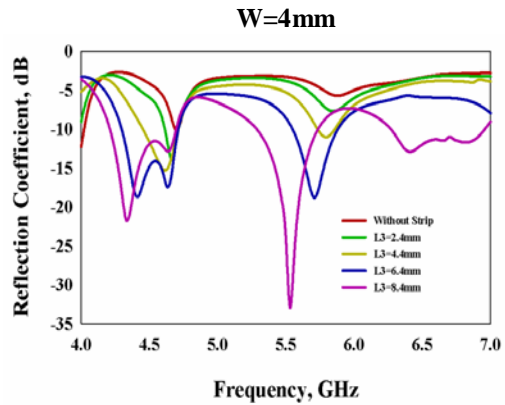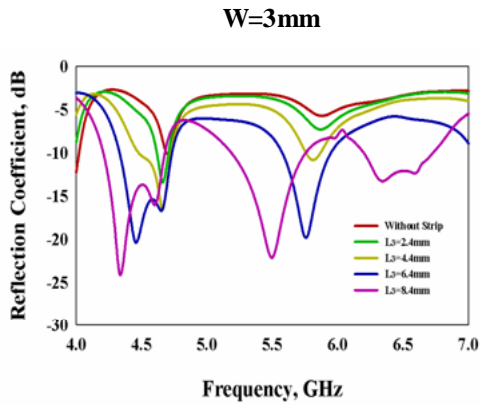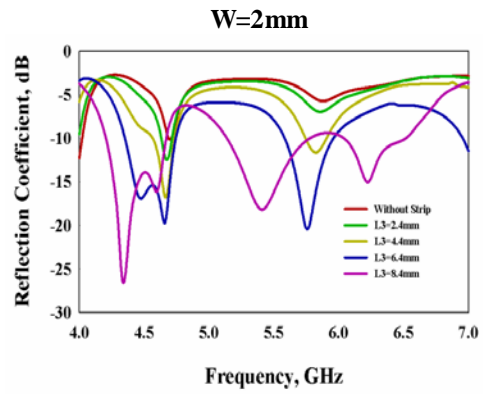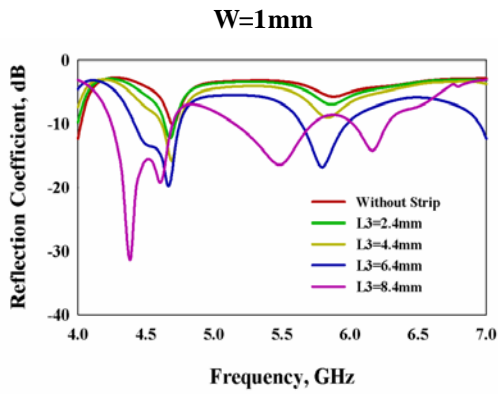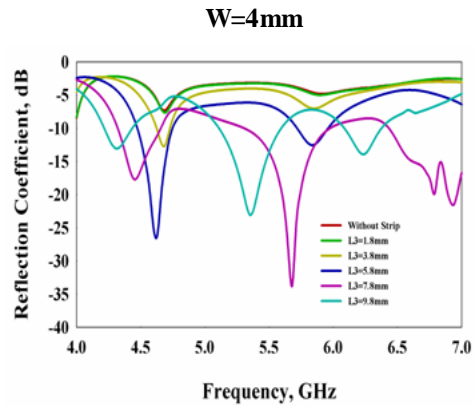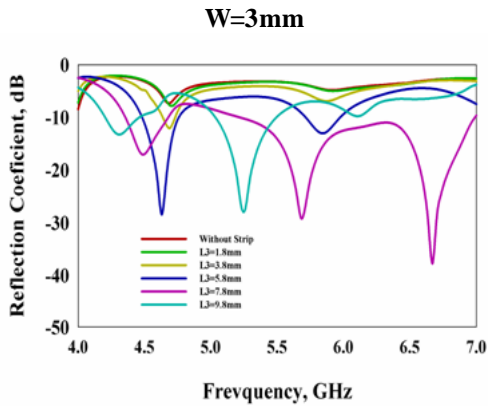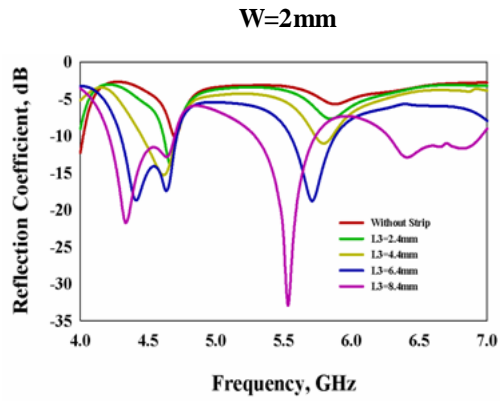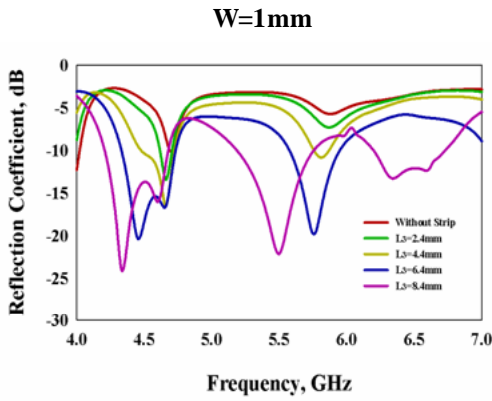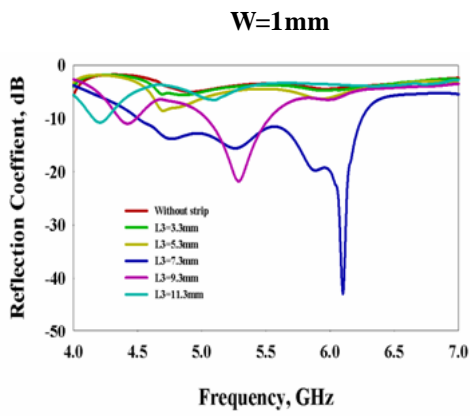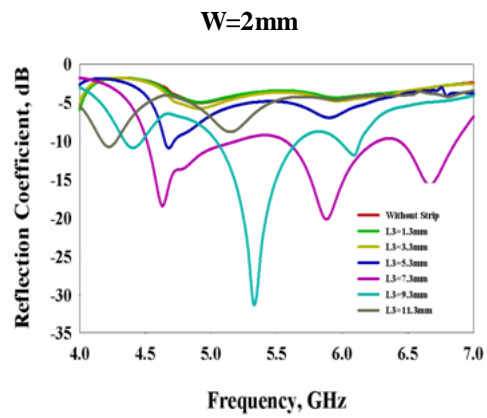
W=1mm

Fig. 4.9

W=2mm

Fig. 4.10

W=3mm

Fig. 4.11

W=4mm

Fig. 4.12

L₂=17.5mm

W=1mm

Fig. 4.13

W=2mm

Fig. 4.14

W=3mm

Fig. 4.15

W=4mm

Fig. 4.16

L$_2$=19.5mm

W=1mm

Fig. 4.17

W=2mm

Fig. 4.18

W=3mm

Fig. 4.19

W=3mm

Fig. 4. 20

L$_2$=21.5mm

W=3mm

Fig. 4.21

W=4mm

Fig. 4. 22

W=3mm

Fig. 4.23

W=4mm

Fig. 4. 24

L₂=23.5mm

W=1mm

Fig. 4.25

W=2mm

Fig. 4. 26

W=3mm

Fig. 4.27

W=4mm
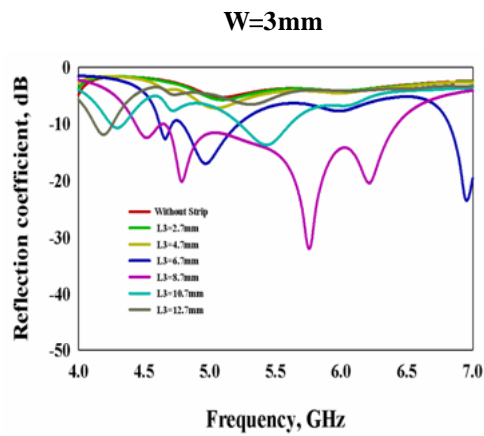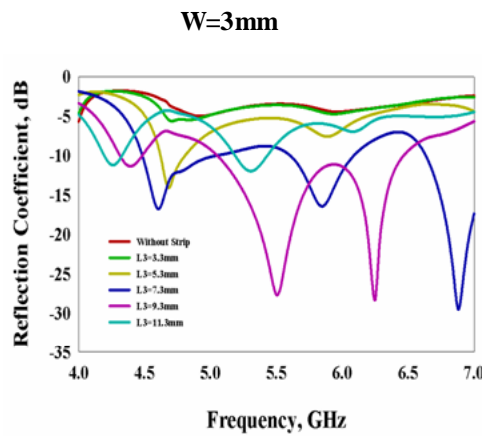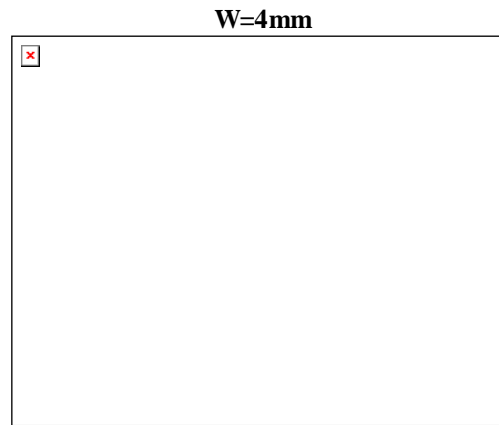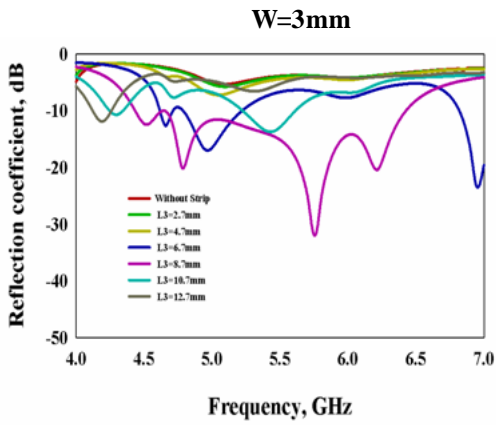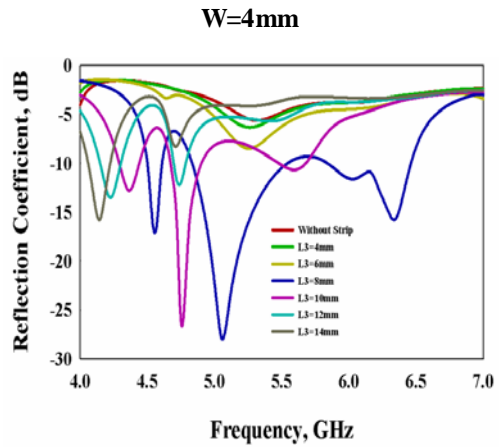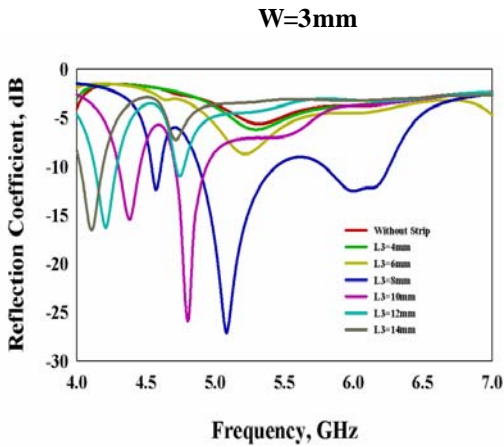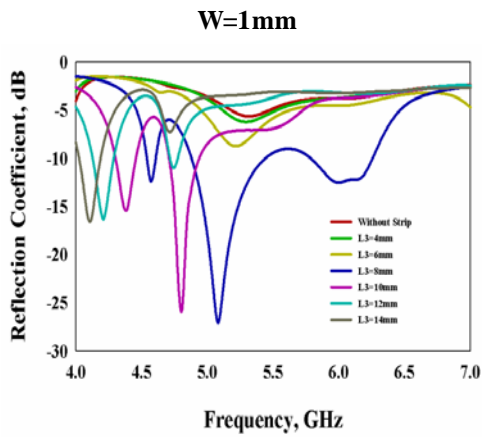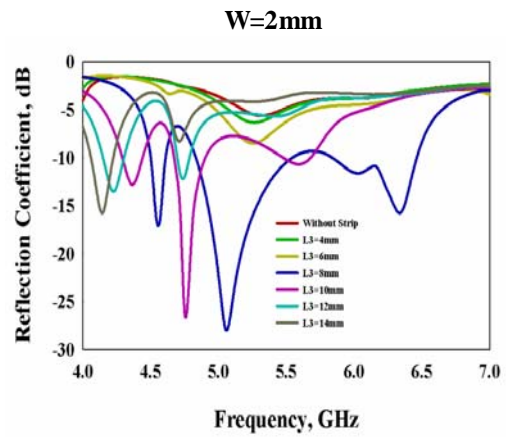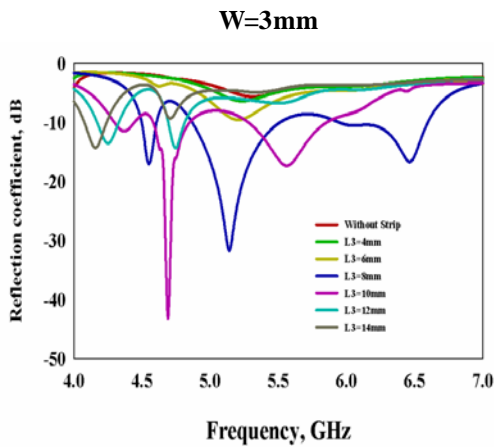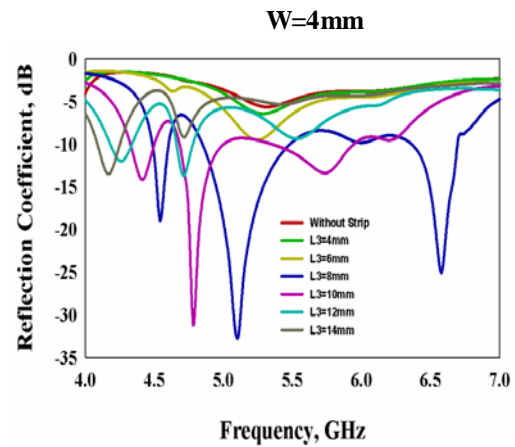
Fig. 4. 28

4.2.3.4 Substrate height variation

Here the parameter under consideration is the height of the patch and the feed substrate. During the analysis the dielectric constant of the substrate is maintained at 4.2. Generally speaking, the height of the substrate plays a crucial role on the microstrip antenna impedance bandwidth characteristics. Usually, increasing the antenna thickness broadens the bandwidth. For a coaxially fed single layer patch antenna, when the substrate height is of the order of 0.05λ, the increased inductive reactance of the probe deteriorates antenna impedance matching performance.

Initially, the height of the patch substrate alone is varied and fig 4.29 shows the effect of the height of the patch substrate on antenna reflection characteristics. It can be seen that below h=1.6mm, the resonances are not properly merged. When the height is increased above 1.6mm, matching for the third resonance starts deteriorating and at h=3.2mm, the third resonance vanishes.
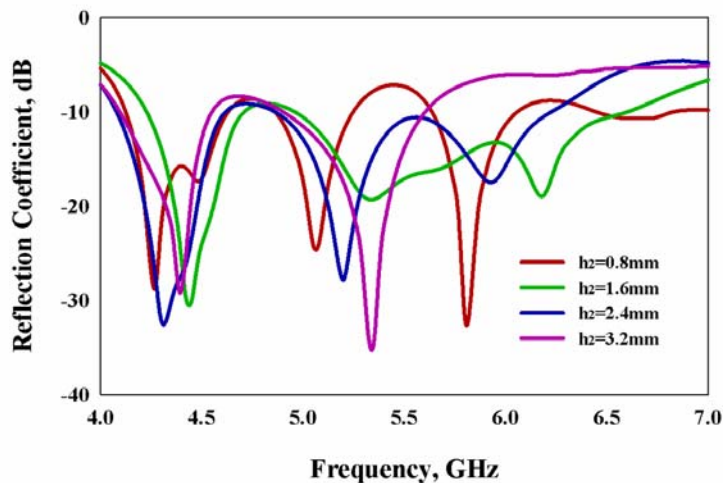
Fig. 4.29 Effect of patch substrate height

Finally, the height of both the feed line and patch substrates are varied. The transmission line width W_f is maintained to have 50 Ω input impedance as per the design equation [3]. The variation is made from 0.8mm to 3.2mm in steps of 0.4mm. Fig. 4.30 shows the effect of substrate thickness on the reflection characteristics of the antenna. It can be seen that below h=1.6mm, the resonances are not properly merged. Increasing the value of height above 1.6mm shifts the lower frequency to the lower side, but impedance matching corresponding to the third resonance is found to be deteriorating. The third resonance vanishes for variations above h=2.4mm because of the poor coupling between the feed line and the patch.
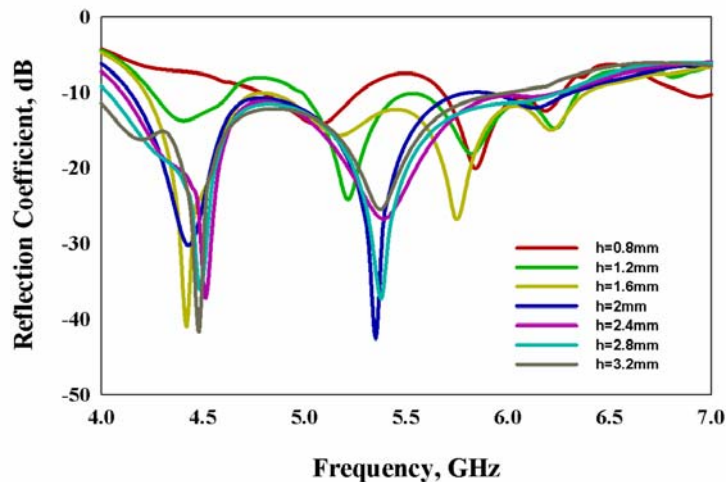
Fig. 4.30 Effect of patch and feed line substrate height variation

4.2.3.5 Feed variation studies

The length of the feed plays an important role on the broadband impedance matching characteristics because it determines the merging between the individual resonances. Here the feed length parameter L_f, measured from the centre of the patch antenna, is varied. The variation in the reflection

characteristics of the antenna with the feed length is shown in fig. 4.31. It is observed that the feed length is not affecting the impedance matching for the first resonant frequency centered around 4.5 GHz. As the feed length is increased from 3.5mm onwards, matching corresponding to the other two resonant frequencies is found to be improving and at the optimum feed length, these two resonances merges together with the initial resonance to give broadband operation.
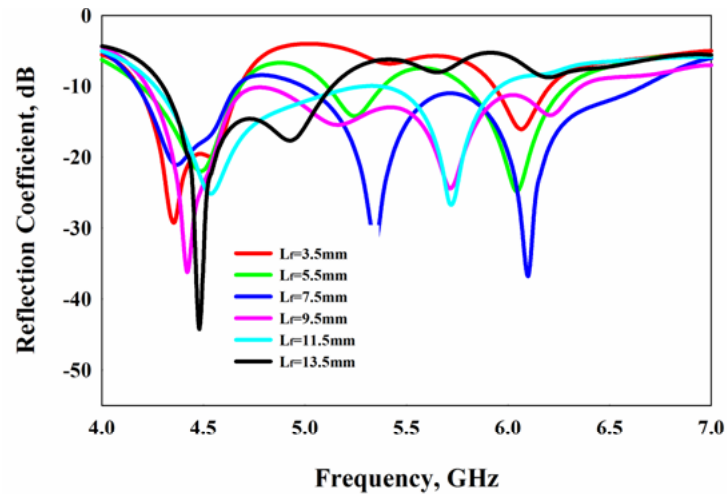
Fig. 4.31 Effect of feed offset L$_f$

4.2.3.6 Radiation Patterns and Gain of the antenna

The radiation patterns of the antenna are taken in both the XZ and YZ planes and it is illustrated in fig. 4.32.
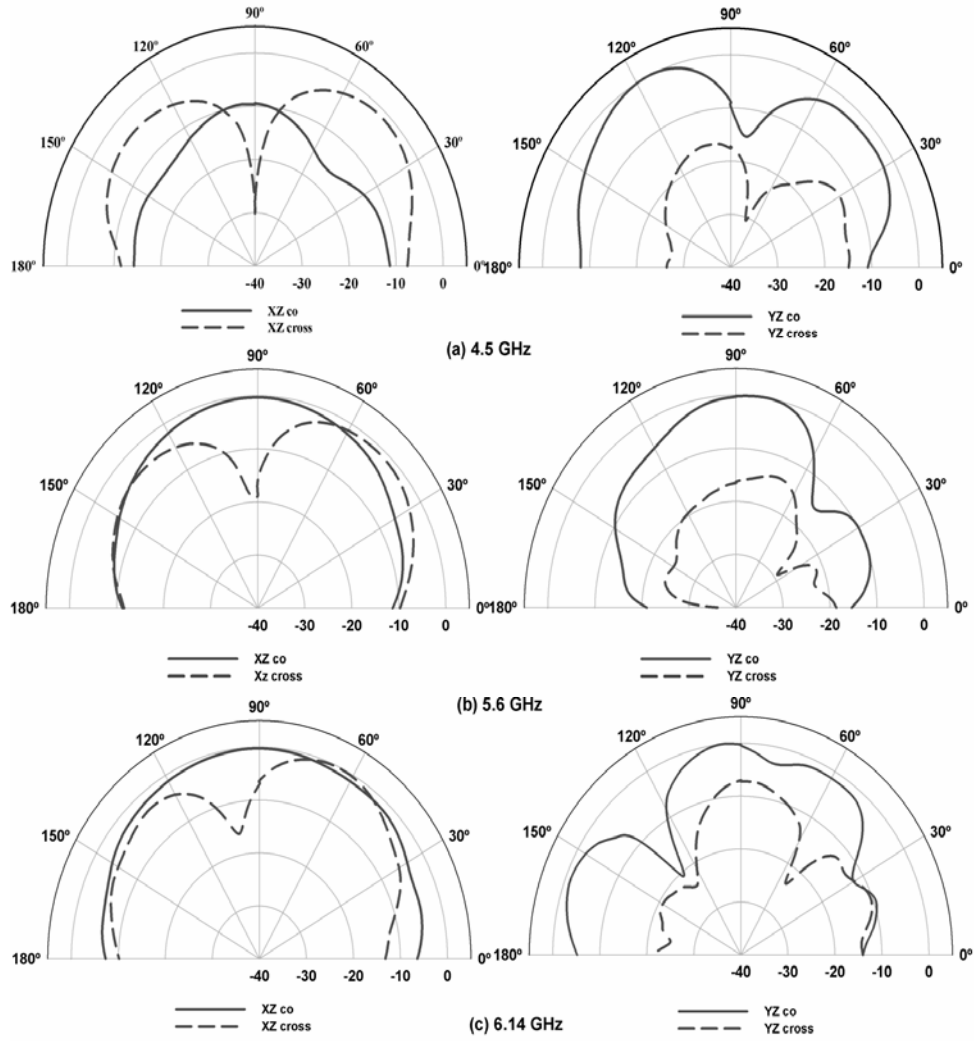
Fig. 4.32 Measured Radiation patterns of the antenna
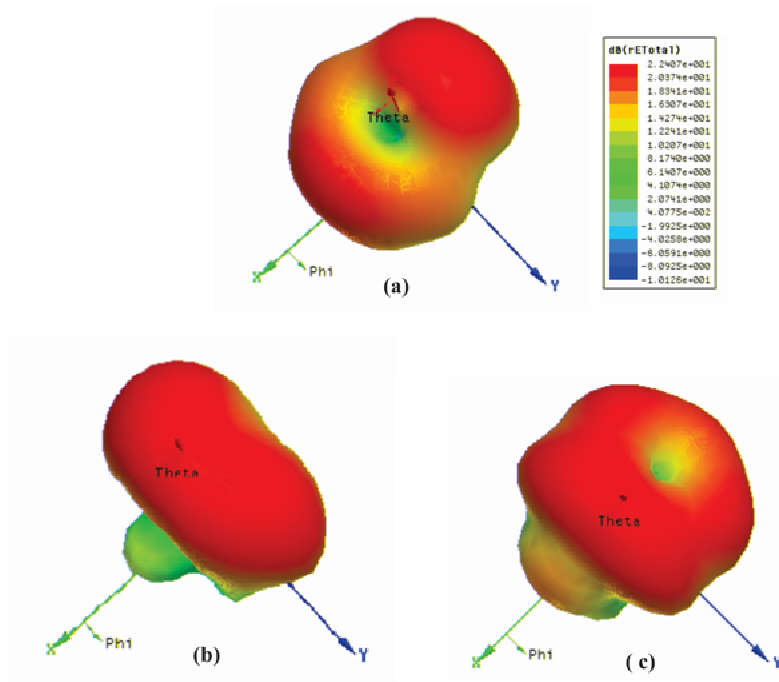
Fig. 4.33 Simulated 3D Radiation patterns of the antenna at a) 4.5 GHz, b) 5.6 GHz and c) 6.14 GHz

The simulated 3D radiation patterns of the antenna at the corresponding resonant frequencies are shown in fig. 4.33.

At 4.5 GHz, the pattern maximum of the YZ co pattern lies at 120^0, which is 30^0 away from the on axis of the antenna. The XZ and YZ plane cross polar isolation is found to be 19.1 dB and 8.1 dB respectively. The 3 dB beam widths are found to be 51.1^0 and 41.1^0 respectively for the XZ and YZ planes. The XZ cross pattern shows a power dip along the on axis and its reason can be found from the surface current pattern at the resonance, which is examined later. For 5.6 GHz resonance, the cross polar isolation is found to be 19 dB and 16.6 dB respectively for both the planes and the corresponding 3 dB beam widths are found to be 58.2^0 and 43^0 respectively. The 6.4 GHz resonance shows a 6.4 dB cross polar isolation for both the planes and their corresponding 3 dB beam

widths are found to be 128.9^0 and 28^0 respectively. The radiation characteristics of the antenna over the entire frequency of operation are studied and the results are tabulated in the table 4.1.

Table 4.1 Cross polarization and beam width characteristics

Frequency, GHz	Cross polar level along the on axis, dB		3 dB Beam width, degrees	
	XZ Plane	YZ Plane	XZ Plane	YZ Plane
4.3	22.5	10.9	49.6	39.4
4.5	19.1	8.2	51.1	41.1
4.7	19.9	7.6	56	41.6
5	24.4	9.8	71.1	62.4
5.3	26	14	77.4	75.8
5.7	15.4	15.4	82.5	38.8
5.9	11.2	11.2	92.8	37.1
6.2	6.7	6.7	118.3	31.4
6.3	6.4	6.4	128.9	28

The measured gain of the proposed antenna is shown in fig. 4.34. The antenna has a peak gain of 5.9 dBi at 4.7 GHz and a least of 2.5 dBi at 6.37 GHz. The reduction in the gain for the higher resonant frequency can be understood by looking on to the surface current pattern at that resonance. It can be seen that the opposing currents on either sides of the strip cancels the fields along the on axis at the field giving a lower gain at that frequency and it can be well understood by looking into the surface current distribution of the antenna described in the following section.
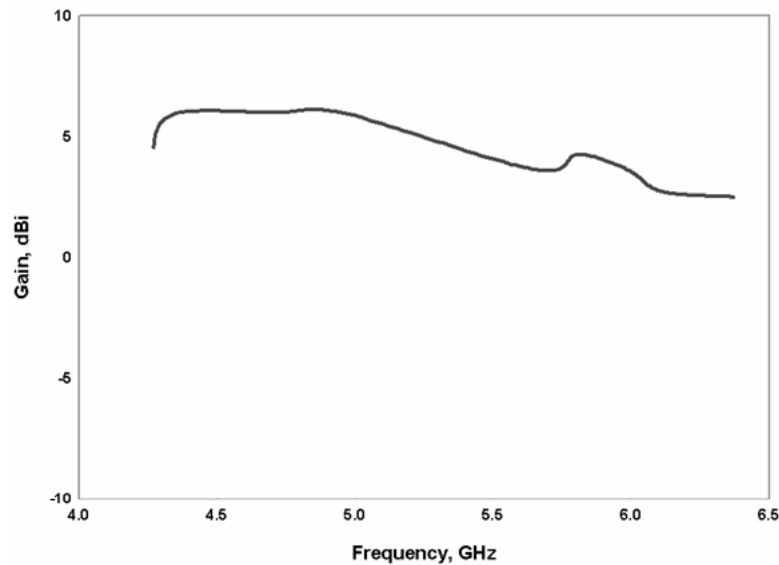
Fig. 4.34 Measured Gain of the antenna

4.2.3.7 Surface current distributions of the antenna

The reflection characteristics of the antenna give a great deal about the resonating frequency of the broadband antenna. The resonant mechanism or the mode formation can be well understood by looking into the surface current distribution of the antenna. The polarization of the antenna and the radiation characteristics can be best understood using these patterns. The simulated surface current distributions of the proposed antenna at the resonant frequencies are shown in fig. 4.35. Corresponding to the resonance at 4.5 GHz, a full wave variation is noted on the top edge of the patch along the strip and a similar variation is noted through the right and left edges of the patch along the Y-direction. This produces two resonances which coalesce to give the first resonance. But the polarization is found to be along the X-axis. This is because the opposing currents on either sides of the strip cancel the field along the on axis at the far field. Due to this type of current pattern, a power dip is noted along the on axis of the antenna for the XZ-cross radiation pattern for the resonance centered around 4.5 GHz. The second

resonance is due to three half wave variations along the sides of the patch in the Y-direction resulting in an almost steady XZ and YZ copolar patterns. According to the parametric analysis performed, the third resonance is majorly affected by the strip length variation. So it was kept in mind that the third resonance should be solely due to the strip. But it is observed in the surface current pattern corresponding to the third resonance that two symmetric full wave variations from the strip to the top right and left edges of the patch is contributing for the third resonance. From this it can be concluded that the third resonance is contributed by the combined effect of the patch and the strip.
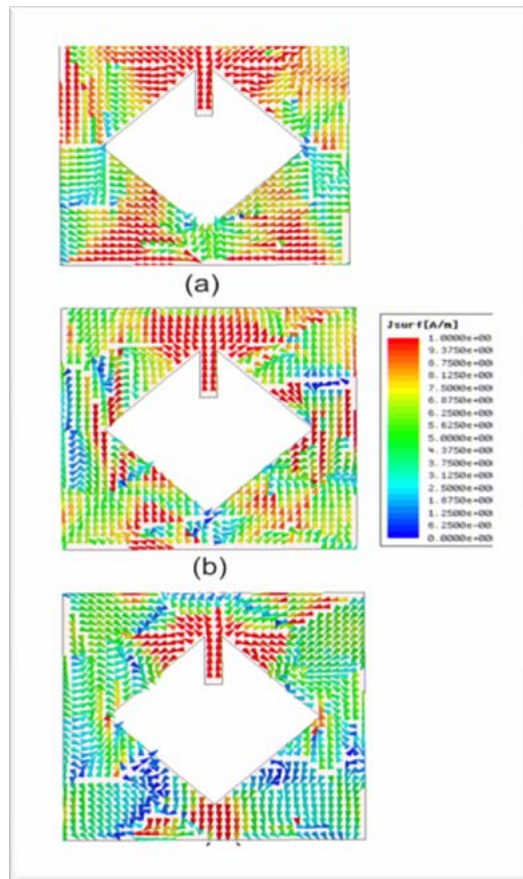
Fig. 4.35 Surface current distributions of the antenna at a) 4.5 GHz, b) 5.6 GHz and c) 6.14 GHz

4.2.3.8 Design equation formulation and validation

The experimental and simulated analysis of the broadband antenna and finally, the surface current pattern analysis of the antenna yield the design equation formulation of the antenna parameters. The design equations are crucial while implementing the antenna on other substrates. The initial step is to design a 50Ω microstrip transmission line.

The antenna parameters are found to be

$L_1 = 0.85\lambda_g$, $L_2 = 0.42\lambda_g$, $L_3 = 0.19\lambda_g$, $W = 0.048\lambda_g$, $L_f = 0.2297\lambda_g$, $h = 0.0387\lambda_g$, $L_g = 1.33\lambda_g$ and $W_g = 1.02\lambda_g$

Where λ_g is the guided wavelength corresponding to the first resonant frequency in the band and is given by

$$\lambda_g = \frac{\lambda}{\sqrt{\varepsilon e}} \text{---} (4.3)$$

Where $\varepsilon_e = \frac{\varepsilon + 1}{2}$ -- (4.4)

The design equations are validated on substrates having different permittivity. The geometric parameters of the antenna are tabulated in table 4.2. Fig. 4.36 shows the reflection characteristics of the antennas with the computed geometric parameters given in the table 4.2.
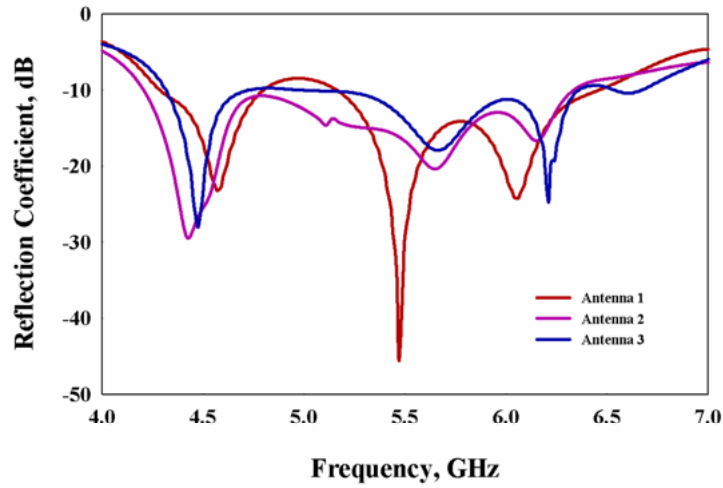
Fig. 4.36 Validation of reflection coefficients of the antennas on different substrates

Table 4.2 Antenna description

	Antenna 1	Antenna 2	Antenna3
ε_r	2.2	4.2	6.15
L_1	44.79mm	35mm	27.42mm
L_2	22.13mm	17.5mm	14.8mm
L_3	10.01mm	7.8mm	6.69mm
W	2.53mm	2mm	1.69mm
L_f	12.1mm	9.5mm	8.09mm
h	2.04mm	1.6mm	1.36mm
L_g	70mm	55mm	46.89mm
W_g	53.75mm	42mm	35.96mm
Percentage Bandwidth	41.1%	38%	38.65%

The important conclusions of this initial analysis can be summarized as

- The metal strip printed on the top corner of the tilted square slot plays a crucial role in achieving broadband impedance characteristics of the square patch antenna.

- The antenna achieves a bandwidth of 38% and it is a suitable choice for the 5.2/5.8 GHz WLAN, HiSWaNa and HYPERLAN applications.

- The impedance matching strip achieves impedance matching for the resonant modes of the patch and in addition the strip along with the patch contributes another third resonance which merges with the resonances of the patch antenna to give broadband operation.

- The strip nullifies the high capacitive reactance offered by the slot for the resonances offered by the patch and the increase in the slot length increases the real and imaginary part of the input impedance, so that the proper selection of the metal strip offers wide band impedance matching property for the antenna.

These interferences initiated to find out the effect of the slot shape on the impedance matching performance of the square patch antenna. For the study, a polygonal slot is incorporated instead of the tilted square slot and a detailed parametric analysis has been performed. The detailed discussions of the polygonal slot loaded square patch antenna are discussed in the following sections.

4.3 Analysis of an electromagnetically coupled strip loaded polygonal slotted microstrip antenna

The previous sections deal with the detailed experimental and simulation studies of the broadband nature of the tilted square slot loaded patch antenna. In this

section, the effect of shape of the slot on the impedance bandwidth characteristics is studied. Here, the tilted square slot of the antenna presented in section 4.2 is replaced by a polygonal slot. The geometry of the proposed design is shown in fig 4.37. Initially a square microstrip patch antenna of dimension L_1XL_1 mm^2 is fabricated on a substrate of dielectric constant 4.2 and height h=1.6mm. The antenna is electromagnetically coupled using a 50Ω printed microstrip transmission line fabricated using the same substrate. The offset distance from the centre of the patch to the top edge of the microstrip feed line is denoted by L_f. A polygonal slot of side dimension L_2 mm is etched on the square patch antenna. Broadband impedance matching characteristics is obtained by inserting the rectangular metal strip on the top portion of the slot as discussed in section 4.2. The dimension of the rectangular strip is denoted by L_3XW mm^2. The total height of the antenna is 3.2 mm. The ground plane dimension selected is L_gXW_g. The antenna is modeled in FDTD with discretization parameters $\Delta x=\Delta y=0.5$mm and $\Delta z=0.4$mm. The computational domain corresponding to this problem contains 150x150x50 number of Yee cells. The antenna is excited with 50Ω microstrip feed line which is modeled using Leubber's feed model as explained in chapter 3. The FDTD analysis will compute the frequency response of the antenna by exciting with a Gaussian pulse. The top view of the FDTD computational domain is shown in fig. 4.37(c).

(a) Top view

(b) Side view

c) Layout of the computational domain
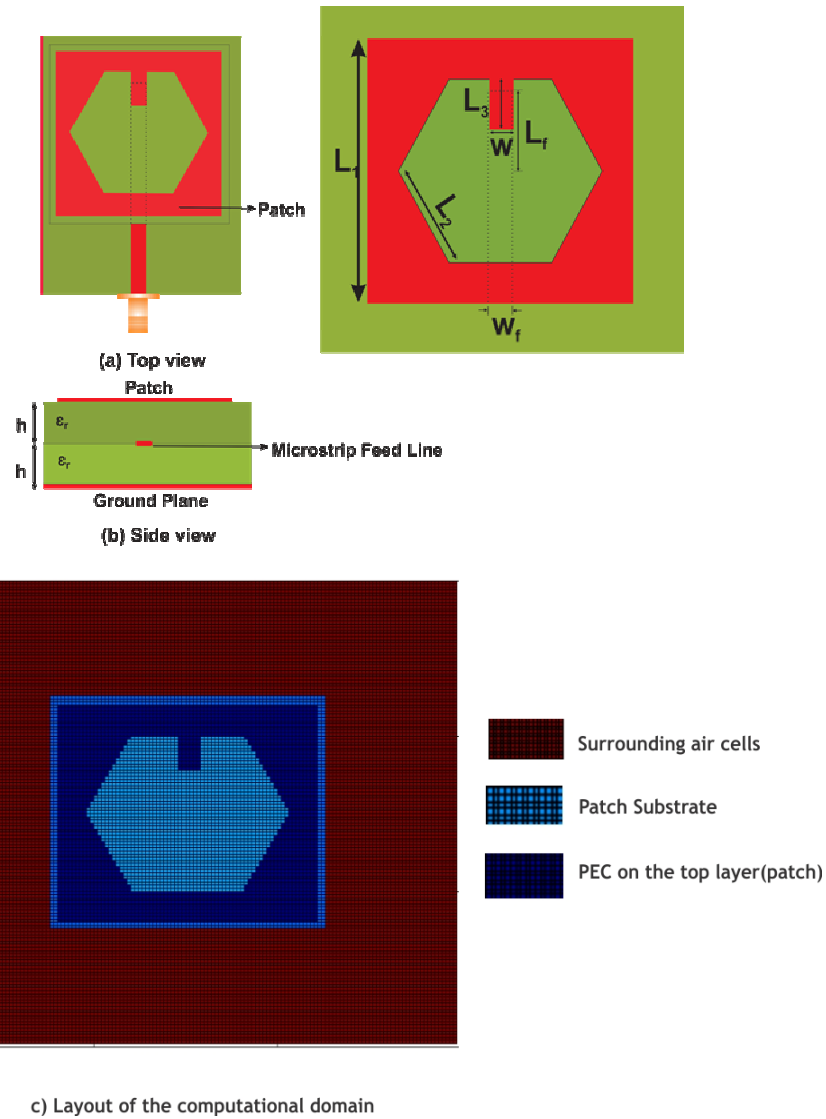
Fig. 4.37 Antenna geometry

4.3.1 Reflection characteristics

The antenna parameters at the optimum design are L_1=35mm, L_2=14.3mm, L_3=4.68mm, W=3mm, L_f=10.55mm, W_f=3mm, L_g=55mm, W_g=44mm. The experimental and simulated reflection characteristics of the polygonal slot loaded broadband microstrip antenna at the optimum design are

shown in fig. 4.38. It can be seen that the experimental and simulation results are in good agreement. It is observed that the antenna effectively merges four resonances to give broadband operation. The 2:1 VSWR bandwidth of the antenna is 45.87% from 4.21 GHz to 6.7 GHz which is higher than that of the tilted square slot loaded patch antenna. The resonances are found to be around 4.28 GHz, 4.62 GHz, 5.8 GHz and 6.35 GHz. The resonant mechanism is found to be similar to that of the strip loaded tilted square slotted microstrip patch antenna and it can be verified using the surface current patterns of the antenna.
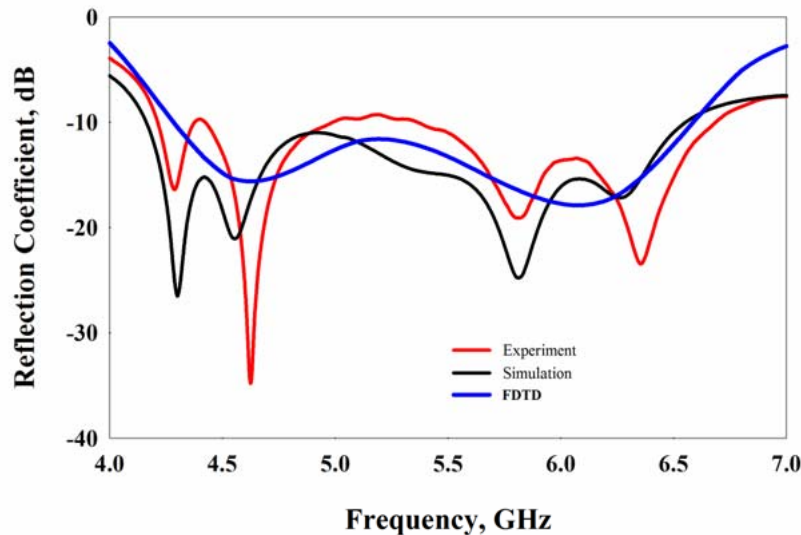
Fig. 4.38 Reflection characteristics

4.3.2 Effect of slot dimension

Similar parametric analysis has been performed to find out the effect of slot and strip dimensions on antenna reflection characteristics as that done for the tilted square slotted antenna. For each slot dimension, the width and length of the strip are varied and the results are summarized from fig. 4.39 to fig. 4.54

L$_2$=10.3mm
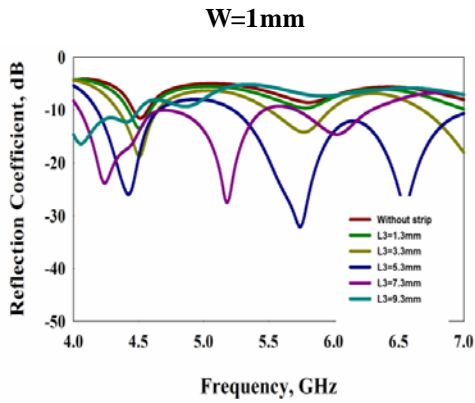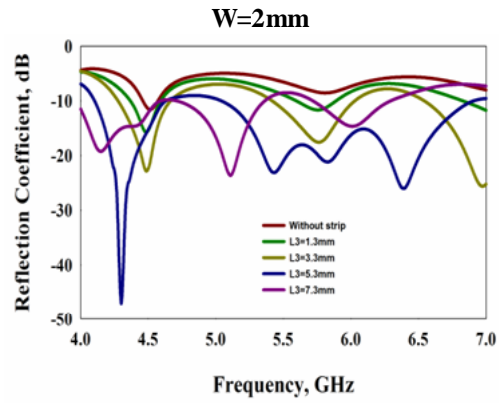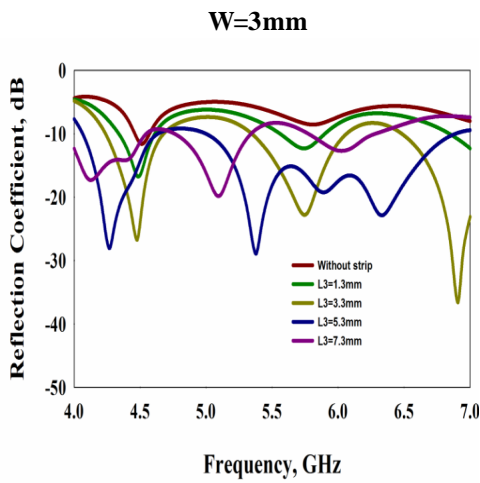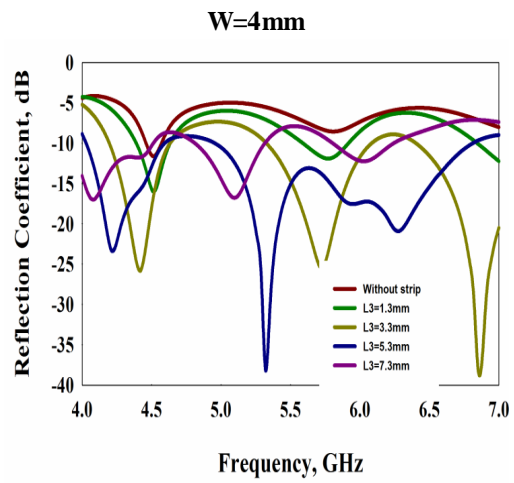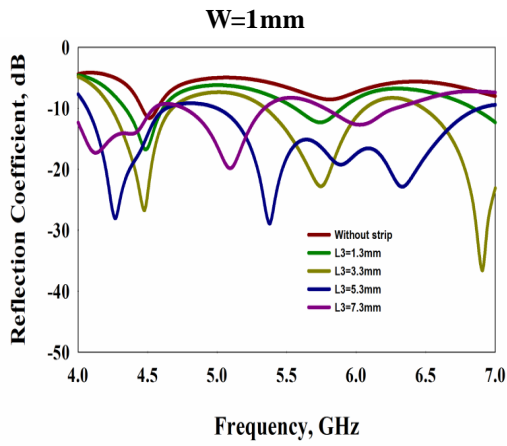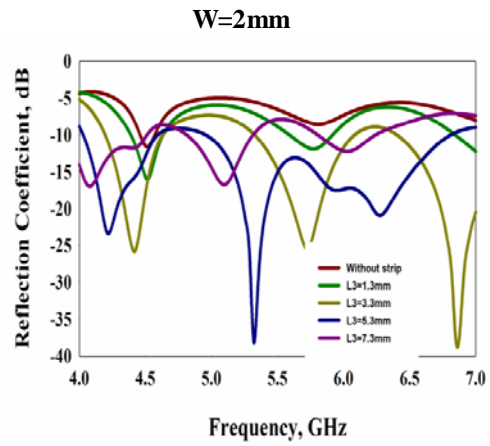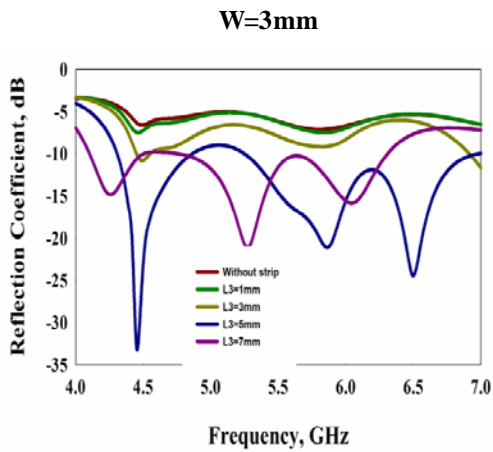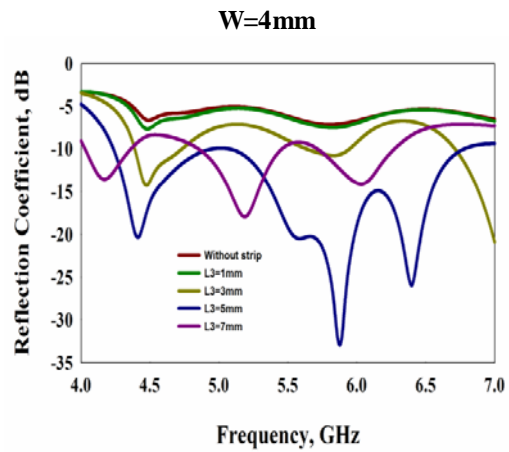
W=1mm

Fig. 4.39

W=2mm

Fig. 4.40

W=3mm

Fig. 4.41

W=4mm

Fig. 4.42

L_2=12.3mm

W=1mm

Fig. 4.41

W=2mm

Fig. 4.42

W=3mm

Fig. 4.43

W=4mm

Fig. 4.44

$L_2=14.3mm$

W=3mm

Fig. 4.45

W=4mm

Fig. 4.46

W=1mm

Fig. 4.47

W=3mm

Fig. 4.48

L_2=14.3mm

W=3mm

Fig. 4.49

W=4mm

Fig. 4.50

W=1mm

Fig. 4.51

W=2mm
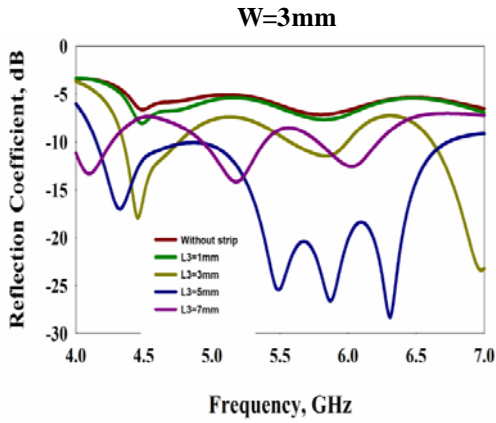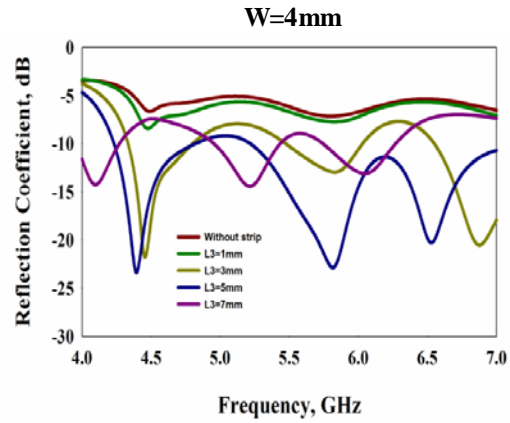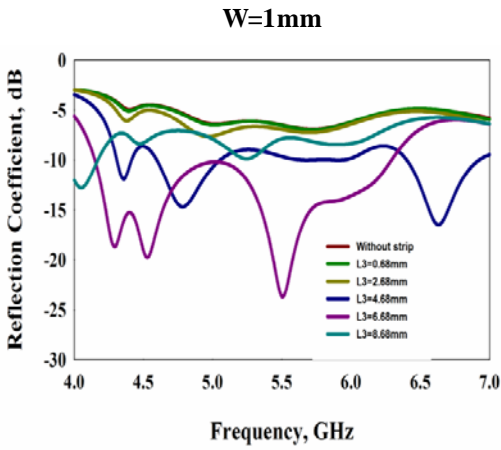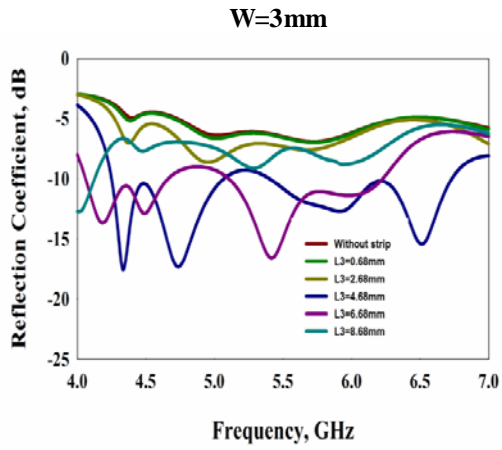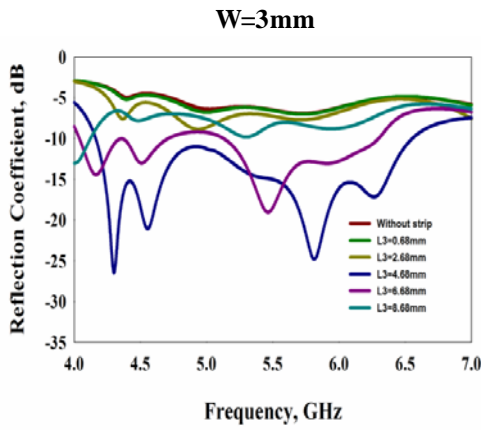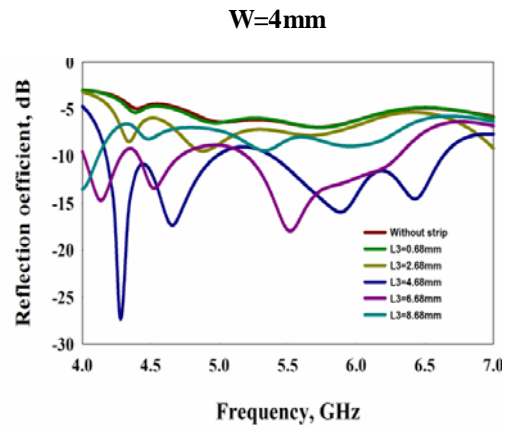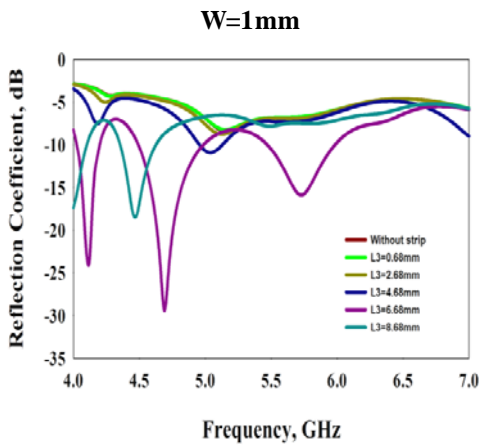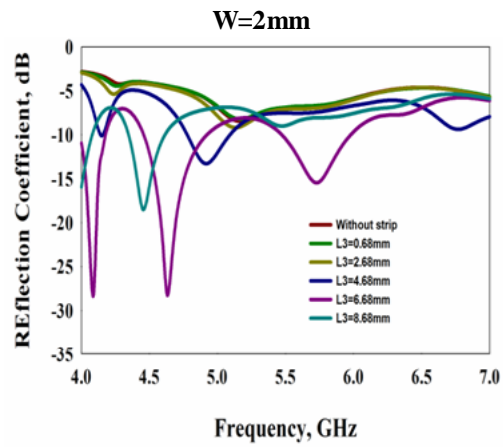
Fig. 4.52

L$_2$=16.3mm

W=3mm   W=4mm
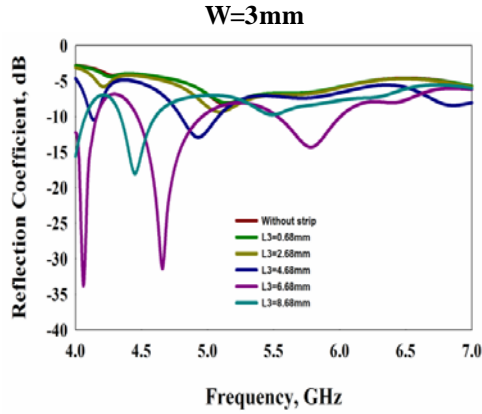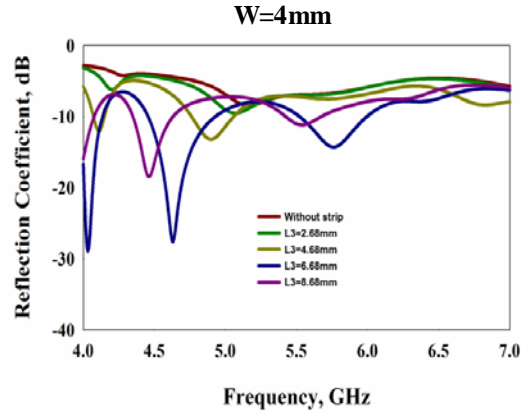
Fig. 4.53   **Fig. 4.54**

4.3.3 Computed Electric field distributions of the antenna

The three dimensional FDTD algorithm gives the electric and magnetic field component values at each cells. With the help of these values one can easily identify the resonant modes of the patch antenna and can easily understand the resonant mechanism. In this section, the electric field distributions on the top surface of the patch antenna are computed and the conclusions arrived for the resonant mechanism of the tilted square slot loaded antenna is validated here.

Fig. 4.55 and fig. 4.56 illustrates the E$_x$ and E$_y$ components of the electric field distributions on the patch surface at 4.28 GHz. A full wave variation from the strip to the right and left edges of the upper side of the patch is observed for the E$_x$ component of the electric field in the Y-direction and due to the cross proximity of the second resonance a full wave variation is observed along the Y-direction. The E$_y$ component shows a full wave variation on the top of the patch which mainly contributes radiation.
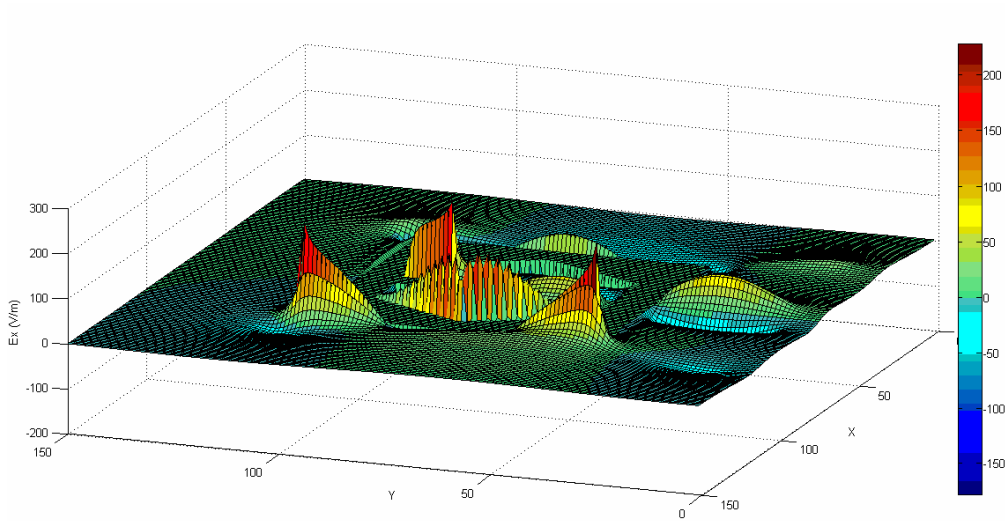
Fig. 4.55 Computed E_x component at 4.28 GHz
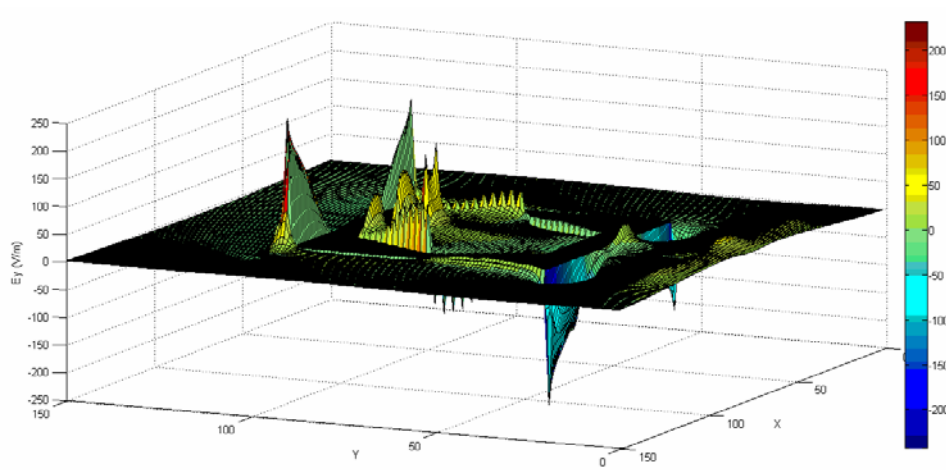
Fig. 4.56 Computed E_y component at 4.28 GHz

The E_x and E_y components of the electric field distributions corresponding to 4.62 GHz resonance is shown in fig. 4.57 and fig. 4.58 respectively. It is observed that the major contribution for radiation is by the fringing E_y component on the corners of the patch antenna. The resonance is majorly caused due to the full wave variation of the electric field along the Y-direction and it can be easily understood by looking into the E_x component.
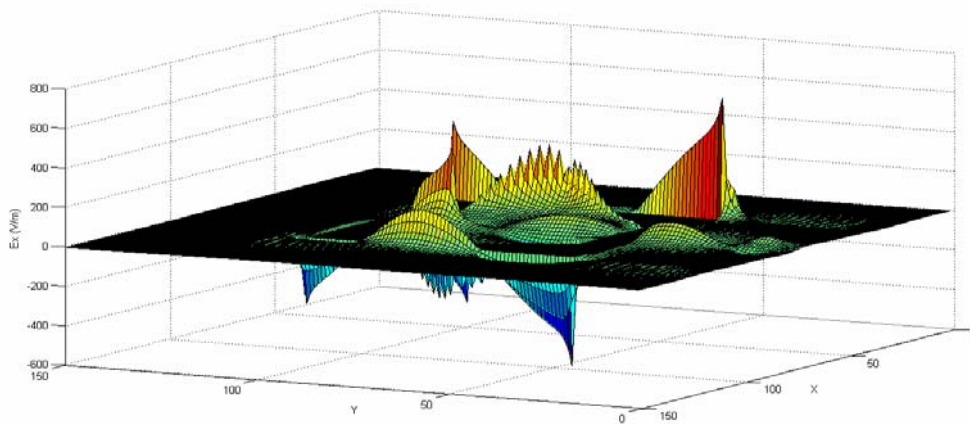
Fig. 4.57 Computed E_x component at 4.62 GHz
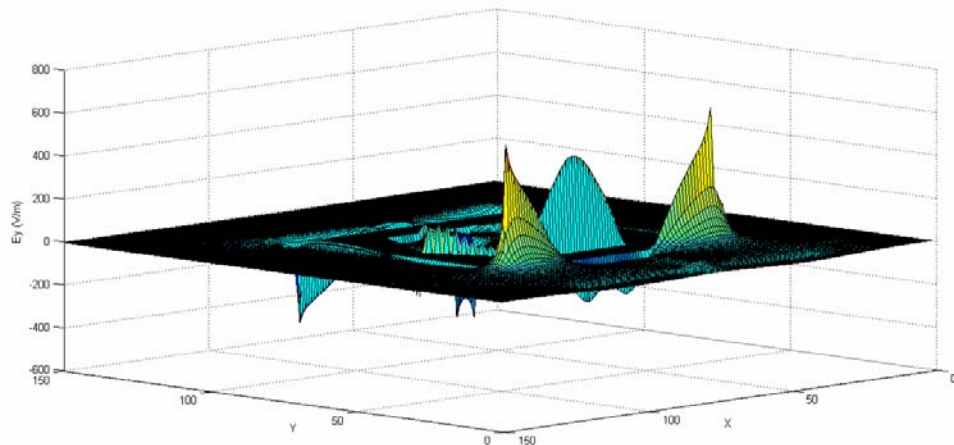
Fig. 4.58 Computed E_y component at 4.62 GHz

The fringing electric fields of the patch antenna at 5.8 GHz are shown in fig 4.59 and fig. 4.60 respectively. Three half wave variations of the E_x component along the sides of the patch antenna along the Y-direction is noted for this resonance. Radiation is majorly contributed by the E_y component of the electric field on the top and bottom corners of the patch antenna so that the polarization is found to be along the Y-direction.
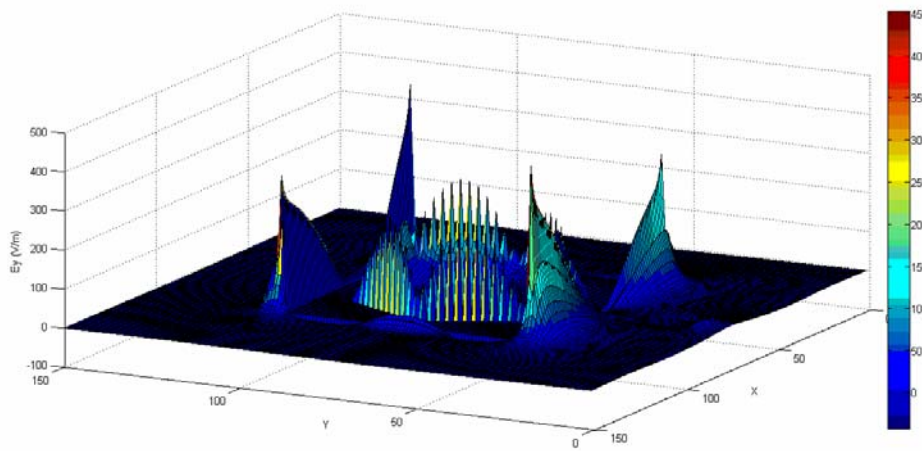
Fig. 4.59 Computed E_y component at 5.8 GHz
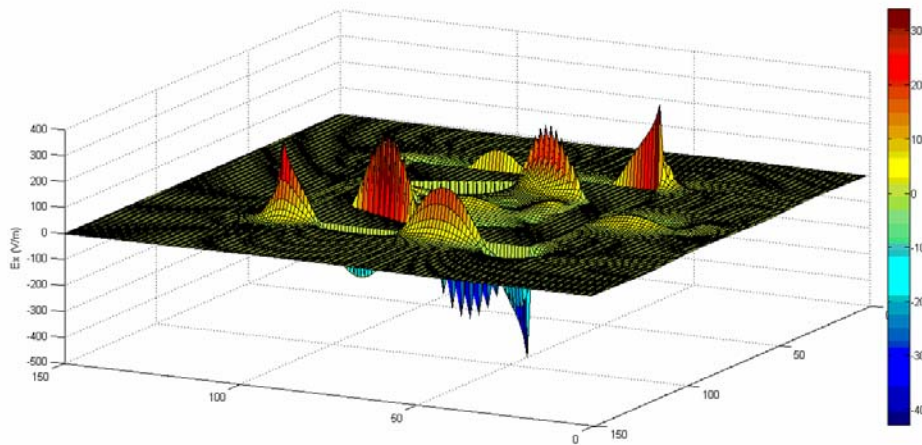
Fig. 4.60 Computed E_x component at 5.8 GHz

It is concluded from the parametric analysis of the tilted square patch antenna that the final resonance is contributed by the combined effect of both the strip and the patch. The electric field distributions of the final resonance centered on 6.37 GHz are shown in fig. 4.61 and fig. 4.62 respectively. A strong contribution from the E_y component on the top edge of the patch just above the strip in noted while the contribution from E_x component is negligible and it is mainly observed on the two sides of the strip with an out of phase distribution.
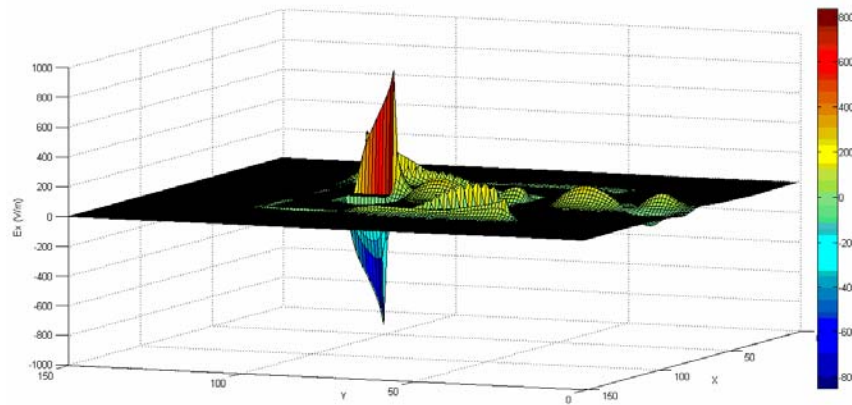
Fig. 4.61 Computed E_x component at 6.37 GHz
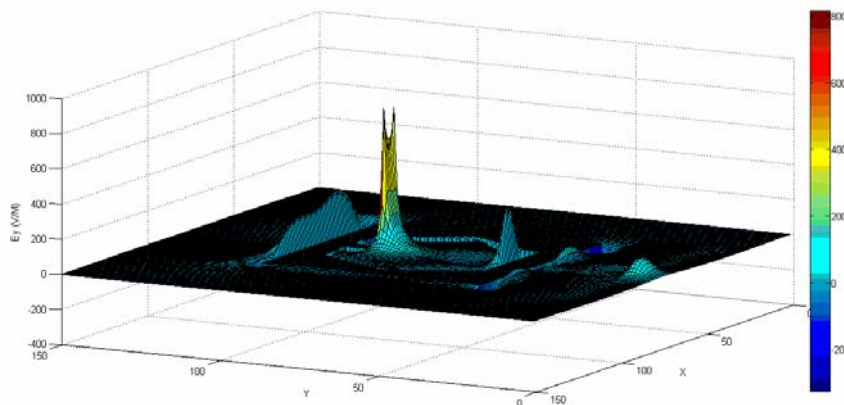
Fig. 4.62 Computed E_y component at 6.37 GHz

4.3.4 Radiation patterns and Gain of the antenna

The radiation patterns of the antenna are measured throughout the entire operating frequency range. The XZ and YZ plane radiation patterns of the proposed antenna at the resonances are shown in fig. 4.63. The simulated 3D radiation patterns of the antenna at the resonant frequencies are shown in fig. 4.64.
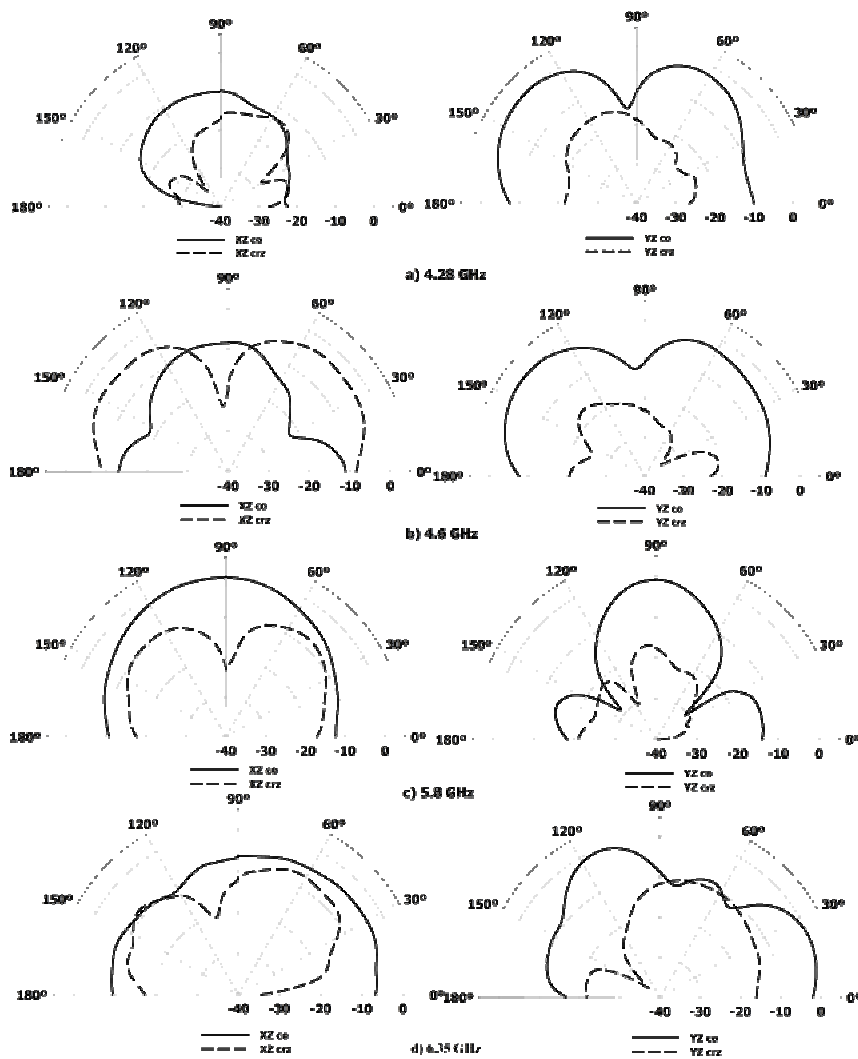
Fig. 4.63 Measured Radiation patterns of the antenna

It can be seen that for the initial two resonances centered around 4.28 GHz and 4.62 GHz, the shape of YZ copolar patterns are almost similar. The XZ copolar patterns show a low powered radiation as compared to the YZ plane copolar patterns. The cross polar isolation for the 4.28 GHz resonance is found to be 7dB and 18.7dB for the XZ and YZ plane patterns   respectively while that corresponding to the second resonance is 8.9 dB for the XZ plane and 12.6 dB for the YZ plane. The XZ plane pattern corresponding to the 5.8 GHz resonance shows broadside radiation coverage as compared to its YZ copolar pattern. Due to three half variations along the edges of the patch along the Y-direction for 5.8 GHz resonance, a power dip along the on axis of the antenna for the XZ cross pattern is observed.
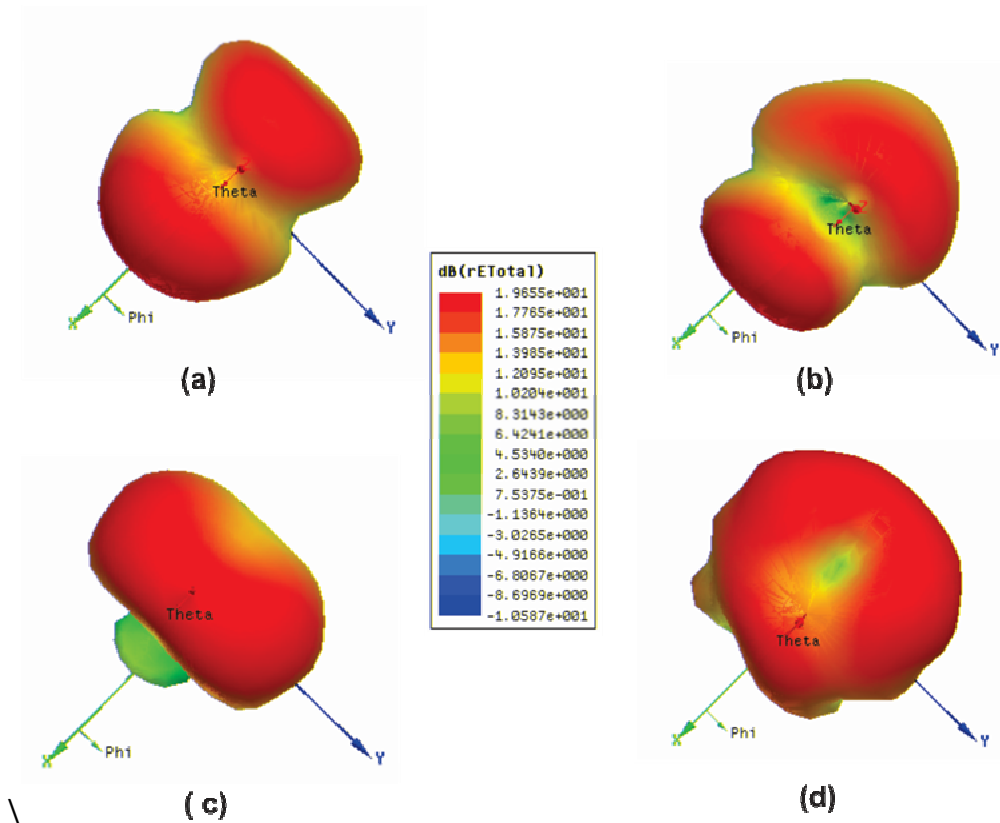
Fig. 4.64 Measured 3D Radiation patterns of the antenna at a) 4.28 GHz, b) 4.62 GHz, c) 5.8 GHz and d) 6.35 GHz

The XZ and YZ plane cross polar isolation is found to be 22.9 dB and 17.5 dB respectively. The final resonance around 6.35 GHz is found to have a very low cross polar isolation as compared the other resonances. The cross polar isolation is found to be 3.7 dB for both the XZ and YZ planes. A detailed study of the radiation patterns of the antenna throughout the entire frequency of operation is performed. It is tabulated in the table 4.3 given below.

Table 4.3 Cross polarization characteristics of the antenna

Frequency, GHz	Cross polarization, dB	
	XZ plane	YZ plane
4.21	5.86	7.89
4.4	7.51	10.33
4.6	9.52	14
4.8	12.56	16.58
5	15.2	15.2
5.2	16	16
5.4	18	18
5.6	25.47	18.6
5.8	22.9	17.5
6	14	14
6.2	7.8	7.8
6.4	2.5	2.5

The gain of the antenna is plotted in fig. 4.65. It is observed that the antenna shows a maximum gain of 6.82 dBi at 6 GHz.
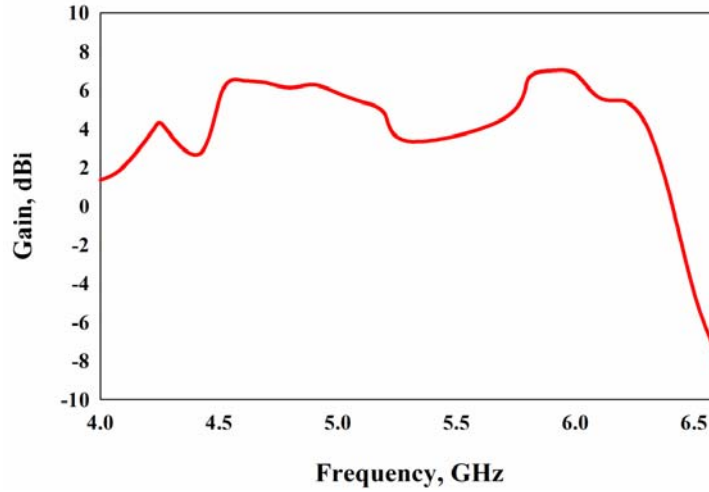
Fig. 4.65 measured gain of the antenna

4.3.5 Design equations of the antenna

Depending upon the parametric analysis performed, the design equations of the antenna are formulated and they can be expressed as $L_1=0.8051\lambda_g$, $L_2=0.3289\lambda_g$, $L_3=0.1076\lambda_g$, $W=0.069\lambda_g$, $L_f=0.2047\lambda_g$, $L_g=1.2652\lambda_g$, $W_g=0.9661\lambda_g$, $h=0.0368\lambda_g$.

Where λ_g is the guided wavelength corresponding to the first resonant frequency in the band and is given by

$$\lambda_g = \frac{\lambda}{\sqrt{\varepsilon e}} \text{ --- (4.5)}$$

Where

$$\varepsilon_e = \frac{\varepsilon+1}{2} \text{ -- (4.6)}$$

The design equations are validated on substrates having different permittivity. The reflection characteristics are shown in fig. 4.66, with their geometrical parameters in table 4.4.
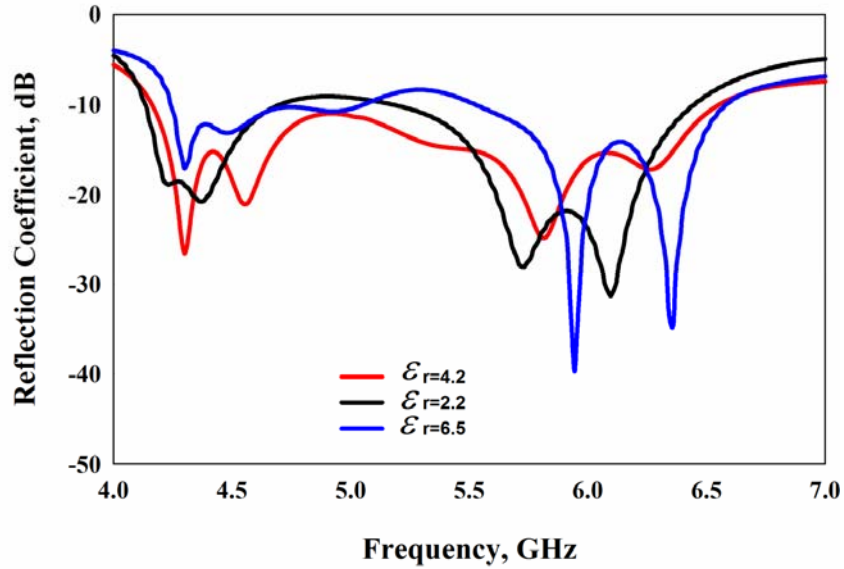
Fig. 4.66 Reflection characteristics of the antenna fabricated on different substrates

Table 4.4 Antenna description

Antenna Parameters	Antenna 1	Antenna 2	Antenna3
ε_r	2.2	4.2	6.5
L_1	48.36	35	28.13
L_2	19.76	14.3	11.4
L_3	6.46	4.6	3.78
W	4.15	3	2.14
L_f	11.34	10.55	7.4
h	2.21	1.6	1.29
L_g	70	55	45.8
W_g	53.5	44	35
Percentage Bandwidth	43.77%	44.6%	43.54%

4.4 An L-strip fed polygonal slotted broadband patch antenna

In order to comply with the modern wideband breast cancer imaging applications, an antenna must cover the 4-9 GHz frequency band and it must have good time domain characteristics. The polygonal slotted broadband microstrip antenna, described in section 4.3, can be effectively utilized for breast cancer imaging applications by suitably exciting higher order modes of the patch antenna without disturbing the initial resonances using an L-strip feed mechanism. Researchers all over the world has effectively utilized the L- feed mechanism to merge the fundamental modes of the patch to the higher order modes in order to get broadband impedance matching performance [4-8]. This technique in effect increases the impedance matching for the higher order modes of the patch in addition to the already existing resonances.

In this section, printed L-strip feeding technique is successfully implemented on the polygonal slotted strip loaded broadband patch antenna discussed in section 4.3. The feed length variation and the time domain analysis are studied in detail in this section.

4.4.1 Antenna geometry

The geometry of the proposed antenna is shown in fig.4.67. The basic structure is the impedance matching strip loaded polygonal slotted electromagnetically coupled mirostrip antenna having geometric parameters L_1=35mm, L_2=14.3mm, L_3=4.6mm, W=3mm, L_f=10.55 mm, h=1.6mm, L_g=55 mm and W_g=44 mm. The feed is modified with a printed L-strip feed mechanism with the L-strip length denoted by L_4=15mm. The antenna is fabricated on a substrate of dielectric constant ε_r=4.2 and the total height of the antenna is 3.2mm.

(a) Top view

(b) Side view
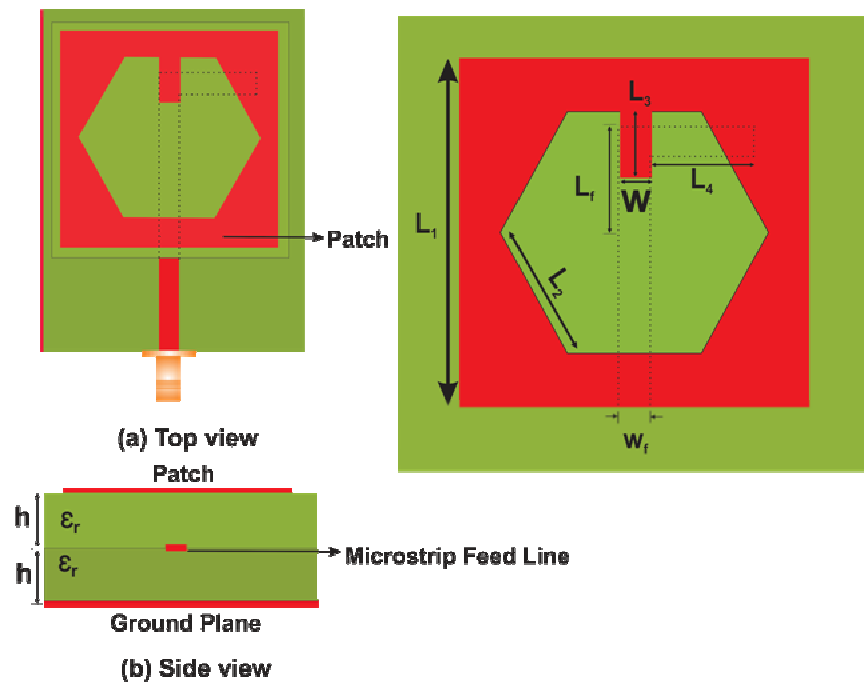
Fig. 4.67 Geometry of the antenna

4.4.2 Reflection characteristics

A rigorous parametric analysis has been performed to find out the optimum length of the L-strip feed to merge the higher order mode resonances to the existing resonances. In order to make the comparison study easier, the reflection characteristics of the polygonal slotted antenna in the 4- 10 GHz frequency span are taken and are shown in the fig.68. It can be seen that broadband operation is achieved by merging four resonances around 4.28 GHz, 4.63 GHz, 5.8 GHz and 6.36 GHz. Also two poorly matched resonances are noted at 8.25 GHz and 9 GHz.

The final design is obtained by properly matching the two higher resonances using printed L-strip feeding mechanism while maintaining L_f same as that of the initial design. The reflection characteristics of the final antenna at the optimum design are shown in fig. 4.69. It is noted that the antenna

exhibits a 2:1 VSWR bandwidth of 74% from 4.35 GHz to 9.5 GHz. The resonances are found to be at 4.5 GHz, 4.8 GHz, 5.9 GHz, 6.7 GHz, 8.1 GHz and 9.2 GHz.
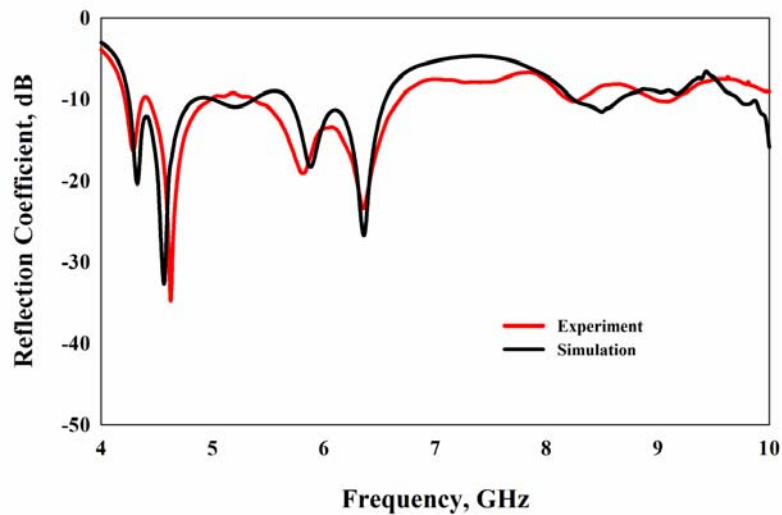
Fig. 4.68 Reflection characteristics of the polygonal slotted broadband antenna
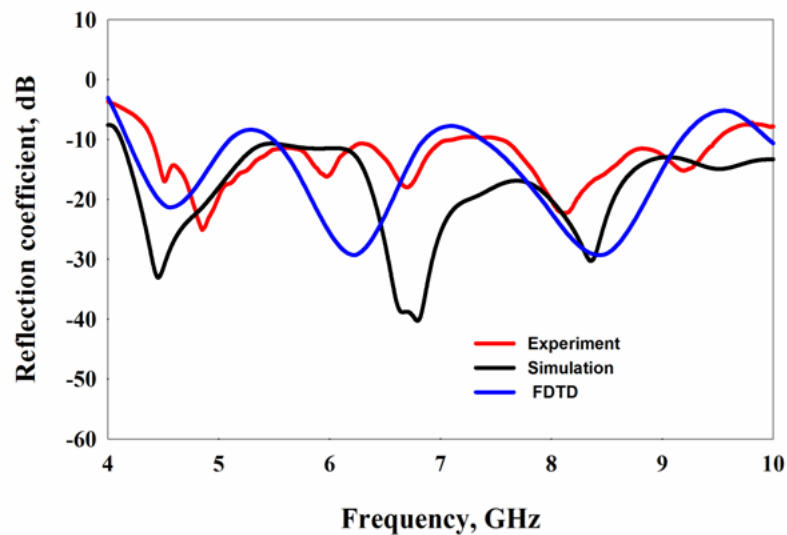
Fig. 4.69 Reflection characteristics of the L-strip fed antenna

4.4.3 Effect of feed strip length L_4

Extensive simulation and experimental studies has been performed to find out the effect of the horizontal strip length L_4 on reflection characteristics and input impedance of the antenna.
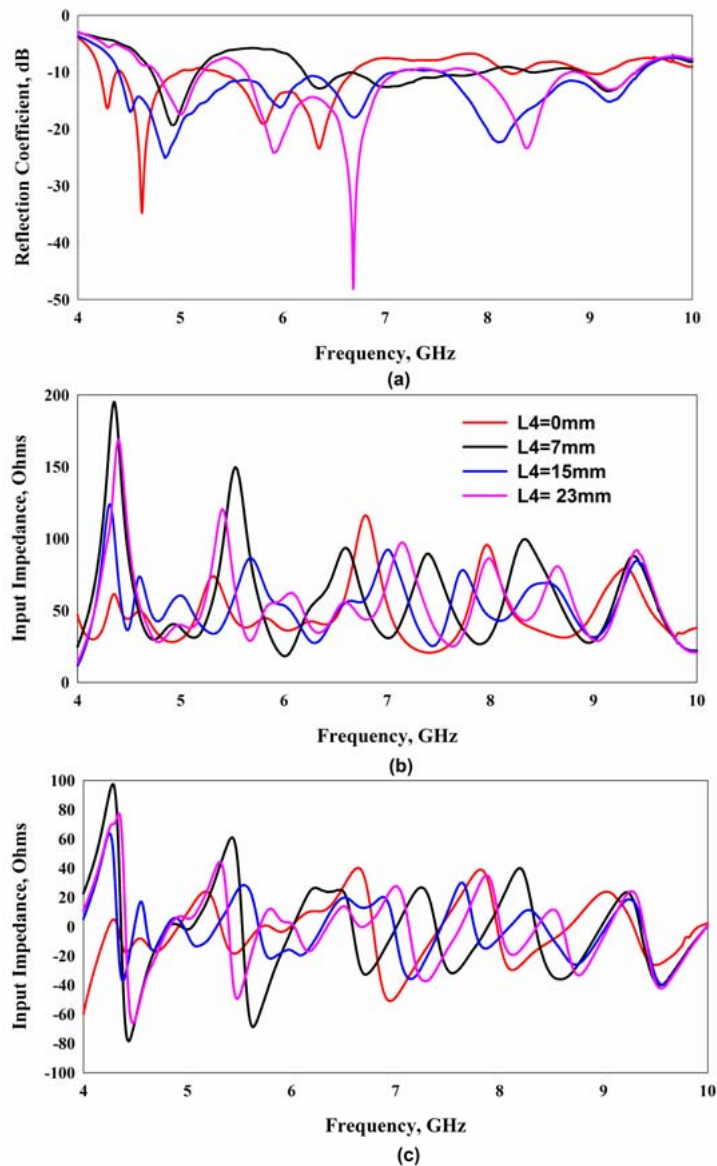
Fig. 4.70 Effect of strip length L_4

Fig.4.70 below describes the variation of reflection characteristics and input impedance with horizontal strip length L_4. It can be seen that by introducing the strip L_4, a slight right shift in the first four resonances is observed. This is due to the change in coupling between the patch and the feed as compared to the initial antenna. A predominant variation in the matching for the first resonance is noted as compared to the other three initial resonances. As L_4 increases, the real part of the impedance corresponding to the first resonance also increases till L_4=7mm (0.21λ_g, where λ_g is the guided wavelength corresponding to the first resonant frequency), then decreases untill L_4=17mm (0.52 λ_g), again increases causing poor matching. Upto L_4=7mm, the imaginary part shifts towards high inductive state and then back to capacitive part upto L_4=17mm. An optimum length of L_4=15mm (0.46 λ_g) is selected to obtain the maximum bandwidth of the antenna.

4.4.4 Radiation patterns of the antenna

The measured XZ and YZ plane radiation patterns of the antenna are shown in fig. 4.71. At 4.5 GHz, a 3 dB beam width of 50^0 is observed in the XZ copolar pattern. The YZ copolar pattern has two symmetric maximas directed along 60^0 and 120^0 respectively. At 5.5 GHz and 5.8 GHz, the half power beam widths are found to be 129^0 and 78^0 respectively in the XZ copolar pattern. At 5.5 GHz, the XZ and YZ cross polar isolation are found to be 10dB and 5 dB respectively and for 5.8 GHz the cross polar isolation is found to be 12 dB in the XZ plane and 7.2 dB in the YZ plane. At 6 GHz, 55^0 beam width and 10.3 dB cross polar isolation are noted in the XZ plane whereas in the YZ plane these are 44.3^0 and 8 db respectively. Also two symmetrical power dips are noted at 139^0 and 45^0 in the YZ plane. The XZ plane radiation pattern at 6.6 GHz shows a 120^0 beam width and 4 dB cross polar isolation. The beam in the XZ plane is shifted by -20^0 from the on axis at 8 GHz and an 8 dB cross polar isolation is observed for both the planes. Due

to the higher order mode radiation, the YZ co polar pattern at 9.2 GHz has two symmetrical power dips at 63^0 and 122^0 and both the planes are having a very low cross polar isolation.
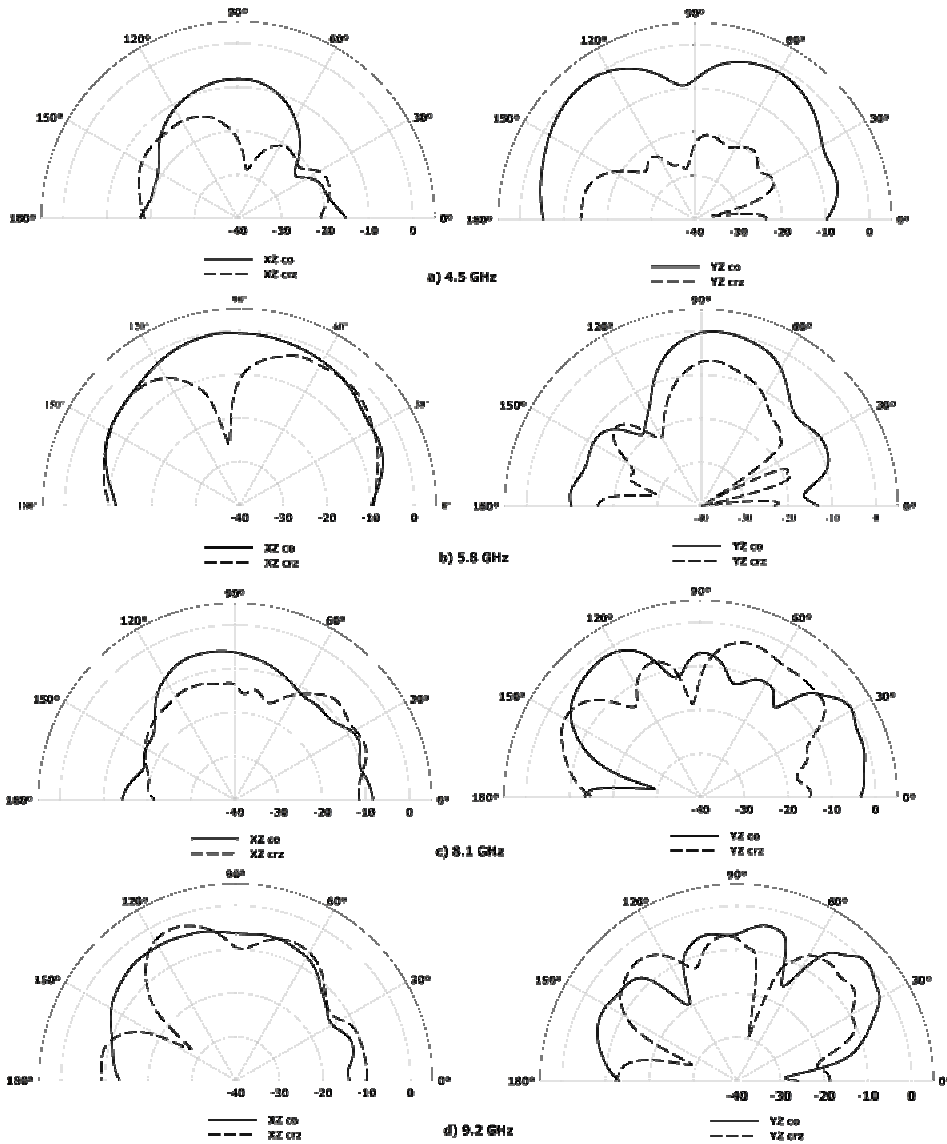
Fig. 4.71 Radiation patterns of the antenna

4.4.5 Gain and efficiency of the antenna

The measured gain and the simulated radiation efficiency of the antenna is shown in fig. 4.72. Gain at the resonances is found to be 4.17 dBi, 4.7 dBi, 5dBi, 3.88 dBi, 4.6 dBi and 5 dBi respectively and has an average gain of 4.09 dBi within the desired band.

The maximum efficiency of the antenna is found to be 72.6% at 4.92 GHz and the average efficiency is found to be 57.2%.

4.4.6 Time domain analysis of the antenna

The experimental time domain analysis is carried out to find out the impulse response of the antenna. This is done by convoluting the fourth order derivative of the Gaussian function [9]
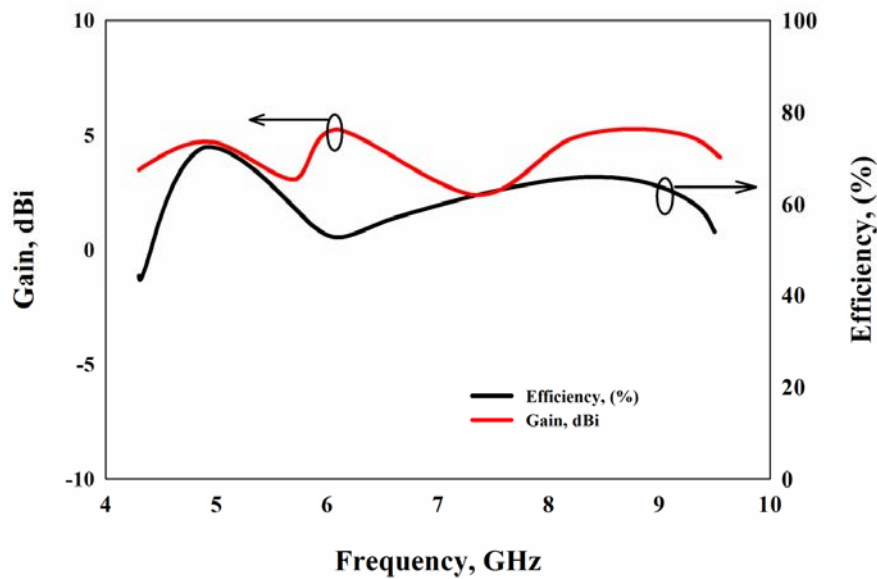
Fig. 4.72 Gain and efficiency of the antenna

$$Vin(t)=A\left[3-6\left(\frac{4\pi}{T^2}\right)t^2+\left(\frac{4\pi}{T^2}\right)^2 t^4\right]e^{-2\pi\left(\frac{t}{T}\right)^2}t^2\quad\frac{V}{m}\quad\text{-----------------------(4.8)}$$

With h(t), the inverse Fourier transform of the transfer function H(w) [10], where

$$H(\omega)=\sqrt{\frac{2\pi RcS_{21}(\omega)e^{\frac{j\omega R}{c}}}{j\omega}}\quad\text{---(4.9)}$$

Where c is the free space velocity and R is the distance between the antennas.
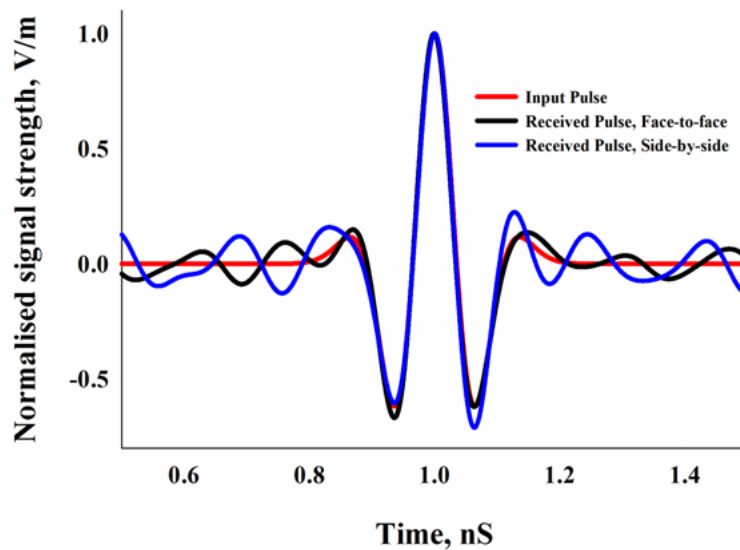
Fig. 4.73 Time domain analysis of the antenna

The received pulse is

$$Vrec(t)=Vin(t)\otimes h(t)\quad\frac{V}{m}\quad\text{--(4.10)}$$

   The input pulse is designed to cover the specified frequency range with the amplitude constant A= 1.6 and the pulse duration parameter T= 67 pS. The

input and output waveforms corresponding to the face to face and side by side orientations of the antenna are shown in fig. 4.73. It can be seen that the face to face and side by side orientations retain the information contained in the transmitted signal with minimum dispersion.

4.5 Conclusions

Two impedance matching strip loaded tilted square slotted and polygonal slot loaded square microstrip antennas are designed to comply with the broadband wireless communication applications. The tilted square slot antenna achieves a bandwidth of 38% and the polygonal slotted antenna has a bandwidth of 45% at the optimum design. The impedance matching strip achieves impedance matching for the resonances offered by the patch and it along with the patch contributes another third resonance and at the optimum strip length, these three resonances merge together to a achieve wide bandwidth for the antenna. The proposed optimum designs are potential candidates in wireless communications systems where compact efficient antennas are in great demand. Finally, L-strip feed mechanism is implemented on the polygonal slotted strip loaded square patch antenna to occupy a very high bandwidth within the 4-9GHz frequency range which is most suited for the ultra wideband imaging applications.

4.6 References

[1]   Ramesh Garg, V.S Reddy, "Edge feeding of microstrip ring antenna," IEEE Transactions on Antennas and Propagation, vol. 51, no. 8, pp. 1941-1946, 2003.

[2]   C.L Mak, K.M Luk, K.F Lee, "Microstrip line fed L-strip patch antenna," IEE Proceedings .Microwave Antennas and Propagation, vol. 146, no.4, pp. 282-284, 1999.

[3]   Ramesh Garg, "Microstrip Antenna Design Handbook", Artech House

[4]   S. Mridula, Sreedevi K. Menon, B. Lethakumary, Binu Paul, C.K Aanandan and P. Mohanan, "Planar L-strip Fed Broadband Microstrip Antenna", Microwave and Optical Technology Letters, Vol. 34, No.2, pp. 115-117, 2002

[5]   Yong-Xin Guo, Kwai-Man Luk and Kai-Fong Lee,"L-Probe Fed Thick-Substrate Patch Antenna Mounted on a Finite Ground Plane", IEEE Trans. Antennas Propag., vol. 51, no. 8, pp. 1955-1963, 2003.

[6]   Jongkuk Park, Hyung-gi Na and Seung-hun Baik, "Design of Modified L-Probe Fed Microstrip Patch Antenna", IEEE Antennas and Wireless Propagation Letters, vol. 3, no. 8, pp. 117-1119, 2004.

[7]   Zhi Ning Chen and M.Y.W Chia, "Broadband Suspended Plate Antennas Fed by Double L-Shaped Strips ", IEEE Transactions on Antennas Propagation, vol. 52, no. 9, pp. 2496-2500, 2004.

[8]   P.Li, H.W Lai, K.M Luk and K.L Lau, "A Wideband Patch Antenna With Cross Polarization Suppression", IEEE Antennas and Wireless Propagation Letters, vol. 3, pp. 211-214, 2004.

[9]   Shih-Yuan, Po-Hsiang Wang, Powen Hsu,"Uniplanar Log-Periodic Slot Antenna Fed by a CPW for UWB Applications", IEEE Antennas and Wireless Propagation Letters, vol. 5, pp. 256-259, 2006.

[10] M. Gopikrishna, Deepti Das Krishna, C.K Aanandan, P. Mohanan and K. Vasudevan, "Design of a compact Semi-Elliptic Monopole Slot Antenna for UWB systems ", IEEE Transactions on Antennas Propagation, vol. 57, no. 6, pp. 1834-1837, 2009.

.....ഇരു.....

INVESTIGATIONS ON STACKED OFFSET SINGLE BAND AND BROADBAND GAIN ENHANCED MICROSTRIP ANTENNAS

The experimental and simulated investigations towards the development of compact gain enhanced microstrip antennas are discussed in this chapter. Principle of stacking is effectively implemented and the position of the upper parasitic patch is offsetted to enhance the gain of single band and broadband square patch antennas, without deteriorating the impedance matching performance of the antenna. Two single band prototypes along with the two slotted broadband designs discussed in the previous chapter are taken here for consideration. Experimental and simulated studies for explaining the gain enhancement mechanism are described in detail in this chapter.

5.1 An overview of gain enhancement techniques for microstrip patch antennas

Researchers all over the world have extensively studied the gain enhancement techniques for microstrip patch antennas. Siew Bee Yeap *et al.* increased the gain of microstrip antennas [1] by partially removing the substrate over which the patch antenna is fabricated. Partial substrate removal reduces the losses due to surface waves and dielectric substrates. It can enhance the gain up to 2.7dBi. A very simple technique to enhance the gain of microstrip antennas is to load the antenna with a superstrate. The measured gain will be maximum, when the superstrate thickness is equal to the one quarter of the wavelength of the wave propagating in the superstrate. Chih-Yu Huang et. al. proposed a compact superstrate loaded broadband microstrip patch antenna [2] with enhanced gain performance. Here, the bandwidth enhancement and size reduction is achieved by chip resistor loading. Gain enhancement to compensate the reduction in gain due to reduction in size of the patch and ohmic loss of chip resistor loading is achieved by the loading of a high permittivity superstrate layer.

Multiple resonator model is an effective technique to enhance the gain of microstrip antennas. It can be done by implementing the patch resonators in a plane as an array or can be stacked vertically. The microstrip antenna arrays [3-6] can enhance the gain of the structure by utilizing a larger area. Microstrip yagi antenna is a modification of the microstrip array which can be used for enhancing the gain of the antenna. Gerald DeJean proposed a microstrip Yagi array configuration [7] utilizing seven microstrip elements, one as the driven element, two reflector elements and four director elements. It can enhance the gain up to 15.6 dBi and it exhibits good F/B ratio around 8-10 dB. But the major disadvantage of such designs is that they are very bulk in size and so they cannot be integrated with microwave monolithic integrated circuits.

So stacking is a reasonable choice for enhancing the gain of microstrip antennas. Stacking can be implemented for increasing the bandwidth of the antenna and also for enhancing the gain of the structure. Nishiyama *et al.* [8] has extensively studied the effect of stacking on microstrip antenna characteristics. They concluded that when the size of the parasitic patch is nearly equal to the fed patch, and the distance between the fed patch and the parasitic patch is approximately 0.1 wavelengths, then the bandwidth is increased. When the distance is approximately half wavelength, then gain enhancement is achieved. They have conducted experimental and simulation studies by varying the spacing between the feed patch and the parasitic patch. It was observed that the space between the feed patch and the parasitic patch acts like a cavity and when the distance between the feed patch and the parasitic patch becomes equal to 0.05λ, the electric field between the patches consists of E_z component mainly and the cavity resonates in the TM_{10} mode. If the distance between the patches is held at 0.25λ, the E_z component is found to be decreasing, while the E_x component increases. When the distance is held at 0.5λ, the electric field between the patches consists of the E_x components and the space between the patches acts like a leaky cavity, which mainly contributes for the radiation. The fringing fields between the patches and the ground become in phase and it enhances the radiation from the antenna, thereby increasing the gain. They have conducted experiments with two parasitic patches; the first parasitic patch for increasing the bandwidth and the other for increasing the gain of the antenna [8]. But the major drawback of stacking is that it occupies a larger volume, since the distance between the patches is of the order of half wavelengths.

The major challenge in the stacked array antenna design is to reduce the volume of the antenna while maintaining good impedance matching and

enhanced gain performance. This chapter describes a simple and effective technique to reduce the volume of the stacked antennas without deteriorating impedance matching performance. Stacking is successfully implemented and the position of the parasitic patch is offsetted to enhance the gain performance of the antenna without increasing the height of the parasitic resonator. Offsetting the position of the upper parasitic patch makes the space between the two patches as a leaky cavity and more fringing fields are observed as compared to the stacked antennas without offset. The fringing fields of the lower and upper patches become in phase and the fields produced by them get added up in the far field giving a high gain at the far field.

A single band square microstrip antenna working around 2.63 GHz and the broadband strip loaded tilted square slotted and polygonal slotted antennas discussed in chapter 4 are taken here for consideration. This technique is comparatively easier to fabricate and is devoid of spacers to support the parasitic patch since the parasitic patch is loaded at a height which is equal to the height of the FR4 substrate. Simulated fringing electric field models are discussed in detail for explaining the gain enhancement mechanism for the antennas. The section starts with an electromagnetically coupled square patch antenna. Then its stacked configurations, with and without offset, along with the comparison study with a two element array configuration, are discussed. Finally, the stacked offset configurations of the tilted square slot loaded and polygonal slot loaded broadband antennas are discussed.

5.2 Electromagnetically coupled square patch antenna

An electromagnetically coupled square patch antenna is discussed in this section. The reflection characteristics of this antenna is taken as the reference, since it acts as the feed patch for the stacked configuration described in the

preceding sections. The square patch antenna having a size of $L_1 X L_1$ mm^2 is fabricated on a substrate of dielectric constant 4.2. The total height of the antenna is found to be 3.2mm including the feed substrate. The patch antenna along with the parameters is depicted in fig. 5.1.

The antenna is excited using a 50Ω microstrip transmission line with feed offset parameter L_2 from the right edge of the patch and its length is denoted by L_f. The ground plane dimension is denoted as $L_g X W_g$.
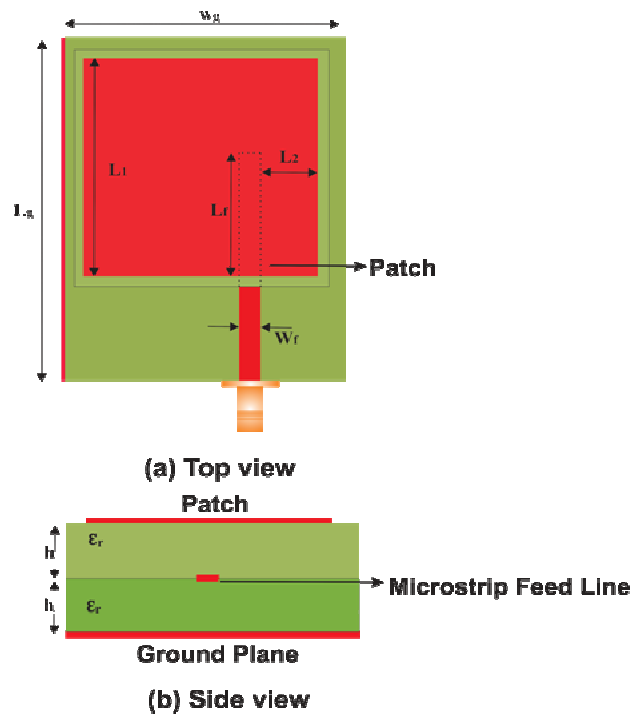
Fig. 5.1 Antenna Geometry

The reflection characteristics of the antenna are shown in fig. 5.2. The fundamental resonance of the antenna is found to be at 2.63 GHz with 4% bandwidth. The antenna parameters are held at L_1=27mm, L_f=17mm, L_2=6.75mm, W_f=3mm, L_g=80mm, W_g=54mm and h=1.6mm. The reflection

coefficient value at the resonance is found to be -21.6 dB and the -10 dB bandwidth of the antenna is 110 MHz.
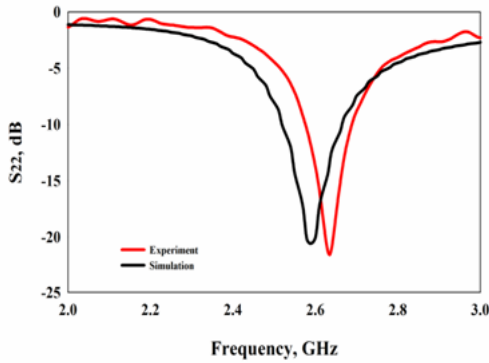
Fig. 5.2 Reflection characteristics
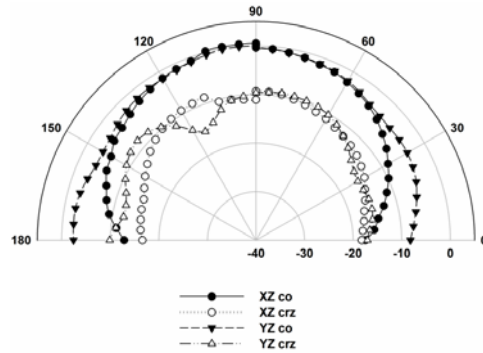
Fig. 5.3 Measured radiation pattern of the antenna

The experimental and simulated radiation patterns of the antenna at the resonant frequency are shown in fig.5.3 and fig.5.4 respectively. It can be concluded that the antenna offers broadside radiation coverage and the pattern maximum lies along the on-axis of the antenna. The cross polar isolation is found to be 10 dB for both the XZ and YZ planes. The estimated gain of the antenna is shown in fig.5.5. The antenna shows a maximum gain of 2.34 dBi at the resonant frequency. The efficiency of the antenna is measured and is found to be 64%.
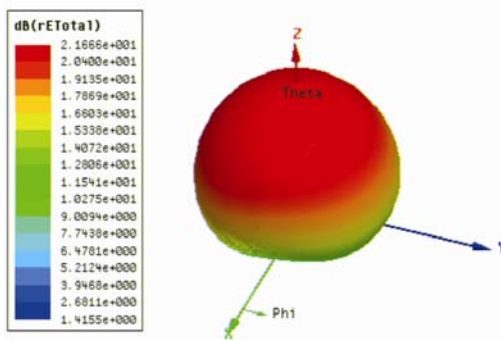
Fig. 5.4 3D Radiation Pattern of the antenna
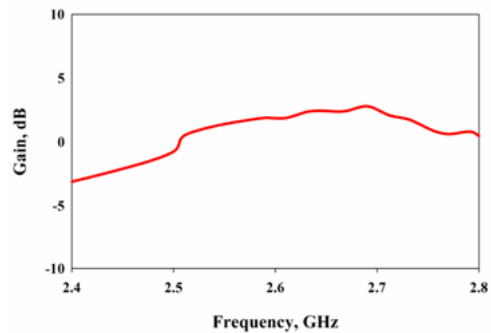
Fig. 5.5 Measured gain of the antenna

5.3 Electromagnetically coupled stacked square patch antenna without offset

This section deals with the stacked configurations of the electromagnetically coupled square patch antenna discussed in the previous section. The section starts with the stacked configuration without any offset in the position of the upper patch and then proceeds into the offset configurations. The geometry of the stacked antenna with the associated parameters is shown in fig. 5.6. Here the separation between the fed patch and the parasitic patch is held at 1.6mm, which is the dielectric thickness of the FR4 substrate. Initially, the offset parameter is made to be L_0=0mm.
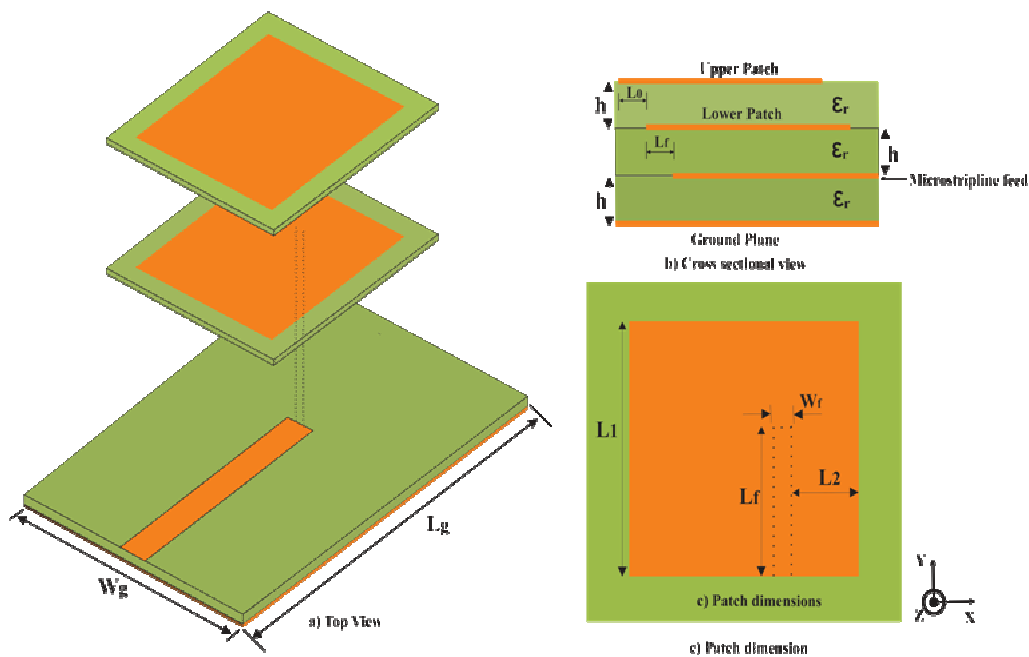
Fig. 5.6 Geometry of the stacked square patch antenna

The antenna parameters are found to be L_1=27mm, L_f=17mm, L_2=6.75mm, W_f=3mm, L_g=80mm, W_g=54mm and h=1.6mm. Care should be taken to mount the parasitic patch over the feed patch. A slight shift in the

position of the parasitic patch will results in change in resonant frequency and hence degradation of impedance matching properties of the antenna.

The reflection characteristics of the antenna are shown in fig. 5.7. The measured and simulated values are in good agreement. The antenna is resonating at 2.48 GHz with the reflection coefficient value of -33 dB and has 5.6% bandwidth (-10 dB bandwidth of 140 MHz) around the resonance. It is observed that the resonant frequency of this stacked configuration is found to be lower than that of the square patch antenna without the parasitic patch as discussed in the previous section. This lower shift is due to the fact that the placement of the upper patch affects the fringing fields of the lower patch, thereby increasing the effective dielectric constant of the lower patch.

The XZ and YZ plane experimental and simulated 3D far field radiation patterns of the proposed antenna are shown in fig. 5.8 and fig. 5.9 respectively. It is observed that the antenna shows broadside radiation characteristics with the pattern maximum directed along the bore sight. The cross polar isolation is found to be 10 dB for both the XZ and YZ planes.

The gain of the stacked antenna is shown in fig.5.10. The antenna shows a maximum gain of 1.78 dBi at 2.48 GHz. The radiation efficiency of the antenna is found to be 38% at the resonance. The reduction in the gain of the antenna can be well explained using the simulated electric field distributions of the antenna. A comparison study of the fringing electric field distributions of the simple patch antenna, stacked patch antenna with and without offset are described in detail in section 5.4.4.
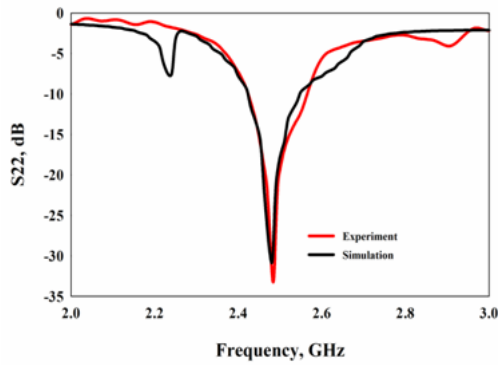
Fig. 5.7 Reflection characteristics   **Fig. 5.8 Radiation pattern at 2.48 GHz**
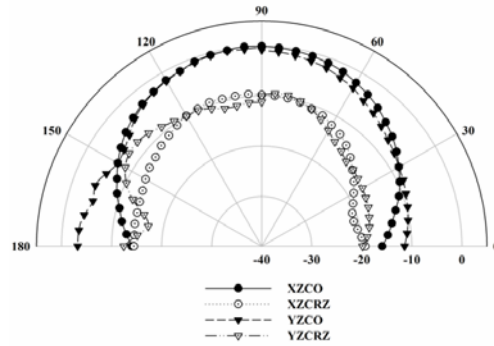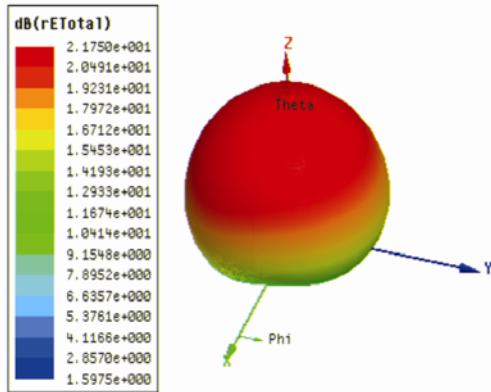
Fig. 5.9 3D Radiation pattern at 2.48 GHz   **Fig. 5.10 Reflection characteristics**
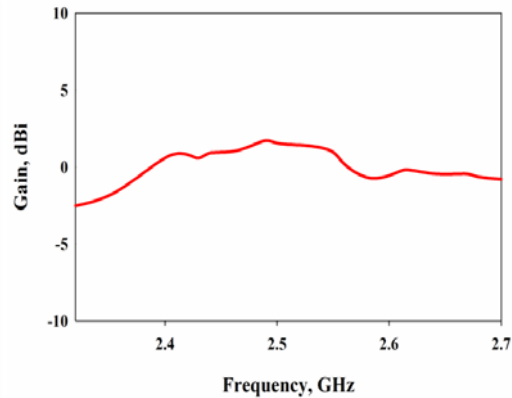
5.3.1 Effect of parasitic loading height

In this section the effect of parasitic loading height on the resonant and radiation characteristics of the stacked patch antenna are studied. The resonant frequency and the gain are the major parameters under consideration. In order to perform the height variation studies, the stacked patch antenna with the geometrical parameters L_1=27mm, L_2=6.75mm, L_f=17mm, L_g=80mm and W_g=54mm printed on the FR4 epoxy substrate is taken into consideration for simulation.

The effect of the stacking height on the reflection characteristics is plotted in fig. 5.11. The height is varied from 0.8mm to 4mm in steps of 0.4mm. It is observed that increase in the stacking height lowers the resonant frequency. Corresponding to the height variation from 0.8mm to 4mm, the resonant frequency shift is from 2.56 GHz to 2.37 GHz. It is observed that corresponding to a stacking height of 0.8mm, the resonant frequency is found to be 2.56 GHz and increase in the stacking height decreases the resonant frequency. Good matching is observed when the stacking height is equal to 1.6mm. Increase in stacking height above 1.6mm deteriorates impedance matching gradually. The cause of the degradation in impedance matching is well explained using the input impedance variation of the antenna. The input impedance variation of the stacked antenna with stacking height is shown in fig. 5.12. It is observed that increasing the height of the parasitic patch will decrease the real part of the input impedance and due to the decrease in the coupling between the patches, the imaginary part of the impedance is shifted towards the inductive side.
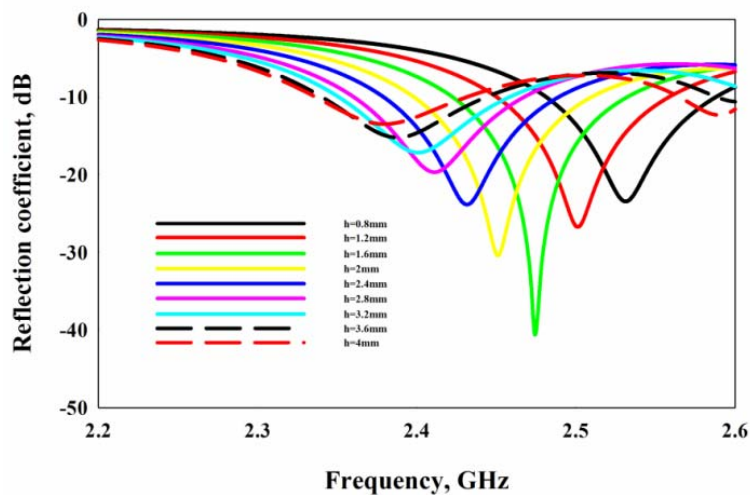
Fig. 5.11 Effect of stacking height on reflection characteristics
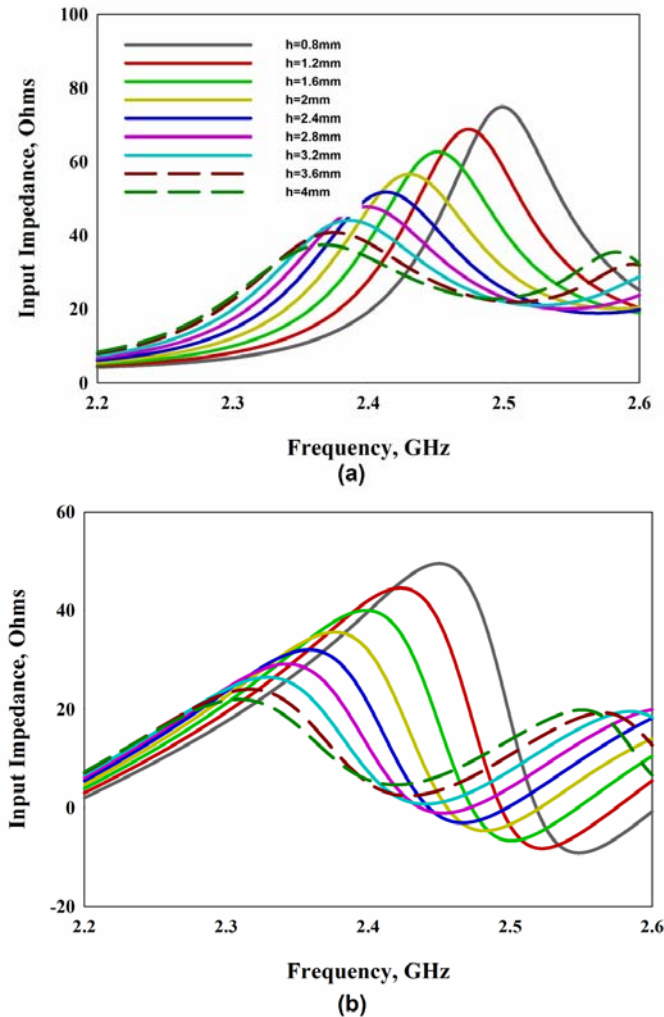
**Fig. 5.12 Effect of stacking height on Input Impedance a) Real part,
b) Imaginary part**

The variation of the gain of the stacked square patch antenna without offset against the stacking height is studied and is tabulated in table 5.1. For a stacked microstrip patch antenna, increase in the stacking height increases the gain of the antenna. The same observation is valid here also. The gain of the simple sqaure patch antenna without the parasitic patch is also taken at the same feed point as that of the stacked antenna without offset as a reference. The

maximum gain achieved for the stacked configuration is only 2.52 dBi at a stacking height of 2.4mm. Increasing the height above 2.4 mm deteriorates the matching performance of the antenna and hence gain decreases gradually. It is observed that the stacking height above 1.6mm can only give an enhanced gain as compared to the standard square patch antenna.

Table 5.1 Height Variation Study

Height, mm	Resonant frequency, GHz	Gain, dBi
0 (Single patch)	2.63	2.3600
0.4	2.6	2.1800
0.8	2.56	2.1700
1	2.54	2.1600
1.2	2.52	2.2300
1.4	2.51	2.2900
1.6	2.5	2.3200
2	2.47	2.5000
2.4	2.46	2.5200
2.8	2.44	2.5100
3.2	2.43	2.4700
3.6	2.42	2.3300

5.4   Stacked Offset Patch Antenna Configurations

In this section, offsetting technique is successfully implemented on the stacked square patch antenna configuration discussed in the previous section. The upper parasitic patch is offsetted in the +Y direction by a displacement of L_0. The geometry of the design is shown in fig. 5.6. Offsetting procedure should

be done with maximum care, because any misalignment of the parasitic patch adversely affects the resonant and radiation behavior of the antenna.

5.4.1 Offset variation studies

The initial aim is to find out the change in the resonant frequency of the structure with offset parameter L_0. A detailed parametric analysis has been carried out to find out the effect of offset parameter on the resonant frequency and is illustrated in fig.5.13. The offset parameter 'L_0' is varied up to 7mm in steps of 1mm.
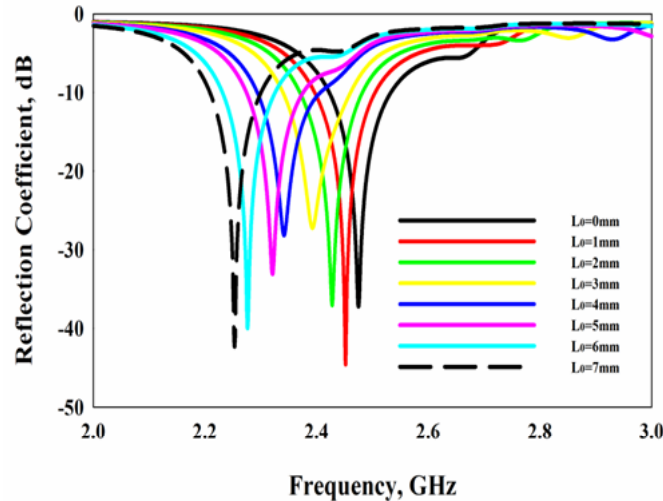
Fig. 5.13 Effect of offset parameter L_0

The other antenna parameters are kept at L_1=27mm, L_2=6.75mm, L_f=17mm, L_g=80mm and W_g=54mm. It is noted that as L_0 increases, the resonant frequency is found to be decreasing.

5.4.2 Stacked offset antenna with L_0=3mm

The experimental realization of the offset configurations were taken for two configurations, one with offset parameter L_0=3mm and the other with

L_0=5mm. Initially the stacked antenna configuration with offset parameter L_0=3mm is taken into consideration. The geometric parameters of the antenna are found to be L_1=27mm, L_2=6.75mm, L_f=17mm, L_0=3mm, L_g=80mm and W_g=54mm. The antenna is printed on the same FR4 substrate and fed via a printed microstrip transmission line fabricated using the same substrate as that of the stacked antenna without offset.
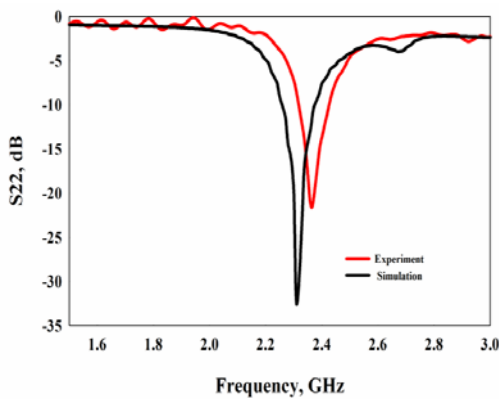
Fig. 5.14 Reflection characteristics   **Fig. 5.15 Measured gain of the antenna**
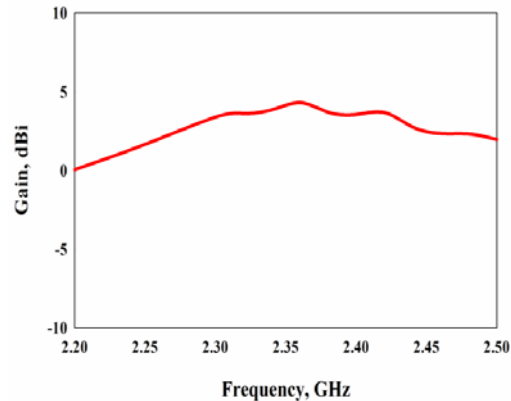
The antenna is found to be resonating at 2.36 GHz with a reflection coefficient value of -21.5dB as depicted in fig. 5.14. The -10dB bandwidth of the antenna is found to be 110MHz with 4.6% bandwidth around the resonance. As compared to the antenna without offset, the antenna is resonating at a lower resonating frequency with 120MHz frequency difference.

The gain of the antenna is measured and it is illustrated in fig.5.15. It is interesting to note that the antenna has a peak gain of 4.49 dBi at the resonating frequency. The experimental and simulated radiation patterns of the antenna at the resonant frequency are shown in fig.5.16 and fig.5.17 respectively. The cross polar isolation is found to be 8.5 dB in both the planes. The 3dB beamwidths are found to be 71^0 and 96^0 in the XZ and YZ planes respectively.
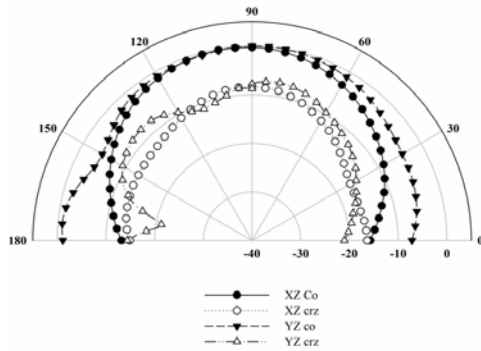
Fig. 5.16 Experimental radiation pattern of the stacked offset antenna with L_0=3mm
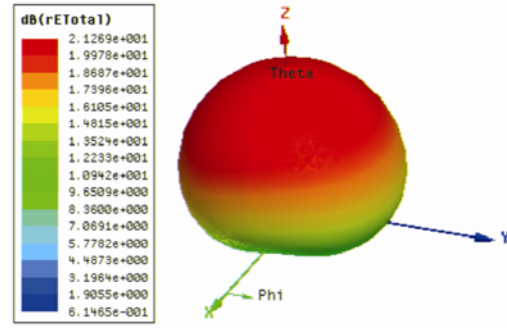
Fig. 5.17 Simulated 3D radiation pattern of the stacked offset antenna with L_0=3mm

5.4.3 Stacked offset antenna with L_0=5mm

Finally, stacked offset patch antenna with offset parameter L_0=5mm is taken into consideration. The reflection and gain characteristics of the proposed design are shown from fig. 5.18 and fig. 5.19 respectively. The antenna parameter are found to be L_1=27mm, L_2=6.75mm, L_f=17mm, L_0=5mm, h=1.6mm, L_g=80mm and W_g=54mm.

The antenna is found to be resonating at 2.3 GHz with a -10 dB bandwidth of 100MHz and the reflection coefficient value at the resonance is found to be –22dB. The antenna has a maximum gain of 4.8 dBi at the resonant frequency which is greater than twice as that of the antenna without offset in the position of the upper patch. The experimental and the simulated 3D radiation patterns of the antenna at the resonant frequency are shown in fig. 5.20 and fig. 5.21 respectively. It is observed that the antenna is showing broadside radiation coverage with a cross polar isolation of 7.7 dB and 5.4 dB in the XZ and YZ planes respectively.
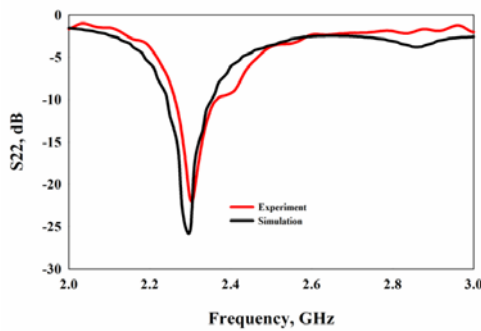
Fig. 5.18 Reflection characteristics
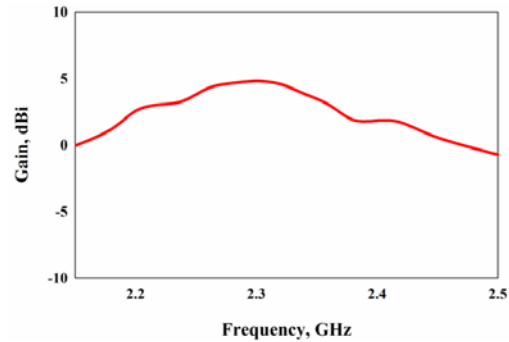
Fig. 5.19 Gain of the antenna
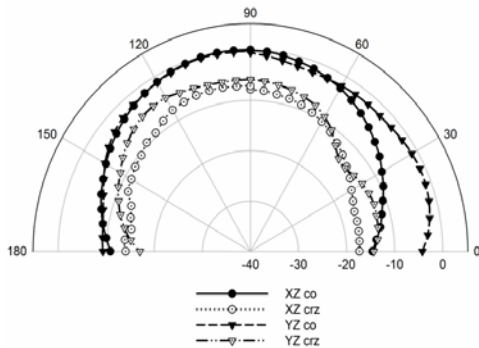
Fig. 5.20 Experimental radiation pattern of the stacked offset antenna with L_0=5mm
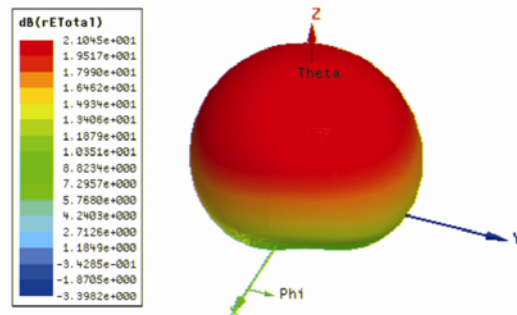
Fig. 5.21 Simulated 3D radiation pattern of the stacked offset antenna with L_0=5mm

5.4.4 Electric field distributions of the antennas

The previous sections deal with the stacked configurations of square patch antenna with and without offset. This section gives an elaborate study of the electric field distributions of the antennas. It gives an idea about the radiation characteristics of the antennas and the reason for gain enhancement is clearly explained here. A comparison study on the radiation patterns of the different stacked configurations discussed in the previous sections is also included. The electric field distributions of the simple patch antenna, stacked patch antenna with L_0=0mm and h=1.6mm and stacked patch antenna with L_0=5mm and h=1.6mm are illustrated in fig. 5.22. It is observed that for a simple square patch antenna, the fringing fields along the radiating edges of the patch acts like two slots separated

by half wavelength which aids the radiation mechanism and is shown in fig. 5.22(a). But the placement of the upper parasitic patch affects the fringing fields of the fed patch and if the two patches are very close to each other, the space between the patches acts like strong cavity and a small fringing field is observed along the periphery of the patch. This gives reduced radiation and hence gain of the antenna is reduced. Offsetting the parasitic patch makes the cavity leaky and more fringing fields are observed along the periphery of the patches. Here the E_x component dominates than that of the E_y component making polarization along the X-axis and hence it gives an enhanced radiation resulting in a high gain as compared to the simple patch antenna and the stacked antenna without offset. The offset in the position of the upper parasitic patch decreases the cross polar isolation slightly in both the planes. This is because of the enhanced radiation provided by the E_y component in the fringing field and it can be best understood by looking into the fringing electric field pattern shown in fig.5.22 (c). Also the increase in offset parameter increases the 3 dB beamwidth in the YZ plane gradually.
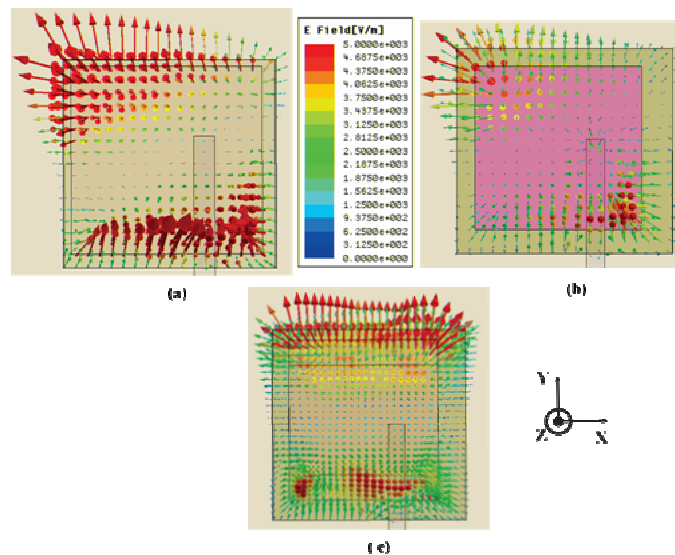
Fig. 5.22 Fringing Electric field distributions of the antennas a) Single patch antenna, b) Stacked patch antenna with L_0=0mm and h=1.6mm and c) Stacked patch antenna with L_0=5mm and h=1.6mm

5.5 The two element array: a comparison study

In this section, a comparative study of the radiation performance of the stacked offset square patch antenna with that of a two element array is carried out. The same square patch antenna used for the construction of the stacked offset patch antenna configuration act as the basic element of the array configuration. The two elements are fed centrally through the Wilkinson power divider arrangement fabricated on FR4 substrate of dielectric constant 4.2. The inter element spacing is made to be half wavelength. The geometry of the proposed two element array antenna is shown in fig. 5.23. The geometrical parameters of the antenna are L_1=27mm, L_f=13mm, L_s=36mm, L_g=85mm and W_g=80mm, h=1.6mm and εr=4.2.
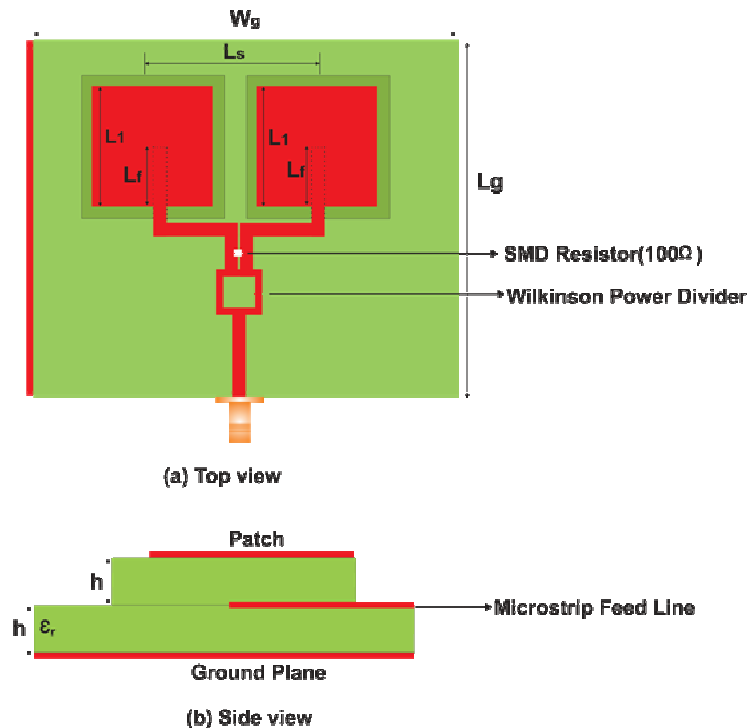
Fig. 5.23 Geometry of the two element array configuration
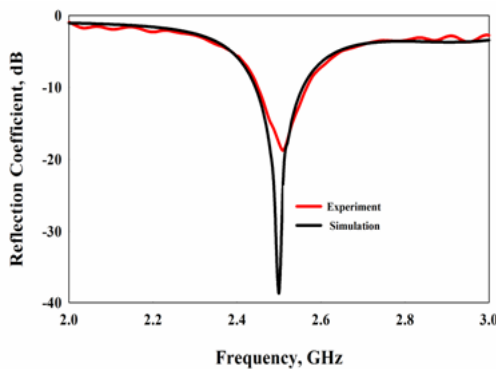
Fig. 5.24 Reflection characteristics of the two element array antenna
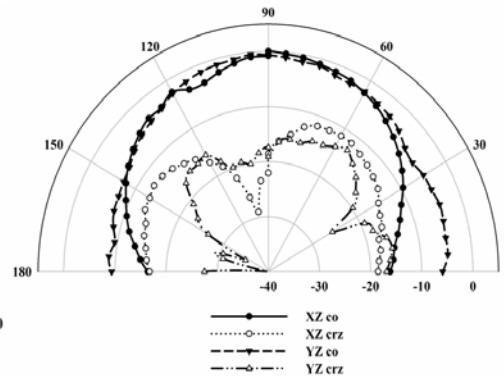
Fig. 5.25 Radiation patterns of the two element array antenna

The experimental and simulated reflection characteristics of the proposed array antenna configuration are shown in fig. 5.24. It is observed that the antenna is resonating at 2.5 GHz. The antenna has a reflection coefficient value of -18.7 dB at the resonance and is exhibiting 4.3% bandwidth from 2.45 GHz to 2.56 GHz.   The gain of the antenna is computed and it has a maximum gain of 5.3 dBi at the resonance.

The XZ and YZ plane measured radiation patterns of the antenna are shown in fig. 5.25. It is observed that the antenna exhibits a cross polar isolation of 17.5 dB for both the planes and the 3 dB beamwidth is found to be 67^{0} for both the planes.

The experimental gain chart for the fabricated designs is shown in fig.5.26. It is noted that the stacked antenna without any offset in the position of the upper parasitic patch shows a gain of 1.69 dBi at the resonant frequency. It is noted that offsetting the position of the upper patch lowers the resonant frequency, but it enhances the gain performance of the antenna. The antenna with offset parameter L_0=3mm is showing a gain of 4.49 dBi whereas the antenna with L_0= 5mm is showing a maximum gain of 4.8 dBi. It is found that

increase in L_0 increases the gain of the antenna. The two element array on the other hand shows a maximum gain of 5.3 dBi, but it occupies a larger volume. It is worthwhile to note that the stacked antenna with L_0=5mm shows a comparable gain performance as compared to the two element array configuration while maintaining satisfactory radiation and matching characteristics with an added advantage of compact mode of operation. It gives a volume reduction of 24.78 % as compared to the two element array configuration.
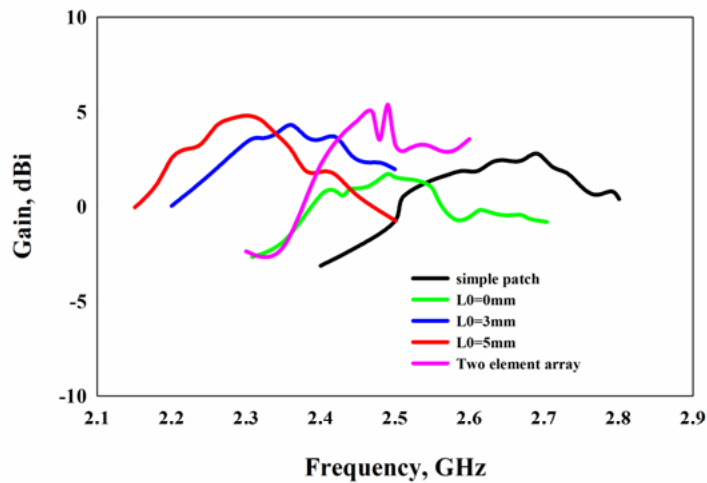
Fig. 5.26 Measured gain of the fabricated antennas

The experimental radiation patterns of the stacked antenna with L_0=0mm and h=1.6mm, stacked offset antenna with L_0=3mm and h=1.6mm, stacked offset antenna with L_0=5mm and h=1.6mm and the array antenna configurations at the resonant frequencies are depicted in fig. 5.27. It is observed that for the stacked antenna without any offset in the position of the upper patch, -10 dB cross polar isolation is observed for both the planes. It shows a 3 dB beamwidth of 74^0 in the XZ plane and 67^0 in the YZ plane. The offset in the position of the upper parasitic patch decreases the cross polar

isolation slightly in both the planes. This is because of the enhanced radiation provided by the E_y component in the fringing field and it can be best understood by looking into the fringing electric field pattern shown in fig. 5.22(c). Also the increase in offset parameter increases the 3 dB beam width in the YZ plane gradually. When L_0=3mm, the cross polar isolation is found to be 8.5 dBi for both the planes. The 3 dB beamwidths are found to be 71^0 and 96^0 in the XZ and YZ planes respectively.

For L_0=5mm, the cross polar isolation is of the order of 7 dB and the antenna shows a 3 dB beamwidth of 77^0 in the XZ plane and 129.5^0 in the YZ plane. For the two element array configuration, a high cross polar isolation is observed and is of the order of 17.5 dB for both the planes. The 3 dB beam with is found to be 67^0 for both the planes.
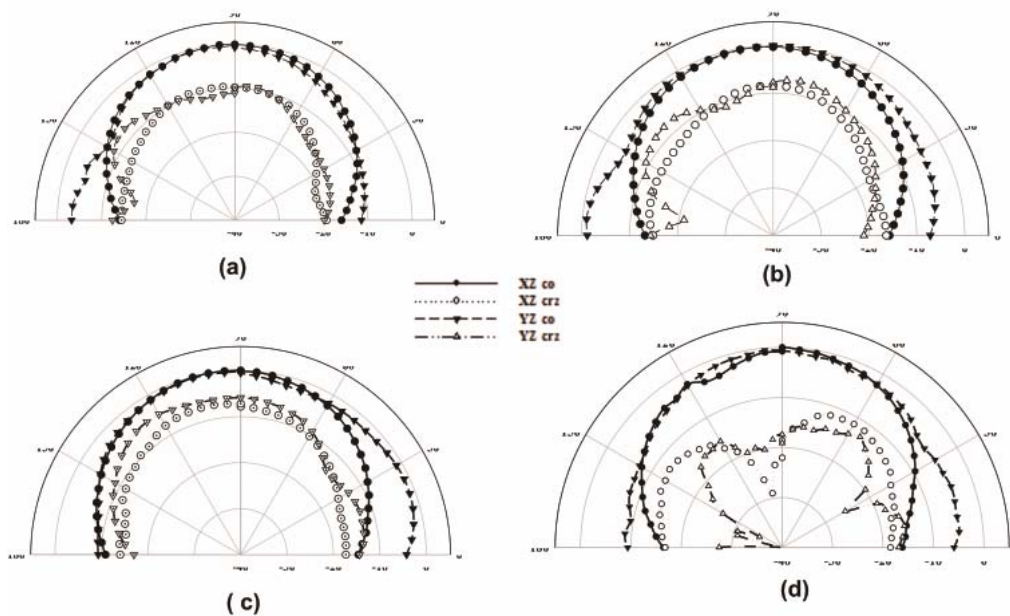
Fig. 5.27 Radiation characteristics of the antennas a) stacked patch antenna without offset, b) stacked offset antenna with L_0=3mm, c) Stacked offset patch antenna with L_0=5mm and d) two element array configuration

The important conclusions arrived from the above studies are summarized below

- Principle of offsetting can be effectively applied on the stacked single band antenna configuration to achieve high gain performance without deteriorating the impedance matching performance of the antenna.

- In conventional stacked high gain antennas, gain enhancement is achieved by stacking the parasitic patch at a height equal to the half wavelength of the resonating frequency. The offsetting technique greatly reduces the volume of the antenna without deteriorating the impedance matching performance of the antenna.

- The single band design working around 2.3 GHz has a stacking height of the order of $0.025\lambda_g$, where λ is the guided wavelength corresponding to the resonant frequency of the antenna and gain of the antenna is found to be 4.8 dBi.

Based on the above important conclusions, the offset stacking technique is applied to the two broadband designs depicted in chapter4 and their detailed studies are discussed in the following sections.

5.6 Stacked offset broadband microstrip patch antennas

In this section, principle of stacking and parasitic patch offsetting is successfully implemented for strip loaded tilted square slot loaded and polygonal slot loaded broadband microstrip antenna designs discussed in chapter 4.

5.6.1 Stacked Tilted Square Slot loaded broadband patch antenna with zero offset

The broadband strip loaded patch antenna discussed in chapter 4 is stacked with the same structure with zero offset in the position of the parasitic

upper patch. The experimental and simulation studies of the structure are discussed in detail in this section.

5.6.1.1 Antenna Geometry

The geometry of the proposed antenna is shown in fig. 5.28. The antenna consists of strip loaded tilted square slotted antenna as the lower patch. The dimensions of this fed patch are found to be L_1=35mm, L_2=17.5mm, L_3= 7.8mm, W=2mm and L_f=10.5mm. The ground plane dimension is selected to be 44X55 mm^2. The patch is fabricated on a substrate of dielectric constant 4.2 and thickness 1.6mm. The antenna is electromagnetically coupled using a 50Ω microstrip transmission line. The transmission line is fabricated using the same substrate. The same patch antenna fabricated on the same substrate is stacked over the initial antenna so that the total height of the antenna is found to be 4.8mm, including the transmission line. The offset parameter is made to be L_0=0mm.
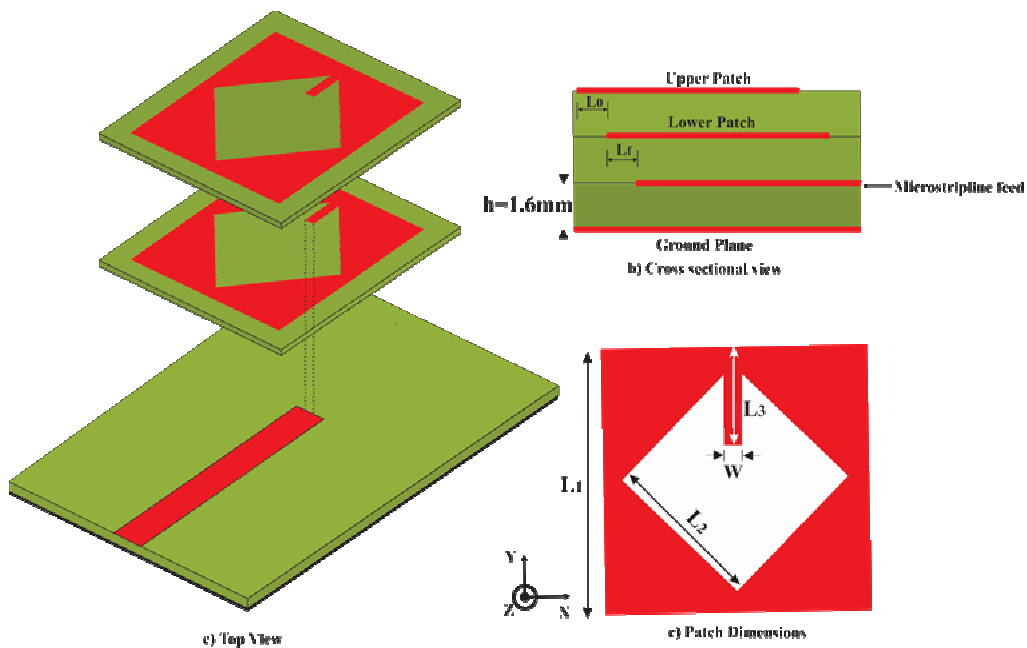
Fig. 5.28 Geometry of the antenna

5.6.1.2 Reflection Characteristics

Fig. 5.29 shows the reflection characteristics of the stacked antenna with zero offset in the position of the upper parasitic patch. The antenna has a 2:1 VSWR bandwidth of 32.51% from 4.07 GHz to 5.65 GHz. It is understood that placement of the upper patch shifts all the resonant frequencies to the lower side. This lower shift is due to the increase in the effective dielectric constant of the driven patch because the parasitic patch affects the fringing field of the driven patch.
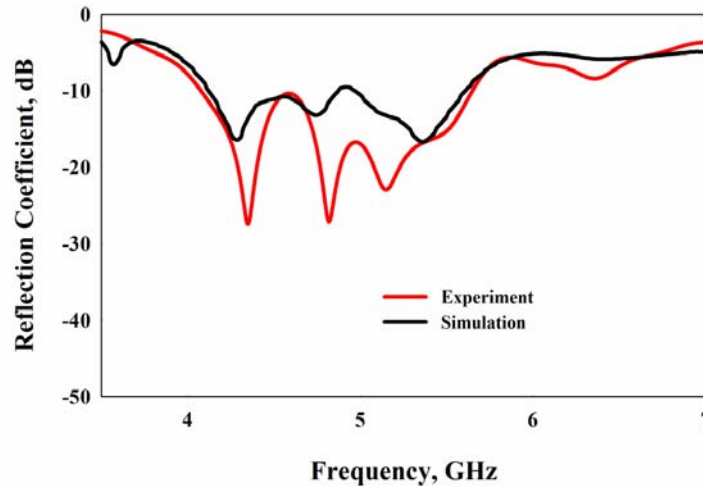
Fig. 5.29 Reflection characteristics of the antenna without offset

It is observed that the minor resonance around 5 GHz for the antenna without the parasitic patch is found to be predominant for the stacked configuration and it is found to be at 4.8 GHz. The other resonances are found to be around 4.3 GHz, 5.1 GHz and at 5.4 GHz.

5.6.1.3 Effect of stacking height

In order to study the effect of the parasitic patch height on antenna reflection characteristics, a thorough parametric analysis has been performed.

Fig. 5.30 shows the effect of stacking height on antenna reflection characteristics. It is found that the parasitic patch height majorly affects the matching for the higher resonant frequencies and the lower resonance is found to be unaffected. When the stacking height exceeds 3.2mm, the lower two resonances will be predominant and the matching for the higher resonance is found to be deteriorating.
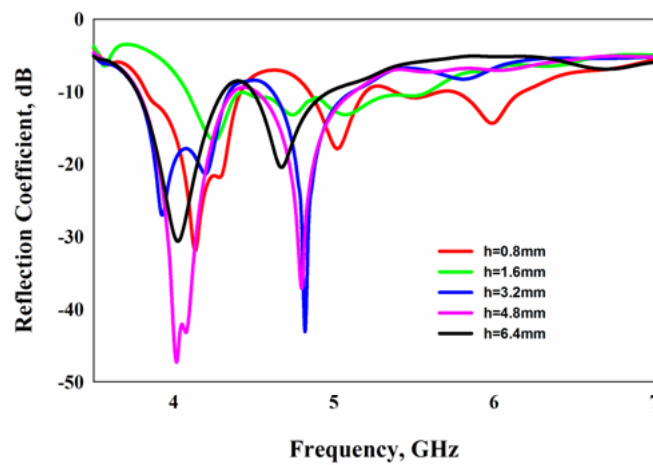
Fig. 5.30 Effect of stacking height

5.6.1.4 Radiation patterns and gain of the antenna

The measured radiation patterns of the antenna at the resonant frequencies are shown in the fig. 5.31. It is observed that the XZ plane radiation patterns are almost identical throughout the entire frequency of operation. For all the resonances, the XZ copolar pattern shows lesser power as compared to the corresponding YZ copolar pattern. The simulated 3D radiation patterns of the antenna at the resonant frequencies are shown in fig. 5.32. The cross polar isolation throughout the entire frequency band of operation for both the planes is studied in detail and is shown in table 5.2.
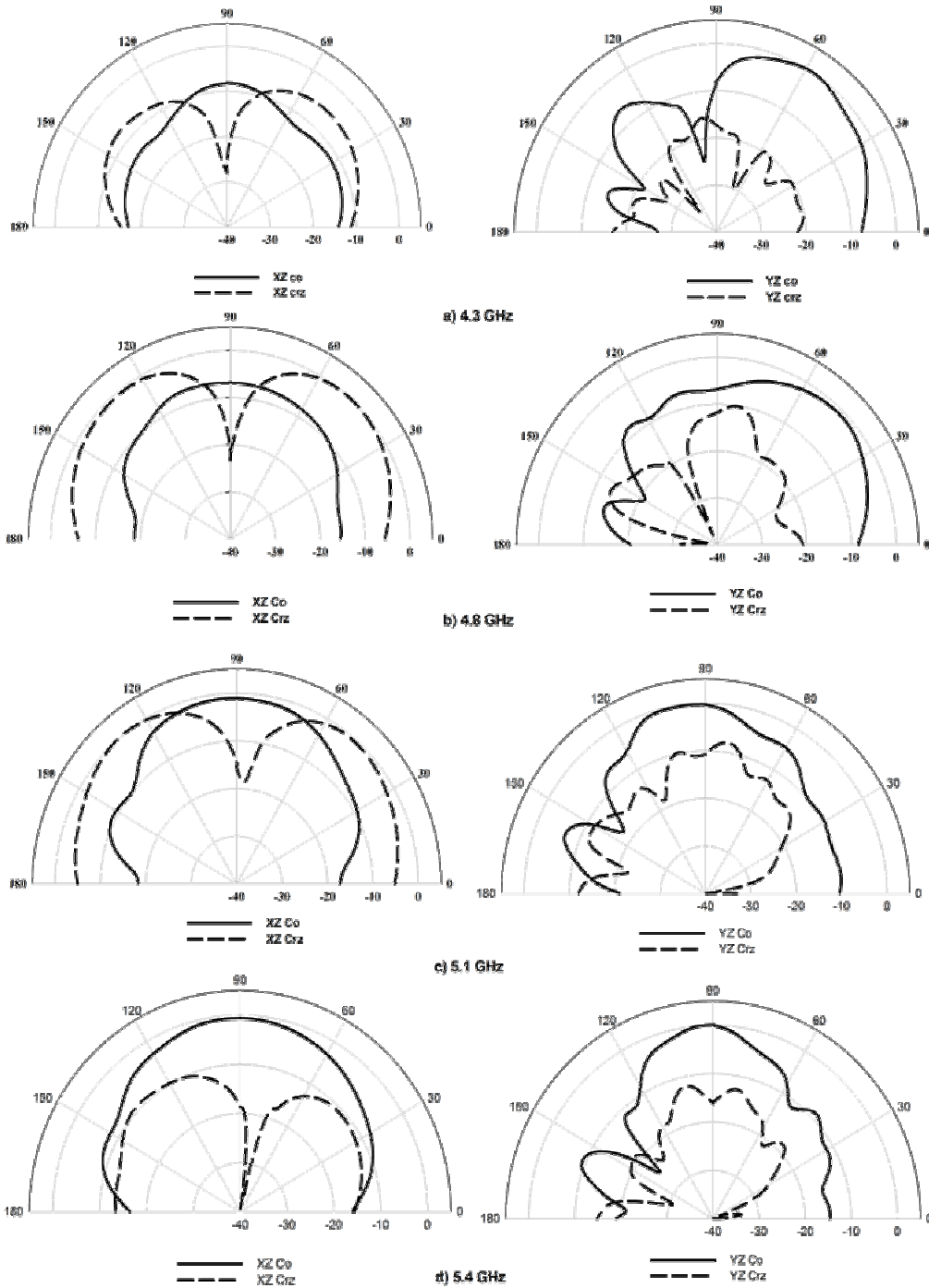
Fig. 5.31 Radiation patterns of the antenna
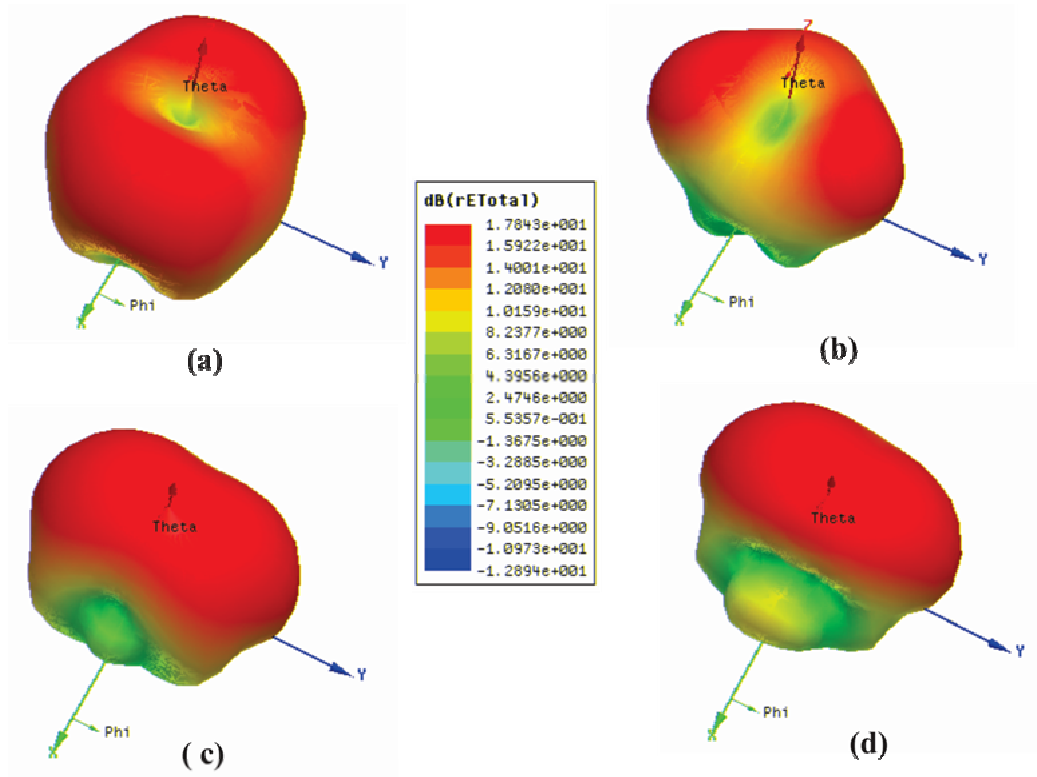
Fig. 5.32 3D Radiation patterns of the antenna at a) 4.3 GHz, b) 4.8 GHz, c) 5.1 GHz and d) 5.4 GHz

Table 5.2 Cross polarization characteristics of the antenna

Frequency, GHz	Cross polarization (dB)	
	XZ Plane	YZ Plane
4.1	15	9
4.3	20	9
4.5	30	7.5
4.7	19.7	5
4.9	15	6.3
5.1	14.25	10.7
5.3	17.9	15.8
5.5	34.7	34.7

The gain of the antenna is shown in fig. 5.33. The maximum gain of the antenna is found to be 8.13 dBi at 5.5 GHz. The average gain of the antenna over the band is only 6.56 dBi.
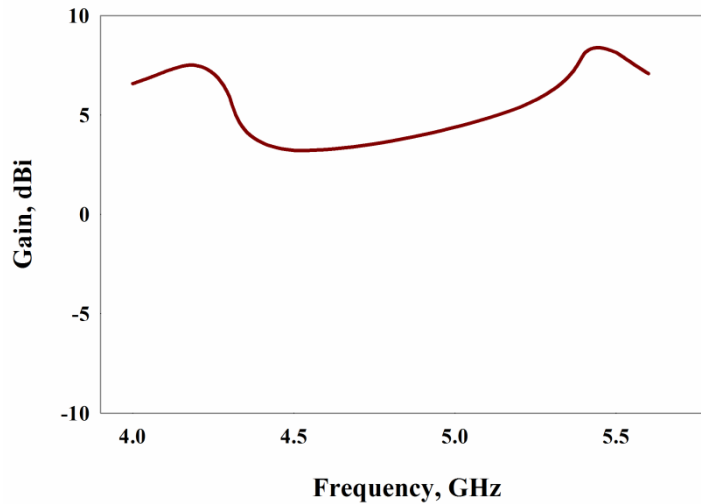
Fig. 5.33 Gain of the antenna

5.7   The stacked offset microstrip antenna

The stacked offset microstrip patch antenna discussed in section 5.7.1 cannot increase the gain considerably, especially for the centre frequencies in the band of operation. This is due to the strong coupling between the feed patch and the parasitic patch. Gain enhancement can be achieved by making the cavity leaky. This is accomplished by offsetting the position of the upper patch along +Y-direction. The experimental and simulation studies guiding into the gain enhancement technique of the antenna are discussed in detail in this section.

5.7.1 Antenna geometry

The geometry of the proposed offset stacked microstrip patch antenna is shown in fig. 5.28. The antenna is obtained by offsetting the position of the

upper patch along +Y direction by a distance L_0 as compared to the antenna without offset. The other antenna parameters remain the same as that of the stacked antenna without offset. The antenna parameters at the optimum design are found to be L_1=35mm, L_2=17.5mm, L_3=7.8mm, W=2mm, L_f=10.5mm, L_0=4mm and h=1.6mm at the optimum design. The antenna is fabricated on a substrate of dielectric constant 4.2.

5.7.2 Reflection characteristics

The reflection characteristics of the stacked offset microstrip patch antenna at the optimum offset distance are shown in fig.5.34. The antenna has a 2:1 VSWR bandwidth of 34.9 % from 3.73 GHz to 5.73 GHz. The wide bandwidth is obtained by merging five resonances centered around 3.8 GHz, 4.27 GHz, 4.76 GHz, 5.1 GHz and 5.49 GHz. It is an interesting observation that the offset in the position of the upper patch introduces an additional lower new resonance around 3.8 GHz which merges together with the other resonances to enhance the bandwidth of the antenna.
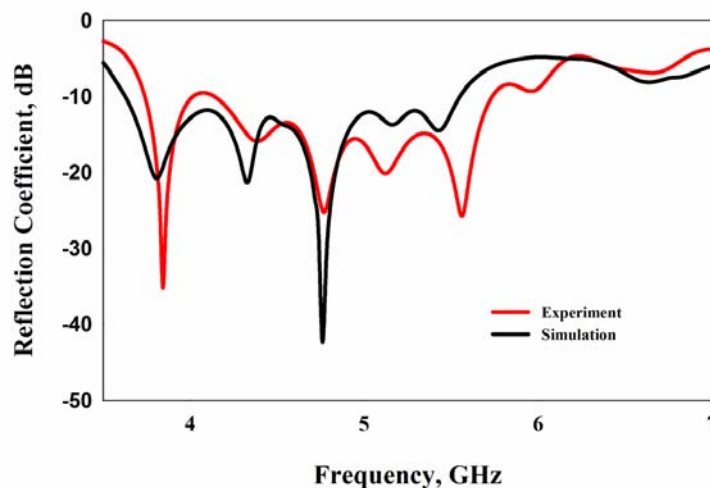
Fig. 5.34 Reflection characteristics of the stacked offset microstrip antenna

5.7.3 Effect of offset parameter

In order to study the effect of offset parameter L_0 on antenna reflection characteristics, a rigorous parametric analysis has been performed. Fig. 5.35 shows the effect of L_0 on antenna reflection characteristics.
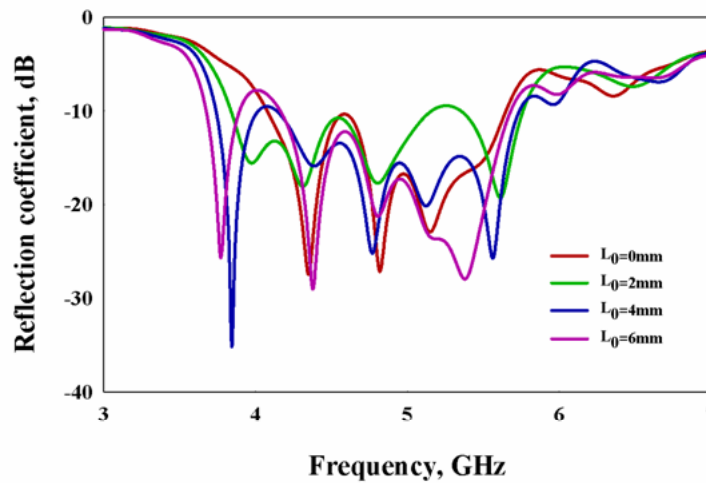
Fig.5.35 Effect of offset parameter L_0 on reflection characteristics

It is observed that offsetting the parasitic patch introduces a lower resonance and as L_0 increases the newly generated resonance shifts towards the lower side from the 4.3 GHz resonance. No predominant shift in the other resonant frequencies is observed. An optimum offset parameter of L_0=4mm is selected to attain the maximum bandwidth of the antenna. It is concluded that the offset structure itself acts as the origin of the newly generated resonance as in [9].

5.7.4 Upper substrate height variation

Here, the effect of the upper substrate height on the reflection characteristics of the antenna is studied. It is shown in fig. 5.36. It can be seen that the antenna attains broadband operation when the substrate thickness is

increased above 1mm. Below h=1mm, the resonances are not properly merged. The maximum available bandwidth is obtained when h=1mm. It is also noted that increasing h above 1mm decreases the percentage bandwidth of the antenna. This is because increase in 'h' above 1mm deteriorates the impedance matching corresponding to the higher resonant frequency.
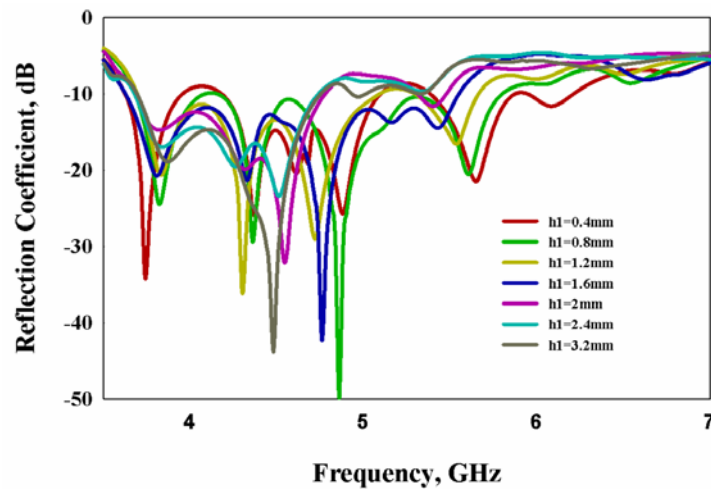
Fig. 5.36 Effect of upper substrate height variation

5.7.5 Radiation pattern and gain of the antenna

The experimental and simulated radiation patterns of the antenna at the resonances are shown in fig.5.37 and fig.5.38 respectively. It is observed that for all the resonances, a symmetrical stable XZ copolar pattern is observed for the entire operating band and the YZ copolar patterns show fluctuations. For the first four resonances the YZ plane cross polar power is lower as compared to that of the XZ plane. The maximum cross polar isolation is found to be 33 dB at 5.1 GHz in the XZ plane and 36.7 dB at 5.49 GHz in the YZ plane patterns. The variation of cross polar level and 3 dB beam width over the entire operating band is studied and is shown in Table 5.3.
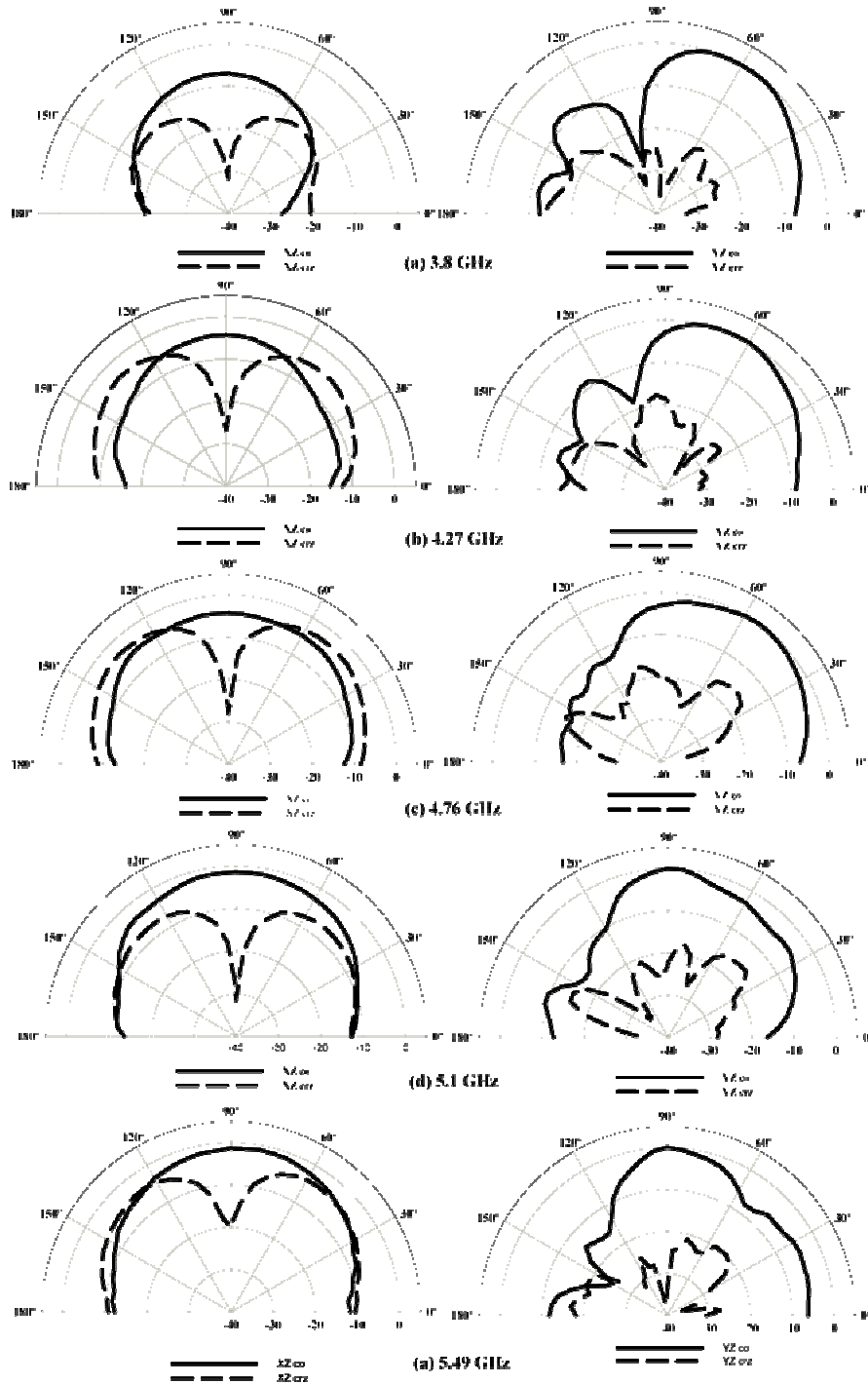
Fig. 5.37 Measured radiation patterns of the antenna
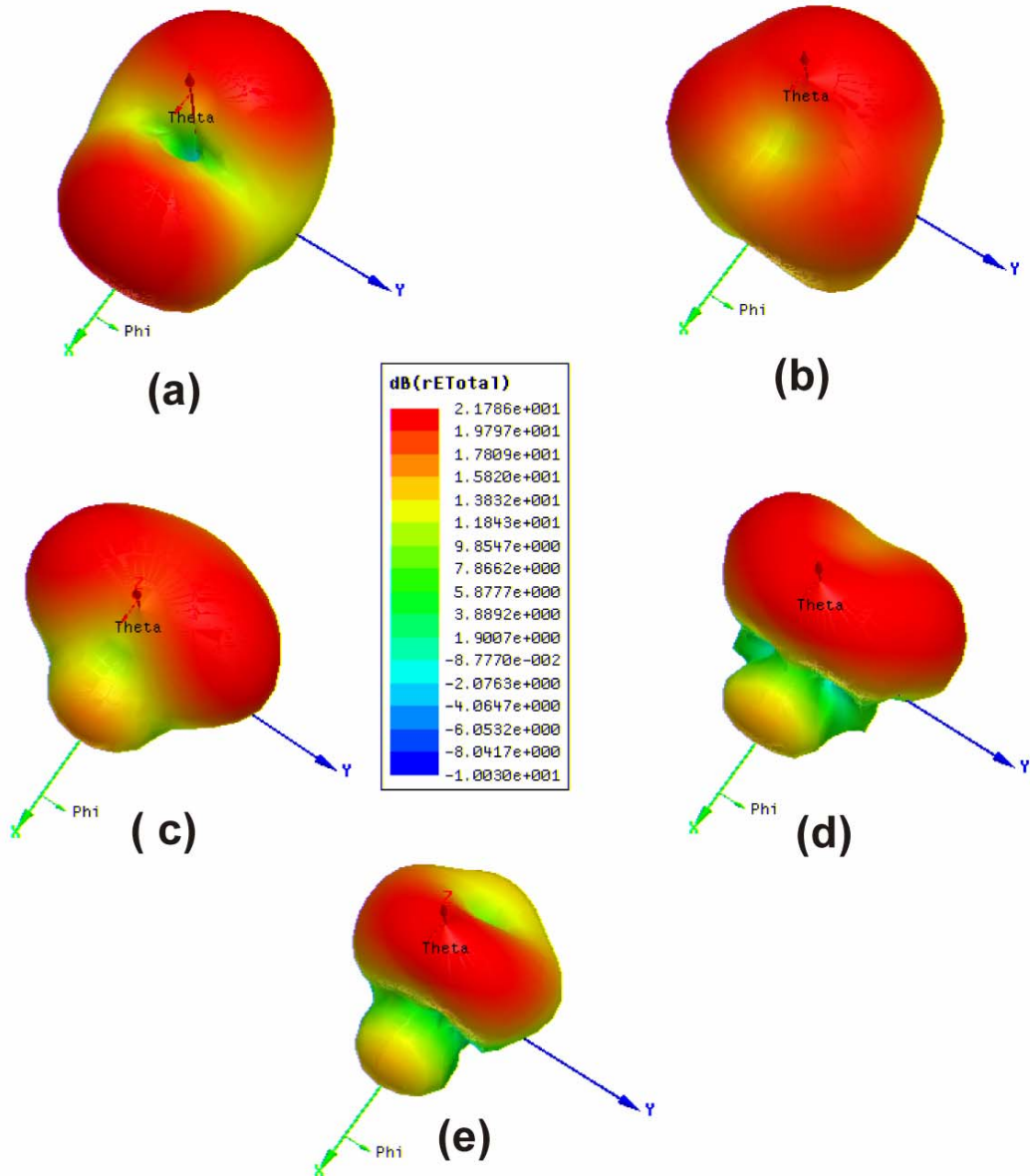
Fig. 5.38 Simulated radiation patterns of the antenna at a) 3.8 GHz, b) 4.27 GHz, c) 4.76 GHz, d) 5.1 GHz and e) 5.49 GHz

Table 5.3 Measured Cross-Polar Level and 3db Beamwidth

Frequency, GHz	Cross polar level along the on axis, dB		3 dB Beam width, degrees	
	XZ Plane	YZ Plane	XZ Plane	YZ Plane
3.75	25.48	18.76	77	53
3.95	22.8	18.8	60.8	50.4
4.15	22.5	15.7	58.6	48
4.35	25.4	15	72.9	59.4
4.55	25.8	15.4	103.6	62.2
4.75	25.7	16.7	111	67
4.95	27.5	20	104.8	75.2
5.15	30	23.4	85.6	31.6
5.35	23.1	29.6	74.3	28.9
5.55	17.5	31.33	80.8	35
5.73	12.5	16.2	119	35

The gain of the antenna is shown in fig. 5.39. The antenna shows a maximum gain of 8.07 dBi at 3.9 GHz which is very much higher than that of a conventional patch antenna fabricated on the same substrate and it is also noted that the gain of the centre resonant frequencies are also enhanced as compared to the antenna with zero offset (L_0=0mm) in the position of the upper patch.
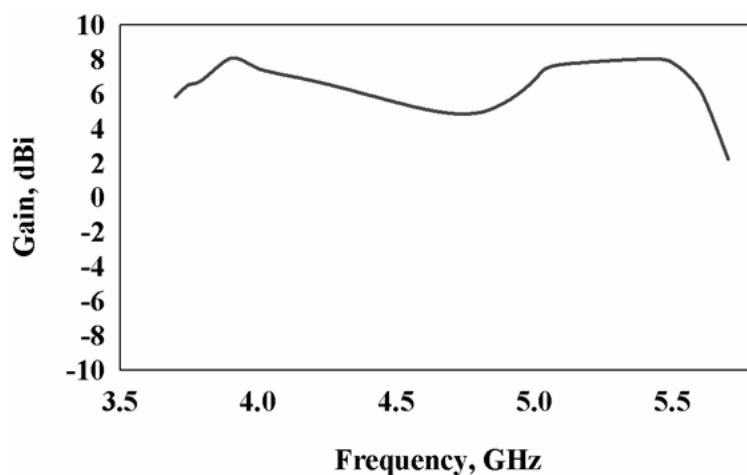
Fig. 5.39 Measured Gain of the antenna

5.8 The offset stacked polygonal slot loaded broadband microstrip antenna

In this section, principle of stacking and offsetting is implemented on the polygonal slot loaded broadband microstrip patch antenna discussed in chapter 4. Here, the offset parameter is maintained at L_0=2mm. The geometry of this final design is shown in fig. 5.40. The other geometrical passssrameters of the antenna are found to be L_1=35mm, L_2=14.3mm, L_3=5.8mm, W=3mm, and L_f=10.55mm. The total thickness of the antenna is found to be 4.8mm.
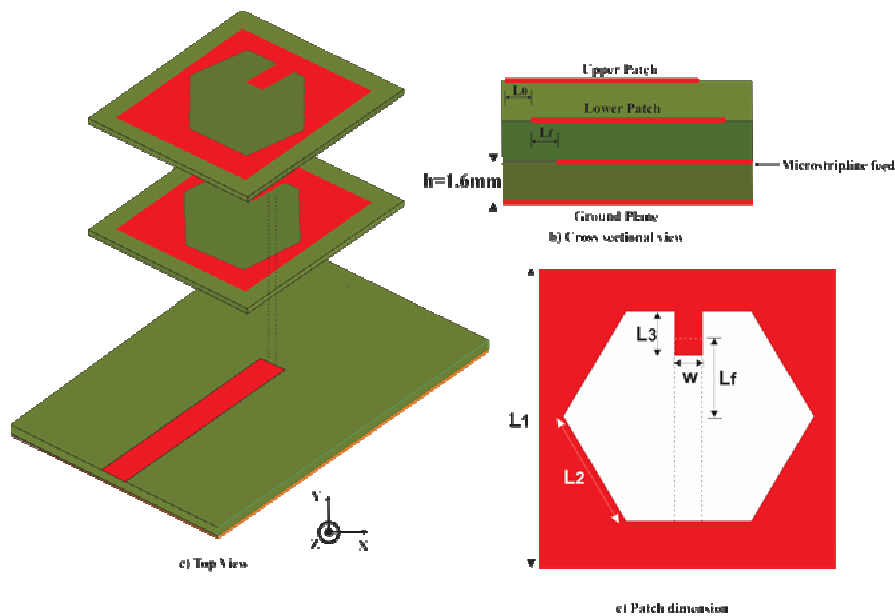
Fig. 5.40 Electric field distributions of the stacked antenna with zero offset

5.8.1 Reflection and Radiation characteristics

The simulated, experimental and computed reflection characteristics of the proposed offset stacked patch antenna are shown in fig.5.41. It is found that the antenna is covering a wide bandwidth from 4.01 GHz to 5.57 GHz having 32.56% bandwidth. The resonances are found to be at 4.18 GHz, 5GHz and 5.37 GHz.
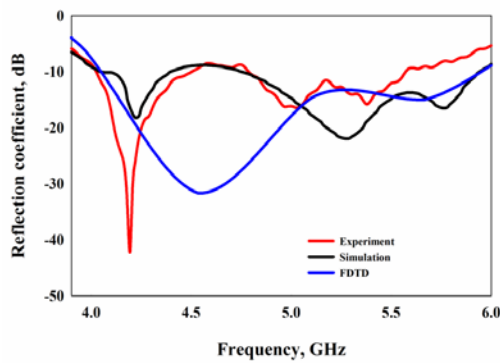
Fig. 5.41 Reflection characteristics of the offset stacked polygonal slotted microstrip antenna with L₀=2mm
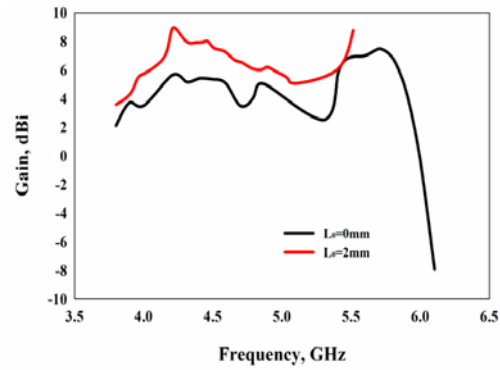
Fig. 5.42 Gain characteristics of the stacked polygonal slotted antenna with and without offset

The gain characteristics of the proposed antenna are shown in fig. 5.42. A comparison study of the gain of the antennas with and without offset is depicted in the same figure. It is observed that the antenna shows better gain characteristics as compared to the antenna without offset throughout the entire frequency of operation. The maximum gain of the antenna is found to be 8.9 dBi at 4.2 GHz.

The experimental radiation patterns of the antenna at the resonant frequencies are shown in fig. 5.43. For all the resonant frequencies, a dip along the on axis of the antenna is noted for the XZ cross polarization patterns. The cross polar isolation is found to be 21 dB, 19 dB and 24 dB for the XZ plane radiation patterns of the antenna at 4.2 GHz, 5 GHz and 5.37 GHz respectively. For the 4.2 GHz resonance, the cross polar power level is 7.2 dB below the co polar power along the on axis in the YZ plane pattern. The resonances centered around 5 GHz and 5.37 GHz shows cross polar isolation of 1.8 dB and 13 dB respectively for the YZ plane pattern.

(a) 4.2 GHz

(b) 5 GHz

(c) 5.37 GHz
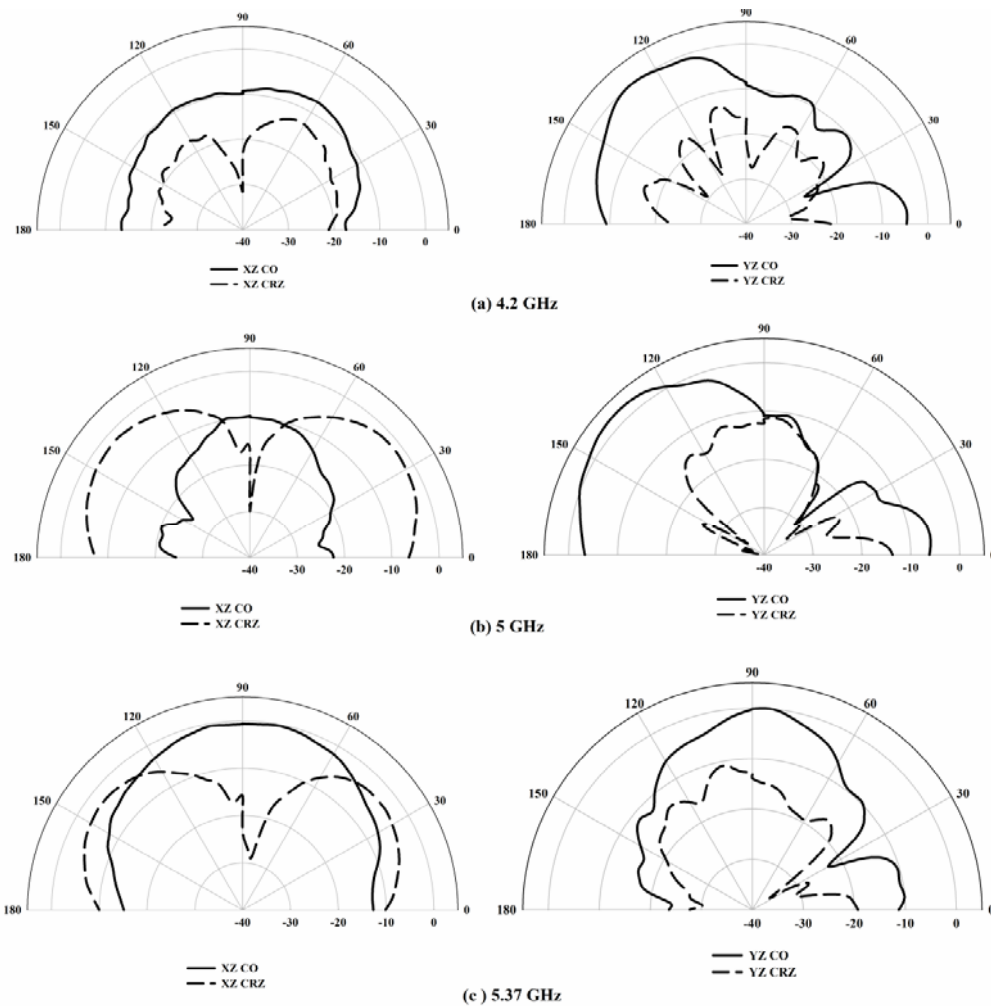
**Fig. 5.43 Reflection characteristics of the offset stacked polygonal slotted microstrip antenna with L_0=2mm**

5.8.2 Fringing Electric field models of the antenna

The fringing electric field models of the antenna are computed using FDTD method. It is concluded from the earlier discussion that, offsetting enhances the fringing electric fields of the patches and it is found that the major contribution is from the E_y component of the electric field. So for this study only the E_y component of the fringing electric field for the top and bottom layer of the patches is taken into consideration here.

The fringing electric fields of the top and bottom patches of the antenna at 4.19 GHz are shown in fig. 5.44 and 5.45 respectively. It is observed that there is a strong contribution from the E_y component on the top and bottom sides of the patches. From the figures, it is observed that the space between the patches acts like a leaky cavity and hence enormous fringing electric fields are noted along the radiating edges of the patches and hence the gain is found to be increased.
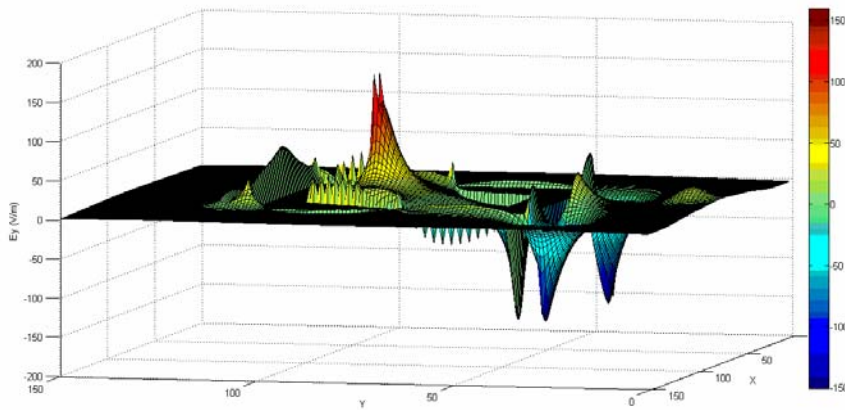
Fig. 5.44 Computed E$_y$ component of Electric field on the upper patch at 4.19 GHz
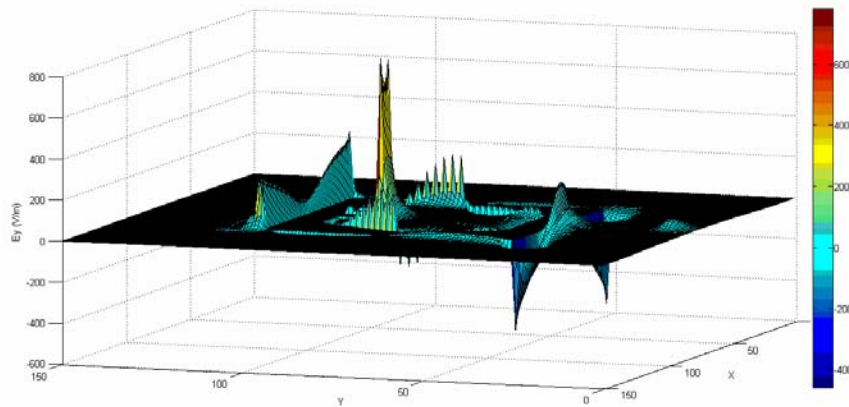
Fig. 5.45 Computed E$_y$ component of Electric field on the lower patch at 4.19 GHz

5.9 Conclusions

The chapter highlighted a novel technique to enhance the gain of single band and broadband microstrip patch antennas. Principle of stacking is successfully implemented and the position of the upper parasitic patch is offsetted to enhance the fringing electric fields of the stacked antenna. The design greatly reduces the separation between the patches without degrading the impedance matching performance of the antenna. The single band design working around 2.3 GHz has a stacking height of the order of $0.025\lambda_g$, where λ is the guided wavelength corresponding to the resonant frequency of the antenna and gain of the antenna is found to be 4.8 dBi. The offset stacked tilted square slotted and polygonal slotted broadband designs exhibits a bandwidth of 34.9% and 32.56% respectively and shows a maximum gain of 8.07dBi and 8.9dBi respectively.

5.10 References

[1] Siew Bee Yeap, Zhi Ning Chen, "Microstrip patch antennas with enhanced gain by partial substrate removal," IEEE Trans. Antennas Propag., vol. 58, no. 9, pp. 2811-2816, 2010.

[2] Chih-Yu Huang, Jian-Yi Wu, Kin-Lu Wong, "High-gain compact circularly polarized microstrip antenna," IEE Electronic Lett., vol. 34, no. 8, pp. 712-713, 1998.

[3] Chi-Lun Mak, Hang Wong, Kwai-Man Luk, "High-gain wide-band single layer patch antenna for wireless applications," IEEE Trans. Vehicular Tech., vol. 54, no. 1, pp. 33-40, 2005.

[4] Herve Legay, L. Shafai, "A self-matching wideband feed network for microstrip arrays," IEEE Trans. Antennas Propag., vol. 45, no. 4, pp. 715-722, 1997.

[5] Herve Legay, L. Shafai, "New stacked microstrip antenna with large bandwidth and high gain," IEE Proc. Microw. Antennas Propag., vol. 141, no. 3, pp. 199-204, 1994.

[6] Chad Kidder, Ming-Yi Li, Kai Chang, "Broadband U-slot patch antenna with a proximity coupled double π-shaped feed line for arrays," IEEE Antennas Wireless Propag. Lett., vol. 1, no. 4, pp. 2-4, 2002.

[7] Gerald R. DeJean, Manos M. Tentzeris, "A New High-Gain Microstrip Yagi Array Antenna with a High Front-to-Back Ratio for WLAN and Millimeter-Wave Applications," IEEE Trans. Antennas Propag., vol.55, no.2, pp.298-304, 2007.

[8] E. Nishiyama, M. Aikawa, S. Egashira, "Stacked microstrip antenna foe wideband and high gain," IEE Proc. Microw. Antennas Propag., vol. 151, no. 2, pp. 143-148, 2004.

[9] E. Rajo-Iglesias, G. Villaseca-Sanchez, C. Martin-Pascual, "Input Impedance Behaviour in Offset Stacked Patches," IEEE Antennas Wireless Propag. Lett., vol.1, pp.28-30, 2002.

…..ജൂ…..

CONCLUSION AND FUTURE PERSPECTIVE

C o n t e n t s	**6.1** *Thesis highlights and Key contributions*
	6.2 *Inferences from the wideband strip loaded slotted patch antenna*
	6.3 *Inferences from the offset stacked single band and broadband high gain designs*
	6.4 *Suggestions for future work*

This chapter highlights the conclusions drawn from numerical, simulation and experimental investigations of broadband and high gain microstrip antennas. The important inferences of the strip loading and offsetting techniques are also presented along with some of the future directions in this area.

6.1 Thesis highlights and Key contributions

This chapter describes the closing stage of the thesis by summarizing the important conclusions drawn from the experimental and simulation studies of the broadband and high gain strip loaded slotted square patch antennas.

An overview of the antenna research along with the state of art technologies in planar antenna designs are highlighted in chapter1.

A broad literature review regarding the development of microstrip antennas and the different technologies used to enhance the bandwidth of microstrip antennas are included in chapter2. The motivation behind the present work regarding the bandwidth enhancement technique persistent towards the current technological developments is explained in detail in this chapter.

Experimental, numerical and simulation studies towards the development of a broadband strip loaded slotted square patch antenna are the core of chapter4. Investigations are carried out on tilted square slot and polygonal slot loaded patch antennas and the resonant mechanism is explained in detail. Simple design equations are formulated and are validated on different substrates. Finally, L-strip feed mechanism is successfully implemented to broaden the bandwidth of the polygonal slotted patch antenna further.

Investigations on the gain enhancement technique for single band square patch antenna and two broadband configurations discussed in chapter4 are discussed in chapter5. Stacking is successfully implemented and the upper parasitic patch is offsetted to enhance the gain of the structure. The technique

effectively reduces the overall volume of the stacked antenna configurations considerably.

6.2 Inferences from the wideband strip loaded slotted patch antenna

The interferences drawn from the experimental and simulation analysis of the strip loaded broadband patch antennas are summarized below.

- By properly optimizing the strip dimensions, the resonances caused by the patch antenna can be effectively matched and can be merged with the resonance offered by the patch and the strip.

- The antenna has a 2:1 VSWR bandwidth of 38% for the tilted square slot structure and 45% for the polygonal slotted structure, making it suitable for 5.2/5.8 GHz WLAN, HIPERLAN2 and HiSWaNa communication bands.

- The impedance matching strip is incorporated on the same plane of the antenna structure and hence it is devoid of spacers required to support the impedance matching strip as in conventional designs and the design reduces fabrication complexities.

- The added metal strip overcomes the high capacitive reactance offered by the lower resonances and it is found that increase in the strip length shifts the imaginary part to the inductive side. The strip acts like a series LC circuit connected in series with the slotted patch antenna.

- The design equations formulated can be used for the validation of the antenna on different microwave substrates.

6.3 Inferences from the offset stacked single band and broadband high gain designs

The interferences drawn from the offset stacked single band and broadband high gain microstrip antennas are summarized below. .

- Principle of stacking is effectively applied and the position of the upper patch is offsettted without deteriorating the impedance matching performance of the antenna for single band and broadband designs.

- In conventional stacked high gain antennas, gain enhancement is achieved by stacking the parasitic patch at a height equal to the half wavelength of the resonating frequency. The offsetting technique greatly reduces the volume of the antenna without deteriorating the impedance matching performance of the antenna.

- In conventional stacked patches, when the separation between the patches is very less, then the space between the patched acts like a strong cavity and it resonates at the TM_{01} mode of the patch antenna and the electric field between them contains mainly E_z component. When the separation between the patches is equal to half wavelength of the resonating frequency of the patch, the space between the patches acts like a leaky cavity, and E_x component dominates and it aids radiation. The offset in the position of the stacked upper patch without increasing the stacking height, in effect, makes the space between the patches as a leaky and hence it enhances the fringing electric fields from the patches and the antenna exhibits high gain performance.

- The single band design working around 2.3 GHz has a stacking height of the order of $0.025\lambda_g$, where λ is the guided wavelength corresponding to the resonant frequency of the antenna and gain of the antenna is found to be 4.8 dBi.

- The offset stacked tilted square slotted and polygonal slotted broadband designs exhibits a bandwidth of 34.9% and 32.56% respectively and shows a maximum gain of 8.07dBi and 8.9dBi respectively.

6.5 Suggestions for future work

The strip loaded broadband patch antenna can be configured for much compact mode of operation by increasing the strip length. It is found from the experimental and simulation studies that the increase in the strip length lowers the resonant frequencies offered by the patch. But the impedance matching performance deteriorates. This is due to the fact that increase in the strip length increases the real part of the impedance and the imaginary part shits towards the inductive side. The impedance mismatch can be overcome by loading a parasitic patch over the antenna. This is because, the placement of the upper patch lowers the input impedance and it suppresses the high inductive reactance and hence a much compact mode of operation can be achieved.

The strip loaded antennas can be made in the form of an array to enhance the band width of the antenna to meets the requirements of ultra wide band radio which uses 3.1 GHz to 10.5 GHz frequency spectrum in the frequency band. Here the patches can be fed with Wilkinson power divider and the distances between the patches can be adjusted so that the resonances offered by each of the strip loaded patch antenna can be merged to give an

extra large bandwidth. Here the number of patched required will be lesser as compared to the existing Ultra Wide Band log periodic designs available in the literature.

The main design concern regarding the implementation of high gain antennas is their suitability in urban environment. We have checked the radiation patterns of the antenna within the anechoic chamber and outside the chamber and no predominant variation in the radiation characteristics is observed. The existing antenna designs used for indoor wireless application have a gain in between 2 dBi and 9 dBi and the antenna is practically grown along with the wireless communication module. So for indoor application, the gain and bandwidth reported by our design is sufficient. The reported antenna can be easily grown with the wireless module, provided that the antenna should be detuned against the near field coupling effects of the RF circuitry. But in a noisy street, signal fading effects will be predominant. In such a situation, we have to go for array designs of the existing antenna for getting improved gain characteristics. In a normal closed array design, the mutual coupling effects will be present and hence steps should be taken to minimize the mutual coupling effects. It includes implementation of broadband PBG ground planes for the entire array structure for the operating band of interest.

.....ജ്ഞ.....

A COMPACT PLANAR DUAL BAND ANTENNA FOR 2.4/5.2 GHZ WIRELESS LAN APPLICATIONS

The thesis presented few broadband designs of slot loaded printed microstrip antennas. In this section the study is extended to a modified printed strip monopole antenna excited by a Finite Ground Coplanar Wave Guide feed to achieve dual band operation. Dual band operation is achieved by properly attaching symmetrical sleeves on the flared monopole strip. The antenna exhibits almost omni-directional radiation characteristics throughout the entire frequency bands of operation which make it an attractive choice for modern wireless communication links, especially the 2.4 GHz/5.2 GHz WLAN applications.

A.1 Introduction

The recent rapid progress in wireless communication demands compact broadband antennas. The usage of ultra wide band antennas for narrow band and multiband applications results in out of band spurious emission in the transmitting mode. Therefore for narrow band applications in multiple frequencies, multi band antennas are preferred. Multi band antennas with quasi omni-directional radiation characteristics will serve as a strong candidate for modern wireless communication systems. Therefore compact multiband printed monopole antennas have aroused wide spread application, especially in low power wireless communication gadgets. Z.N Chen [1] et. al have extensively studied the impedance and radiation characteristics of thin wire, thick wire, planar and roll monopoles mounted over a finite ground plane. It is observed that they exhibit a percentage bandwidth of 25%, 40%, 53% and 71% respectively. The coupling between the rolls of the monopole and the spiral structure introduces parasitic inductance and capacitance which in turn introduces an new resonance which merge together with the existing resonance yielding a high impedance bandwidth. However the ground plane dimension and its orientation with respect to the radiator is a serious issue concerning with its integration with wireless communication systems. Therefore the research community has gone towards the development of planar printed monopole antennas in which the ground plane can be printed on the same substrate. Two types of major feeding mechanisms are usually employed, either microstrip feed or coplanar wave guide feed.

Ammann et. al [2] studied the effect of ground plane dimension on the impedance bandwidth of a microstrip line fed printed monopole antenna. They concluded that ground plane truncation excites additional resonant

mode which enhances the bandwidth of the antenna. Manoj Joseph et. al [3] studied the dual band performance of a microstrip line fed truncated ground plane monopole antenna by deliberately placing an offsetted rectangular metal strip on the ground plane. It is interesting to observe that a U-shaped current pattern excited on the monopole strip to the ground strip via the ground plane causes the lower resonance other than the resonance caused due to the monopole itself.

In this study, top loading and symmetrical add on sleeves are utilized in a CPW monopole antenna to achieve compact dual band operation.

A.2 Evolution of the antenna

The evolution of the antenna geometry is shown in fig. A.1. The basic geometry is derived from a coplanar waveguide fed printed monopole antenna. Fabrication is done on an FR4 epoxy substrate of relative dielectric constant 4.4. The width of the main monopole arm and the gap between the ground and the main arm are designed to obtain 50Ω impedance matching [4].
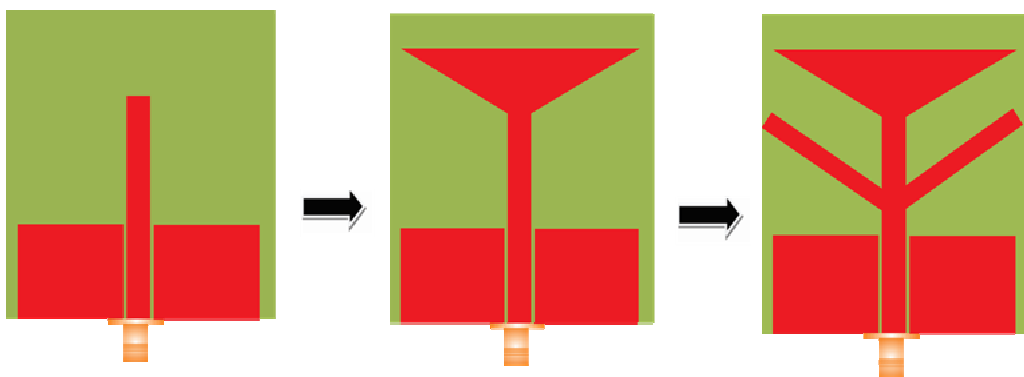
Fig. A.1 Evolution of the antenna

A.2.1 Analysis of a CPW fed strip Monopole antenna

The analysis of the CPW fed printed strip monopole is discussed in this section. The initial design parameters for the strip monopole antenna are, L_g =15mm, W_g=10mm, g=0.35mm, W_c = 3mm, L_m= 20mm, h=1.6mm and ε_r=4.4. The geometry of the antenna is shown in fig.A.2. The reflection characteristics of this basic monopole design are shown in fig. A.3. It is evident from the figure that the strip monopole is resonating at 2.58 GHz with a 2:1 VSWR bandwidth of 15% covering 2.41 GHz to 2.80 GHz.
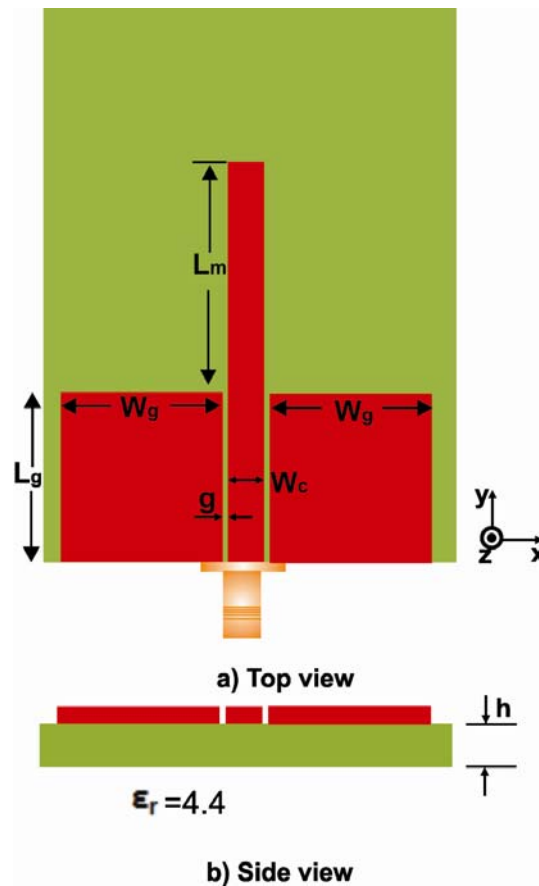
Fig. A.2 Geometry of the CPW fed monopole antenna
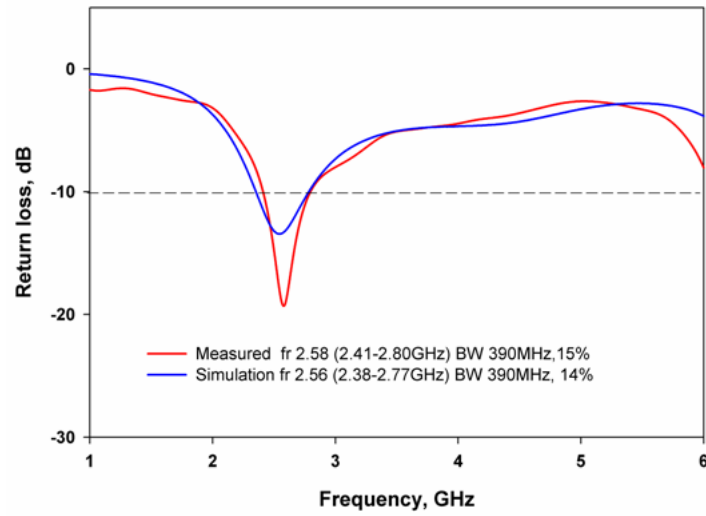
Fig. A.3 Reflection characteristics of the CPW fed monopole antenna

A.2.1.1 Resonance in CPW fed strip Monopole antenna

In order to study the resonance mechanism in the strip monopole antenna, the surface current patterns are utilized. The simulated surface current density distribution on the surface of the monopole is shown in fig. A.4.
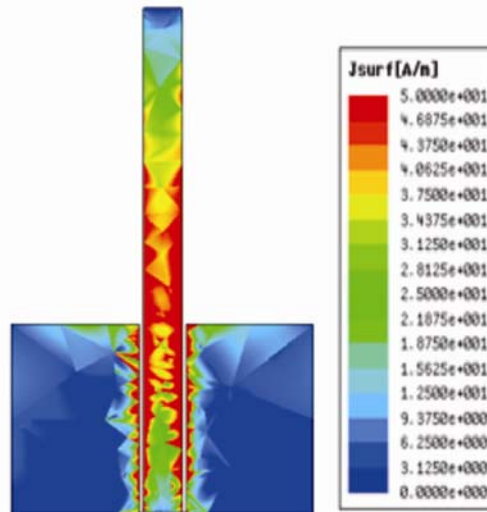
Fig. A.4 Surface current distribution of the CPW fed monopole antenna

It is noted that a current minima is observed at the top of the monopole and a maxima is observed at the bottom near the ground plane ending. This is nearly a quarter wave variation along the length of the monopole corresponding to the resonance.

A.2.1.2 Polarization and Radiation patterns

The polarization of the antenna can be verified directly from the current density plot in the vector form at the resonance as shown in fig A.5. It is found that the monopole strip itself has a strong contribution at the resonance while the ground plane has feeble effect. It is noted that the current at the top edge of the monopole are equal and opposite in phase. Therefore they cancel each other at the far field and do not contribute for any radiation. It is also observed that the current direction through the strip monopole is along the Y-direction which results in linearly polarized radiation along the Y- direction.
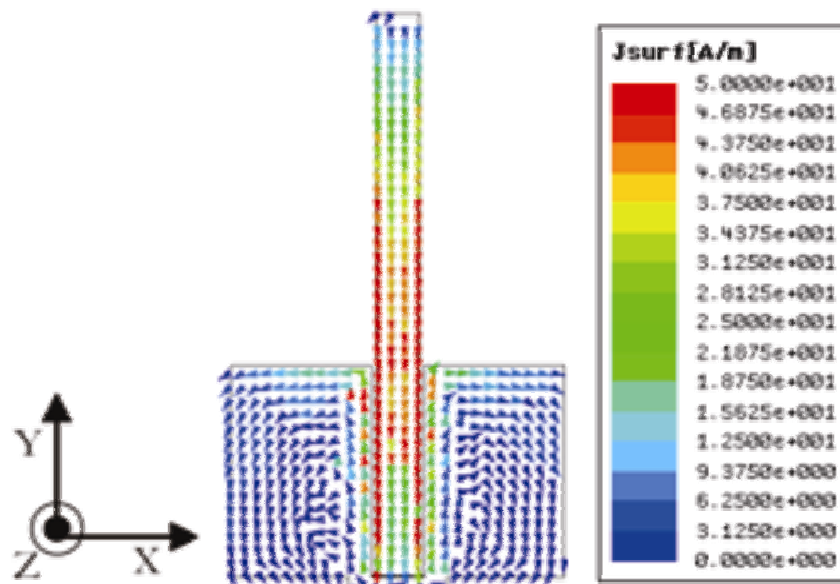
Fig. A.5 Vector Surface current distribution of the CPW fed monopole antenna
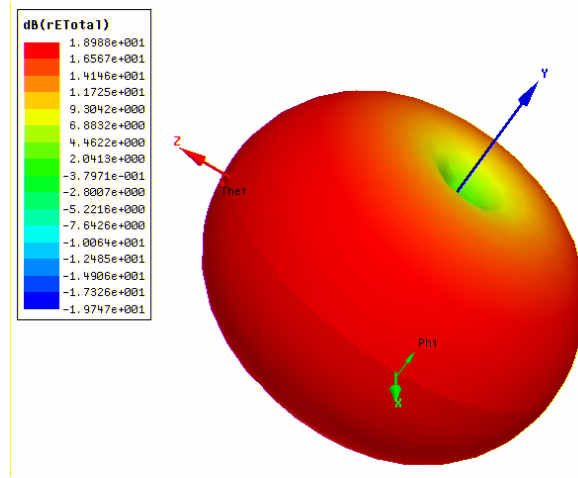
Fig. A.6 Simulated 3D radiation pattern of the antenna

The simulated 3D radiation patterns of the proposed monopole antenna at 2.56 GHz is shown in fig. A.6. It is evident that the monopole is exhibiting almost omni-directional radiation pattern in the H-plane and a figure of eight pattern along the E-plane.

The measured XZ and YZ plane copolar and cross polar radiation patterns of the antenna at the resonant frequency is shown in fig. A.7.
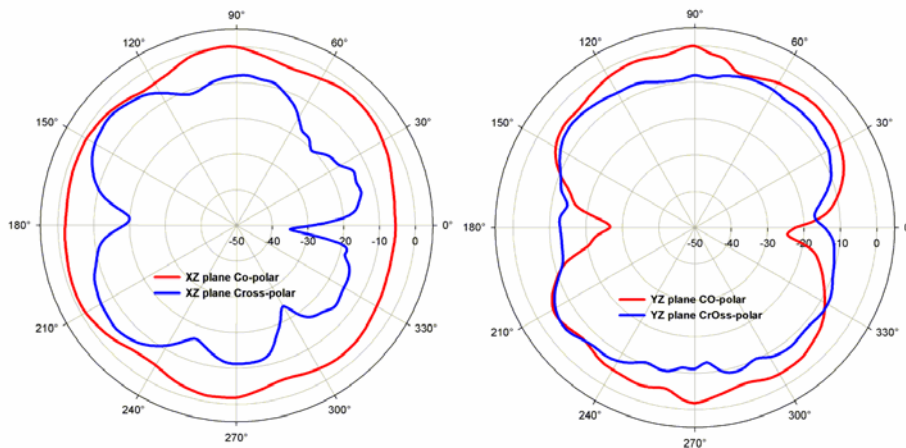
Fig. A.7 Measured radiation patterns of the antenna

The experimental results confirm the radiation behavior obtained through simulation and it is observed that the strip monopole has almost omni-directional radiation coverage in the XZ plane and is highly directional in the YZ plane.

A.2.1.3 Gain and Efficiency

The measured gain of the antenna is depicted in fig. A.8. A peak gain of 4 dBi is observed at 2.6 GHz and the gain remains almost constant throughout the entire band of operation. The average radiation efficiency is found to be 75% in the operating band.
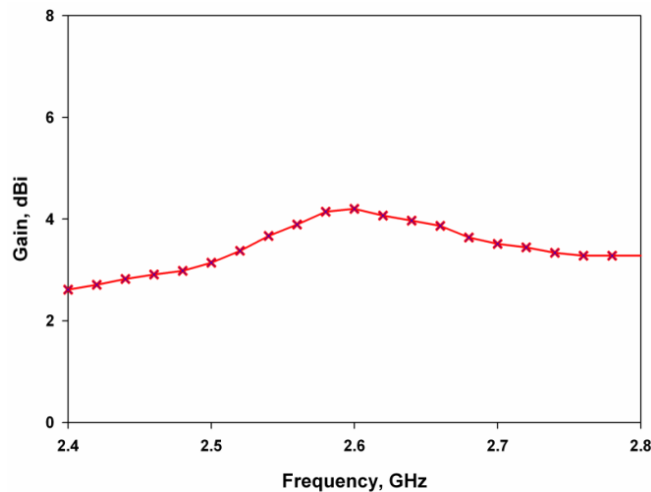
Fig. A.8 Measured Gain of the antenna

A.2.2 Analysis of a CPW fed flared Monopole antenna

It is concluded from the previous section that coplanar waveguide fed strip monopole is an efficient radiator and its omni-directional radiation characteristics make it suitable for modern wireless communication gadgets. In this section, a more compact mode of operation is achieved by top loading a

flared structure over the strip monopole while maintaining the same radiation characteristics of the ordinary strip monopole.

A.2.2.1 Geometry of the flared monopole antenna

The geometry of the flared monopole antenna is shown in fig. A.9. It is a slight modification of the coplanar waveguide fed strip monopole antenna. A flaring with dimension L_f and W_f is introduced in the coplanar waveguide fed strip monopole antenna so that L_m is maintained to be constant for both the designs. The antenna parameters are found to be $L_g = 15$mm, $W_g = 10$mm, $g = 0.35$mm, $W_c = 3$mm, $W_f=23$mm, $L_m = 20$mm, $L_f=10$mm, h=1.6mm and $\varepsilon_r=4.4$.
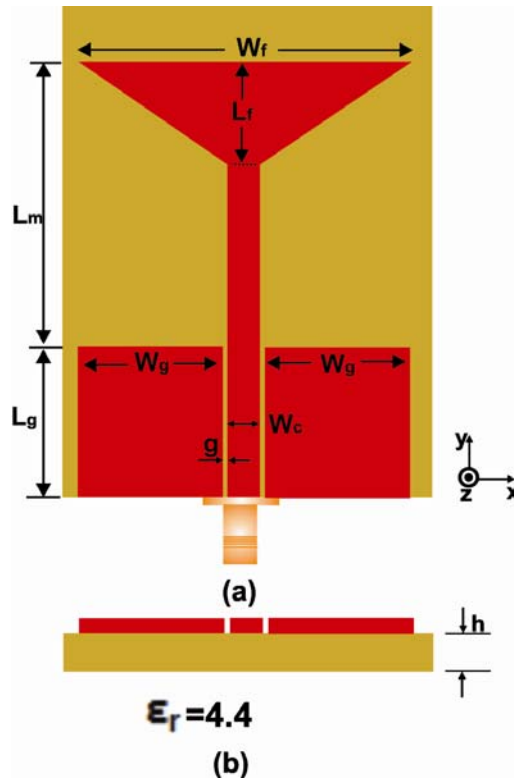
Fig. A.9 Geometry of the CPW fed flared monopole antenna

A.2.2.2 Reflection characteristics

The experimental and simulated reflection characteristics of the proposed flared monopole antenna are shown in fig. A.10. The antenna shows a resonance at 2.14 GHz in experiment with 370 MHz bandwidth from 1.97 GHz to 2.34 GHz. The simulation shows 360 MHz bandwidth from 1.92 GHz to 2.28 GHz around the resonance of 2.08 GHz.
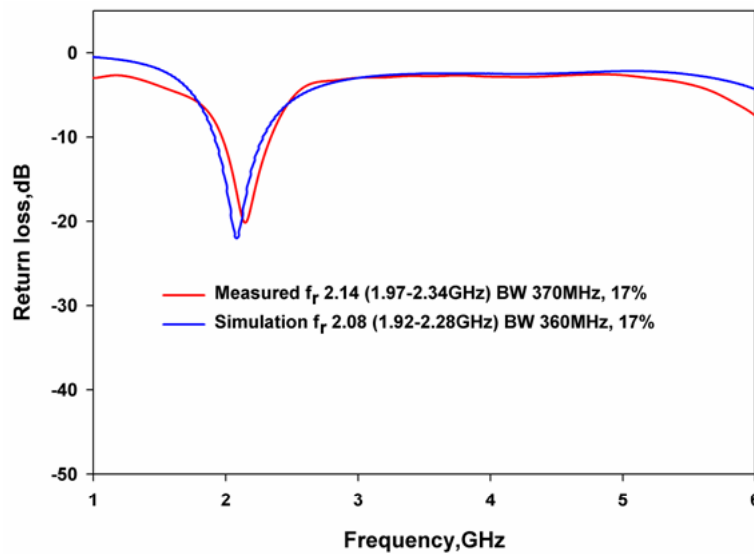
Fig. A.10 Reflection characteristics of the CPW fed flared monopole antenna

A.2.2.3 Radiation patterns

The simulated 3D radiation pattern of the flared monopole antenna is shown in fig. A.11. It is observed that the flared monopole is also providing almost omni-directional radiation pattern. Also it is interesting to note that flaring introduced in the coplanar waveguide fed strip monopole antenna doesn't disturb the radiation pattern. The experimental radiation patterns of the antenna at 2.14 GHz are illustrated in fig. A.12.
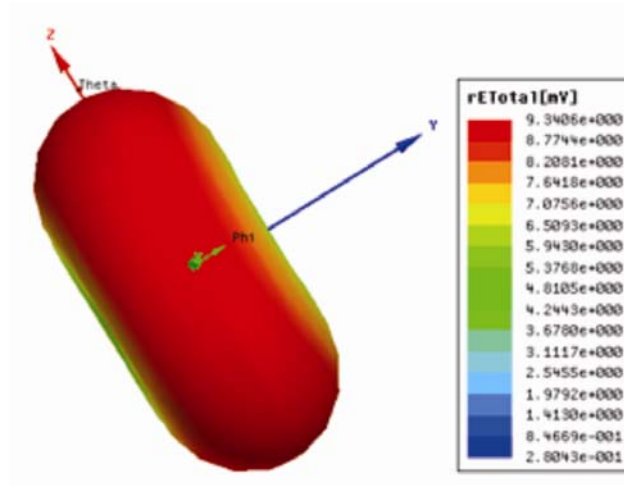
Fig. A.11 3D Radiation patterns of the CPW fed flared monopole antenna
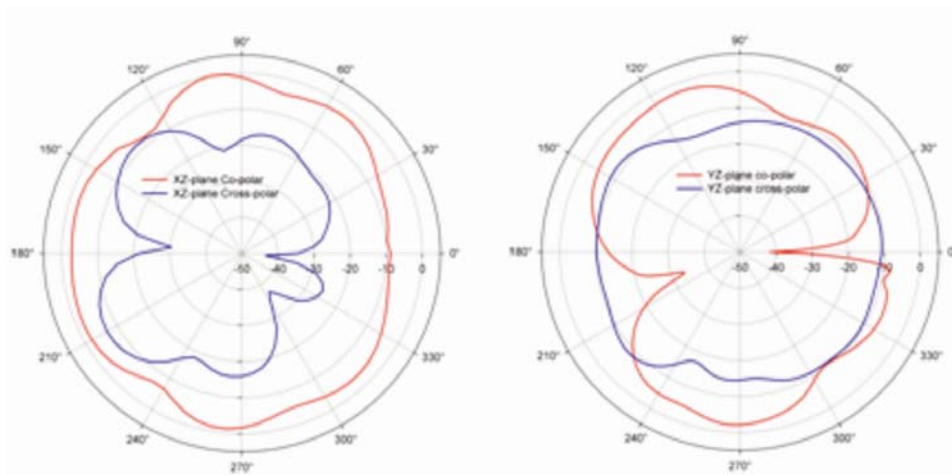
Fig. A.12 Measured radiation patterns of the antenna

A.2.2.4 Gain and Efficiency

The measured gain of the antenna is depicted in fig. A.13. It is observed that the gain remains almost constant throughout the entire operating band. It is also worth to note that the gain remains almost unaltered by the introduction of flaring. The maximum gain is found to be 4 dBi. The average efficiency is found to be 75%.
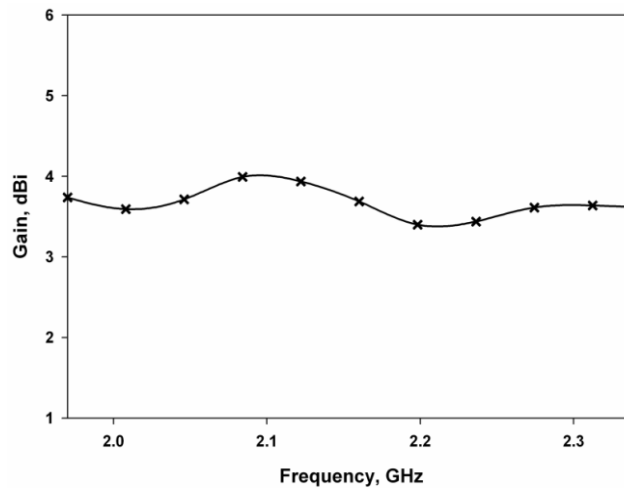
Fig. A.13 Measured Gain of the antenna

A.2.3 Dual Band flared monopole with V-element

Two symmetrical metal sleeves are incorporated on the flared monopole structure in order to excite another resonant mode so as to obtain a dual band antenna. The geometry of the proposed antenna is shown in fig. A.14.
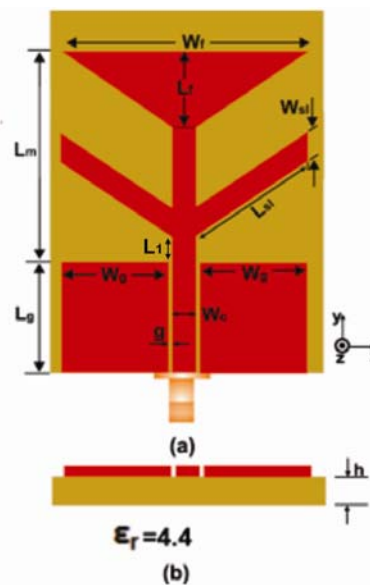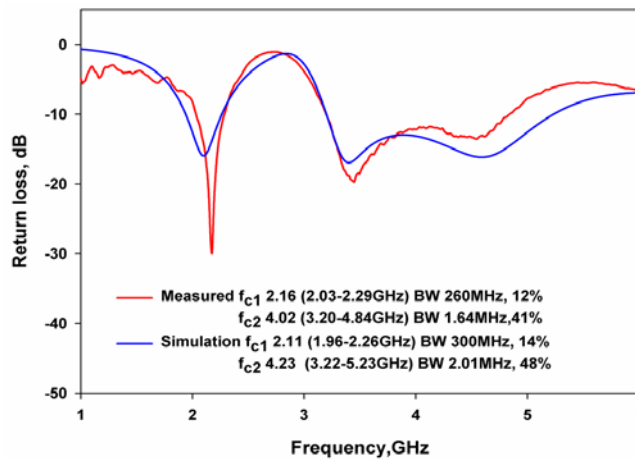

Fig. A.14 Geometry of the CPW fed flared monopole antenna with attached sleeves

Two symmetrical V-sleeves of dimension L_{sl}=15mm and W_{sl}=2.5 mm are incorporated on the monopole main arm in order to get the second resonant band. The antenna parameters are found to be L_g =15mm, W_g = 10mm, g = 0.35mm, W_c=3mm, W_f=23mm, L_m=20mm and L_f=10mm, h=1.6mm, L_{sl}=15mm, W_{sl}=2.5 mm, L1=2.5mm and ε_r=4.4.

A.2.3.1 Reflection characteristics

The input reflection coefficient of the flared monopole antenna integrated with the symmetrical V-sleeves is shown in fig. A.15. The measured results show a lower resonance around 2.16 GHz from 2.03 GHz to 2.29 GHz and the second band is centered around 4.02 GHz with a fractional bandwidth of 41% from 3.2 GHz to 4.84 GHz.

**Fig. A.15 Reflection characteristics of the CPW fed flared monopole antenna with attached sleeves**

A.2.3.2 Resonances in the attached V-sleeve antenna

The simulated surface current density of the antenna at 2.11 GHz is shown in fig. A.16. It is clear from the plot that the lower resonance is caused due to the quarter wave current variation on the flared monopole. The intensity of current on the attached V-sleeves is negligible as compared to that in the flared monopole.
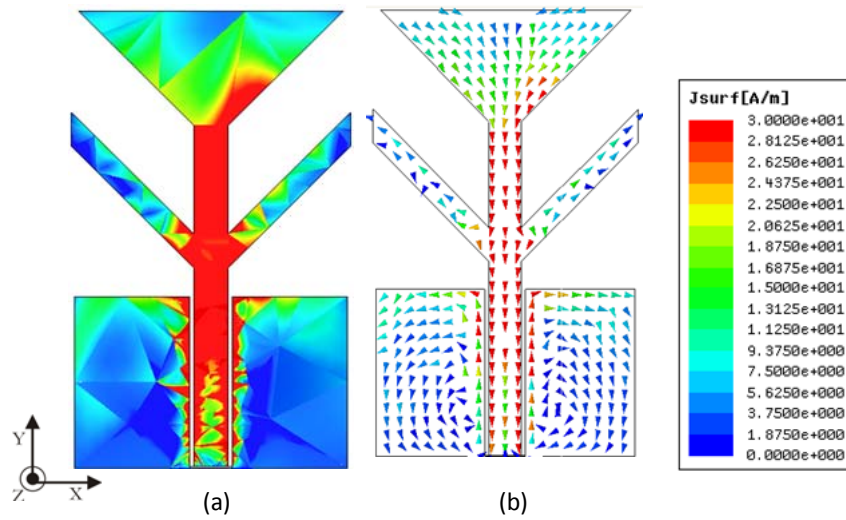
Fig. A.16 Surface current distributions of the CPW fed flared monopole antenna with attached sleeves at 2.11 GHz

The surface current distributions of the antenna at 4.23 GHz is shown in fig. A.17. It can be concluded that the second resonant band is contributed by the attached V-sleeves and the contribution on the flared arm is negligible.
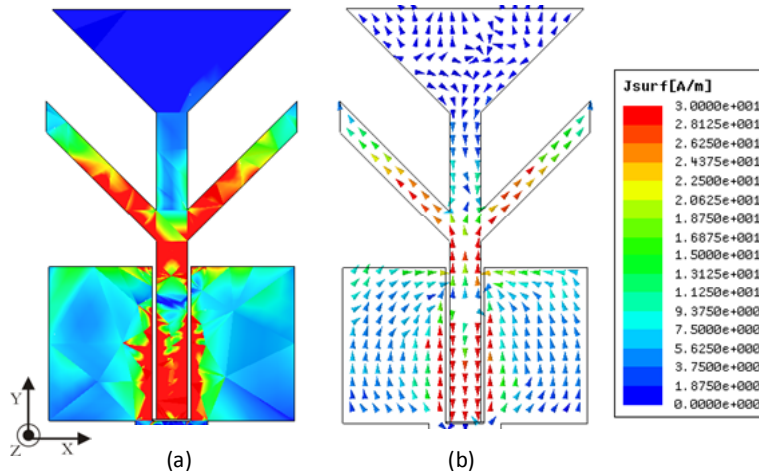

Fig. A.17 Surface current distributions of the CPW fed flared monopole antenna with attached sleeves at 4.23 GHz

A.2.3.3 Radiation patterns

The simulated 3D radiation patterns of the antenna at both the resonant bands are shown in fig. A.18. It is observed that the antenna exhibits its omni-directional radiation characteristics as that of the strip monopole antenna.
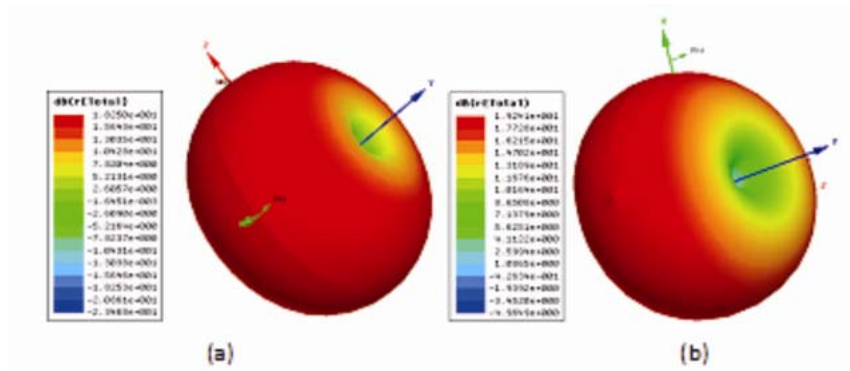
Fig. A.18 3D Radiation patterns of the antenna at a) 2.11 GHz and b) 4.23 GHz
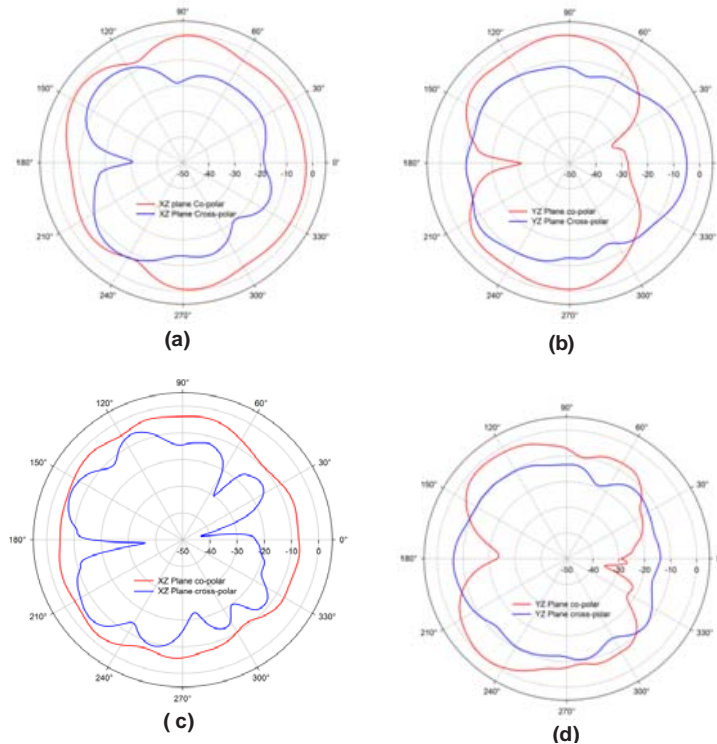
Fig. A.19 Measured radiation patterns in the two orthogonal planes at 2.16GHz [fig (a)-(b)] and at 4.0 GHz [fig(c)-(d)].

The simulated radiation patterns are validated in the two standard planes and are shown in fig. A.19. It is observed that the antenna has a wide coverage in the XZ plane and is directional in the YZ plane.

A.2.3.4 Gain and Efficiency

The peak gain of the antenna at the two resonant bands is shown in fig. A.20. The antenna shows almost constant gain throughout the two resonant bands. The antenna has a peak gain of 3.5 dBi in the first resonant band and 3.9 dBi in the second resonant band.
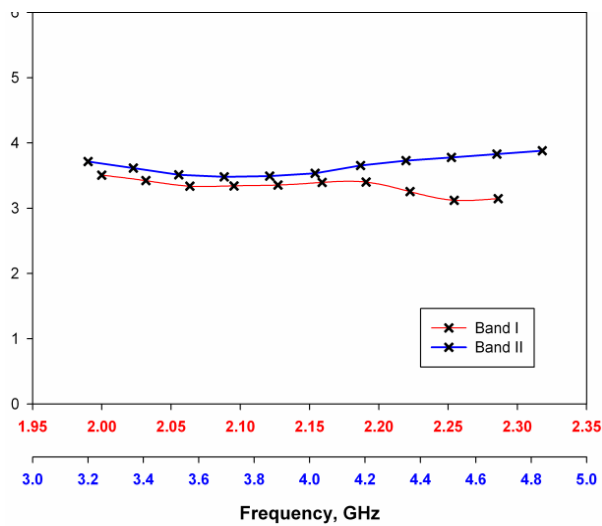

Fig. A.20 Measured gain of the antenna

The radiation efficiency is measured using Wheeler cap method. The measured average efficiency of the antenna are 65% and 73% for the first and second resonant band respectively.

A.3 References

[1] Z.N Chen, M.Y.W Chia and M.J Ammann, "Optimisation and comparison of Monopoles", IEE Proceedings-Microwave Antennas and Propagation, Vol. 150, No.6, December, 2003.

[2] M.J Ammann and M. John, "Optimum Design of the Printed Strip Monopole", IEEE Antennas and Propagation Magazine, Vol. 47, No.6, December, 2005.

[3] Manoj Joseph, Rohith K. Raj, M.N Suma and P. Mohanan, " Compact Dual-Band Antenna for DCS/2.4 GHz WLAN Applications" Microwave and optical Technology Letters, Vol. 48, No.5, May, 2008.

[4] R. Garg, P. Bhartia, I. Bahl and A. Ittitiboon, Microstrip Antenna Design Handbook, Norwood, MA, Artech House, 2001,

.....ജാ.....

▌▌▌ **Citations** ▌▌▌

[1] Reference to the paper **Sarin V P**, Nishamol M S, Deepu V, C K Aanandan, P Mohanan and K Vasudevan "Wideband printed microstrip antenna for wireless communications" *IEEE Antennas and Wireless Propagation Letters*, Vol.8, pp.779-781, 2009 in

a) "A Compact CPW fed Slotted Patch Antenna for Dual Band Applications". Wen-Chung Liu; Chao-Ming Wu; Nien-Chang Chu; , *IEEE Antennas and Wireless Propagation Letters*, VOL. 9, 2010,

b) "Wideband Slot Antenna for WLAN Access Points" Medeiros, C.R.; Lima, E.B.; Costa, J.R.; Fernandes, C.A.;*IEEE Antennas and Wireless Propagation Letters*, VOL. 9, 2010,

c) "Microstrip line Fed Modified Sierpinsky Fractal Monopole Antenna for Dual Wideband Applications" Choukiker, Y.K., Behera, S.K., IEEE International Conference on Communication Control and Computing Technologies (ICCCCT), 2010.

d) "Investigations of a crossed exponentially tapered slot printed antenna for UWB ranging" Medeiros, Carla R, Costa, Jorge R. Fernandes, Carlos A.;, IEEE Proceedings of the Fourth European Conference on Antennas and Propagation (EuCAP), 2010

e) "Parasitically Loaded CPW fed Monopole Antenna for Broadband Operation" W.L Chung, and Tseng Yen Jui;, IEEE Transactionson Antennas and Propagation, vol. 59 (2), No.6, 2011.

f) "Review Paper for Circular Microstrip Patch Antenna", Sonali Jain, Rajesh Nema, International Journal of Computer Technology and Electronics Engineering (IJCTEE), vol.1, issue 3, 2012.

[2]   Reference to the paper "A Dual band dual polarized electromagnetically coupled microstrip antenna for WLAN 5.2/5.8GHz applications", **Sarin V P**, Nishamol M S ,Gijo Augustine, P Mohanan, C K Aanandan and K Vasudevan, IEEE Antennas and Propagation society International Symposium(APS-2008) in

  a)   "Dual Polarisation Microstrip Patch Array Antenna for WLAN Applications". Mohd Shah, M.; Suaidi, M.K.; Abdul Aziz, M.; Kadir, M.F.A.; Rahim, M., 3rd European Conference on *IEEE* Antennas and Propagation, EuCAP 2009.

  b)   "A Novel dual band and dual polarized antenna for WLAN Systems " Shihua Wang; Kitchener, D.; Xiaodong Chen; Parini, C., 5th European Conference on *IEEE* Antennas and Propagation, EuCAP 2011.

[3]   Reference to the paper "A Wideband Stacked Offset Microstrip Antenna with Improved Gain and Low Cross Polarisation", **Sarin V.P**, Nishamol M.S, Tony D, C.K Aanandan, P. Mohanan and K. Vasudevan, IEEE Transactions on Antennas and Propagation, Vol. 59, issue 4, 2011 in "Bandwidth and Gain Enhancement of an Aperture Antenna with Modified Ring Patch", M.M Honari, A. Abdipour and G. Moradi, IEEE Antennas and Wireless Propagation Letters, Vol. 10, 2011.

…..ഇരുൽ…..

List of Publications

International Journals

[1] **Sarin V P**, Nishamol M S, Tony D, C K Aanandan, P Mohanan and K Vasudevan "A broadband L-strip fed printed microstrip antenna" *IEEE Transactions on Antennas and Propagation*, Vol.59, pp.281-284, 2011.

[2] **Sarin V P**, Nishamol M S, Tony D, C K Aanandan, P Mohanan and K Vasudevan "A Wideband stacked offset microstrip antenna with improved gain and low cross polarization" *IEEE Transactions on Antennas and Propagation*, Vol.59, pp. 1376 - 1379, 2011.

[3] **Sarin V P**, Nishamol M S, Deepu V, C K Aanandan, P Mohanan and K Vasudevan "Wideband printed microstrip antenna for wireless communications" *IEEE Antennas and Wireless Propagation Letters*, Vol.8, pp.779-781, 2009.

[4] Gijo Augustine, Bybi P.C, **Sarin V.P**, C K Aanandan, P Mohanan and K Vasudevan "A Compact Dual-Band Planar Antenna for DCS-1900/PCS/PHS,WCDMA/IMT-2000 and WLAN Applications" *IEEE Antennas and Wireless Propagation Letters*, Vol.7, pp.108-111,2008.

[5] **Nishamol M S**, Sarin V P, Tony D, C K Aanandan, P Mohanan and K Vasudevan "An Electronically Reconfigurable Microstrip Antenna with Switchable Slots for Polarization Diversity" *IEEE Transactions on Antennas and Propagation*, Vol.59, pp. 3424 - 3427, 2011.

[6] **Sarin V P**, Nishamol M S, Gijo Augustine, C K Aanandan, P Mohanan and K Vasudevan "An Electromagnetically coupled dual band dual polarized microstrip antenna for WLAN applications", **Microwave and optical technology letters**, July 2008.

[7]   Nishamol M S, **Sarin V P** , Gijo Augustine, Deepu V, C K Aanandan, P Mohanan and K Vasudevan " Compact dual frequency dual polarized cross patch antenna with an X-slot", **Microwave and optical technology letters**, December 2008.

[8]   Nishamol M S**, Sarin V P,**Tony D, C K Aanandan, P Mohanan and K Vasudevan "Single feed circularly polarized V slot antenna for GPS applications" Accepted for publication in **Microwave and optical technology letters**.

[9]   Nishamol M S, **Sarin V P**, Tony D, C K Aanandan, P Mohanan and K Vasudevan "Design of frequency and polarization tunable microstrip antenna", **Microwave Review Journal**, vol.16, No.2, December 2010.

[10] Nishamol M S, **Sarin V P**, Tony D, C K Aanandan, P Mohanan and K Vasudevan "Broadband printed V- slotted cross patch antenna for IEEE802.11a/WiMAX/GHiperLAN2 applications", **Progress In Electromagnetic Research Letters**, Vol. 19, 155-161, 2010.

[11] **Nishamol M S**, Sarin V P, Tony D, C K Aanandan, P Mohanan and K Vasudevan "Varactor Controlled Frequency and Polarization Reconfigurable Microstrip Antenna" **RF and microwave computer-aided engineering**-Accepted.

[12] Tony D, **Sarin V P**, Nishamol M S**,** , C K Aanandan, P Mohanan and K Vasudevan "CPW fed slotted planar antenna for wireless communications " **Microwave and optical technology letters**-Accepted.

[13] **Sarin V P**, Nishamol M S, Tony D, C K Aanandan, P Mohanan and K Vasudevan "Compact High Gain Stacked Offset Single Band and Broadband Microstrip Antennas as an Alternative to Normal Stacked and Array Configurations" *Microwave and optical Technology Letters,* Communicated.

International and National Conferences

[1] **Sarin V P**, Nishamol M S ,Tony D, P Mohanan, C K Aanandan and K Vasudevan, " Strip loaded slotted patch antenna for wireless applications" IEEE Applied Electromagnetics Conference(AEMC-2009), Kolkata, India.

[2] **Sarin V P**, Nishamol M S ,Gijo Augustine, P Mohanan, C K Aanandan and K Vasudevan, " A Dual band dual polarized electromagnetically coupled microstrip antenna for WLAN 5.2/5.8GHz applications" IEEE Antennas and Propagation society International Symposium(APS-2008), San Diego, USA.

[3] **Nishamol M S** , Sarin V P, Tony D, P Mohanan, C K Aanandan and K Vasudevan "Frequency and polarization tuning of a cross patch antenna using capacitive loading" International conference on Communications and signal processing (ICCSP 2011), February 2011, NIT, Calicut, Kerala, India.

[4] Gijo Augustine, Bybi P C, **Sarin V P**, Nishamol M S, P Mohanan, C K Aanandan and K Vasudevan, " compact dual band antenna for handheld wireless communication gadgets" IEEE Antennas and Propagation society International Symposium(APS-2008), San Diego, USA.

[5] Gijo Augustine, Bybi P C, **Sarin V P**, Nishamol M S, P Mohanan, C K Aanandan and K Vasudevan, "compact dual band planar antenna for IMT-2000 application" International conference on microwave antenna propagation and remote sensing (ICMARS-2008).

[6] Gijo Augustine, Bybi P C, **Sarin V P**, Nishamol M S, P Mohanan, C K Aanandan and K Vasudevan, " A compact dual band planar antenna for IMT-2000 and WLAN applications" Proceedings of IEEE Applied Electromagnetic conference, 19-20, December 2007, Kolkata, India.

[7] Nishamol M S , **Sarin V P**, Tony D, P Mohanan, C K Aanandan and K Vasudevan, " Single feed circularly polarized cross patch antenna" IEEE Applied Electromagnetics Conference(AEMC-2009), Kolkata, India.

[8] Nishamol M S, **Sarin V P**,P Mohanan, C K Aanandan and K Vasudevan ' Single feed miniaturized cross patch antenna" International conference on Recent advances in microwave theory and applications (Microwave 2008), 21-24 November 2008,Jaipur, Rajasthan.

[9] **Sarin V P**, Nishamol M S , Tony D, Sreejith M. Nair, P Mohanan, C K Aanandan and   K Vasudevan, ' A Broadband microstrip antenna for wireless applications' National Conference on Electronics, February 2011,BPC College , Piravom, Kerala

[10] **Sarin V P**, Nishamol M S , Deepu V, Sujith R,P Mohanan, C K Aanandan and K Vasudevan, 'Broadband microstrip antenna for wireless applications' National symposium on Antennas and Propagation (APSYM 2008), 29-31 December 2008,CUSAT, KERALA, INDIA.

[11] Nishamol M S, **Sarin V P**, Deepu V, Sujith R, P Mohanan, C K Aanandan and K Vasudevan 'Cross patch antenna with an X slot for polarization switching" National symposium on Antennas and Propagation (APSYM 2008), 29-31 December 2008,CUSAT, KERALA, INDIA.

[12] **Sarin V P,** Nishamol M S, Tony D, Sreejith M. Nair and K Vasudevan, "A Broadband Microstrip Antenna for Wireless Applications" National Conference in Electronics, February, 2011, B.P.C College, Piravom, Kerala, India.

…..ജ്ഞ…..

SARIN V.P

Senior Research Fellow
Centre for Research in Electromagnetics and Antennas
Department of Electronics
Cochin University of Science and Technology
Cochin-22, Kerala, India
Email: sarincrema@gmail.com

Objective

A motivated scholar having keen interest in Microwave electronics with specialization in Printed antenna technology, seeking a position in R&D level.

Research Achievements

- **Student Author Award** in IEEE Applied Electromagnetic Conference (AEMC-09) held at Kolkata.

- Qualified University Grants Commissions **JRF/NET** in 2007.

- Published papers in International Journals like IEEE, Wiley etc., National and International Symposia.

Education

M.Sc Applied Electronics
School of Technology and Applied Science,
Edappally, Kerala, India.
Score: First Rank (First class with Distinction)

Training

- Attended a one day work shop on recent advances in Microwave Theory and Applications (Microwave 08) in Jaipur, India.

- Completed 6 months training in Indian Satellite Research Organization (ISRO) during Master's Thesis, and theoretically analyzed an HF RADAR array for predicting the jet velocity associated with the ionospheric plasma instabilities

Technical Papers Presented

- Presented the paper "Single feed miniaturized cross patch antenna" in IEEE International conference on Recent advances in microwave theory and applications (Microwave 2008), 21-24 November 2008, Jaipur, Rajasthan.

- Presented the paper "Strip loaded slotted patch antenna for wireless applications" in IEEE Applied Electromagnetics Conference (AEMC-2009), Kolkata, India.

- Presented the paper 'Broadband microstrip antenna for wireless applications' in National symposium on Antennas and Propagation (APSYM 2008), 29-31 December 2008, CUSAT, Kerala, India.

Publications

International Journal	: 12
National & International conference	: 12

Computer Proficiency

C, C^{++}, MATLAB, Assembly Level Programming, VDSP, VHDL, Ansoft HFSS, Designer, Zeland IE3D, Zeland FIDELITY, Microwave Office, Microstripes, and CST Microwave Studio.

….. හⓒ…..

Index

3

3D radiation pattern · 125, 144, 145, 167, 173, 185, 211, 214, 215, 219

A

Aanandan · 30, 54
Anechoic Chamber · 70, 71, 71,100
Antenna design · 79, 158, 180, 161, 221
Array-18, 19, 26, 27, 28, 32, 37, 39, 46, 47, 48, 49, 55, 56, 159, 198, 160, 161, 162, 166, 167, 168, 169

B

Bandwidth · 3, 5, 12, 14, 53, 54, 57, 58, 59, 61, 70, 97, 100, 71, 75, 104, 105, 106, 113, 114, 121, 160, 161, 163, 166, 172, 173, 177, 187, 188, 189, 193, 197,
Bose -2
Buried feed-8

C

Cavity Model-9, 10
Coaxial feed-7
CPW · 56, 158, 207, 208, 209, 210, 212, 213, 214, 215, 216, 217, 218
Current distribution -126, 127, 128, 209, 210, 218,

D

Dual band-205,216

E

E plane -31
Efficiency-7,19,24,32,36
Electric field -5,11,74,78,80, 84,90,94,104,139,142,161,174,195,202
Electromagnetic radiation · 19
Excitation technique-6

F

FFT -99,112
Finite Difference Time Domain - 11,14,39,77,78
Finite element method- 11,76
Flow chart · 98
Fringing- 5,141,142,161,166,174,195,202

G

Gain- 5,13,28,32,38,46,70,73,104,123,126,155,160,180,212,215,220
Green's function method-12

H

Heinrich Rudolf Hertz-2
HFSS - 76
HP 8510C · 68,69

I

Impedance matching - 13,26,33,38,68,70,104,161,201,207
Inferences · 199,201

J

James Clark Maxwell-2

K

Kraus -3

L

Low profile-3,18
L-strip-40, 44, 46, 105, 144, 200

M

Maxwell · 3, 59, 79, 101, 102, 103
Method of moments-11

…..ಜ಼ಀ಼…..